Residual Crashes and Injured Occupants with Lane Departure Prevention Systems

Luke E. Riexinger

Dissertation submitted to the faculty of the Virginia Polytechnic Institute and State University in partial fulfillment of requirements for the degree of

Doctor of Philosophy

In

Biomedical Engineering

Hampton C. Gabler, Chair

Warren N. Hardy, Co-Chair

Zachary Doerzaph

Douglas J. Gabauer

Scott Gayzik

Feng Guo

22 March 2021

Blacksburg, Virginia

Keywords: Active Safety, Lane Departure Warning, Event Data Recorder, Crash Avoidance Modeling, Rollover Injury Model

Residual Crashes and Injured Occupants with Lane Departure Prevention Systems

Luke E. Riexinger

ABSTRACT

Every year, approximately 34,000 individuals are fatally injured in crashes on US roads [1]. These fatalities occur across many types of crash scenarios, each with its own causation factors. One way to prioritize research on a preventive technology is to compare the number of occupant fatalities relative to the total number of occupants involved in a crash scenario. Four crash modes are overrepresented among fatalities: single vehicle road departure crashes, control loss crashes, cross-centerline head-on crashes, and pedestrian/cyclist crashes [2]. Interestingly, three of these crash scenarios require the subject vehicle to depart from the initial lane of travel. Lane departure warning (LDW) systems track the vehicle lane position and can alert the driver through audible and haptic feedback before the vehicle crosses the lane line. Lane departure prevention (LDP) systems can perform an automatic steering maneuver to prevent the departure.

Another method of prioritizing research is to determine factors common among the fatal crashes. In 2017, 30.4% of passenger vehicle crash fatalities involved a vehicle rollover [1]. Half of all fatal single vehicle road departure crashes resulted in a rollover yet only 12% of fatal multi-vehicle crashes involved a rollover [1]. These often occur after the driver has lost control of the vehicle and departed the road. Electronic stability control (ESC) can provide different braking to each wheel and allow the vehicle to maintain heading. While ESC is a promising technology, some rollover crashes still occur. Passive safety systems such as seat belts, side curtain airbags, and stronger roofs work to protect occupants during rollover crashes. Seat belts prevent occupants from moving inside the occupant compartment during the rollover and both seat belts and side curtain airbags can prevent occupants from being ejected from the vehicle. Stronger roofs ensure that the roof is not displaced during the rollover and the integrity of the occupant compartment is maintained to prevent occupant ejection.

The focus of this dissertation is to evaluate the effectiveness of vehicle-based countermeasures, such as lane departure warning and electronic stability control, for preventing or mitigating single vehicle road departure crashes, cross-centerline head-on crashes, and single vehicle rollover crashes. This was accomplished by understanding how drivers respond to both road departure and cross-centerline events in real-world crashes. These driver models were used to simulate real crash scenarios with LDW/LDP systems to quantify their potential crash reduction. The residual crashes, which are not avoided with LDW/LDP systems or ESC, were analyzed to estimate the occupant injury outcome. For rollover crashes, a novel injury model was constructed that includes modern passive safety countermeasures. The results for road departure, head-on, and control loss rollover crashes were used to predict the number of crashes and injured occupants in the future. This work is important for identifying the residual crashes that require further research to reduce the number of injured crash occupants.

Residual Crashes and Injured Occupants with Lane Departure Prevention Systems

Luke E. Riexinger

GENERAL AUDIENCE ABSTRACT

Every year in the US, approximately 34,000 individuals are fatally injured in many different types of crashes. However, some crash types are more dangerous than other crash types. Drift-out-of-lane (DrOOL) road departure crashes, control loss road departure crashes, head-on crashes, and pedestrian crashes are more likely to result in an occupant fatality than other crash modes. In three of these more dangerous crash types, the vehicle departs from the lane before the crash occurs. Lane departure warning (LDW) systems can detect when the vehicle is about to cross the lane line and notify the driver with beeping or vibrating the steering wheel. A different system, called lane departure prevention (LDP), can provide automatic steering to prevent the vehicle from leaving the lane or return lane. In control loss crashes, the vehicle's motion is in a different direction than the vehicle's heading. During control loss, it is easier for the vehicle to roll over which is very dangerous. Electronic stability control (ESC) can prevent control loss by applying selective braking to each tire to keep the vehicle's motion in the same direction as the vehicle's heading. If a rollover still occurs, vehicles are equipped with passive safety systems and designs such as seat belts, side curtain airbags, and stronger roofs to protect the people inside. Seat belts can prevent occupants from striking the vehicle interior during the rollover and both seat belts and side curtain airbags can prevent occupants from being ejected from the vehicle. Stronger roofs ensure that the roof is not displaced during the rollover to prevent occupants from being ejected from the vehicle.

The focus of this dissertation is to estimate how many crashes LDW, LDP, and ESC systems could prevent. This was accomplished by understanding how drivers respond after leaving their lane in real crashes. Then, these real crash scenarios were simulated with an LDW or LDP system to estimate how many crashes were prevented. The occupants of residual crashes, which were not prevented by the simulated systems, were analyzed to estimate the number of occupants with at least one moderate injury. Understanding which crashes and injuries that were not prevented with this technology can be used to decide where future research should occur to prevent more fatalities in road departure, head-on and control loss crashes.

ACKNOWLEDGEMENTS

I would first like to acknowledge my advisor, Dr. Clay Gabler, for his profound influence over more than just this dissertation but my career, and my life. From the moment I met him, he inspired me to use my knowledge to evaluate ways of protecting people from vehicle crashes. While he was a secret celebrity and highly regarded for his research, he was always interested in my success more than his own. Thank you for asking me challenging research questions, writing red comments all over my manuscripts, and listening to many late-night practice presentations to develop me into an effective researcher. Thank you Dr. Gabler for always encouraging me to push myself to complete another paper and always placing your confidence in me to figure out the next tough problem that could make transportation safer.

Special thanks to my committee members, Dr. Warren Hardy, Dr. Doug Gabauer, Dr. Zac Doerzaph, Dr. Feng Guo, and Dr. Scott Gayzik, for their review and input on this dissertation. Your advice and support were essential for completion of this work and I know it will continue throughout my career.

I would like to thank the Toyota Collaborative Safety Research Center for funding me, this research, and the opportunity to present this work at many conferences. I would like to specifically acknowledge Rini Sherony and Takashi Hasegawa-san for their insights on this research and having confidence in me to continue their projects. Thank you to Mitch Garber for recognizing an opportunity to investigate driver reaction times and David Fortenbaugh for his contribution and input.

My personal thanks to my lab mates: Whitney Tatem, David Holmes, Grace Wusk, Max Bareiss, Sammy Haus, Morgan Dean, and Colin Smith. You all are my friends, not my co-workers, and I could not have completed this work without your advice, input, and friendship over the years. I would like to acknowledge the many interns who I worked closely with to develop the NCHRP 17-43 database, the cross-centerline database, and the NCHRP 17-88 database. I would specifically like to mention Shannon King, for her help developing the rollover injury risk curve as well as Andrew Galloway and Joe Gopiao for their work analyzing the residual road departure and head-on crashes. You all inspired me to consider academia and continue to work with students like you.

I would like to thank my parents for installing a good work ethic in me and demonstrating how to find success. For years, you have taught me how to work and reminded me to take breaks, especially when stuck on a problem. Thank you for encouraging me to get my dachshund Lucy, who makes sure I do not work too much or at least pause to give her a belly rub. Most of all thank you for showing me how to find joy in what God has provided and trust him through all that life throws at you. Thank you to my grandparents for their prayer and advice throughout my life. Finally, I would also to acknowledge the overabundance of blessings from God in my life. I cannot express how overwhelming it is to have such a close loving family, work which I enjoy, a mind I can use to protect lives, and friends who support me. I do not know exactly what my future holds but I know that God has and will continue to guide me.

TABLE OF CONTENTS

TABLE OF FIGURES

TABLE OF TABLES

1 INTRODUCTION

Every year, approximately 34,000 individuals are fatally injured in crashes on roads in the US [1]. These fatalities occur across many types of crash scenarios, each of which has its own set of causation factors. One way to prioritize research on a preventive technology for a specific crash scenario is to look at number of occupant fatalities relative to the total number of occupants involved in this crash scenario. According to Kusano, four crash modes are overrepresented among fatalities: single vehicle road departure crashes, control loss crashes, cross-centerline head-on crashes, and pedestrian/cyclist crashes [2]. Interestingly, two of these crash scenarios require the subject vehicle to depart from the initial lane of travel before the crash occurs. Another method of prioritizing research is to determine factors common among the fatal crashes. In 2017, 30.4% of passenger vehicle crash fatalities involved a vehicle rollover [1]. Half of all fatal single vehicle road departure crashes resulted in a rollover yet only 12% of fatal multi-vehicle crashes involved a rollover [1].

The focus of this dissertation is to evaluate vehicle-based countermeasures to prevent or mitigate single vehicle road departure crashes, cross-centerline head-on crashes, and single vehicle rollover crashes.

1.1 Crash Scenarios

1.1.1 Road Departure Crashes

Drift-out-of-lane (DrOOL) road departure crashes typically consist of an unaware driver unintentionally leaving their lane of travel, departing from the road, and colliding with a fixed roadside object such as a tree or guardrail. Road departure crashes are one of the most dangerous crash modes. From 2007 to 2011, drift-out-of-lane road departure crashes accounted for one-third of all crash fatalities despite accounting for less than 10% of all crashes [2].

1.1.2 Cross-Centerline Head-On Crashes

DrOOL cross-centerline head-on crashes consist of a vehicle unintentionally crossing the centerline and colliding with a vehicle traveling the opposite direction. Head-on collisions are particularly dangerous due to the large deceleration experienced upon impact since the vehicles were moving in opposite directions. Head-on collisions are overrepresented in fatal outcomes. Head-on crashes comprise only 4% of non-intersection crashes but account for 49% of fatalities in non-intersection crashes [3].

1.1.3 Rollover Crashes

A vehicle rollover can be either end-over-end or lateral. End-over-end rollovers are extremely rare and consist of a very large pitch such that the vehicle does not remain on its wheels. More commonly, rollovers occur in the lateral direction due to significant vehicle roll. Rollovers can occur after an impact

with another vehicle, but they are more common in single vehicle collisions [1]. In 2017, 30.4% of passenger vehicle crash fatalities involved a vehicle rollover [1]. Ejection is a key contributor to occupant injury with over 40% of the fatalities in rollovers due to occupant ejection. However, not every fatally injured occupant involved in a rollover was ejected from the vehicle. Another confounding factor is that the vehicle may collide with fixed objects or other vehicles in addition to the rollover.

1.2 Countermeasures

1.2.1 Lane Departure Warning/Prevention Systems

The high severity of DrOOL road departure and head-on crashes has been a key motivation for the development of active safety systems, such as lane departure warning (LDW) systems. LDW systems are designed to alert the driver, through audible, visual or haptic signals, that the vehicle has inadvertently left the lane of travel [4]. Ideally, the driver reacts to the warning and returns to the lane, preventing an impact (Figure 1). However, the effectiveness of a warning system is limited by the reaction time of the driver and the ability of the driver to return to the road without impacting any roadside objects [4]. The reaction time of a driver to a haptic or audible LDW system can vary from as low as 0.38s to 1.36s [5]. Additionally, LDW effectiveness is dependent on the evasive action taken by the driver. Lane departure prevention (LDP) systems remove the need for the driver to react to prevent DrOOL crashes by automatically steering the vehicle back toward the original lane. Some LDP systems can provide steering input before departing the lane and may also be referred to as lane keeping assist (LKA) systems. Unlike lane centering systems, LKA systems may oscillate within lane and may stop any maneuver after departing the lane.

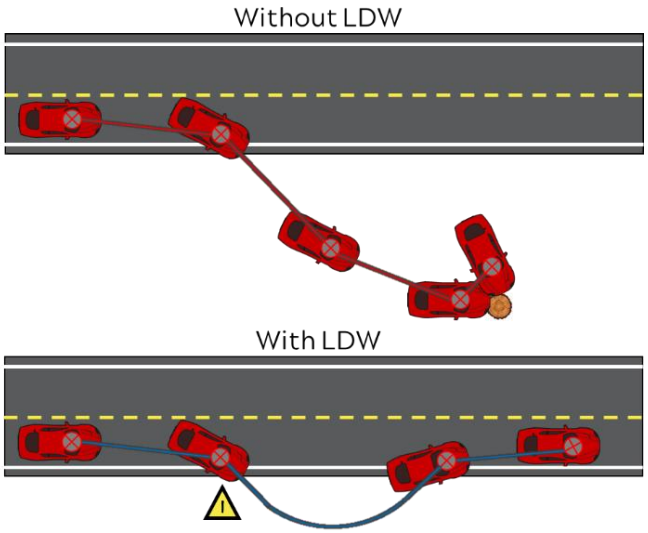

Figure 1. Example of a LDW system preventing a road departure crash by inducing a driver maneuver.

From 2011 to 2015, almost 50% of all moderate to fatal injuries occurred in crashes that could benefit from LDW/LDP systems [6]. Over 65% of these LDW/LDP applicable scenarios were DrOOL road

departure crashes. Riexinger found that roughly 80% of drivers in drift-out-of-lane road departure crashes responded with a steering maneuver [6]. Kusano estimated that between 29-32% of drift-out-of-lane road departure crashes could be prevented with an LDW system [7]. Similarly, Scanlon estimated that 26% of drift-out-of-lane road departure crashes could be prevented with an LDW system and 32% with an LDP system [8]. Several studies have estimated the effectiveness of LDW in road departures, however due to the higher relative speed that the subject vehicles approach each other during a head-on collision, the effectiveness of LDW and LDP systems may be different in this mode than in road departures (Table 1). Cicchino estimated the number of lane departure crashes, including head-on crashes, that were prevented by LDW/LDP systems using insurance claim information. The estimated benefit is lower than other simulated studies since drivers can disable the LDW system and it combines the effect of many system types.

Table 1. Summary of LDW/LDP effectiveness estimates in the literature.

Source	System Type	Effectiveness
Cicchino 2018 [9]	Single vehicle road departure, head-on, sideswipe crashes in US	11% (LDW/LDP)
Sternlund 2017 [10]	Single vehicle road departure, head-on crashes on high-speed roads in Sweden	53% (LDW/LDP)
Riexinger 2018 [4]	Single Vehicle Road Departure crashes in US	16.7%-21.5% (LDW) 24.3% (LDP)
Scanlon 2015 [8]	Single Vehicle Road Departure crashes in US	26.1% (LDW) 37.3% (LDP)
Kusano 2014 [7]	Single Vehicle Road Departure crashes in US	29%-32% (LDW)

1.2.2 Infrastructure

The geometry and construction of the road and roadside environment is carefully considered to reduce the number and severity of these lane departure crashes. The Roadside Design Guide (RDG) specifies design countermeasures such as rumble strips, a clear zone width, traffic barriers [11]. Rumble strips are an infrastructure countermeasure similar to a LDW system. When a vehicle crosses the lane and contacts the rumble strip, an audible and haptic warning is delivered to the driver. Often this allows the driver to safely return to the lane [12, 13]. The RDG also specifies a clear zone along the road where potential roadside hazards should either be removed or protected by a traffic barrier. For highways, the recommended clear zone width is 10 m [11]. For hazards that cannot be removed, the RDG can recommend the installation of a traffic barrier such as a guardrail, concrete barrier, or cable barrier [11]. One method for supporting the installation of a longitudinal barrier uses the RSAP program to estimate if there is an overall reduction in the crash cost that offsets the installation of the barrier [14]. The installed barriers are

tested to conform with the crash standards indicated in the Manual for the Assessment of Safety Hardware [15].

1.2.3 Electronic Stability Control

Electronic stability control (ESC) is an active safety feature that detects wheel slip and applies selective braking to each tire to maintain vehicle heading. Previous studies have shown that ESC systems are effective in preventing control loss crashes. ESC has been estimated to prevent up to 50% of all crashes with serious or fatal injuries and could prevent 20% of all non-rear end crashes (Table 2).

Table 2. Summary of ESC effectiveness values and methods in the literature.

Source	Method	Population	ESC Effectiveness
Farmer, 2004 [16]	Induced exposure method compared identical makes and models	All crashes	1%
		Single Vehicle	50%
		Single Vehicle Rollover	74%
Erke, 2008 [17]	Combined multiple values computed across many studies	Single Vehicle	49%
		Loss of control	41%
		Rollover, injuries	69%
		All, non-rear-end	22%
Dang, 2004 [18]	Quasi-induced exposure compared to multi-vehicle crashes	Single Vehicle Passenger Cars	35%
		Single Vehicle SUVs	67%
	Quasi-induced exposure compared to multi-vehicle crash fatalities	Single Vehicle Passenger Car fatalities	30%
		Single Vehicle SUVs fatalities	63%
Papelis, 2010 [19]	Simulator study with SUV and passenger vehicles to test loss of control	180 cases	24.6%
Lie, 2006 [20]	Induced exposure method compared identical makes and models	All, non-rear-end	16.7%
		Serious/fatal, non-rear-end	21.6%
		Single vehicle, wet roads	56.2%
		Single vehicle, icy roads	49.2%
		Single vehicle, dry roads	24.8%

1.2.4 Rollover Passive Safety

In the event of a rollover, passive safety features, such as seat belts, side curtain airbags, and stronger roofs, may reduce the risk of serious injury to the passengers. Seat belts can prevent occupant ejection and injury by restraining the occupant to the seat rather than exiting or moving around inside the

vehicle during a rollover crash. Side curtain airbags deploy during a rollover to block common occupant ejection portals such as the side windows. Stronger roofs prevent injury by reducing the amount of roof deformation during a crash. Stronger roofs can also prevent occupant ejection by providing additional support to the widows and windshield from breaking open.

Five main studies have attempted to relate occupant injury to rollover characteristics. The first, by Digges, sought to characterize rollover injuries based on the vehicle class, occupant belt use, ejection, and number of quarter turns using cases from NASS/CDS 1995-2001. The analysis was limited to front seat occupants over the age of 12. Digges found that occupants not wearing their seatbelt or occupants that were ejected had a higher risk of injury [21]. However, this study did not report an injury risk model. The second study, by Conroy, did construct an injury risk model but did not include the coefficients. Conroy used CIREN cases from 1996-2004 and NASS/CDS cases from 1998-2002 [22]. The cases were restricted to rollovers in which the vehicle had no other significant impacts during the crash. Additionally, only non-ejected, front seat occupants were included in the analysis. The logistic injury model used multiple predictor variables including belt use, intrusion, far-side position, age, height, rollover initiation type, number of quarter-turns, vehicle body type. Conroy found that roof intrusion was a significant indicator of injury. Funk et al. found that belt use was the best predictor of ejection likelihood, with side curtain airbags the next best predictor [23]. Using the Abbreviated Injury Score (AIS), a medically relevant injury scale, Funk, Cormier, and Manoogian developed a fatality model and model for serious injuries with maximum AIS greater than 3 (MAIS 3+) [24, 25]. The model they developed for predicting AIS 3+ injuries included the number of quarter turns, ejection, BMI, and age as predictors. However, the model did not use seat belts as a predicting variable. Flannagan constructed a logistic model to predict MAIS3+F injury during a rollover based on the occupant age, belt use, roof intrusion, model year, rural road, occupant ejection, and occupant sex [26].

1.3 Driver PRT

Driver perception-response time (PRT) is a key component in many human factors analyses done during the investigation and reconstruction of automotive crashes. Krauss identified four basic stages of PRT: detection, identification, decision, and response [27]. Once a potential hazard enters the field of view, the driver must first detect the hazard and then acquire enough information about the scenario to determine whether an evasive action is required. Next, if necessary, the driver must decide and execute an evasive action such as braking or steering.

Understanding the PRT of a truly unexpected situation, like a cross-centerline encroachment, is difficult to accurately assess. Research on the topic of PRT has tended to involve studies using simulators or closed tracks (which by their nature can detach the driver from feeling a sense of connection to the road

and risks that come with real driving) or retrospective analyses of crashes in which parameters such as PRT can only be estimated rather than directly measured. Olson and Sivak assessed PRT to unexpected roadway hazards when cresting a hill [28]. In a "surprise" condition, the 50th percentile perception time, measured as the time difference from the "first possible sighting of the obstacle" to the release of the accelerator pedal, was found to be 0.6 to 0.7 seconds. The 50th percentile response time, measured from accelerator pedal release to brake pedal application, was approximately 0.4 seconds, summing for a total PRT of approximately 1.1 seconds. The researchers also found that the 95th percentile PRT was approximately 1.6 seconds. Lerner released crash barrels in front of unsuspecting drivers [29]. 87% of drivers reacted, with 43% steering and braking, 36% steering only, and 8% braking only. Mean brake PRT was 1.5 seconds with an 85th percentile PRT of 1.9 seconds. In a study by Broen and Chiang , the average brake response time of 100 drivers in a simulator reacting to an undefined unexpected obstacle was found to be 1.33 seconds [30]. D'Addario and Donmez investigated brake and steer reaction times to three different hazards (a left-turn across path, a pedestrian entering the roadway, and a right-incursion vehicle) while in a driving simulator [31]. The median brake reaction times were 0.88 seconds (pedestrian), 1.32 seconds (right-incursion vehicle), and 2.02 seconds (left-turn across path). The researchers stated that only the left-turn across path hazard had sufficient data to assess steer reaction times, for which a median time of 1.87 seconds was reported.

To better understand the effect of distractions on the driver reaction time in car following scenarios, Gao and Davis used a naturalistic driving study [32]. Naturalistic studies may provide more accurate measurements of driver reaction time since event is happening during a normal driving scenario rather than in a controlled environment such as a test track or simulator [33]. For 40 attentive drivers responding to a lead vehicle, the mean measured reaction time was 1.57 seconds for crash and near-crash events.

Table 3. Summary of some previously measured PRT response times.

Source	Experimental Design	Situation Type	Driver PRT (s)
Olson and Sivak (1986) [28]	Controlled Test Site	Object in lane revealed during hill crest	1.1
Lerner (1993) [29]	Controlled Test Site	Barrels released	1.5
Broen and Chiang (1996) [30]	Simulator	Obstacle	1.33
D'Addario and Donmez (2019) [31]	Simulator	Pedestrian	0.88
Gao and Davis (2017) [32]	SHRP 2	Car Following Events	1.57

Most studies that measure the driver's PRT focus on either rear-impact crashes or single-vehicle collisions. In particular, the current driver models of detection in car following scenarios are based on

changes in the visual angle of the lead vehicle [34]. However, in cross-centerline crashes, the detection of an encroaching, oncoming vehicle may not require an increase in visual angle. Additionally, the commonly studied PRT scenarios may have different evasive actions than cross-centerline scenarios. Based on the 100-Car Naturalistic Driving Study, drivers applied the brakes alone in 70% of car following near-crash scenarios, but only 19% in oncoming vehicle near-crashes [35]. Based on event data recorders from cross-centerline crashes, Riexinger (2019) showed that 80% of drivers performed both a braking and steering evasive action before the impact with the encroaching vehicle [36].

The most comprehensive and pertinent analysis to the current study is the 2016 work of Markkula et al., who used the Second Strategic Highway Research Program (SHRP 2) and Analysis of Naturalistic External Datasets (ANNEXT) projects to investigate braking in emergency situations during real/on-road driving [37]. Looking at rear-impact crashes and near-crashes, the researchers found that brake onset almost always occurred within a half-second of some visually discernible physical reaction by the driver to the collision threat such as a change in posture, facial expression, or leg position. That research group also expressed that brake reaction times may not be a meaningful measure of driver behavior in surprise emergencies, such as path intrusions, and that reaction times determined in one study may not generalize to other scenarios.

2 DATA SOURCES

2.1 Summary

To estimate the future benefit of LDP and ESC systems for lane departure crashes, this dissertation utilizes multiple datasets that are detailed in the following sections (Table 4).

Table 4. Summary of data sources.

Dataset	Represented Population	Data Type	Chapter Utilized
FARS	All fatal, police-reported crashes	Basic crash, vehicle, and occupant information	3, 7, 12
NASS/GES	Sample of all police-reported crashes	Basic crash, vehicle, and occupant information	3, 7, 12
NASS/CDS	Sample of all police-reported crashes with a vehicle towed due to damage	In-depth investigation: scene diagram, photographs, injury records	3-10, 12-15
CISS	Sample of all police-reported crashes with a towed vehicle	In-depth investigation: scene diagram, photographs, injury records	6, 10, 13, 15
Virginia Tech EDR Database	EDR data extracted from NASS/CDS and CISS cases	Vehicle measurements before and during the crash	4-6, 8-10, 13-15
NCHRP 17-43	Drool road departure crashes from NASS/CDS	Detailed road, roadside, and encroachment information	3-6
Cross-Centerline Database	Head-on crashes from NASS/CDS	Detailed road and encroachment information	7-10
SHRP 2	Naturalistic driving	Vehicle dynamics and multiple video recordings during trips	11
IIHS Vehicle Dataset	Passenger vehicles	IIHS safety ratings and available safety technology by vehicle model	12-15
NHTSA Component Test Database	Passenger vehicles	Roof SWR by vehicle model	12, 13, 15
National Household Travel Survey	US households	Basic driving/vehicle information: vehicle age, miles travelled	6, 10, 15

2.2 FARS

The Fatality Analysis Reporting System (FARS) is a census of every fatal vehicle crash in the US since 1975 [38]. Because every crash in FARS includes at least one fatality, FARS includes only the most severe vehicle crashes. Based on the police reports, FARS contains useful information about the road, environment, vehicles, and occupants involved in the crash.

2.3 NASS/GES and CRSS

The National Automotive Sampling System General Estimation System (NASS/GES) is a database containing a probability sample of police reported crashes from 1988 to 2015 [39]. Every crash in the database is assigned a weight such that the entire database is representative of all police reported crashes in the US. Based on the police reports, NASS/GES contains useful information about the road, environment, vehicles, and occupants involved in the crash. The Crash Report Sampling System (CRSS) is the successor to NASS/GES and contains crashes after the case year 2015. Both NASS/GES and CRSS are useful datasets for understanding the overall crash populations in the US.

2.4 NASS/CDS and CISS

The National Automotive Sampling System (NASS) Crashworthiness Data System (CDS) data set is a representative sample of all crashes in which at least one passenger vehicle was towed away [40]. Every case in NASS/CDS is assigned a weight to represent the total number of similar crashes that occurred in the US during that case year. NASS/CDS provides detailed information on each case including vehicle deformation, crash causation factors, a scaled scene diagram of the crash, and occupant injury information records. Each case in the data set includes a scaled scene diagram with the vehicle trajectory and impact locations. If possible, the vehicle delta-v is calculated from an energy reconstruction based on the crush profile of the vehicle using Win-Smash [41-43]. NASS/CDS contains crash data from 1979 to 2015. The Crash Investigation Sampling System (CISS) is the successor to NASS/CDS and currently contains crash since 2017 [44].

2.5 EDR Database

The Virginia Tech Event Data Recorder (EDR) Database is a collection of the information retrieved from EDRs in vehicles involved in real-world crashes that were investigated in NASS/CDS from 2000 to 2015. The EDR database is continuing to expand to also include cases from CISS 2017. Most recently manufactured vehicles have an EDR installed, which records basic vehicle information in the event of a crash. The EDR database is a unique source of direct measurements of vehicle speed before and during a crash. The EDR records data, such as delta-v, during the crash to capture the crash pulse. Additionally, five seconds of pre-crash information, such as vehicle speed, throttle position, brake activation and engine RPM,

are also recorded. Some advanced EDRs record information such as the steering-wheel position, the activation of electronic stability control (ESC) and the activation of the antilock brakes system (ABS). EDRs have been shown to accurately measure the crash delta-v within 14% [42] and are frequently used to understand driver precrash behavior [45, 46].

2.6 NCHRP 17-43

The National Cooperative Highway Research Program (NCHRP) 17-43 database is under development at Virginia Tech as a part of a grant from the National Academies of Science [47, 48]. The NCHRP 17-43 database contains supplementary data for a total of 1,581 single vehicle road departure crashes from NASS/CDS case years 2011 to 2015. The supplementary data includes numeric trajectories, speed reconstructions, and detailed roadside information extracted from the NASS/CDS cases. It has been used to understand the nature of road departure crashes into barriers [49], understand driver behavior [6, 36], and to predict the benefits of LDW [4, 50].

In the NCHRP 17-43 database, there were 97 cases with reconstructed impact speeds and pre-crash speeds captured by an associated event data recorder (EDR). The reconstructed impact speed was compared to the last recorded pre-crash speed. The reconstructed impact speed was on average 14% lower than the EDR impact speed (Figure 2). Most of this error can be attributed to the known 13% underestimation of the delta-v using WinSMASH [42].

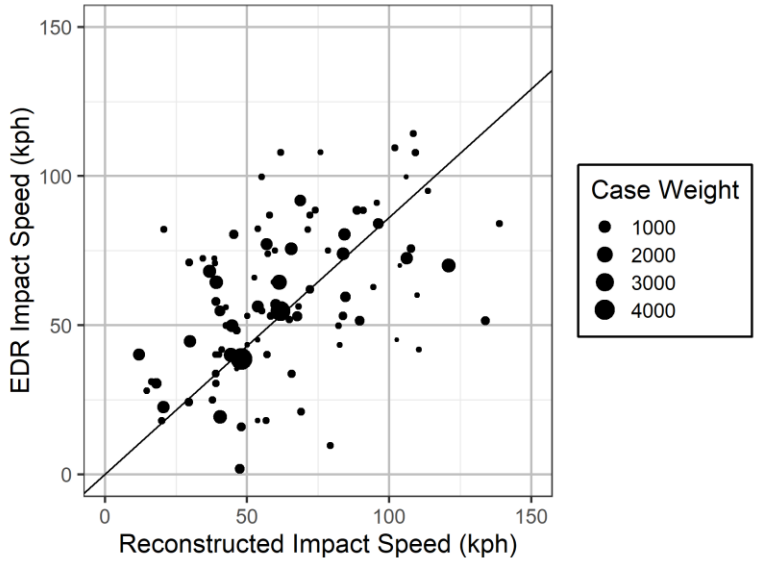

Figure 2. Comparison of reconstructed impact speeds with EDR recorded speeds.

2.7 Cross-Centerline Database

The Virginia Tech Cross-Centerline database contains 232 NASS/CDS cross-centerline crashes where at least one passenger vehicle had EDR information available. I developed this dataset for to

understand the nature of head-on crashes and to evaluate possible countermeasures. Similar to the NCHRP 17-43 database, this contains the trajectory positions and headings of every vehicle involved.

The crashes in the Cross-Centerline database were selected from NASS/CDS 2011-2015. Every case was categorized into a crash scenario based on the ACCTYPE, PREMOVE, and PREEVENT variables. This crash scenario excludes loss of control crashes but can include rollovers. To be included in the database, the crash scenario must be a lane departure that resulted in a crash with a vehicle traveling in the opposite direction. Additionally, at least one vehicle involved in the crash must have EDR information available (Table 5).

Table 5. Cross-Centerline database inclusion criteria.

	Number of Cases	Weighted Number of Cases
NASS/CDS 2011-2015	16,536	7,468,762
Lane Departure: Opposite Direction Crash	694	184,522
EDR Information for at Least One Vehicle	232	68,296

2.8 SHRP 2

The second strategic highway research program (SHRP 2) is the world's largest naturalistic driving dataset, containing nearly two petabytes of data [51]. The primary vehicle of over 3,400 drivers was equipped with a data acquisition system that recorded information from three-axis accelerometers, three-axis rate sensors, a global positioning system, forward radar, vehicle network data, lane position, and four video feeds (front, rear, driver's face, and driver's hands). The SHRP 2 event data also includes whether the driver was distracted or engaged in a secondary task based on a review of the driver video. Every trip was recorded during the three-year period and captured 8,769 crashes or near-crash events. The current study utilized the forward-facing video and the 10 Hz time-series data of vehicle acceleration, brake pedal activation, yaw rate, and steering wheel angle from crash and near-crash scenarios [52].

2.9 NHTSA Component Test Database

The vehicle SWR was also retrieved from the NHTSA Component Test Database [53]. This database provided a collection of the roof crush tests completed to ensure vehicle compliance with FMVSS 216. Test results are available up to model year 2008. The FMVSS 216 testing procedure prescribes moving a rigid, unyielding test block at a rate of 13 mm/s to a maximum displacement of 127 mm [54]. The roof SWR is computed as the force divided by the unloaded weight of the vehicle. The FMVSS 216 test defines the vehicle roof SWR as the maximum roof SWR within the first 127 mm of roof deformation. FMVSS 216 requires both sides of the vehicle be tested.

2.10 IIHS Vehicle Dataset

The Insurance Institute for Highway Safety (IIHS) maintains vehicle safety information and the availability of safety systems in vehicles [55]. These publicly available records of make-model specific

safety equipment were used to determine the roof strength to weight ratio (SWR) and ESC availability. The IIHS ESC availability dataset has four variables for each row: the model year, make, model information, and ESC availability. The model information variable is a string that contains the model of the vehicle and may contain the trim, body type, number of doors, etc. The model information string was parsed into seven variables: model, cab type, drive type, series, hybrid, number of doors, and body style. Possible ESC availably options included, “Standard”, “Optional”, and “Not Available”. If the ESC availability database did not include a vehicle and the model year was 2012 or newer, the vehicle was assumed to be compliant with FMVSS 126. Otherwise, if the database did not include a vehicle make/model, it was assumed to not have ESC. IIHS measures the roof SWR following the FMVSS 216 test procedures except the test block displacement is limited to 5 mm/s [56]. The SWR data from IIHS was organized by vehicle make, model, and model year.

2.11 National Household Travel Survey

The National Household Travel Survey (NHTS) is a publicly available dataset containing personal and household travel information [57]. The NHTS is conducted by the Federal Highway Administration (FHWA) every five to eight years to collect basic information about travel habits. The survey data from 2001, 2009, and 2017 was used to estimate the age distribution of vehicles in the US fleet based on the vehicle miles travelled (VMT). Each trip in the NHTS was weighted by the case weight (WTTRDFIN) times the miles travelled during the trip (VMT_MILE). The age distribution by VMT was calculated for each individual case year. The average vehicle age distribution was determined by averaging the proportion of vehicles of a given model year. The average was used to smooth out the effects of the 2008 recession, which heavily influenced the sales of vehicles and the number of miles travelled during that time (Figure 3).

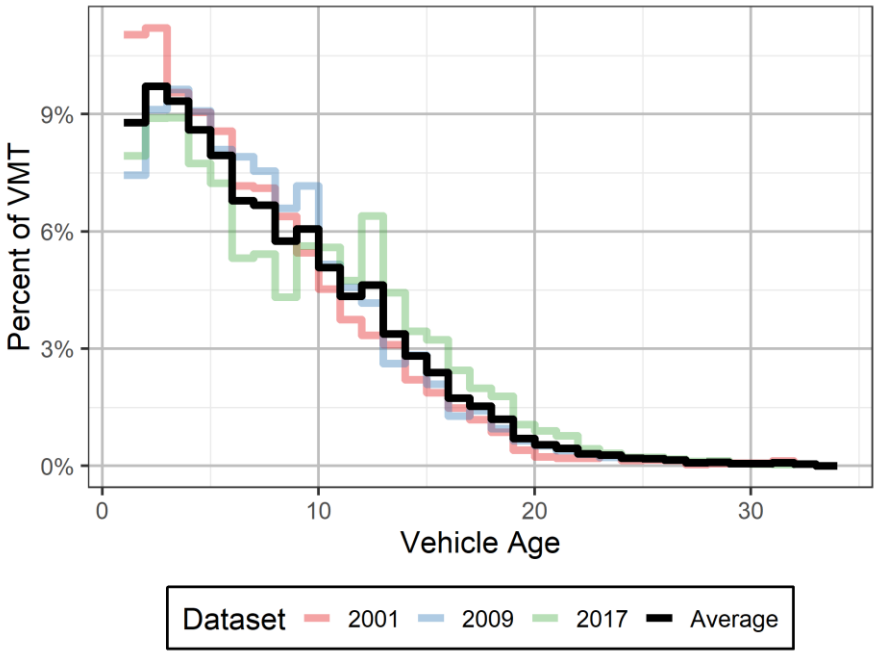

Figure 3. Age distribution of vehicles in the US fleet by survey year.

The average age distribution of vehicles based on the 2001, 2009 and 2017 NHTS data was compared to the NASS/CDS age distribution for the corresponding case year range of 2001 to 2015. Overall, the vehicle age distribution of the US fleet, weighted by VMT, closely follows the age distribution of vehicles involved in a crash with at least one towed vehicle (Figure 4).

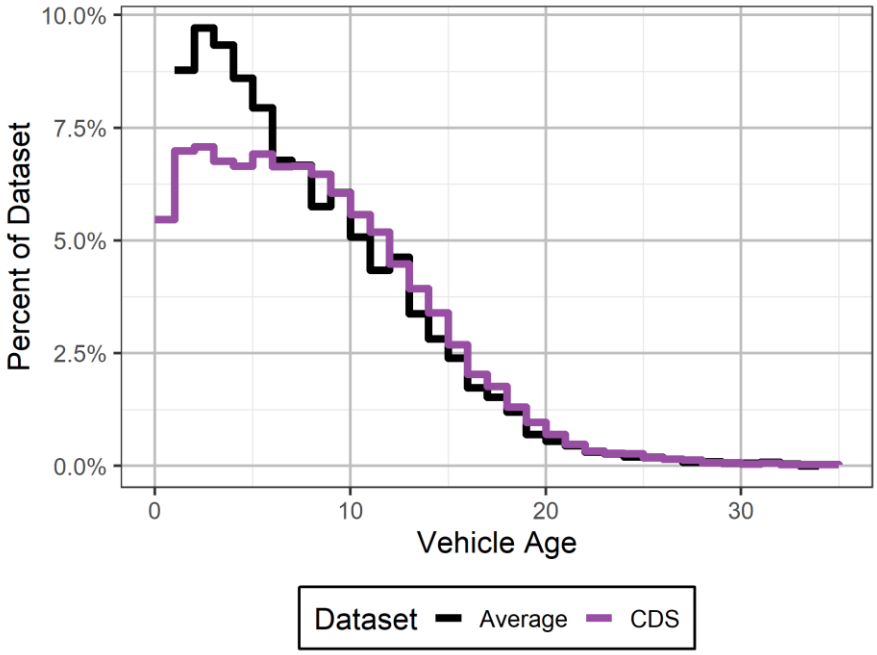

Figure 4. The age distribution of vehicles in NASS/CDS 2001-2015 compared to the average age from the 2001, 2009 and 2017 NHTS studies.

3 CHARACTERIZATION OF ROAD DEPARTURE CRASHES

3.1 Purpose

The objective of chapter 3 was to determine the frequency of and to characterize DrOOL road departure crashes in the U.S. as a basis for evaluating active safety countermeasures.

3.2 Approach

3.2.1 Data Selection

All recorded single vehicle road departure crashes that occurred between 2011 and 2015 were extracted from NASS/GES, NASS/CDS, and FARS. These three databases were selected to cover a large range of crash severities from police reported crashes (GES), and moderate to fatal injurious crashes (CDS), to fatal crashes (FARS). Moderate injury is defined in NASS/CDS based on the Abbreviated Injury Scale (AIS), a clinically relevant scale of injury severity [25]. Additionally, the NCHRP 17-43 database was used to gain insight into the roadside features during DrOOL road departure crashes. The weighted number of cases from NASS/CDS and NASS/GES were used for the analysis.

The two most common types of road departure crashes were DrOOL and control loss road departure crashes (Figure 5). LDW and LDP systems are the primary countermeasure for preventing DrOOL road departure crashes while ESC is the primary counter measure for control loss road departure crashes. Only DrOOL road departure crashes were considered in this characterization since the following chapters will focus on LDW and LDP countermeasures (Table 6).

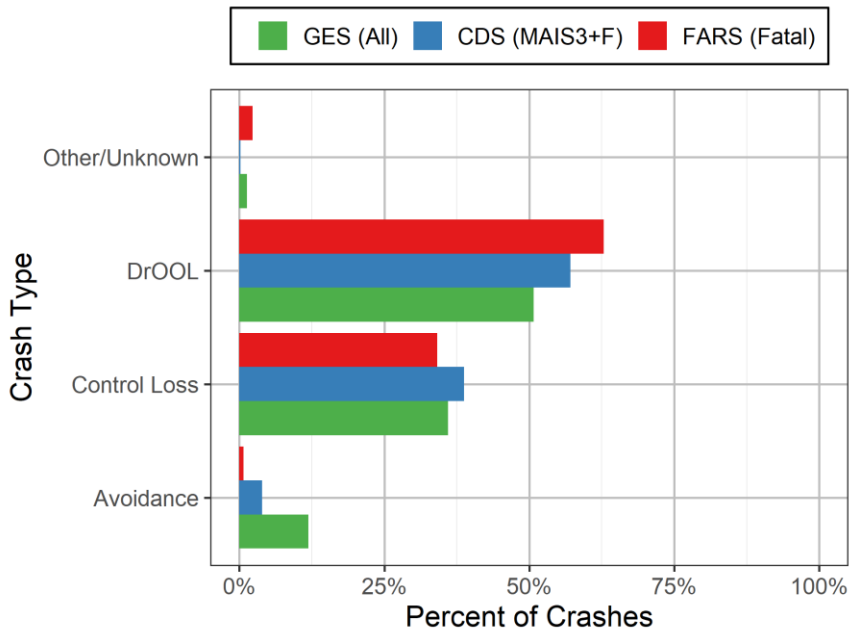

Figure 5. Distribution of types of single vehicle road departure crashes.

Table 6. Number of analyzed cases across each of the datasets.

Dataset	Population	Injury Severity	Weighted Crashes (unweighted)	Weighted Occupants (unweighted)
NASS/GES	All Police-Reported DrOOL Crashes	All	2,160,271 (24,497)	2,817,202 (32,999)
NASS/CDS	Tow-Away DrOOL Crashes	MAIS 3+F	26,890 (335)	28,386 (374)
FARS	DrOOL Crashes with a Fatally Injured Occupant	Fatal	29,663	31,947
NCHRP 17-43	Tow-Away DrOOL Crashes	MAIS 3+F	17,366 (207)	18,352 (231)

3.2.2 Analyzed Parameters

For every DrOOL road departure crash in each database, factors were analyzed from four main characteristics: road/environment, vehicle, driver, and occupants (Table 1). The road/environment characteristic was analyzed for each case since every vehicle and occupant in the crash interacts with a road/environment.

Table 7. Data elements for in-depth characterization.

	Characteristic	Factors	Data Source
Crash Causation	Road/Environment	Speed Limit	All
		Road Alignment	All
		Number of Lanes	All
		Weather Condition	All
		Surface Condition	All
		Roadway Lighting	All
		Shoulder Width	NCHRP 17-43
		Clear Zone Width	NCHRP 17-43
		Lane Markings	NCHRP 17-43
		Object Struck	NCHRP 17-43
	Driver	Avoidance Maneuver	All
		Demographics (age, sex)	All
		Alcohol Involvement	All
		Drug Involvement	All
		Pre-crash Maneuvers	All
Injury Causation	Vehicle	Model Year	All
		Rollover	All
	Occupants	Demographics (age, sex)	All
		Belt Use	All
		Ejection	All
		Seat Location	All

3.3 Results

Fatal DrOOL road departure crashes were overrepresented on 55 mph roads and underrepresented at speeds below 35 mph (Figure 6). This may be due to the fact that slower moving vehicles likely have a lower crash delta-v, which reduces the chance of a fatal injury. Most DrOOL road departure crashes occur on straight sections of roads (Figure 7). Fatal road departure crashes are overrepresented on curved roads.

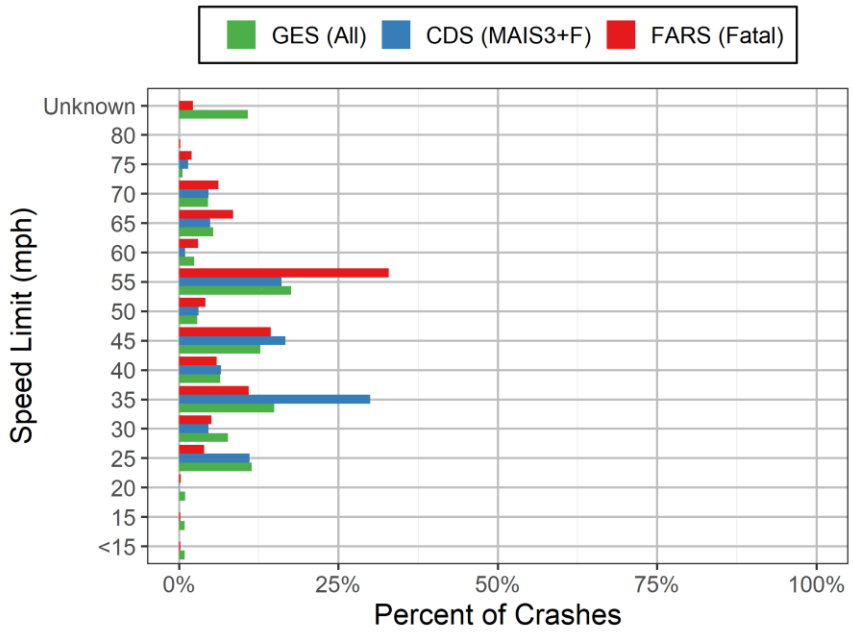

Figure 6. Distribution of speed limit among DrOOL road departure crashes.

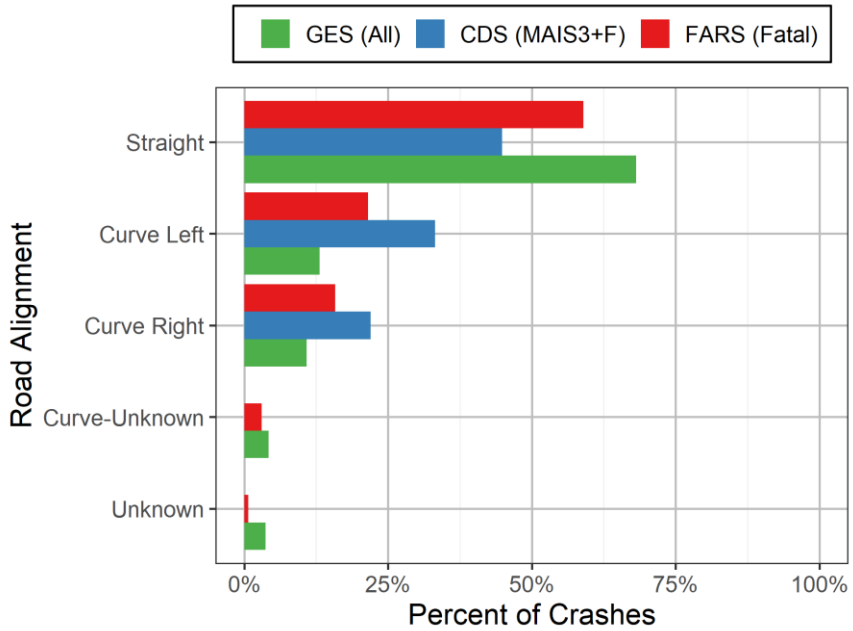

Figure 7. Distribution of road alignment for DrOOL road departure crashes.

Two-lane roads were the most common location of DrOOL road departure crashes but these roads are also one of the most common roadway types in the US (Figure 8). Following the NASS/CDS definition, this counts all lanes on undivided roads and the lanes in the same direction for divided roads. Fatal crashes were nearly as common at night in the dark as during the day (Figure 9). This may be due to an increased number of drowsy or intoxicated drivers at night.

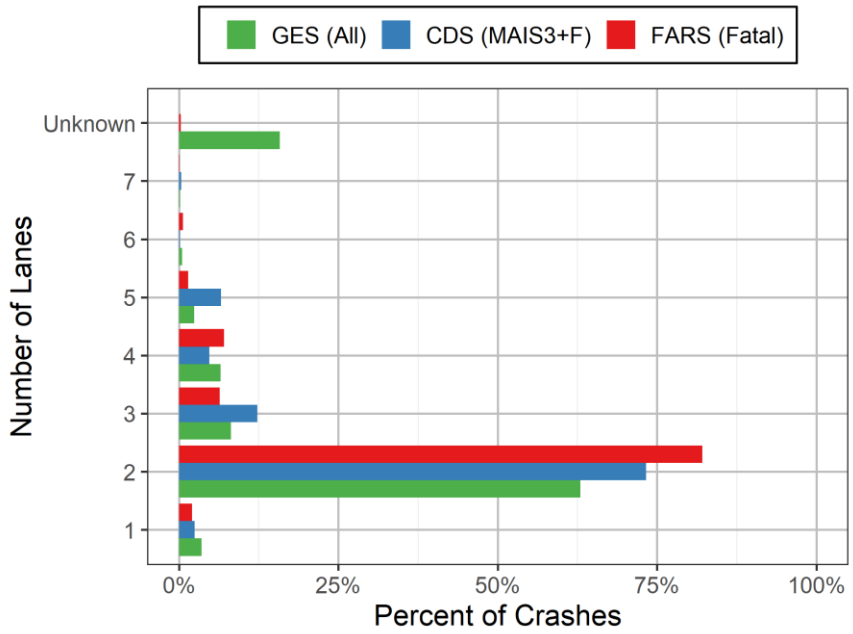

Figure 8. Distribution of lanes for DrOOL road departure crashes.

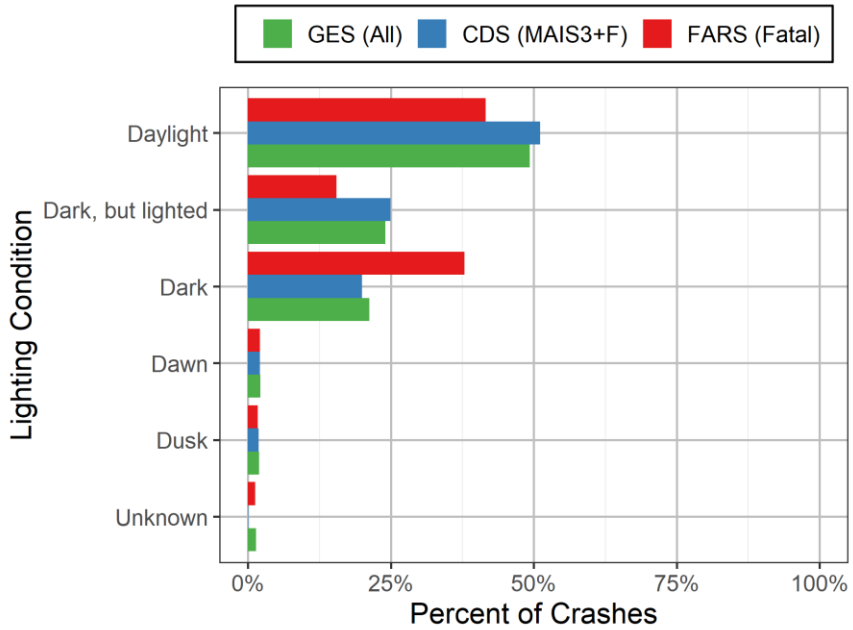

Figure 9. Distribution of lighting conditions for DrOOL road departure crashes.

Most crashes occurred during typical clear days with dry roads (Figure 10 and Figure 11). Fatal crashes may be underrepresented during the rain with wet roads because drivers travelling more cautiously.

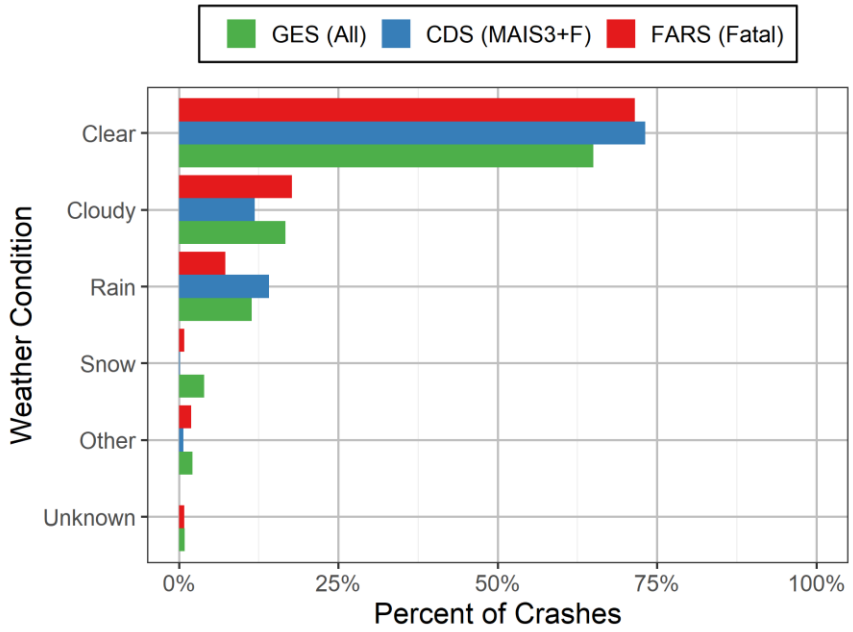

Figure 10. Distribution of weather conditions during DrOOL road departure crashes.

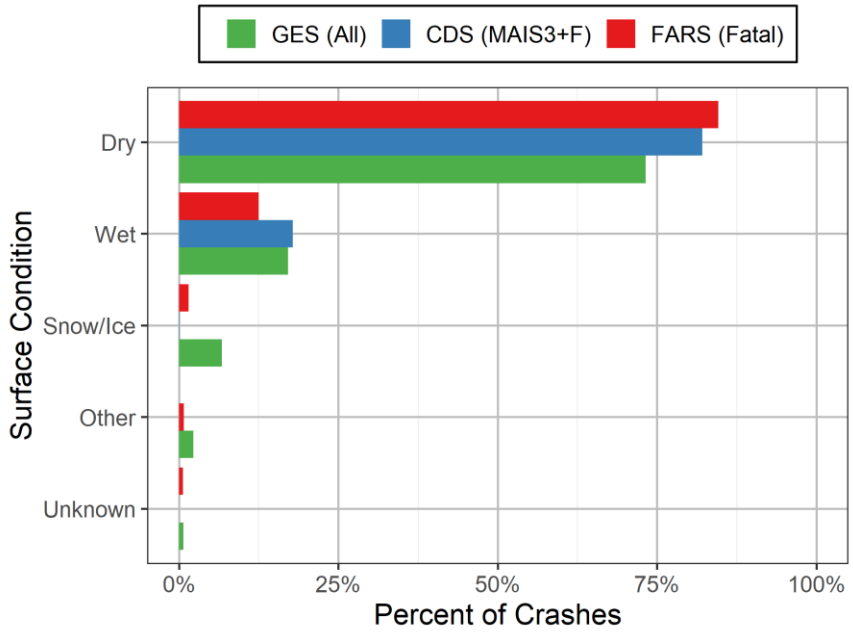

Figure 11. Distribution of surface conditions for DrOOL road departure crashes.

In almost all cases in FARS, NASS/CDS, and NASS/GES, there was either no evasive maneuver or the maneuver was unknown (Figure 12). Because of the lack of insight from these datasets, Chapter 4 will characterize the evasive actions using EDR information. Fatal DrOOL road departure crashes were far more likely to involve a rollover than less severe crashes (Figure 13).

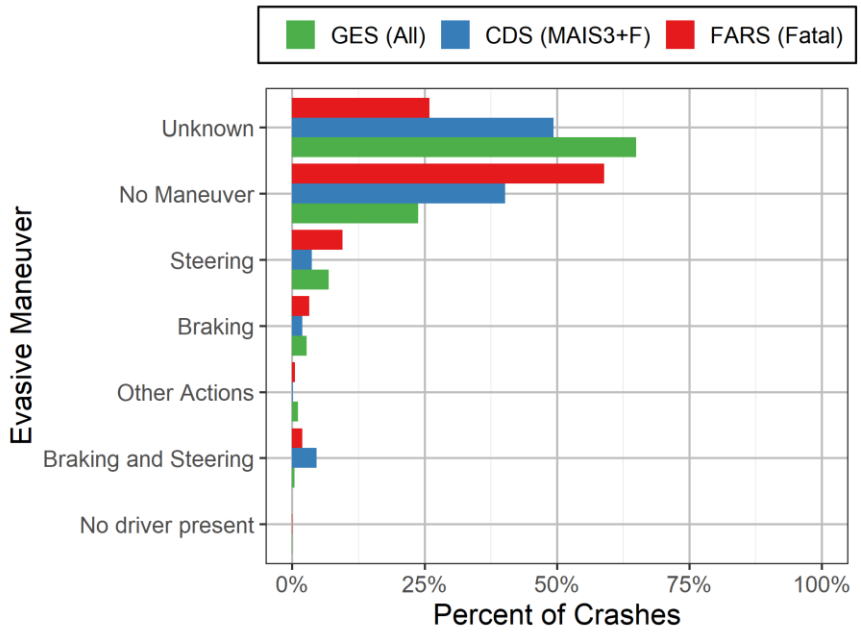

Figure 12. Distribution of driver evasive maneuvers for DrOOL road departure crashes.

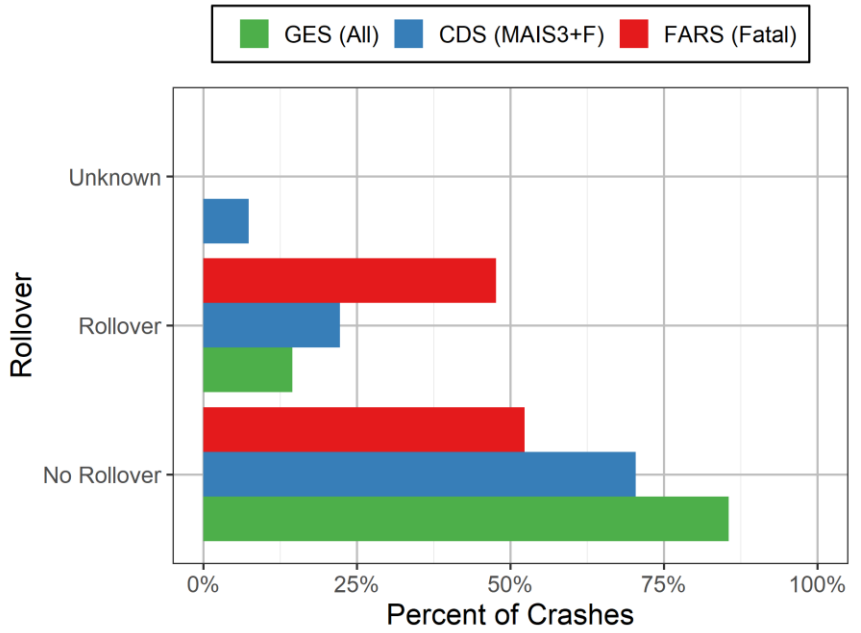

Figure 13. Occurrence of rollovers during DrOOL road departure crashes.

Most drivers in these crashes were relatively young; 40% of drivers were at most 25 years-old (Figure 14). More severe crashes tended to have older drivers, which may indicate that older drivers are more susceptible to serious injuries. Most of the drivers were male (Figure 15).

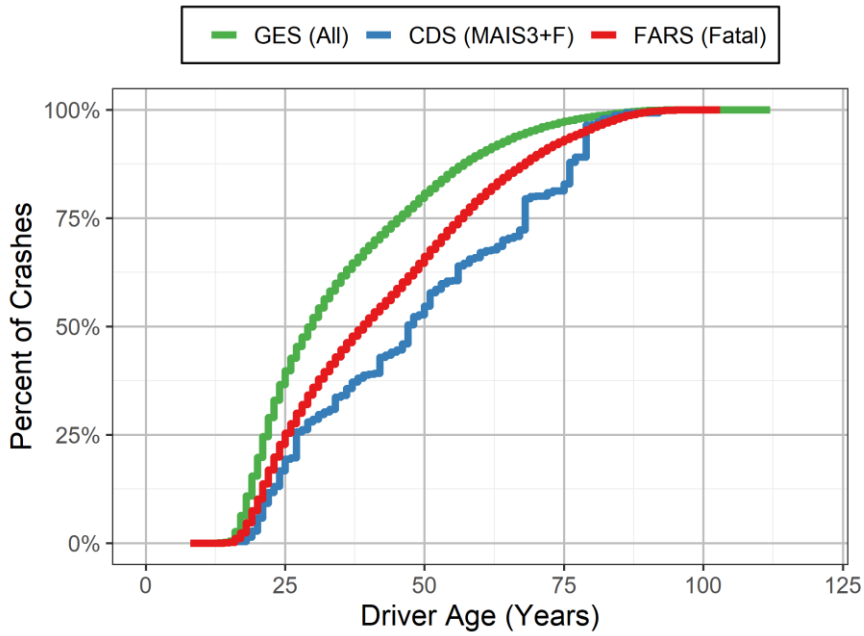

Figure 14. Distribution of driver age in DrOOL road departure crashes.

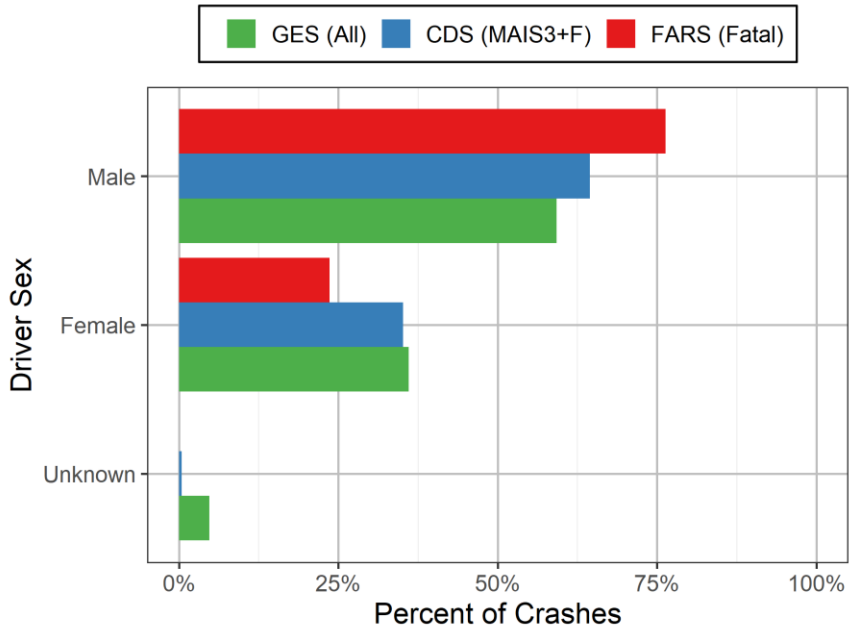

Figure 15. Distribution of driver sex DrOOL road departure crashes.

More severe crashes were overrepresented among cases that involved alcohol or other impairing drugs (Figure 16 and Figure 17). However, it should be noted that these counts are based on police assessment of alcohol or drug involvement and may not always rely on a test. This could bias the results toward none or unknown involvement.

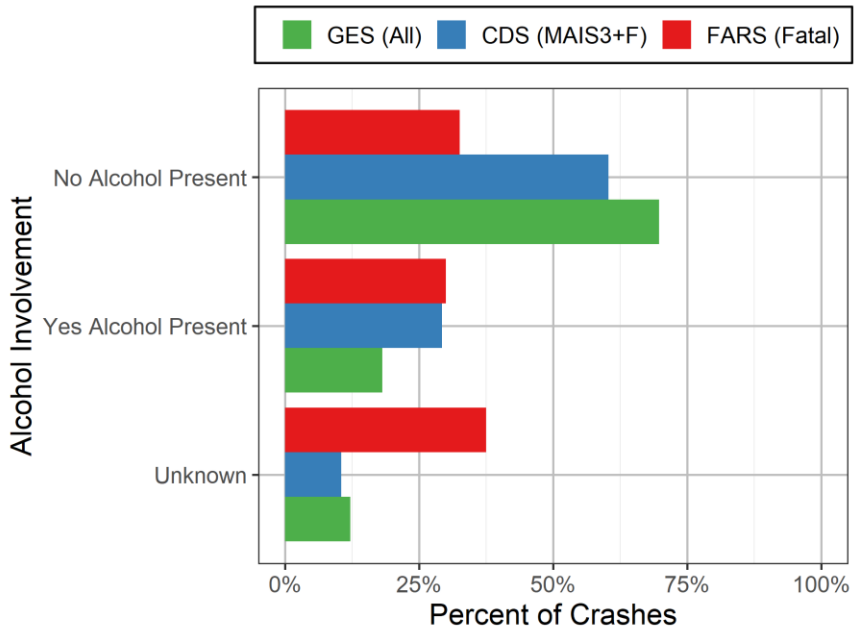

Figure 16. Involvement of alcohol in DrOOL road departure crashes.

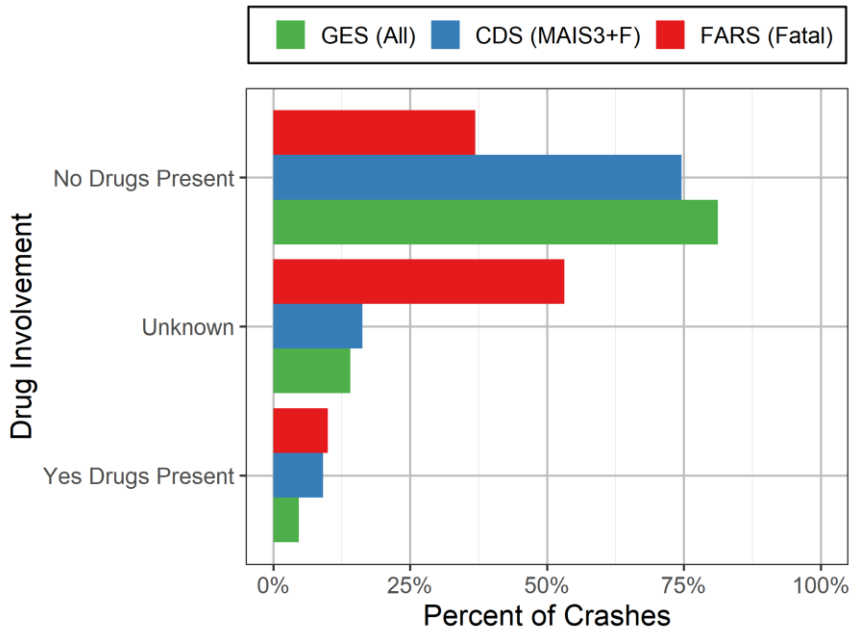

Figure 17. Drug use among drivers in DrOOL road departure crashes.

Before departing the road, nearly all drivers were not attempting any maneuver such as turning on to a new road (Figure 18). The model year of vehicles in fatal DrOOL road departure crashes is shifted left from all DrOOL road departure crashes, which may indicate that newer vehicles protect occupants better (Figure 19). CDS does not follow the same curve because NHTSA purposely sampled vehicles that were less than 10 years old.

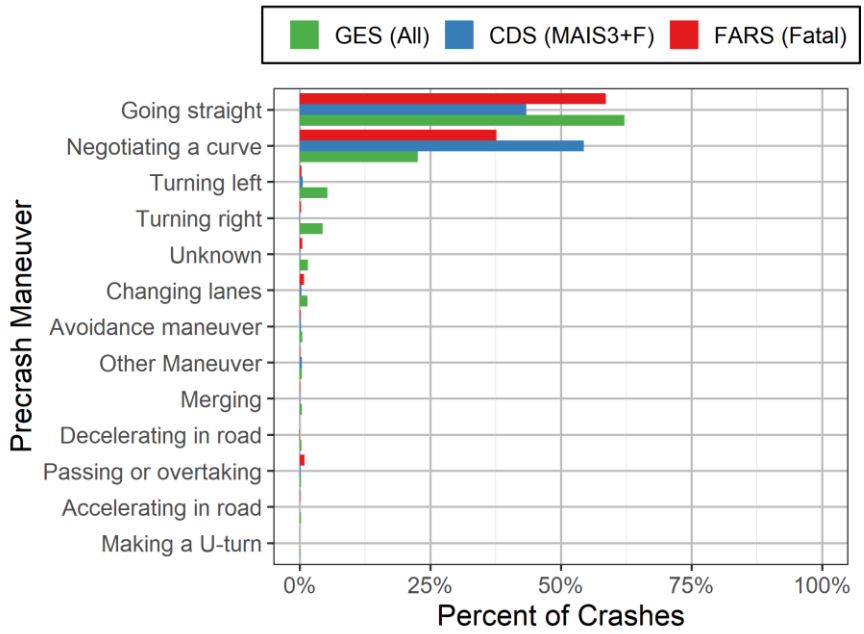

Figure 18. Distribution of maneuvers before departing the roadway.

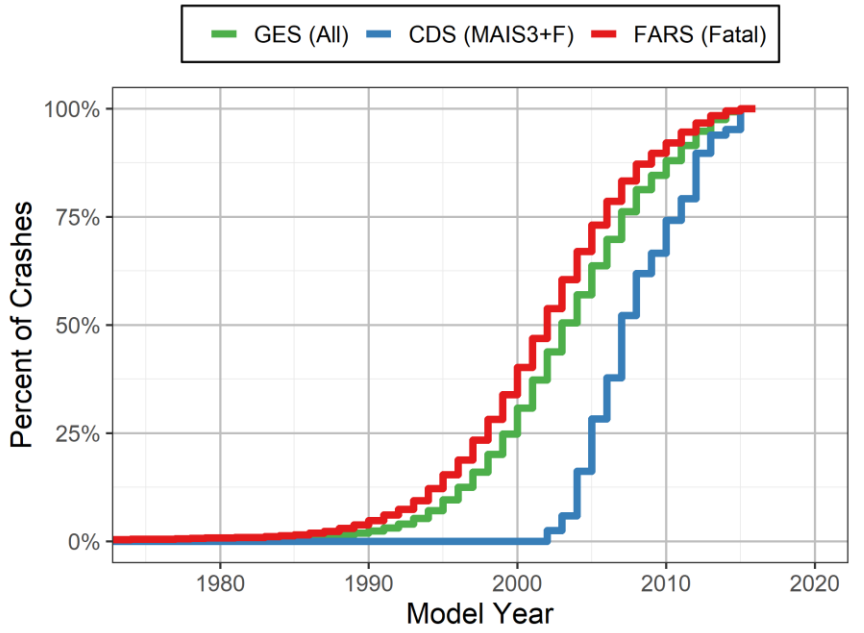

Figure 19. Distribution of vehicle model year in DrOOL road departure crashes.

Over three-quarters of the occupants in DrOOL road departure crashes are in the driver seat (Figure 20). Since most of these crashes are single occupant crashes, there is a drastic increase in the age distribution after occupants reach licensing age (Figure 21). Similar to the driver age distribution, more severe crashes tended to have older occupants.

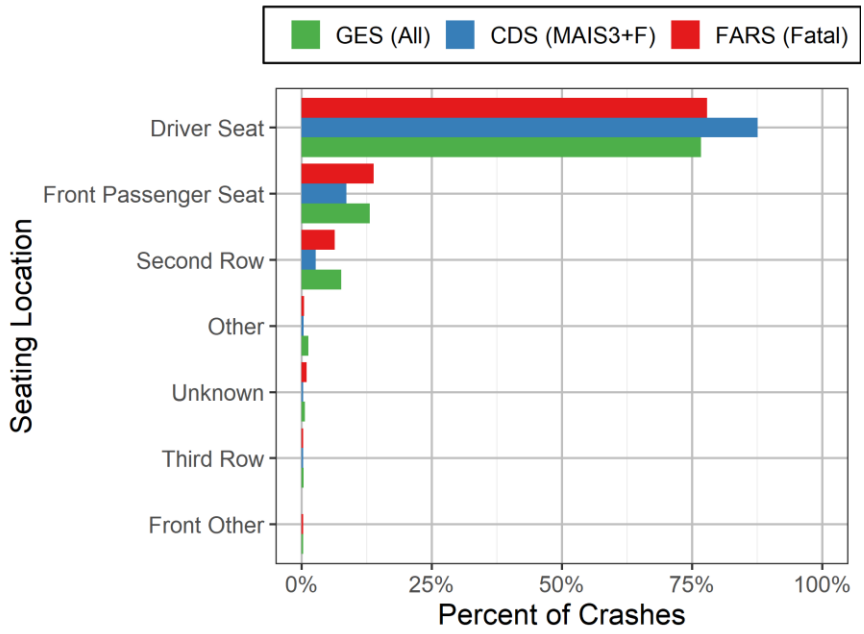

Figure 20. Distribution of occupant seating location.

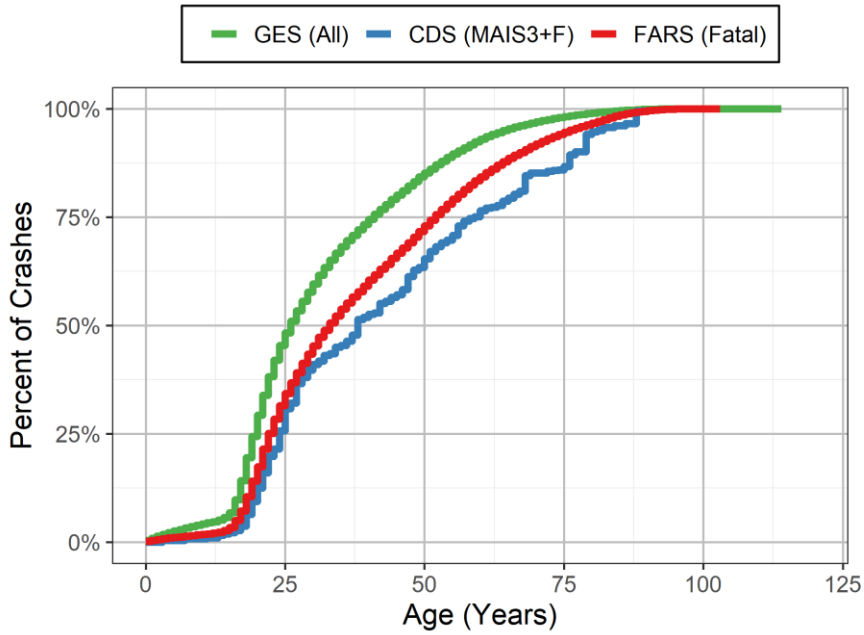

Figure 21. Age distribution of occupants in DrOOL road departure crashes.

Fatal and MAIS 3+F injured occupants were overrepresented among unbelted occupants and ejected occupants (Figure 22 and Figure 23).

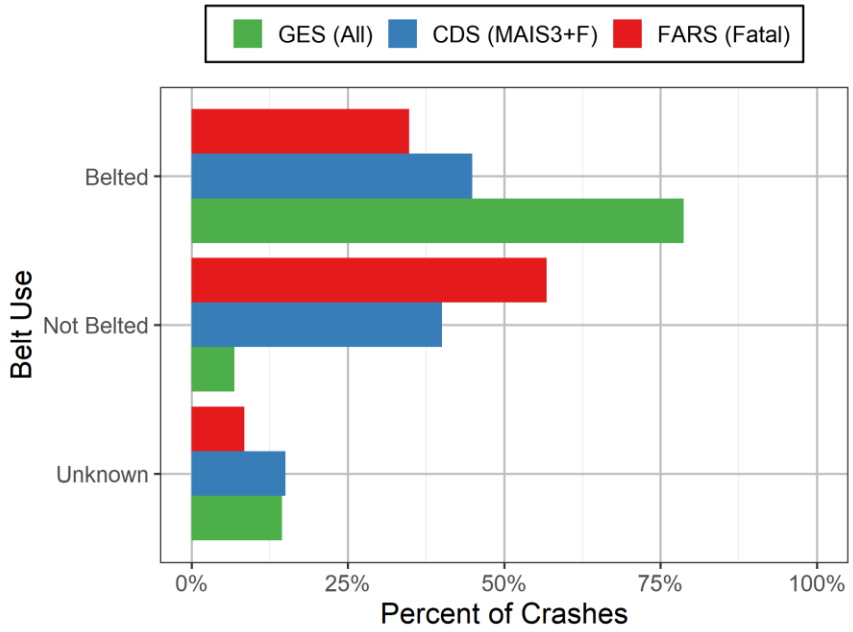

Figure 22. Distribution of occupant belt use in DrOOL road departure crashes.

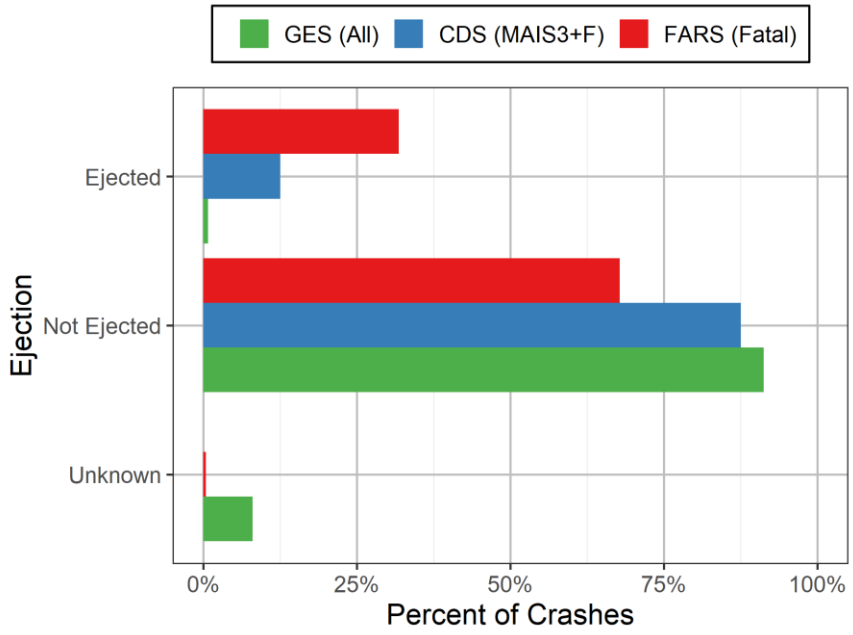

Figure 23. Distribution of ejection occurrence in DrOOL road departure crashes.

Similar to drivers, most of the occupants in DrOOL road departure crashes were male (Figure 24).

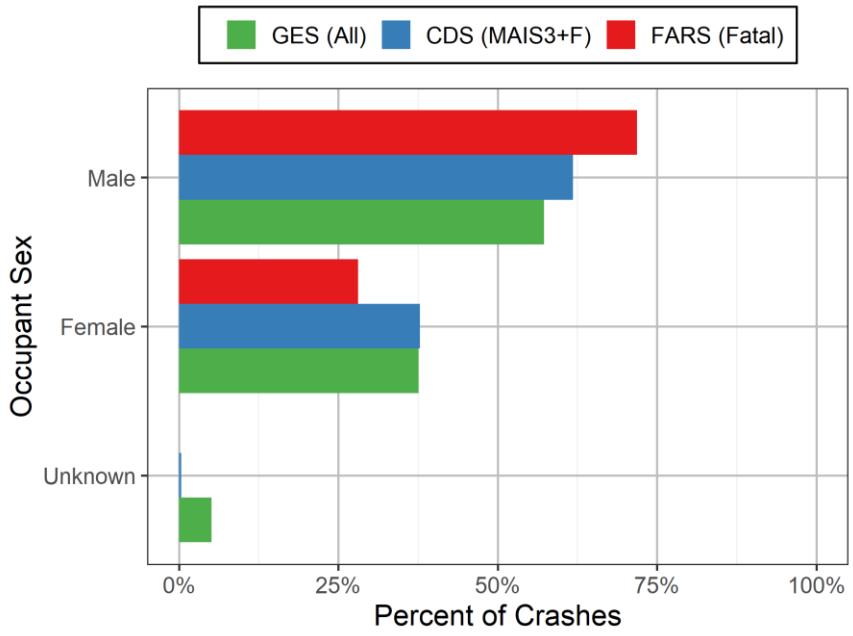

Figure 24. Distribution of occupant sex in DrOOL road departure crashes.

Narrow objects, such as poles and trees, were the most common hazard struck first in DrOOL road departure crashes (Figure 25). Curbs were 26% of the "Other" roadside hazards struck first.

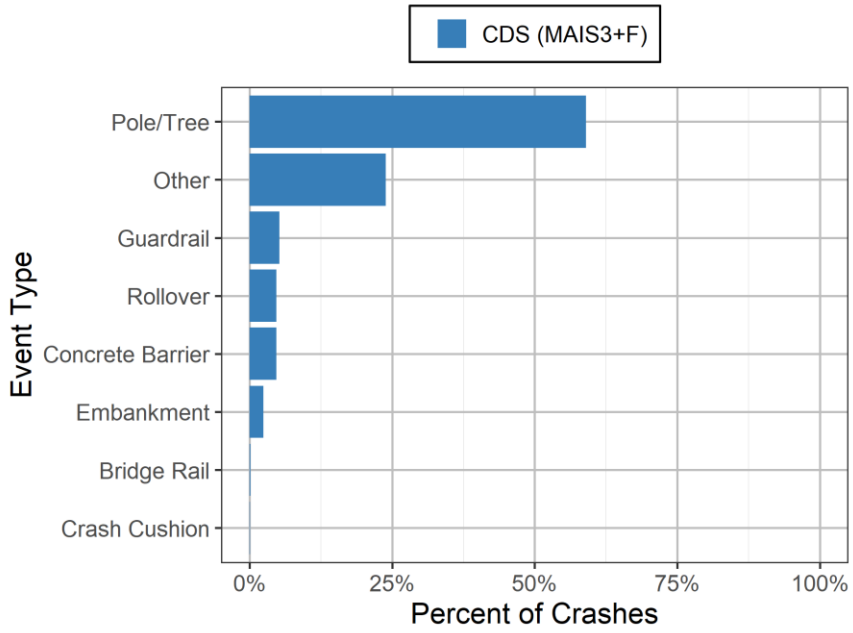

Figure 25. Distribution of the type hazard first contacted in DrOOL road departure crashes.

Over 40% of the weighted DrOOL road departure crashes occurred in a location without a shoulder (Figure 26). Additionally, half of the DrOOL road departure crashes occurred in locations where the measured clear width was less than 2.5 m (Figure 27). Less than 5% of the crashes occurred in locations with a measured clear zone width greater than 10 m. The lack of a shoulder and a small clear zone may limit the ability for drivers to recover from a departure.

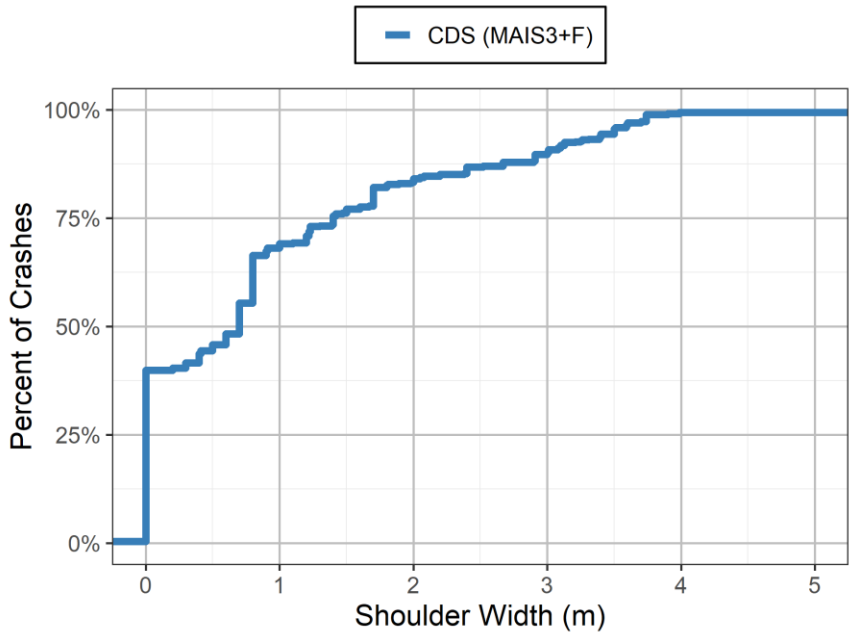

Figure 26. Distribution of the shoulder width at the road departure location.

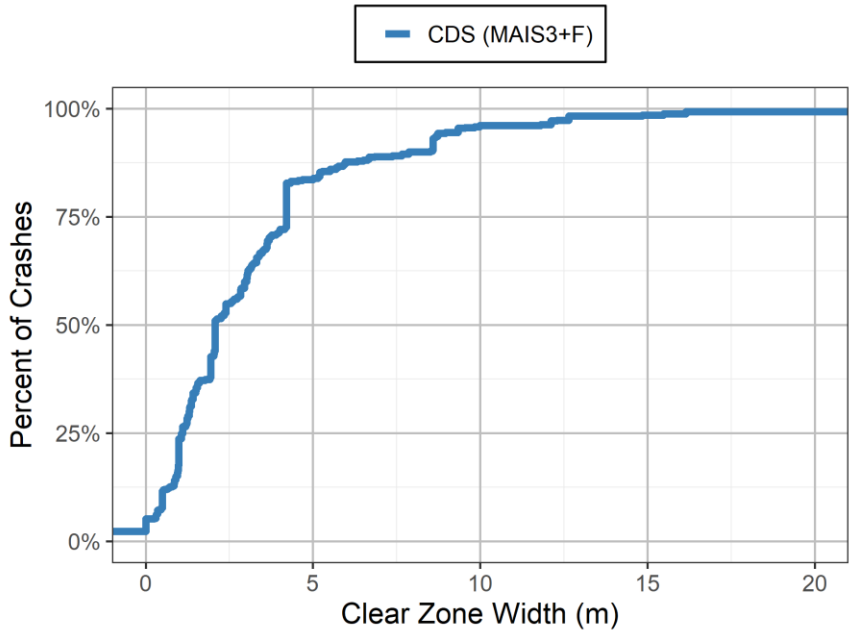

Figure 27. Distribution of the clear zone width at the road departure location.

Solid white lines were the most common lane marking for right side departures and double solid yellow lines were the most common lane marking for left side departures (Figure 28). Over 20% of the crashes occurred in a location with no lane marking. This could make it more challenging for LDW and LDP systems to identify a road departure.

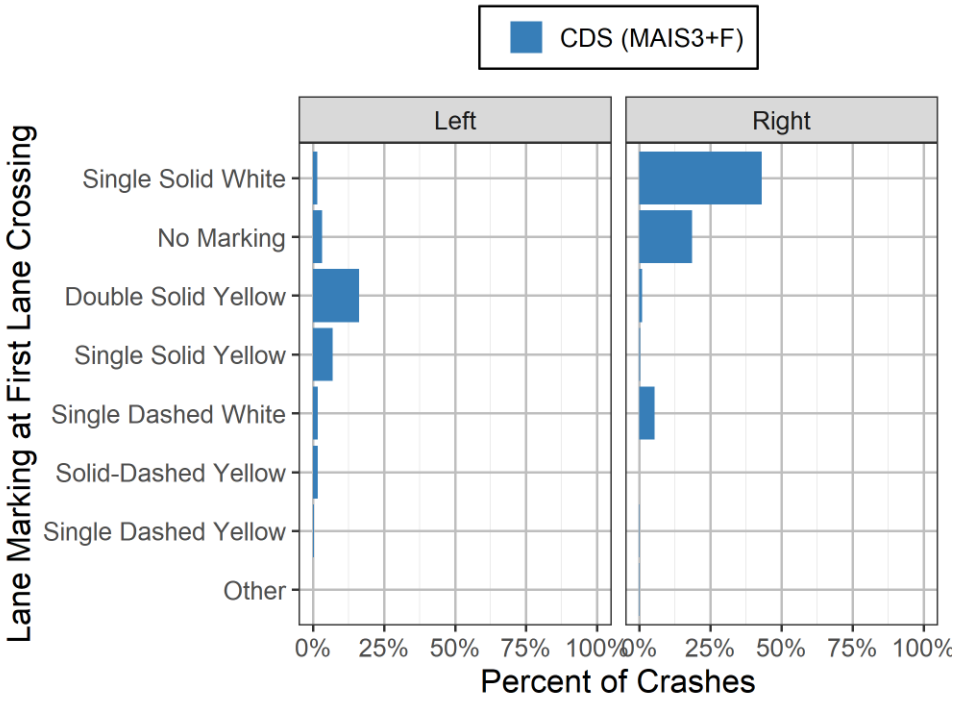

Figure 28. Distribution of lane markings for left and right DrOOL road departure crashes.

3.4 Conclusions

Most DrOOL road departure crashes occur on straight, 2-lane roads on clear days. Male drivers are more likely to be involved in these crashes. Older drivers are more likely to be fatally injured in the event of a DrOOL road departure crash. This analysis revealed two potential challenges road departure countermeasures. Missing lane lines may make it challenging to identify a departure event. In addition, the lack of a shoulder combined with a small clear zone may reduce the chances of the vehicle recovering back onto the roadway.

4 CHARACTERIZATION OF DRIVER EVASIVE ACTIONS IN ROAD DEPARTURE CRASHES

4.1 Purpose

While driver reaction time has been extensively investigated, little has been published on the type of evasive maneuvers taken by the driver to recover from a road departure. The purpose of this chapter is to understand what evasive maneuvers drivers perform while attempting to avoid roadside obstacles after a road departure and to develop a driver behavior model.

4.2 Methods

4.2.1 Case Selection Criteria

To be included in the study, NASS/CDS cases with supplemental trajectory data from the NCHRP 17-43 database must also have EDR information available. At the time this study was completed, the NCHRP 17-43 was not completed and contained only 992 cases. To ensure that the EDR event recorded corresponds to the impact described in the NASS/CDS case, only cases in which the EDR either recorded an airbag deployment or had a delta-v greater than 8 kph were selected [4, 6, 45, 50]. When an airbag deploys, the data is locked into the EDR and cannot be overwritten by lower severity impacts. A delta-v of 8 kph is a significant crash, and it is unlikely that a more significant event could occur to overwrite the data. To ensure that the EDR events align with the NASS/CDS events, the first event in the NASS/CDS case must have the largest delta-v. This selection criteria is the same as that used by Scanlon to analyze intersection crashes [45] and is summarized in Table 8.

Table 8. Case selection criteria.

Criteria	Cases	Weighted Cases
NCHRP 17-43	992	343,494
EDR Information Available	252	92,241
Airbag Deployment or Delta-V > 8 kph	239	88,422
First Impact Most Severe	123	53,660
Pre-crash Information Available	97	44,439

4.2.2 EDR Reconstruction Methodology

To understand the evasive actions attempted by the driver, only the pre-crash data recorded after the initial lane departure is relevant. Assuming constant acceleration between EDR velocity measurements, the distance traveled by the vehicle is computed. The time of the initial lane departure was calculated at the moment when the EDR-computed distance is greater than the trajectory distance (Figure 29). Additional distance was added for cases in which the vehicle crossed at least one lane before departing the road. The

additional distance was computed by assuming a straight path from the point of lane departure to the point of road departure and that the vehicle departed the lane with the same angle as it departed the road (Eq. 1).

$$\text{Lane Distance} = \frac{\text{Lane Width}}{\cos(90 - \text{Road Departure Angle})} \quad (1)$$

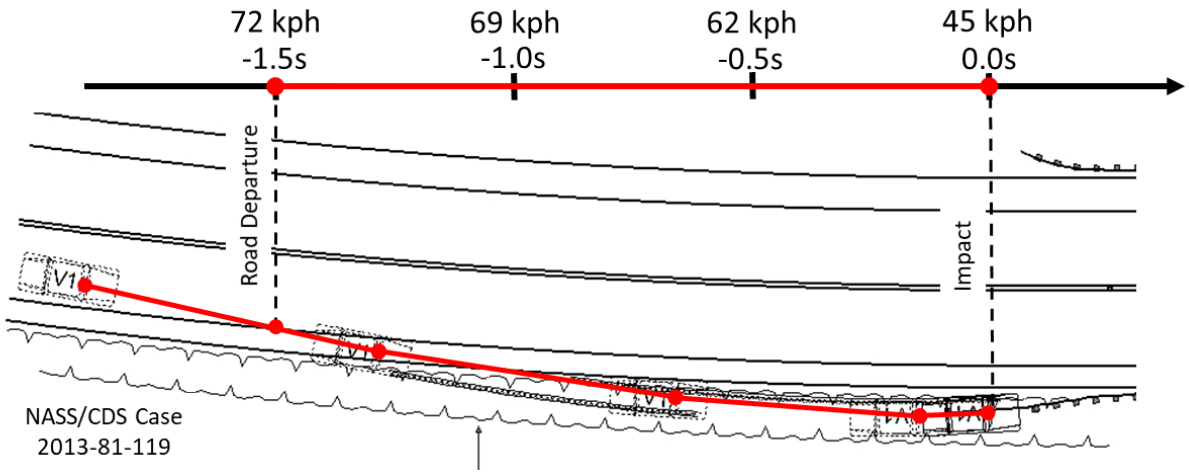

Figure 29. Example alignment of EDR pre-crash velocity with the trajectory information to determine the time of initial lane departure. The red segment represents the time traveled after departing the lane but before impacting the guardrail.

4.2.3 Steering Angle

In this study, evasive steering was defined as a yaw rate greater than 4 deg/s, using a convention consistent with earlier naturalistic driving studies [35]. A criterion for evasive steering based on the steering wheel angle was computed by relating the steering wheel angle to the yaw rate. EDR pre-crash data with both yaw rate and steering-wheel angle were used to determine the relationship between the two parameters. This excluded rollover crashes because they often are not tracking before tripping. The time-series data from ten tracking vehicles in NASS/CDS and NCHRP 17-43 was used to form a linear model relating the yaw rate to steering wheel angle before the crash. The steering-wheel angle is proportional to the yaw rate by a factor of 4.4 (Figure 30). The threshold for evasive steering based on steering-wheel angle was, therefore, 17.5º.

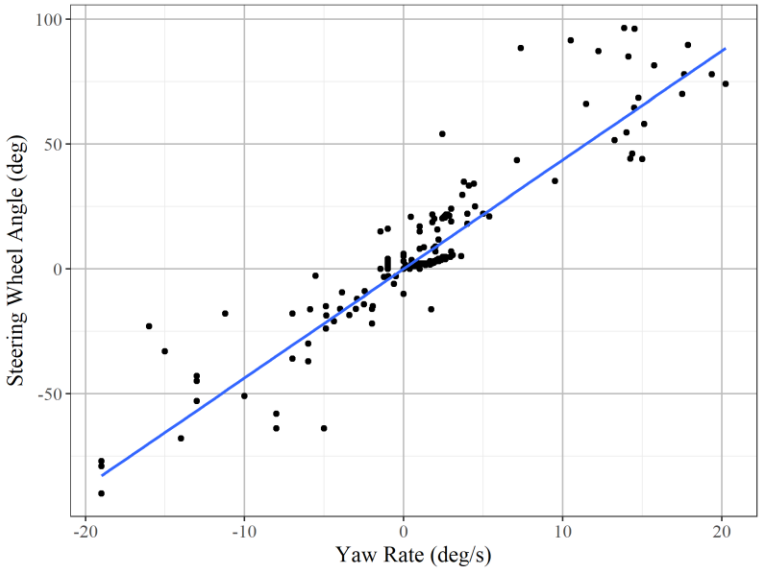

Figure 30. Average relationship between steering-wheel angle and yaw rate.

4.3 Results

The evasive maneuvers performed by the drivers and their frequency are summarized in Table 9. Steering was the most common driver response, followed by braking. There were 16 cases with both steering and braking data. The majority of drivers responded by only steering (Table 10). The combined maneuvers will be utilized in the following chapter as the foundation for the driver behavior model.

Table 9. Evasive maneuvers in DrOOL road departure crashes.

Parameter	Action Performed	Cases Available	Percent of Cases	Action Performed (weighted)	Weighted Cases	Percent of Weighted Cases
Brake	40	92	43.4%	20,556	40,849	50.3%
Accelerate	27	52	51.9%	8,829	21,307	41.4%
Steer	15	17	88.2%	7,813	8,985	87.0%
Yaw	10	15	66.7%	2,493	4,671	53.4%
ABS	4	16	33.3%	329	9,029	3.6%
ESC	4	12	25.0%	752	3,680	20.4%

Table 10. Combination of evasive maneuvers in DrOOL road departure crashes.

Parameter	Action Performed	Percent of Cases	Action Performed (weighted)	Percent of Weighted Cases
No Avoidance	1	6.3%	1,111	17.5%
Brake and Steer	5	31.3%	485	7.6%
Steer Only	9	56.3%	4,694	73.9%
Brake Only	1	6.3%	60	0.9%

4.4 Discussion

As discussed in Chapter 3, NASS/CDS is inadequate for drawing conclusions about driver evasive maneuvers because in over 50% of the cases, the response was unknown (Figure 12). The driver maneuver was determined by the crash investigator based on physical evidence, such as tire marks. However, as the

scene was investigated up to two weeks after the crash, much of the visible evidence was likely missing. Therefore, NASS/CDS is not an adequate source for understanding driver maneuvers. Unlike NASS/CDS, the use of supplementary EDR information provides a direct measurement of the driver response to road departure. This is why more cases in NASS/CDS record the driver as performing no evasive maneuver before the crash than what was recorded in the EDR. Both the EDRs and NASS/CDS determine steering and braking as the most common evasive maneuvers.

In the majority of road departure crashes – 67.1% of cases and 56.2% of weighted crashes – the vehicle was travelling faster than the speed limit (Figure 31). In 43 of the 82 cases, the vehicle was travelling more than 8 kph (5 mph) over the speed limit. The median departure speed was determined to be 54.7 kph. Very few road departure crashes occurred at speeds below 25 kph (Figure 32).

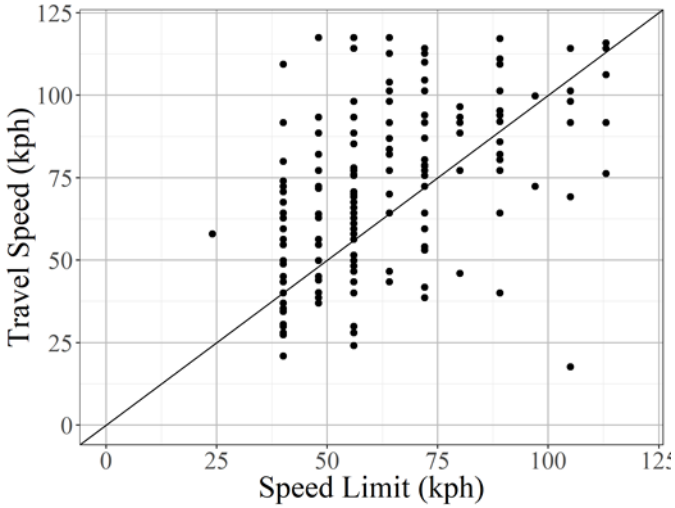

Figure 31. Vehicle speed compared to the posted speed limit. Cases above the line represent vehicles travelling faster than the posted speed limit.

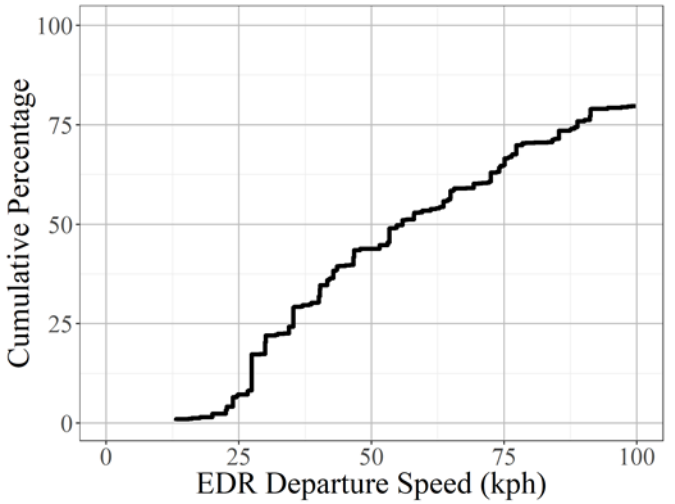

Figure 32. Cumulative distribution of the departure speed.

The distance traveled to the site of impact from the initial lane departure is related to the time from the departure to the impact (Figure 33). This is closely correlated with the departure speed, as expected. Within each time to impact, vehicles travelling faster will cover more distance before impact than slower vehicles. The difference between the distance traveled by slow- and fast-moving vehicles increases with time. Thus, the variation in distance traveled to impact is larger with a longer time to impact.

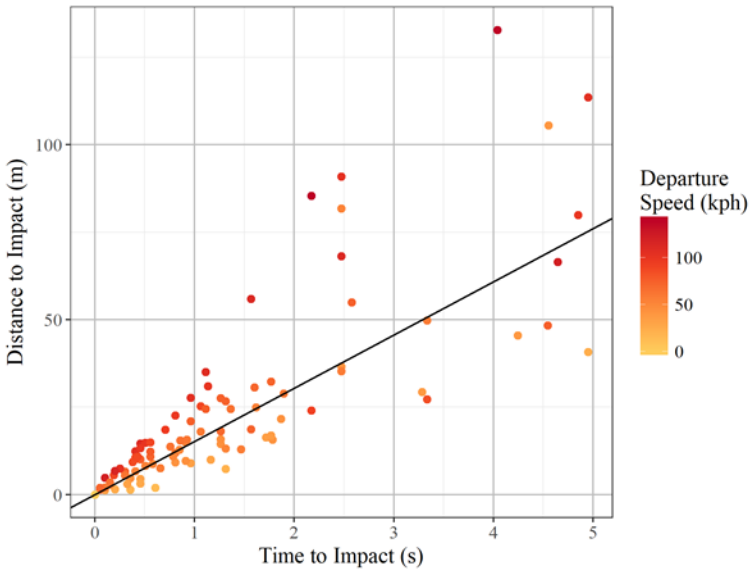

Figure 33. Relationship between the distance traveled and the time to impact. The slope of the line represents the median departure speed of 54.7 kph.

As many of the crashes occurred close to the road and at high speeds, many drivers did not have sufficient time to react. Typical reaction times to LDW systems are between 0.38 s and 1.36 s [5]. Therefore, individuals with a fast reaction time of 0.38 s could not respond to an LDW in 23.4% of crashes. Individuals with a slow reaction time of 1.36 s could not respond to an LDW in 71% of crashes (Figure 34). LDW systems require sufficient time for the driver to react to the warning and perform an evasive maneuver. A lane departure prevention (LDP) system may be more effective in avoiding these crashes by providing a steering input immediately when the vehicle begins to leave the lane.

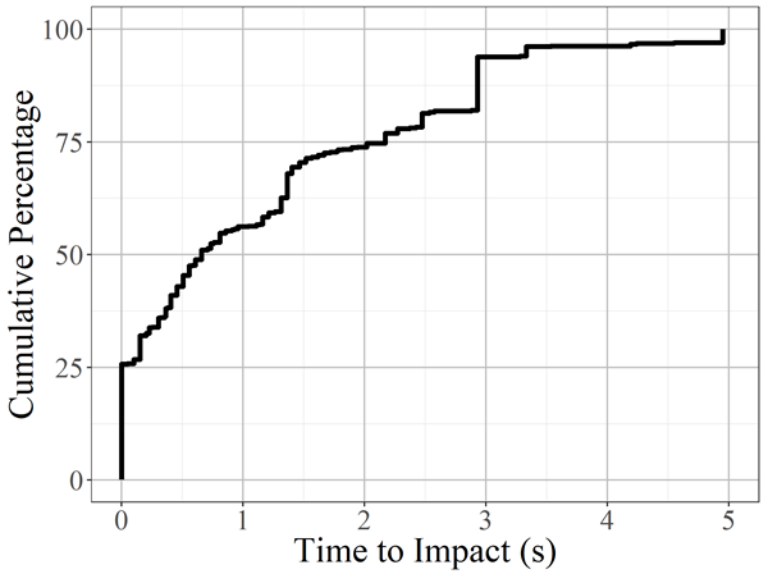

Figure 34. Distribution of time from road departure to time of impact.

The deceleration was computed using a linear regression of the amount of time the driver was braking as a function of the change in velocity. The average deceleration of the vehicle due to braking was 0.41 g (Figure 35). This is less than the 0.58 g evasive braking present in intersection crashes [45]. One reason for this difference is there is likely a lower coefficient of friction between the tires and the ground when off the road compared to when the vehicle is on pavement. In addition, evasive actions off the road and in intersections may be different. The braking is similar to the "comfortable deceleration" value of 0.34 g defined in AASHTO's Green Book [58].

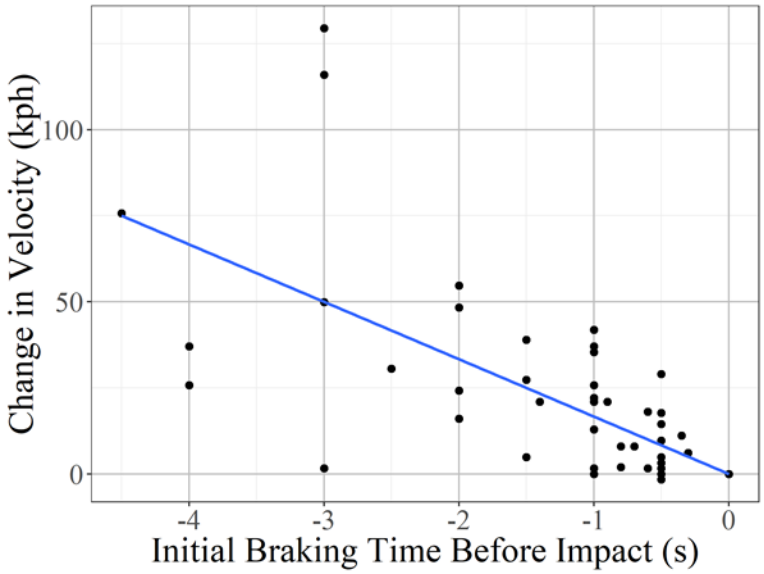

Figure 35. Vehicle deceleration from braking before impact.

4.5 Limitations

This study analyzed only those road departures that resulted in crashes with downloaded EDR data. Accordingly, conclusions cannot be made about what driver maneuvers are successful in avoiding a crash in road departure scenarios. However, the purpose of LDW systems is to reduce the number of road departure crashes, which is represented in these data. Because of the low sampling rate of EDR precrash data, the temporal error for the length of a braking or steering response can be up to 1 s. This is particularly large for cases when the drive responded just before impact.

Within this dataset, more EDRs recorded steering wheel angle than yaw rate. However, the threshold to indicate a steering maneuver based on steering wheel angle may not be accurate for all vehicles. The yaw rate resulting from a given steering wheel angle is highly dependent on the vehicle geometry such as the track width, the suspension, and the speed of the vehicle. However, a steering wheel angle of 17° would be higher than necessary to maintain lane position, which indicates a steering maneuver.

The majority of drivers responded to the road departure by performing some steering maneuver. In over 70% of the cases in which the driver performed an evasive steering action, the driver turned in the direction of the road. This method cannot exclude the possibility of non-evasive steering actions such as the driver falling asleep and causing the vehicle to turn away from the road. These results are also limited by the small number of cases that had the EDR steering or yaw rate data available. The same limitation applies to the activation of ABS and ESC before the crash.

4.6 Conclusions

LDW applicable crashes account for a small portion of crashes but comprised almost 50% of all MAIS3+F injuries. Drivers tend to react to a road departure with an evasive steering action back in the direction of the road. The second most frequent maneuver was braking, which had an average deceleration of 0.41 g. The following chapter will utilize the driver model to predict which crashes could be prevented with LDW/LDP systems.

5 ESTIMATED BENEFIT OF ROAD DEPARTURE CRASHES BY LDW

5.1 Purpose

The purpose of this chapter was to predict the number of DrOOL road departure crashes after fleet-wide deployment of LDW/LDP systems.

5.2 Approach

5.2.1 Data Selection

NASS/CDS drift-out-of-lane road departure crashes from 2011 to 2015 were selected for estimating the effectiveness of LDW/LDP systems. These are the latest five years available in NASS/CDS. For each of these cases, the NCHRP 17-43 database was used to provide the associated coded trajectory of the vehicle before the crash. Only cases with an associated EDR download were included. The EDR pre-crash velocity data was used to determine the vehicle's speed along the trajectory. To be included in our study, the first event had to be the most severe [45]. Additionally, the EDR needed to record either an airbag deployment or a delta-v greater than or equal to 8 kph (5 mph). The airbag deployment locks the EDR data preventing subsequent events from overwriting EDR data. The delta-v requirement ensures a crash with significant damage. Another impact that did not deploy the airbag would be unlikely to overwrite these events. Finally, the EDR must have recorded values for the pre-crash velocity to be used in this study.

If the vehicle departed the road more than once before the crash, it was assumed that an LDW/LDP system would have had no effect because the driver would already be aware of the departure. Overall, there were 81 vehicles in the simulation dataset. After applying NASS/CDS sampling weights, this represented an estimated 29,315 real world crashes (Table 11).

Table 11. Case selection criteria.

	Number of Cases	Weighted Cases
NCHRP 17-43	1,580	504,999
With EDR	270	94,943
Air bag deployment or delta v > 5 mph	184	60,707
First event most severe	97	37,647
Single departure cases	81	29,315

5.2.2 Crash Environment

To accurately predict the benefits of LDW systems for road departure crashes, the environment where the crash occurred must also be modeled. The most important aspect of the crash environment was the road geometry. The road curvature at the point of departure was retrieved from the NCHRP 17-43 database. If the vehicle crossed at least one lane before departing the road, then the first lane line crossed

was utilized. The roadside object that was impacted in the original crash was assumed to be a 1 m by 1 m box located at the point of impact.

5.2.3 Vehicle Model

The vehicles in the crash were represented by a rectangle with a length and width equivalent to the overall length and width from NASS/CDS of each vehicle. The vehicle dynamics were modeled as a point with a time step of 0.01s (Eq. 2-7)

$$a_{t+1} = a_t + Jerk_t * dt \quad (2)$$

$$v_{t+1} = v_t + a_t * dt \quad (3)$$

$$\dot{\Psi}_{t+1} = \dot{\Psi}_t + \ddot{\Psi}_t * dt \quad (4)$$

$$\Psi_{t+1} = \Psi_t + \dot{\Psi} * dt \quad (5)$$

$$x_{t+1} = x_t + v_t * \Delta t * \cos(\Psi_t) \quad (6)$$

$$y_{t+1} = y_t + v_t * \Delta t * sin(\Psi_t) \quad (7)$$

The total force exerted by the tires was limited to 1g. Therefore, any combination of steering and acceleration could not exceed 1g (Eq. 8). If the 1g limit was exceeded, then the braking force was maintained, and the steering was scaled down such that the magnitude was equal to 1g.

$$9.8 > \sqrt{(a)^2 + \left(\dot{\Psi}v\right)^2} \; where \quad (8)$$

$$a = longitudinal\ acceleration\ \left(m * s^{-2}\, {}^{m}/_{s^2}\right)$$

$$\dot{\Psi} = Yaw\ rate\ \left({}^{deg}/_{s}\right)$$

$$v = longitudinal\ velocity\ ({}^{m}/_{s})$$

5.2.4 Crash Reconstruction

To define the velocity along the vehicle's trajectory, the last EDR pre-crash velocity was assumed to be the impact velocity. The velocity was assumed to vary linearly between EDR measurements to compute the distance traveled [4]. Beginning at the point of impact, the pre-crash velocity was mapped to the vehicle trajectory (Figure 36). The travel speed was defined to be the speed of the vehicle when its center of mass crossed the lane line.

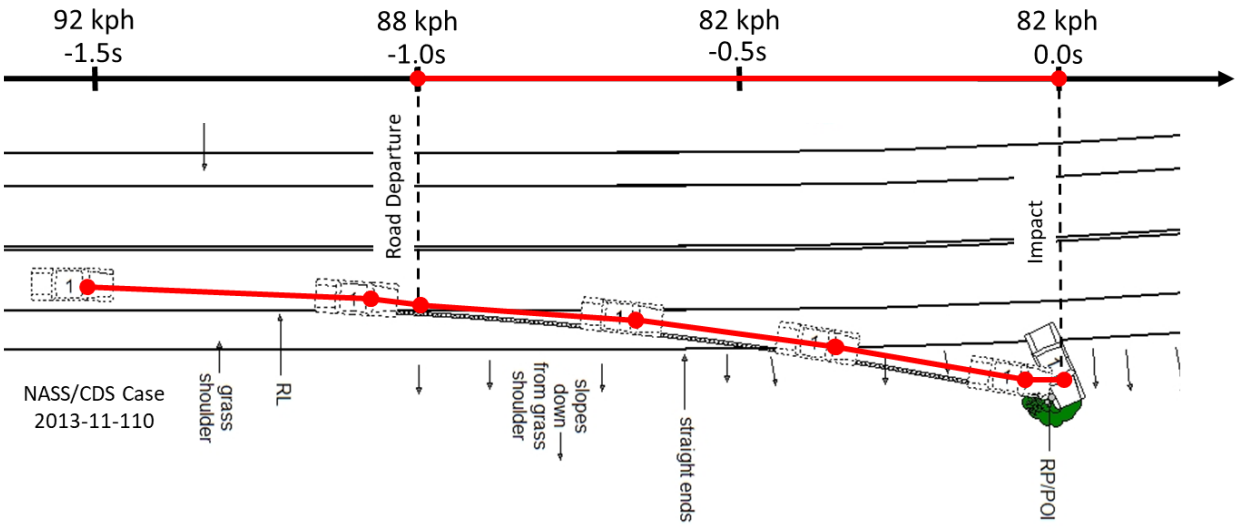

Figure 36. Mapping EDR pre-crash velocity to crash trajectory.

5.2.5 Driver Model

The vehicle steering was controlled by a proportional-integral-derivative (PID) controller with the following parameters: $K_d = 0$, $K_i = 0.1$, $K_p = 743.5$. The PID controller parameters were determined by manually tuning such that the error was reduced quickly (K_d), with minimal offset (K_i), and with minimal overshoot (K_d) to a right-angle turn. The PID controller was minimizing the distance between the predicted vehicle center in half a second to the intended path of the vehicle. The 0.5s look-ahead was used to more closely resemble how humans drive; drivers do not steer based on their current position but where they will be. Additional length equal to 0.5s of travel was added to the end of the trajectory because the steering model looked ahead 0.5s. Initially, the PID controller keeps the vehicle on the crash trajectory but after the driver reacts, the controller moves the vehicle back to the original lane of travel.

The vehicle starts at the reconstructed initial velocity. The driver applies a constant deceleration over the whole trajectory such that the vehicle would be travelling at the impact speed at the original impact location. After the warning was delivered, the driver did not react instantaneously. There was a reaction period during which the vehicle continued to travel as before until the driver reacts. Our model considered two driver reaction times: 0.38s and 1.36s. The 0.38s and 1.36s reaction times model a fast and slow driver reaction time to either a haptic or audible warning [5].

Once the driver has reacted to the warning, our study considered two different braking magnitudes (0.0g, and 0.45g) and three different maximum turning rates (0 deg/s, 11.4 deg/s, and 34.1 deg/s) based on EDR data from intersection and rear-end crashes. [45, 59]. Thus, there were six different possible driver maneuvers, which included no-braking and medium braking maneuvers as well as no-steering, light, and heavy steering maneuvers. Each of the six evasive maneuvers were then weighted based on the overall likelihood of a driver performing each specific maneuver based on the driver model developed in Chapter

4. (Table 12). The steering maneuver was governed by the PID controller, which tried to steer the vehicle back into the original lane of travel.

Table 12. Relative frequency of driver evasive actions.

	No Braking (0g)	Heavy Braking (0.45g)
No Steering (0 deg/s)	17.5%	0.9%
Light Steering (11.4 deg/s)	36.95%	3.8%
Heavy Steering (34.1 deg/s)	36.95%	3.8%

5.2.6 LDW/LDP Algorithm

LDW and LDP algorithms are highly proprietary. Our model investigated 6 hypothetical LDW systems and 2 hypothetical LDP systems (Table 13). There were two simulated activation speeds for the LDW and LDP systems: a standard activation and an expanded activation. The standard system activated when the vehicle was travelling faster than 50 km/h. This higher speed threshold is intended to prevent activations in locations, such as intersections and parking lots, where there may be many lane lines. The expanded activation system would deliver a warning at speeds over 20 km/h if the driver was distracted and over 50 km/h otherwise. There were four different activation time to lane crossing (TTLC) thresholds simulated for the LDW and LDP systems. The standard LDW system activated when the vehicle crossed the lane line or a TTLC of 0 s. The advanced LDW system activated when the TTLC was less than 0.5s. The human-machine interface (HMI) LDW system delivered a warning at 0.5 s TTLC if the driver was alert and 1.2s TTLC if the driver was distracted. The LDP system always activated at 1.0 s TTLC. Together, these systems represent the range of real LDW/LDP system TTC thresholds and activation speeds [60]. For both the human driver and the LDP system, the goal of the vehicle was to return to the original lane of travel.

Driver distraction data was determined by the CDS crash investigator for all 81 simulated cases in the study. If the investigator determined that the driver had “looked but not seen” then it was assumed that an HMI system would interpret that the driver is attentive. If the investigator was not sure if the driver was distracted, it was assumed that the driver was attentive. This assumption would give the driver the latest warning and highest activation speed, which is the least favorable system configuration. Based on this assumption, of the data set, in approximately 67% of the cases the driver was distracted.

Table 13. Eight simulated LDW and LDP systems with different activation speeds and times.

System Design	Activation Speed	Activation TTLC
LDW	>50 km/h	0.0 s before lane crossing
LDW with Expanded Speed	>20 if distracted >50 otherwise	0.0 s before lane crossing
Advanced LDW	>50 km/h	0.5 s before lane crossing
Advanced LDW with Expanded Speed	>20 if distracted >50 otherwise	0.5 s before lane crossing
HMI LDW	>50 km/h	1.2s before lane crossing if distracted 0.5 s before lane crossing otherwise
HMI LDW with Expanded Speed	>20 if distracted >50 otherwise	1.2 s before lane crossing if distracted 0.5 s before lane crossing otherwise
LDP	>50 km/h	1.0 s before lane crossing
LDP with Expanded Speed	>20 if distracted >50 otherwise	1.0 s before lane crossing

5.2.7 LDW/LDP Effectiveness

The LDW effectiveness for 8 different systems was estimated based on the 2 reaction times, and 6 different vehicle maneuvers for each of the 81 cases. This resulted in a total of 7,776 simulations of road departure crashes collisions. These simulations were performed on multiple CPU cores by a custom python script. Each simulation was weighted based on the frequency of each driver evasive action if the system was of the LDW model or weighted based on the case weight if the system was of the LDP model. A crash was predicted to be prevented with an LDW/LDP system if the vehicle successfully returned to the initial lane of travel (Returned) or came to a stop (Stopped). A crash was predicted to not be prevented if the vehicle impacted the roadside object (Crashed) or the vehicle was moving away from the road and not decelerating (Parted).

5.3 Results

In our dataset, 52% of cases were travelling below 50 kph and would not have received any warning for the base LDW and LDP systems (Figure 37). In cases where the driver was believed to be distracted, 6.2% of the cases were traveling below the advanced system activation speed of 20 kph (Figure 38). This meant that in 6.2% of the cases the advanced LDW/LDP system would not have activated and the original crash would not have been prevented.

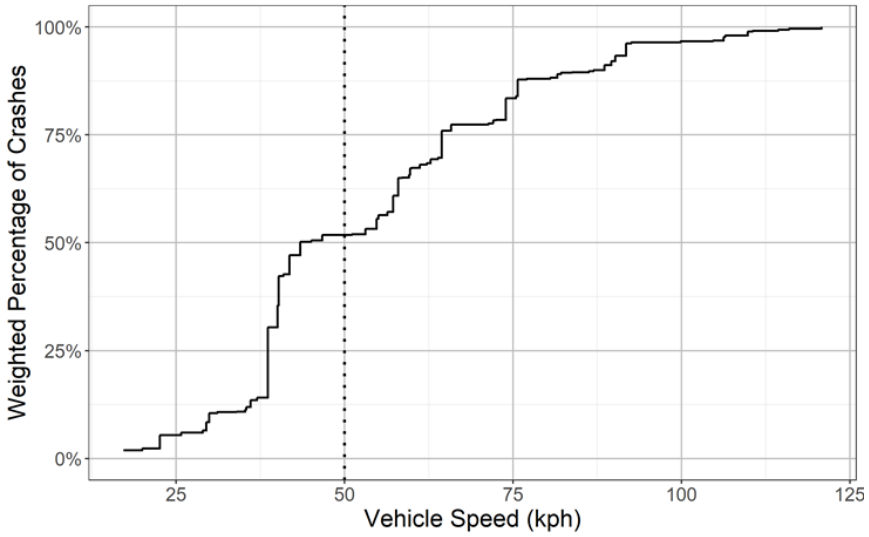

Figure 37. Cumulative distribution of departure speeds for standard system models.

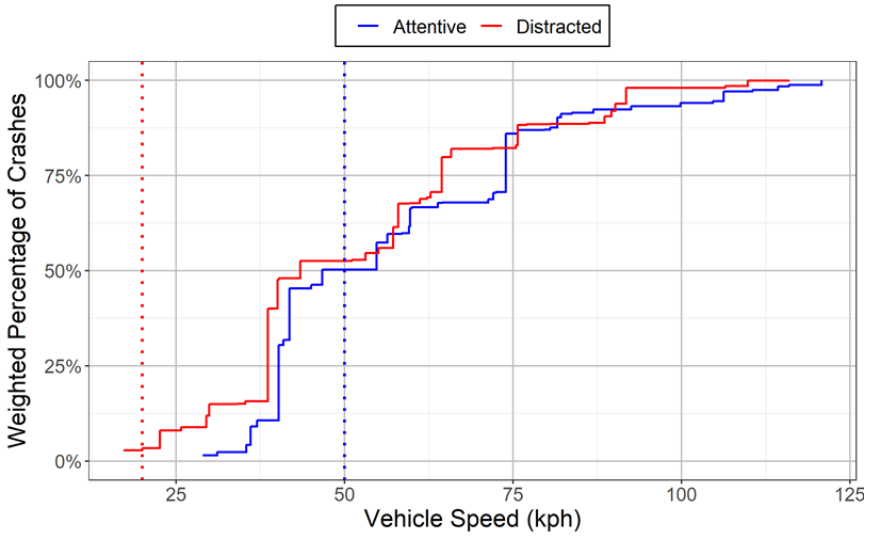

Figure 38. Cumulative distribution of departure speeds for expanded speed models and driver distraction data.

Each of the eight system types was analyzed and a general system benefit was determined. The overall system benefit was defined to be the percentage of cases in which the system successfully avoided a crash, compared to the percentage of cases in which the crash still occurred. The baseline model was defined as a vehicle without an LDW or LDP system in which the vehicle followed the original crash trajectory. The breakdown of the benefit of each system type is shown in Figure 39. The LDP model that could activate at 20 km/h if the driver was distracted, had the highest overall benefit of 67%. The LDW model with the advanced HMI system to provide earlier warning times and a lower activation speed had a crash reduction comparable to the LDP system with an activation speed of 50 km/h. The baseline LDW model provided the smallest benefit since it activated much later than the other systems.

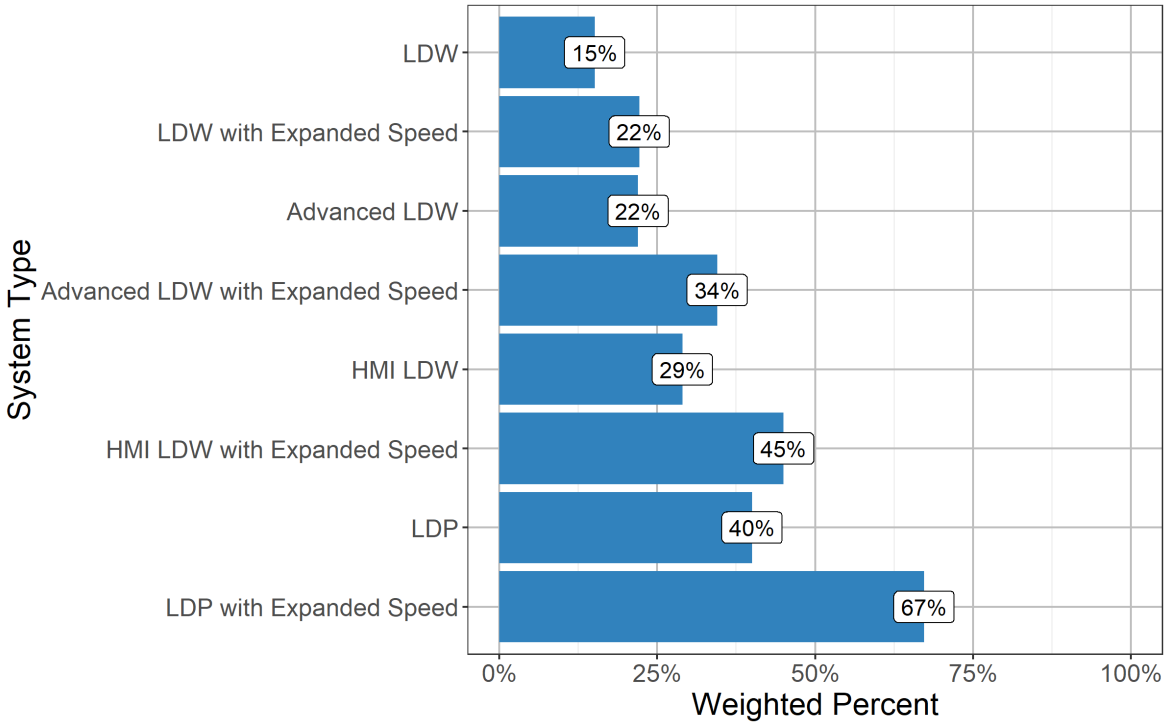

Figure 39. Summary of system benefits. Each group represents the overall benefit that would be seen if all 81 simulated cases were equipped with each specific system type.

The crash avoidance benefit of the LDW system increased for systems that delivered an earlier warning (Figure 40). LDP systems always activated at 1.0 s TTLC and reacted immediately, which produced a greater crash reduction than LDW systems. Systems that can activate at lower speeds when a driver is distracted have a higher benefit than its counterpart because the system activates for a greater proportion of cases.

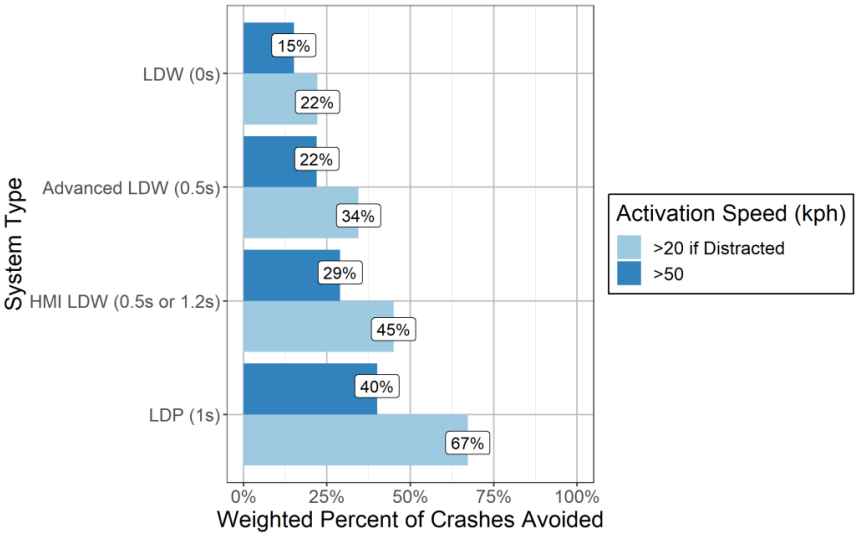

Figure 40. Weighted percent of crashes avoided for each system model and activation speed.

5.4 Discussion

For the baseline LDW system, the predicted crash benefit was 15%. In 2018, Riexinger predicted the crash benefit of LDW systems to be between 16.7% and 21.5% depending on the reaction time or 19.1% on average [4]. The main difference between these two values is the current LDW system only activates if the vehicle is travelling faster than 50 km/h, in which 52% of cases were travelling below 50 km/h and did not receive any warning (Figure 37). Since this study's LDW system activates for half as many cases as the previous studies the benefits are significantly reduced. Even with an HMI system that allows the LDW system to activate at 20 km/h, if the driver is distracted, still does not activate for 6.2% of the simulated cases (Figure 38), which causes the benefit from those systems to also be reduced. The predicted benefit of LDP systems was higher than the previous estimates by Kusano and Scanlon [7, 8] (Table 14).

Table 14. Summary of previous LDW studies on road departure crashes.

Study	Case Selection	LDW/LDP Effectiveness
Riexinger 2018 [4]	Single Vehicle Road Departure crashes in US	16.7%-21.5% (LDW) 24.3% (LDP)
Scanlon 2015 [8]	Single Vehicle Road Departure crashes in US	26.1% (LDW) 37.3% (LDP)
Kusano 2014 [7]	Single Vehicle Road Departure crashes in US	29%-32% (LDW)
This Study	Single Vehicle Road Departure crashes in US	15% (LDW) 40% (LDP)

The base Advanced LDW system predicted a benefit of 22%, and the base HMI LDW system predicted a benefit of 29%. This is a 7% and 14% increase in benefit compared to the base LDW model. Riexinger showed that the highest benefits are to be expected when driver reaction times are the lowest [4]. The Advanced and HMI LDW systems, which activate some time before a lane crossing, effectively turn a long reaction time into a quicker reaction. If the driver is not distracted, then the Advanced LDW and HMI LDW systems behave in the same way and provide a warning at 0.5s TTLC. However, in the cases where the driver is distracted, the HMI LDW system will provide the much greater warning time of 1.2s TTLC, which increases the crash benefit over the Advanced LDW system.

Expanded speed models had a higher benefit than the same model but with a standard 50 kph cutoff speed. The Advanced LDW system with the expanded activation speed had a benefit of 34%, which was 12% more than the base advanced LDW system. The HMI LDW system with the expanded activation speed showed a benefit of 45%, which is a 16% increase from the same system that only activated at speeds greater than 50 km/h. Despite activating for almost 40% more cases, the highest benefit for expanding the activation speed was roughly 27% in the LDP system.

Similar to the previous study [4], many road departure crashes were not avoided in the simulations because there was very little time for the driver to respond. The time available for the driver to respond is

largely dependent on the location of the roadside hazard and the speed of the vehicle. Often the fastest driver reaction time (0.38s) and even an early warning of 0.5 s TTLC, left very little time for the driver to steer or brake to avoid the object (Figure 41). There was a clear boundary below which the vehicle always crashed in the simulation. These cases correspond to scenarios where the driver did not have enough time to respond before impact.

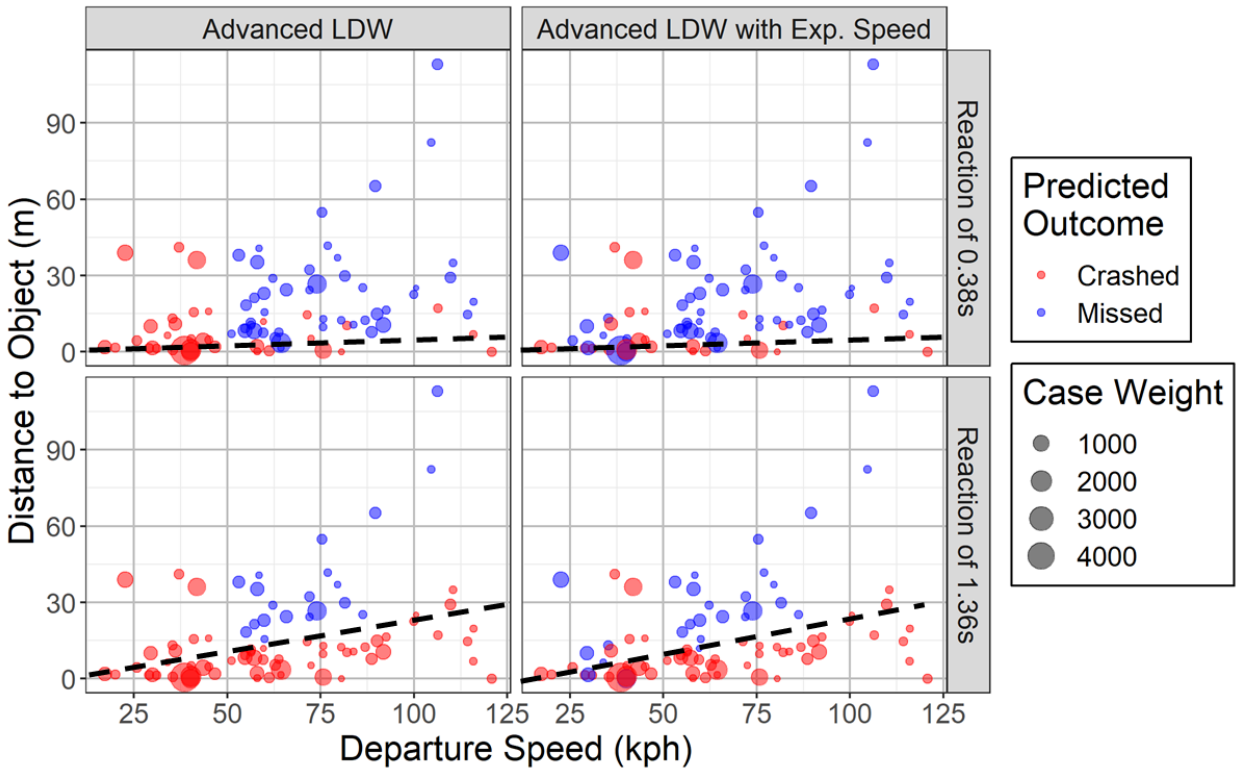

Figure 41. The outcome of each crash based on the departure speed and the straight-line distance to the impacted object from the point of departure for each reaction time for Advanced LDW and Advanced LDW with Expanded Speed Simulations with Heavy Steering and Heavy Braking.

Figure 42 displays the same relationship as Figure 41 but for the HMI LDW and HMI LDW with Expanded Speed systems, where the driver would be given a warning of either 0.5s or 1.2s before lane departure, depending on if the driver is distracted or not. For all the cases in which the driver was not distracted, the HMI LDW system behaved the same way as Advanced LDW system and received the same outcome. The added benefit of the HMI LDW system comes from the cases in which the driver was distracted, as this increases the TTLC that the warning is delivered. With a driver reaction time of 0.38s, the driver response starts to approach that of the LDP systems and hazards close to the road are able to be avoided. However, for a reaction time of 1.36s, the driver still does not start reacting until after the lane crossing event, and many of the objects close to the road, especially where the vehicle is moving very fast,

are still not avoided with the HMI LDW system. Despite the earlier warning time for distracted drivers, the HMI system was often limited by the driver reaction time.

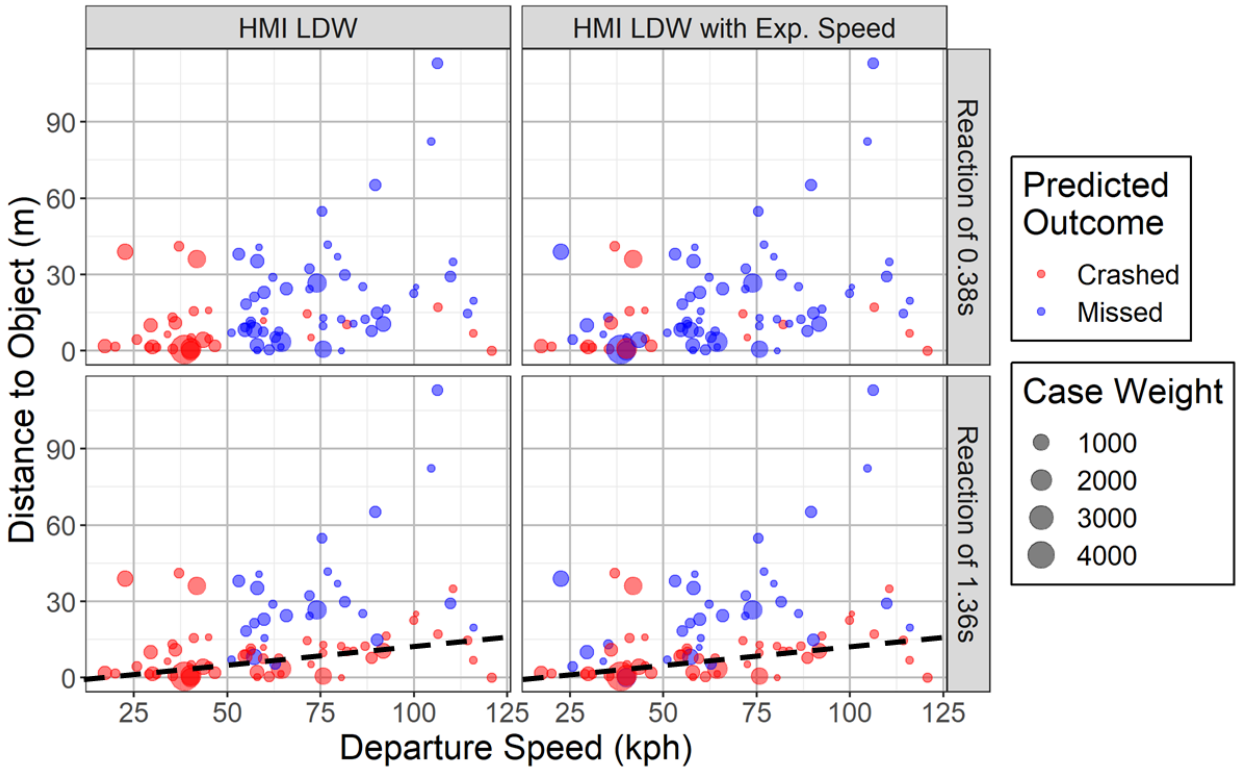

Figure 42. The outcome of each crash based on the departure speed and the straight-line distance to the impacted object from the point of departure for each reaction time for Advanced LDW and Advanced LDW with Expanded Speed Simulations with Heavy Steering and Heavy Braking.

For LDP systems, the vehicle begins steering immediately and does not require driver input. Unlike the LDW systems, a lower boundary does not exist for avoided crashes (Figure 43). This indicates that a LDP system with a 1.0 s TTLC is able to respond before each crash. Some road departure crashes still occurred because the vehicle was unable to completely maneuver out of the path of the hazard. The cases in which the simulated vehicle crashed were based on the unique circumstances of each crash. For example, crashes in which the vehicle departed the roadway at a very large departure angle may be difficult to safely return to the road.

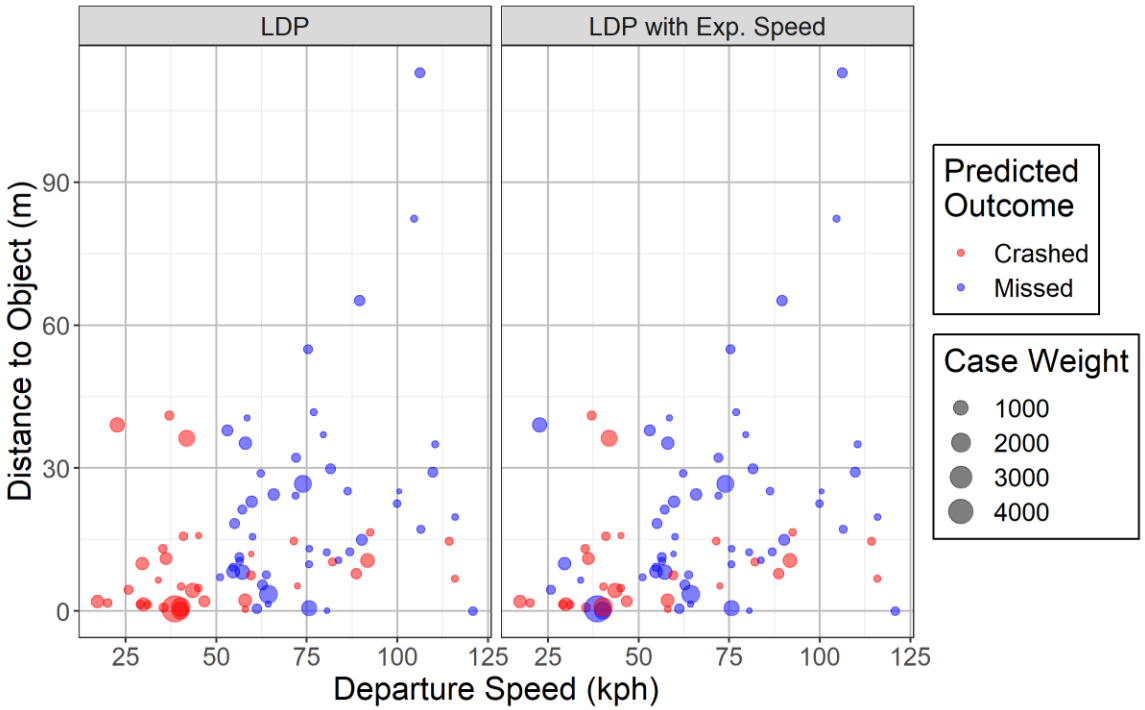

Figure 43. The outcome of each crash based on the departure speed and the straight-line distance to the impacted object from the point of departure for LDP and LDP with Expanded Speed Simulations.

5.5 Residual Crashes

The discussion that follows examines the residual crashes remaining after installation of the LDP with Expanded Speed. The LDP+Expanded Speed model predicted a crash reduction fraction of 68%, the largest safety benefit of all investigated LDW/LDP systems. In our dataset of 81 original crashes, our simulations predicted that 55 cases could be avoided. However, in 26 cases the crash was not avoided. The LDP system was not limited by the driver reaction time as the LDP system activates immediately. Based on the in-depth review of the 26 residual crashes, the crash related factors were grouped into four categories:

- Cases where there was no system activation.
- Cases where the impacted object was within one vehicle width to the travel way/point of departure.
- Cases where the departure angle was relatively large.
- Cases where the vehicle misses the roadside object but does not successfully return to the road due to a very fast departure speed or come to a stop.

Table 15 shows the completed breakdown of the residual crashes into each of these categories. From each category, an example case was chosen for the discussion in this report.

Table 15. Summary of LDP residual crashes by category.

Category	Crashes	Percent	Weighted Crashes	Percent
No System Activation	13	46.4%	5509	57.4%
Close Roadside Object	4	14.2%	1358	14.1%
Large Departure Angle	8	28.6%	1789	18.6%
Parted due to fast speed	3	10.7%	946	9.9%

5.5.1 Cases where there was no system activation

In 13 of the 26 residual crashes, the system did not activate, and there was no difference in the crash outcome, with or without the active safety system. The LDP system did not activate because the vehicle was traveling below the speed threshold. If the speed was under 50 kph, and the driver was not distracted, or if the speed was under 20 kph and the driver was distracted, the system did not activate for these cases and no maneuver was applied. Of the 13 cases in this category, the driver was distracted in 2 cases and not distracted in 11. Figure 44 shows a sample case overlaid onto the original scene diagram for that case. Both the original path and the simulated path are displayed. For cases in which the system did not activate, both the original and simulated vehicle trajectories were identical.

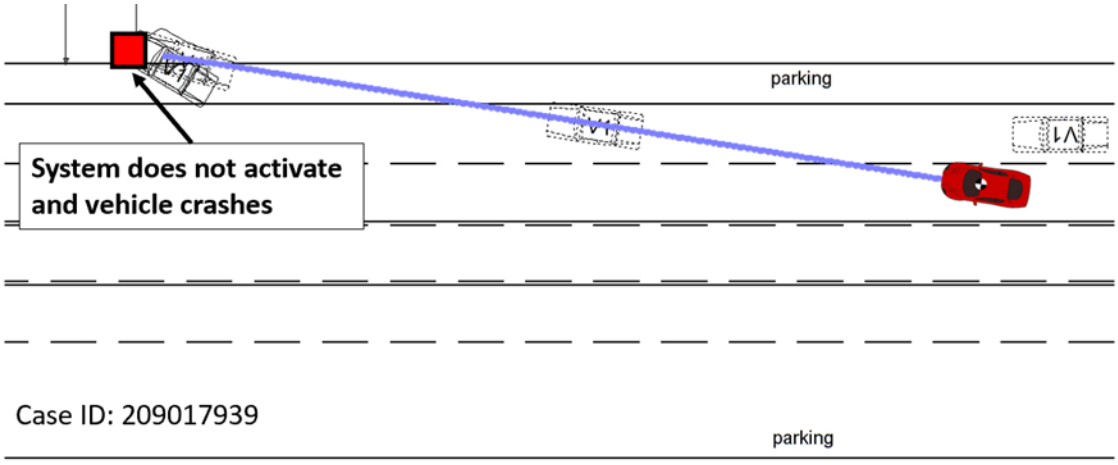

Figure 44. Sample case showing simulated path for in which there was no system activation.

5.5.2 Cases where the impacted object was within one vehicle width to the travel way/point of departure

In 4 of the 26 residual crashes, the impacted object was found to be within one vehicle width of the point of departure. In these cases, the vehicle did not fully leave the roadway in the original crash. All five cases where the vehicle CG did not depart the lane to contact the object, the impacted object was a pole. In these cases, the vehicle does not need to leave the lane at all. In these scenarios, the vehicle was not traveling on an interstate our highspeed roadway (median = 58 kph, max = 75 kph) and because of this the system tends to activate when the vehicle is already very close to the object.

Figure 45 displays an example residual crash in which the impacted object was located at the point of departure. In this case, the vehicle begins to turn 1s before the crash, but is unable to travel laterally

enough to move out of the way of the object. In these cases, the vehicle was still traveling in its original lane when it struck the object.

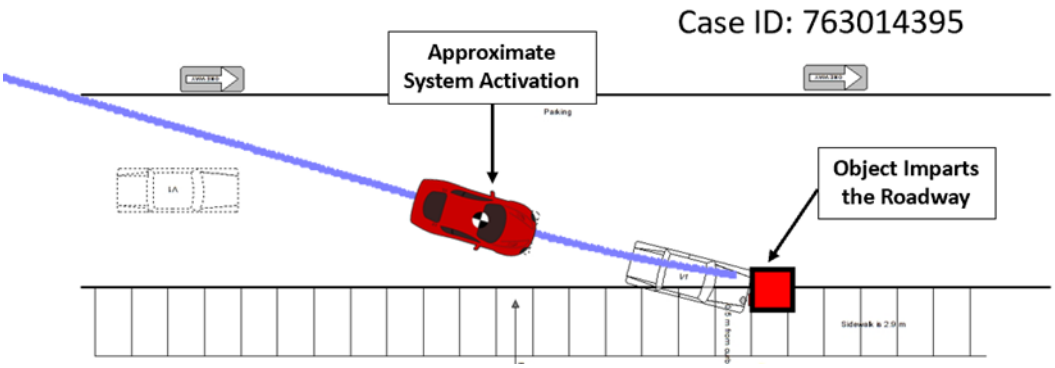

Figure 45. Sample case involving a residual crash in which the impacted object was close to the roadway/point of departure.

5.5.3 Cases where the departure angle was relatively large

In 8 of the 26 residual crashes, a large departure angle was the primary factor for the crash outcome. These crashes are inherently difficult to avoid because larger departure angles require longer recovery paths than cases with smaller departure angles. For a given departure angle, the vehicle will attempt to traverse a curved path of constant radius that is determined based on the maximum yaw rate. Before travelling toward the roadway, the vehicle will continue to travel towards the object until reaching the maximum lateral offset. If the departure angle is large, the maximum lateral extent is also larger, and the recovery path may still intersect the object. A shallower departure would shift the trajectory of the vehicle closer to the road so that the path of the vehicle no longer intersects with the object (Figure 46).

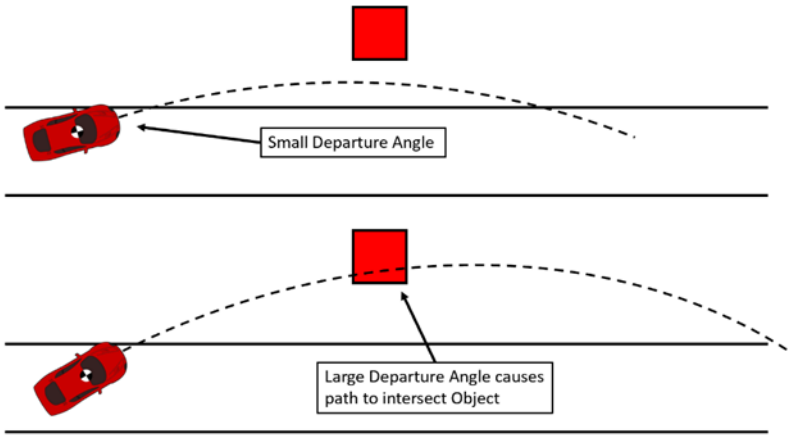

Figure 46. Effect of departure angle on traversed path of the vehicle

Figure 47 displays a sample case where the crash occurred because of steep angle. In this case, if the vehicle had departed at a shallower angle, the impacted object is far enough away from the roadway that the vehicles path would most likely steer clear of the object and return to the road.

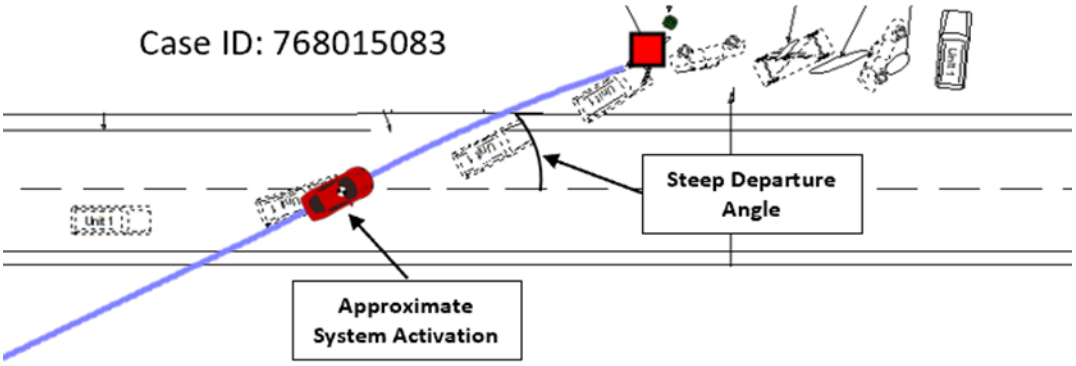

Figure 47. Sample case of a residual crash in which the vehicle departs at a steep angle

5.5.4 Cases in which the vehicle misses the object but does not successfully re-enter the roadway due to large departure speed

In 3 of the 26 residual crashes, the vehicle avoided the impacted object, but the vehicle was unable to return to its initial lane. This simulation is equivalent to a crash due to the likelihood of the vehicle impacting another roadside object. It was assumed that parted outcomes were equivalent to a crash outcome despite avoiding the object, since the vehicle does not return to the road and would likely collide with another object. The vehicle was unable to return to the road due to the speed at which the vehicle is traveling and the curvature of the road. There are two aspects of vehicle physics that are involved in these scenarios. For these simulations it was assumed that the vehicle was neither accelerating or decelerating and maintained its original departure speed. The first being the actual turning radius that the vehicle takes during the simulation. Equation 8 shows the relationship between vehicle speed and vehicle yaw rate. If the turning radius is larger than the road radius of curvature, then the vehicle will never return to the road.

$$turing\ radius = \frac{|\vec{v}|_{vehicle}}{\emptyset_{vehicle}} \tag{8}$$

The second being that the total acceleration of the vehicle is limited to 1g by the friction between the tires and the road. This limit affects the maximum possible turning radius that the vehicle may make. Equation 9 shows the relationship with how this effect turning radius based and turning speed.

$$1g \geq \frac{|\vec{v}|^2{}_{vehicle}}{r_{turning}} \tag{9}$$

In the parted outcomes, the roadway radius was smaller than the turning radius of the vehicle calculated using Equation 2. In these scenarios, the roadway "turns away" from the vehicle faster than the vehicle can turn towards the road. Figure 48 shows a sample case overlaid on the original scene diagram that shows this relationship. When using equation 3 to calculate the maximum possible turning radius for the vehicle, based on the departure speed, it was found that two cases could have been able to return

successfully if the yaw rate was increased, however in one case the maximum curvature that the vehicle could take was still greater than that of the road.

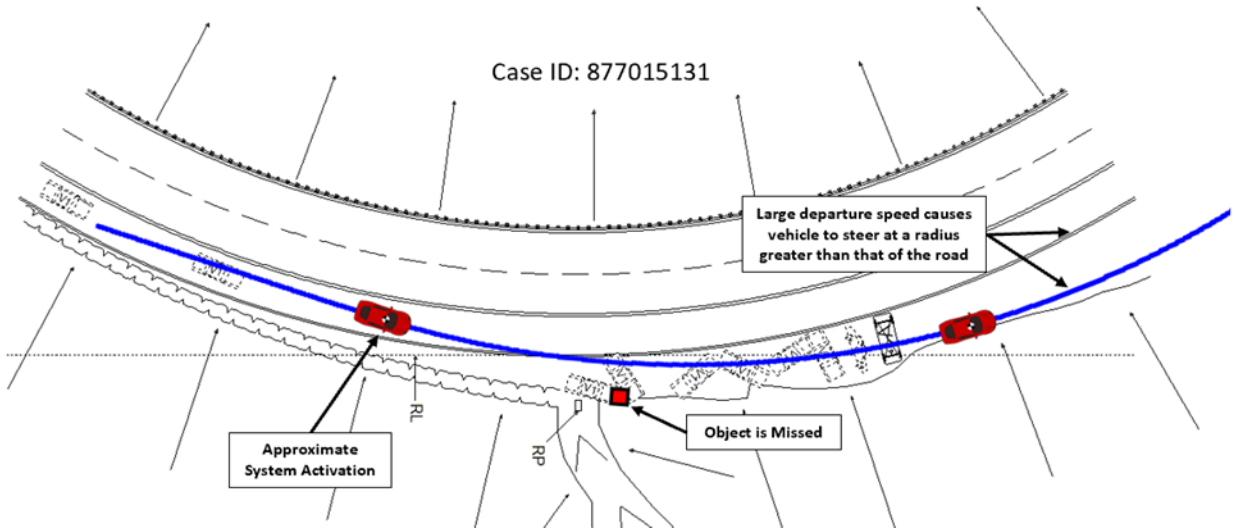

Figure 48. Sample case in which the vehicle misses the impacted object but does not return to the roadway due to the curvature of the road

5.6 Limitations

Our study excluded cases with multiple departures. Additionally, this study assumed that the first impacted object was the only roadside object to be avoided, which may increase the effectiveness estimates. The simulation also assumed that no drivers would overcorrect and depart again. In addition, this study does not include other lane departure crash modes such as control loss and head-on crashes.

For this analysis, the study assumed a uniform size for the impacted object across all trajectories. In reality, the object size varies greatly between case to case. This would then affect which case vehicles would crash and which case vehicles would miss the object as a small object is easier to miss than a larger one. This method of analysis would not be ideal for longitudinal barriers, in which the vehicle may be in contact for more than one trajectory point, however it does work well for trees/poles, which make up 68.8% the impacts used in this study.

Another limitation to the study was that the friction coefficient is assumed to be constant for every case. This would affect a select few cases where road conditions, such as rain and snow, or a change in surface type decreased the turning/braking effects. This study did not account for the grade of the road which could alter the deceleration of the simulated vehicles. However, this effect is likely overcome by any braking performed by the driver.

The vehicle model limited the acceleration to 1 g. This represents the upper limit of the tire force available for a maneuver. Due to tire tread, the driving surface, and the shape of the vehicle, the actual tire force is likely much lower.

The driver distraction during the original crash was determined based on the CDS investigator. Driver distraction was often unknown and could be underreported during interviews with the driver. Unless the investigator indicated the driver was distracted, the assumption was that the driver was attentive. This is a conservative assumption since every modeled system would deliver the warning later or at higher activation speed.

There are a number of sources of error which present a challenge to identify the error on the benefit estimates for each system. These error sources include the CDS sampling error, vehicle location in the scene diagram, EDR temporal sampling error, EDR measurement error, distribution of driver maneuvers, and the error associated with the driver response time. Despite the assumptions necessary to compute the benefit estimates, the trends found when comparing the systems would be unaffected. Future studies could utilize a monte carlo simulation technique which would allow for the overall error to be estimated.

5.7 Conclusions

The estimated effectiveness LDW systems in road departure crash scenarios was 15%. However, more advanced LDW systems that could deliver warnings before leaving the lane had a higher predicted benefit of 22% to 29%. LDP systems performed the best and had an estimated effectiveness of 40%. Any system that could activate at lower speeds also had an increased benefit. The LDP systems, which could activate up to 1 s before the lane departure, were shown to not be limited by the time to impact unlike previous systems. Instead, the majority of crashes with an LDP system occurred because the vehicle was not travelling above the activation threshold. In the cases where the LDP system did activate, the vehicle was unable to avoid the object and return to the road because either the object was very close to the road edge, the vehicle departed at a large angle, or the vehicle was travelling too quickly to return to the road given the LDP system's steering limit. These four residual crash types should be the priority of future road departure crash technology.

6 PREDICTING THE FUTURE OF ROAD DEPARTURE CRASHES

6.1 Purpose

The purpose of this chapter is to estimate the reduction of DrOOL road departure crashes and injuries in the future due to LDW and LDP systems.

6.2 Methodology

6.2.1 Data Selection

There were 81 vehicles in the simulation dataset from Chapter 5. After applying NASS/CDS sampling weights, this represented 29,315 real world crashes.

6.2.2 LDW/LDP Crash Benefits

The crash reduction benefits of LDW/LDP systems in road departure crashes was estimated in chapter 5 (Figure 49). The model predicted that LDW systems would prevent between 15% and 45% of road departure crashes depending on the system configuration. LDP systems were more effective and were predicted to prevent up to 67% of road departure crashes. For any crash that was avoided in the model, the probability of injury was set to zero. Because the driver reacted to the warning system, the impact speed changed, which may have changed the probability of injury.

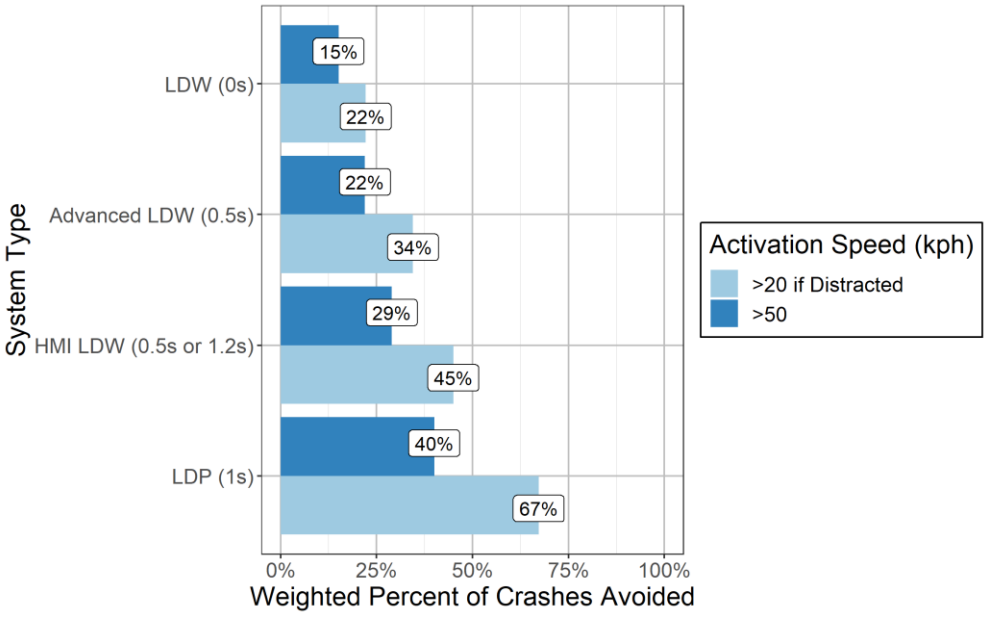

Figure 49. Weighted percent of crashes avoided for each system model and activation speed.

6.2.3 Injury Model

The probability of front occupant sustaining an MAIS 2+F injury for road departure crashes was estimated using the injury model developed by Bareiss using NASS/CDS frontal crashes [61]. The logistic injury model has seven inputs: delta-v, belt use, sex, age, crash compatibility, BMI, and striking location (Table 16). Higher injury severity models lacked enough injured cases to construct a detailed model of occupant injury. The injury model was constructed based on the injury data of front seat occupants at least 12 years old involved in a frontal crash with another vehicle. For road departure crashes, however, the subject vehicle impacted a roadside object not another vehicle. Thus, in road departure crashes the crash compatibility and striking location were zero. The delta-v for road departure crashes was estimated to be 67% of the impact velocity to match the actual number of injured occupants. Of the 81 simulated cases, 58 cases involving 71 occupants contained all the information necessary to utilize the injury model. Since the simulated cases were DrOOL road departure crashes, no cases involved control loss which could result in a side impact. If the vehicle stopped or returned to the lane, the probability of an occupant sustaining a MAIS2+F injury was assumed to be zero. For crashed and parted simulation outcomes, the last velocity was assumed to be the impact velocity.

Table 16. Frontal impact injury model [61].

Variable	Parameter	Estimate	Standard Error	p-value
Intercept	--	-6.516	0.863	<0.001
Total Delta-V	Delta-V (kph)	0.090	0.019	<0.001
Belt Use	Belted	-0.769	0.396	0.054
Sex	Male	-0.891	0.333	0.008
Age	≥65	1.070	0.492	0.031
Crash Compatibility	Car Struck LTV	1.222	0.368	0.001
BMI	BMI (kg/m^2)	0.084	0.021	<0.001
Striking Location	Rear	-1.455	0.501	0.004

6.2.4 Estimating Injury Benefit and Population Attributed Risk

The population attributed risk, or injury benefit, for multiple covariates was computed following Bruzzi's methodology, which applies the logistic model to the population with countermeasures [62]. For each simulated system configuration, the estimated number of injuries was computed using Equation 10 below. The standard errors from the logistic model were used in the calculation to compute 95th percentile confidence intervals of all estimates. The estimated injury reduction for each system configuration was computed relative to the predicted number of injured occupants in the baseline configuration.

$$Predicted\ Injuries = \sum_{i=1}^{71} Probability\ of\ Injury * Case\ Weight \qquad (10)$$

6.2.5 Future Fleet Prediction

The annual number of crashes in the US is related to the annual vehicle miles traveled (VMT), which is an estimate of exposure. In 2015, there was an estimated 3.1 trillion miles traveled in the US [63]. The annual VMT historically increases by about one percent each year (Eq .11) [63]. Based on a 1% annual increase, the future annual VMT was estimated (Figure 50).

$$Future\ VMT = VMT_{2015} 1.01^{(year-2015)} \tag{11}$$

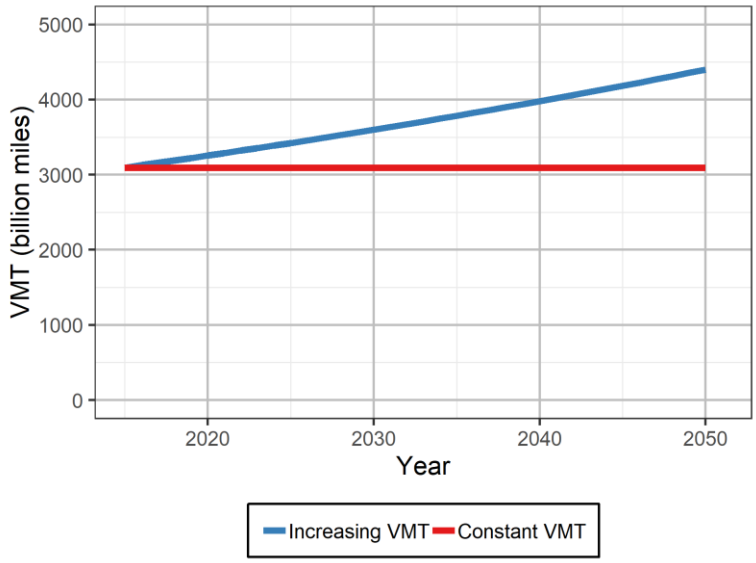

Figure 50. Annual vehicle miles traveled (VMT) by year.

In order to predict the number of crashes that could occur in the future, it was assumed that the crash rate, the number of crashes per VMT, remained constant (Eq. 12). The annual crash rate for DrOOL road departure crashes was computed based on the average annual number of crashes in NASS/CDS 2010 to 2015. There were on average 131,923 road departure crashes annually (acctype = 1 or 6) involving a single passenger vehicle that did not rollover. The estimated crash rate for road departure crashes was 43.3 crashes per billion VMT. The ratio of MAIS2+F injured front seat occupants was computed using the same methodology. In NASS/CDS, if the vehicle's model year was greater than 10 years old, a full investigation was not performed. This means that the occupants of these old vehicles are missing injury information. To account for these injured occupants, the ratio of injured occupants to total occupants was assumed to remain constant between the known and unknown occupants. For road departure crashes, there were 130,786 known front seat occupants at least 12 years old with 15,344 injured occupants resulting in an injury rate of 11.7%. Overall, there was an estimated 15,608 occupants injured in road departure crashes without a rollover. The estimated injured occupant rate for road departure crashes was 5.1 injured occupants per billion VMT.

$$Crash\ Rate_{2015} = \frac{Number\ of\ Crashes\ in\ 2015}{(VMT_{2015})(1 - LDP\ Penetration * LDP\ Effectiveness)} \quad (12)$$

The predicted number of future road departure crashes is dependent on the penetration of LDW systems into the US fleet. The fleet penetration of LDW was estimated by HLDI in 2018 [64] (Figure 51).

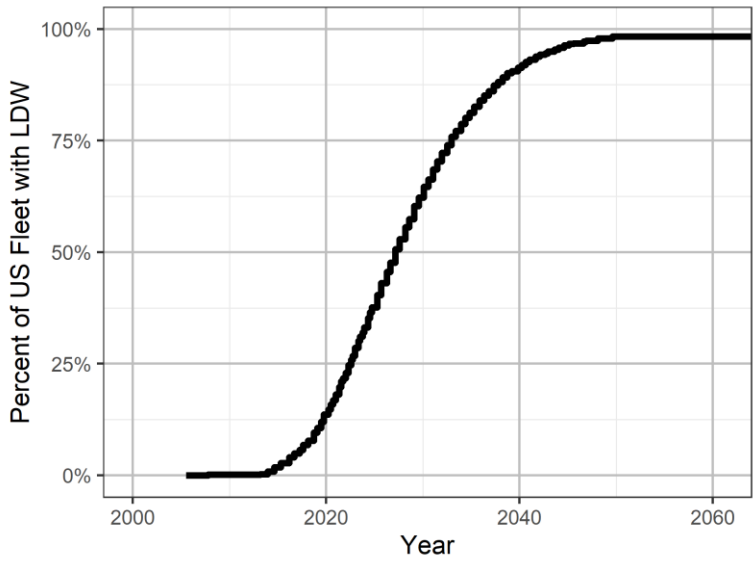

Figure 51. Fleet penetration of LDW in the US fleet as predicted by HLDI.

The crash reduction was computed as the product between the annual VMT, crash rate, LDW effectiveness, and the probability that the vehicle had LDW (Eq. 13). The same process was used to estimate the number of MAIS2+F injured front seat occupants (Eq. 14). In NASS/CDS, if the vehicle's model year was greater than 10 years old, a full investigation was not performed. This means that the occupants of these old vehicles are missing injury information. To account for these injured occupants, it was assumed that the ratio of injured occupants to total occupants remained constant between the known and unknown occupants.

$$Predicted\ Crashes = VMT * Crash\ Rate * LDW\ Eff_c * P(LDW)_i \quad (13)$$

$$Predicted\ MAIS2+F\ Injured\ Occupants = VMT * Injury\ Rate * LDW\ Eff_i * P(LDW)_i \quad (14)$$

6.3 Results

6.3.1 Residual Injuries

The 58 simulated crashes used to predict the reduction in MAIS 2+F injured persons contained 71 occupants of which 29 occupants sustained at least one MAIS2+F injury. This represents 3,066 MAIS 2+F injured occupants in road departure crashes nationally. For the baseline simulation, which represents the original crash outcome, the injury model predicted 3,060 MAIS 2+F injured occupants (Table 17). The expanded activation speed systems had a small increase in injured occupant reduction compared to the base system. The injury reduction is modest since the additional crashes prevented with the expanded activation

threshold are at low impact velocities and have a lower probability of an MAIS2+F injured occupant. The LDP with expanded speed was the only system to not have an injury benefit larger than the crash benefit. This is because nearly all of the additional crashes avoided with the expanded speed system were missing occupant injury information or did not result in an injury.

Table 17. The predicted injury benefit for each simulated system.

Simulation	Percent Crash Reduction	MAIS 2+F Injured Occupants with CI	Percent MAIS 2+F Injured Occupant Reduction with CI
Baseline	0%	3,060 ± 570	0%
LDW	15%	2,540 ± 200	17% ± 17%
LDW with Expanded Speed	22%	2,510 ± 200	18% ± 17%
Advanced LDW	22%	1,950 ± 160	36% ± 13%
Advanced LDW with Expanded Speed	34%	1,910 ± 160	37% ± 13%
HMI LDW	29%	1,680 ± 150	45% ± 11%
HMI LDW with Expanded Speed	45%	1,630 ± 150	47% ± 11%
LDP	40%	1,280 ± 370	58% ± 14%
LDP with Expanded Speed	67%	1,230 ± 150	60% ± 14%

6.3.2 Future Fleet Benefit

Using the 67% crash effectiveness of LDP with the expanded activation speed for road departure crashes and the market penetration, an estimated 26.1% of crashes will be prevented in 2025 (Figure 52). The predicted number of MAIS2+F injuries was reduced by 23.3% by 2025 (Figure 53).

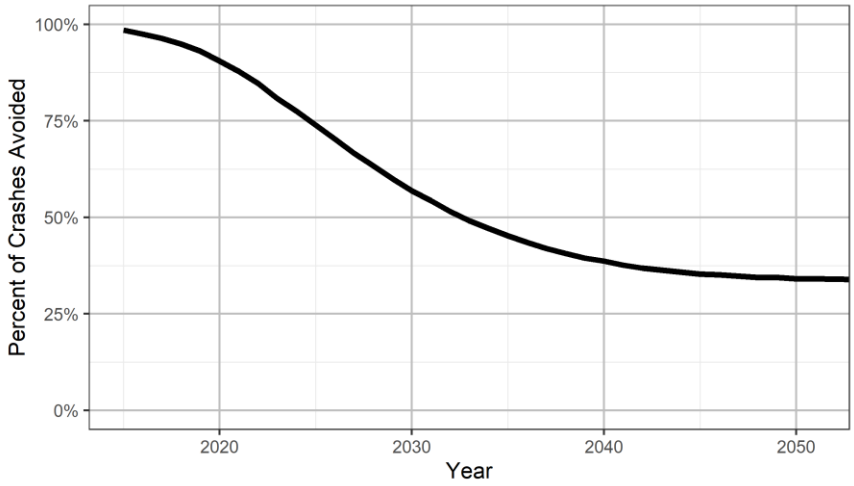

Figure 52. Predicted percent of road departure crashes avoided by LDP.

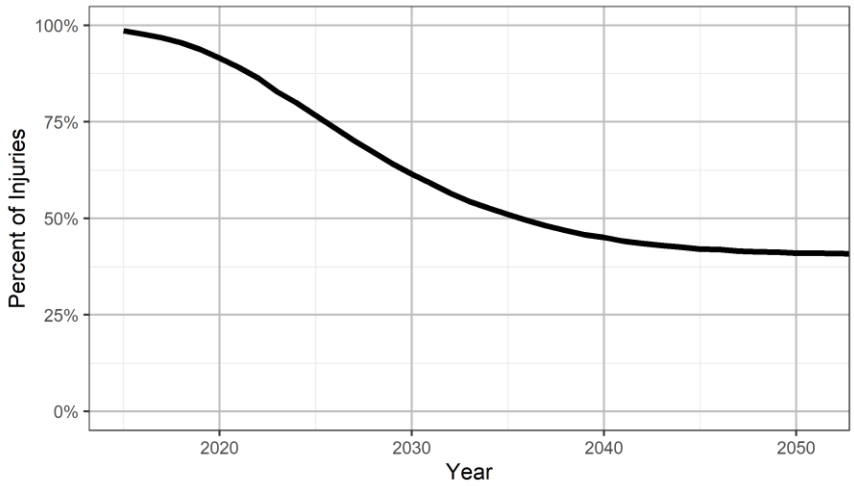

Figure 53. Predicted percent of MAIS2+F injured occupants in road departure crashes prevented by LDP.

In 2025, there will be an estimated 107,851 road departure crashes with LDP resulting in 13,229 MAIS2+F injured occupants assuming an increasing VMT (Figure 54 and Figure 55).

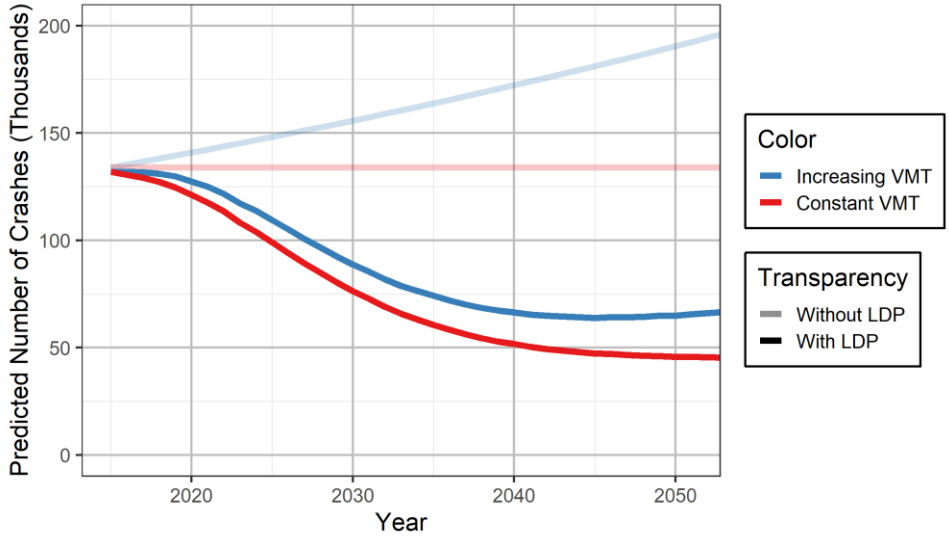

Figure 54. Predicted number of road departure crashes.

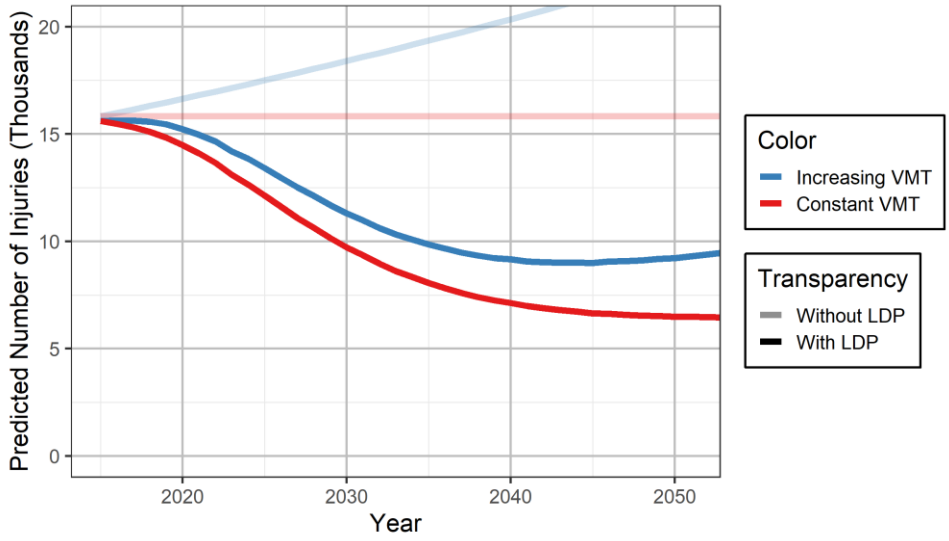

Figure 55. Predicted number of MAIS2+F injured occupants in road departure crashes.

6.4 Discussion

The introduction of LDP systems, which can activate before leaving the roadway, has the potential to greatly reduce the number of DrOOL road departure crashes and their resulting injuries. The crash and injury prediction for increasing VMT was always higher than for a constant VMT because it was assumed that the number of crashes increases with VMT. This relationship predicts that the increase in crashes will surpass the benefit from LDP systems entering the fleet in 2046 and the number of DrOOL road departure crashes and resulting injuries will begin to increase. Continued development of road departure prevention systems will be necessary to reduce the number of crashes after 2046.

6.4.1 Validation

The CISS dataset from 2017 to 2019 was used to identify DrOOL road departure crashes to understand how the future predictions compare over this short time frame. For reference, the average crashes and injured occupants in CDS from 2011 to 2015, which was used as the initial point for the prediction model, and the values from CDS in 2015 are provided as reference (Table 18). Since CISS has a slightly different sample population, NHTSA provided a new variable for case year 2019 that allows a CDS equivalent population to be determined. In general, the estimated crashes and injuries in CISS are higher than the predicted values but are also much higher than the values reported in CDS for the same population. In addition, the sampled CISS cases are more likely to have known occupant injury outcomes because they resampled if the injuries in recent vehicles were unknown. Within CISS, the number of tow-away DrOOL road departure crashes changed by over 45,000 crashes. The large variance in CISS cases makes it challenging to compare with the prediction since it is unlikely that the actual number of road departure crash would have these fluctuations.

Table 18. Comparison of CISS 2017 to 2019 to the predicted DrOOL crashes and injured occupants.

Case Year	CDS/CISS (Actual)		Prediction (Constant VMT)		Prediction (Increasing VMT)	
	Crashes	MAIS2+F Injured	Crashes	MAIS2+F Injuries	Crashes	MAIS2+F Injured
2010-2015	131,923	15,608	131,923	15,608	131,923	15,608
2015	113,331	13,686	-	-	-	-
2016	-	-	130,576	15,466	131,895	15,622
2017	216,577	27,713	129,140	15,314	131762	15,625
2018	196,950	28,560	127,165	15,105	131,057	15,567
2019	169,987	22,269	124,651	14,839	129,764	15,447
2019 (CDS Equivalent)	168,413	22,246	124,651	14,839	129,764	15,447

6.4.2 Limitations

The injury model predictions are largely dependent on the delta-v of the frontal crash. Because roadside objects have varying geometry, mass, and deformation extents, estimating the delta-v is often unclear. The impact speeds were scaled to estimate the delta-v to match the actual crash injury outcomes in the baseline configuration.

The simulations assumed the LDP system was always activated and the driver would not intervene during the automated steering. In some real LDP systems, the system deactivates if the driver provides steering input or pedal application. The LDW/LDP systems were simulated in isolation and did not consider any possible interactions with other active safety systems such as AEB.

These predictions assumed that the VMT, the number of crashes, the number of injuries in DrOOL road departure crashes, in the absence of LDW/LDP systems, only increases by 1% each year. This methodology cannot account for sudden changes to the transportation habits of Americans due to events such as world-wide pandemics. This methodology also assumed that the best simulated system, LDP with expanded activation, would follow the LDW market penetration curve. More advanced systems, like this one, would likely arrive later to the market than LDW systems and LDW systems would be phased out.

6.5 Conclusions

LDW was predicted to reduce the number of injured front occupants by 17% in road departure crashes. LDW/LDP systems that activate earlier or at lower speed thresholds had higher injury benefits. The best system, LDP with expanded activation speed, was predicted to reduce the number of injured front seat occupants by 60%. In 2025, there will be an estimated 26% reduction in road departure crashes and a 23% reduction in injured front seat occupants due to the market penetration of these systems.

7 CHARACTERIZATION OF HEAD-ON CRASHES

7.1 Purpose

The objective of chapter 7 was to determine the frequency of and to characterize head-on crashes in the U.S. as a basis for evaluating active safety countermeasures.

7.2 Approach

7.2.1 Data Selection

All recorded opposite direction crashes that occurred between 2011 and 2015 were extracted from NASS/GES, NASS/CDS, and FARS. These three databases were selected to cover a large range of crash severities from police reported crashes (GES), and moderate to fatal injurious crashes (CDS), to fatal crashes (FARS).

The two most common opposite direction crashes were sideswipe and cross-centerline head-on crashes (Figure 56). Fatal and moderate injury crashes were overrepresented among cross-centerline head-on crashes. In contrast, sideswipe crashes were much less likely to result in a moderate to fatal injury. Therefore, for the remainder of this dissertation, cross-centerline crashes will be the focus (Table 19).

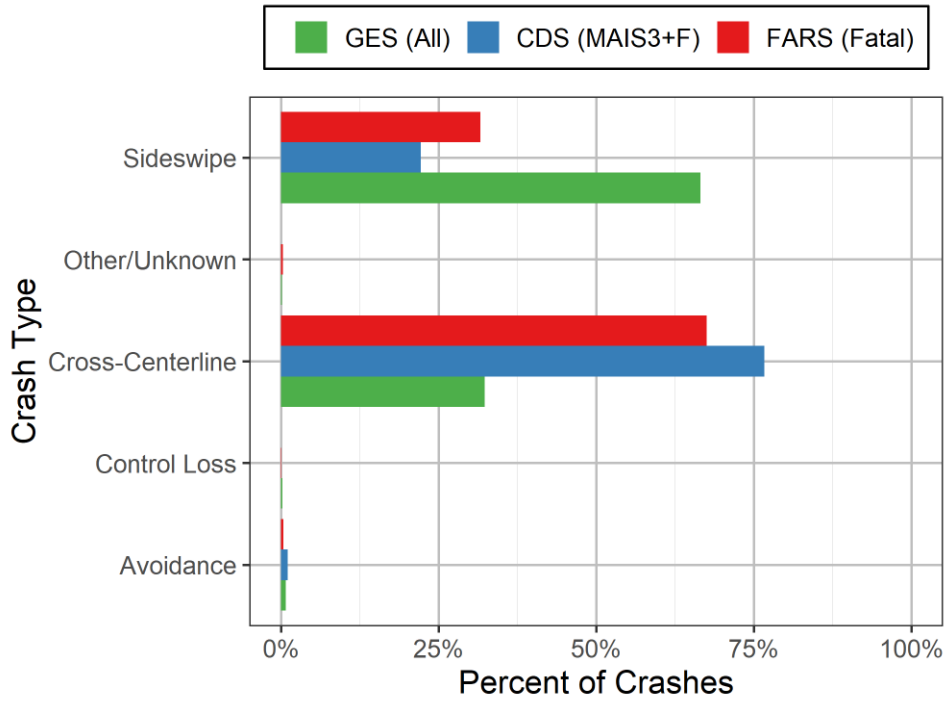

Figure 56. The distribution of opposite direction crash types.

Table 19. Number of analyzed cases across each of the datasets.

Dataset	Population	Injury Severity	Weighted Crashes (unweighted)	Weighted Occupants (unweighted)
NASS/GES	All Police-Reported DrOOL Crashes	All	171,082 (3,045)	481,941 (8,763)
NASS/CDS	Tow-Away DrOOL Crashes	MAIS 3+F	13,711 (136)	16,553 (171)
FARS	DrOOL Crashes with a Fatally Injured Occupant	Fatal	12,695	15,765

7.2.2 Analyzed Parameters

For every DrOOL head-on crash in each database, factors were analyzed from four main characteristics: road/environment, vehicle, driver, and occupants (Table 1). The road/environment characteristic was analyzed for each case since every vehicle and occupant in the crash interacts with a road/environment.

Table 20. Data elements for in-depth characterization.

	Characteristic	Factors	Data Source
Crash Causation	Road/Environment	Speed Limit	All
		Road Alignment	All
		Number of Lanes	All
		Weather Condition	All
		Surface Condition	All
		Roadway Lighting	All
	Driver	Avoidance Maneuver	All
		Demographics (age, sex)	All
		Alcohol Involvement	All
		Drug Involvement	All
		Pre-crash Avoidance Maneuvers	All
Injury Causation	Vehicle	Model Year	All
		Rollover	All
	Occupants	Demographics (age, sex)	All
		Belt Use	All
		Ejection	All
		Seat Location	All

7.3 Results

Fatal head-on crashes were overrepresented on 55 mph roads and underrepresented at speeds below 35 mph (Figure 57). This may be due to the fact that slower moving vehicles likely have a lower crash delta-v, which reduces the chance of a fatal injury. Most head-on crashes occur on straight sections of roads (Figure 58).

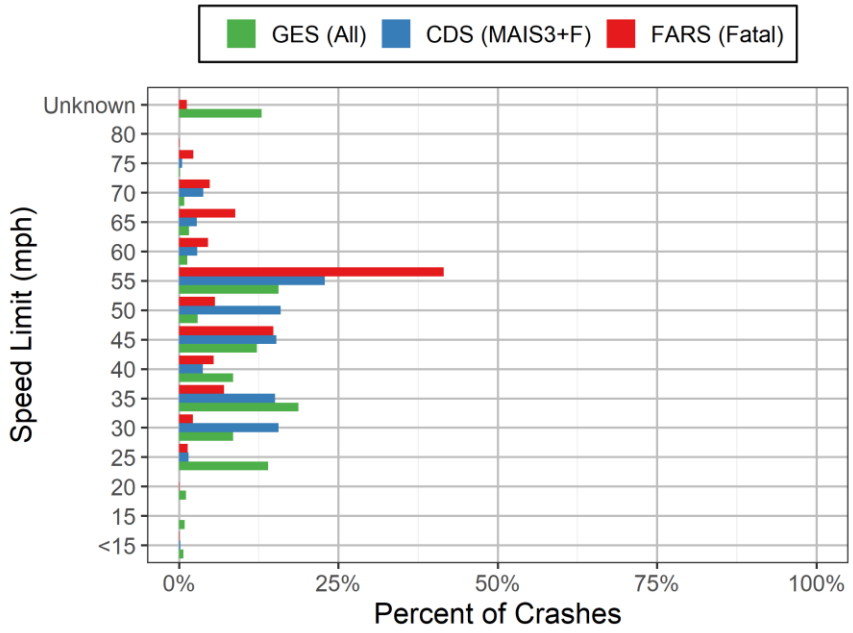

Figure 57. Distribution of speed limit among cross-centerline head-on crashes.

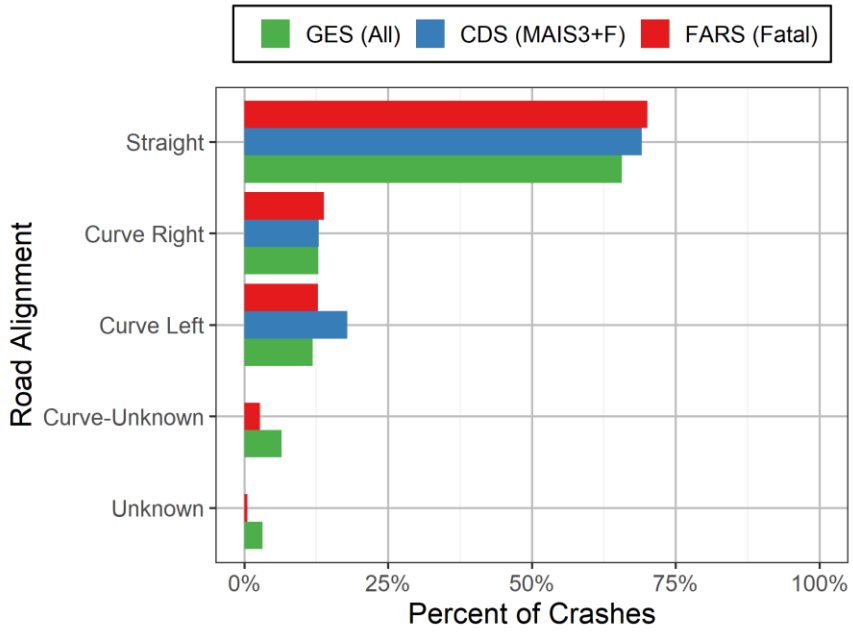

Figure 58. Distribution of road alignment for cross-centerline head-on crashes.

Two-lane roads were the most common location of head-on crashes but these roads are also one of the most common roadway types in the US (Figure 59). Following the NASS/CDS definition, this counts all lanes on undivided roads and the lanes in the same direction for divided roads. Unlike road departure crashes in Chapter 1, more than half of all head-on crashes occurred during the day (Figure 60).

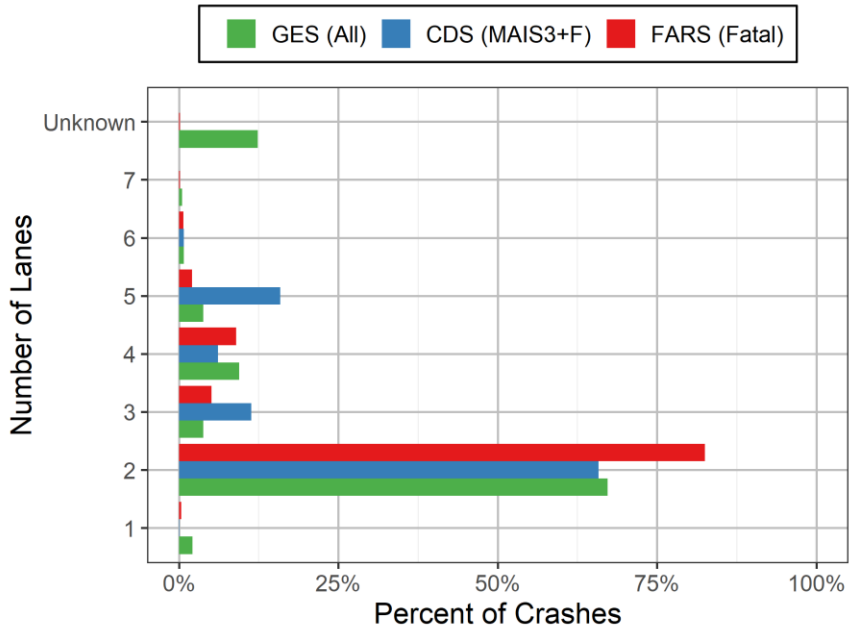

Figure 59. The number of lanes for head-on crashes.

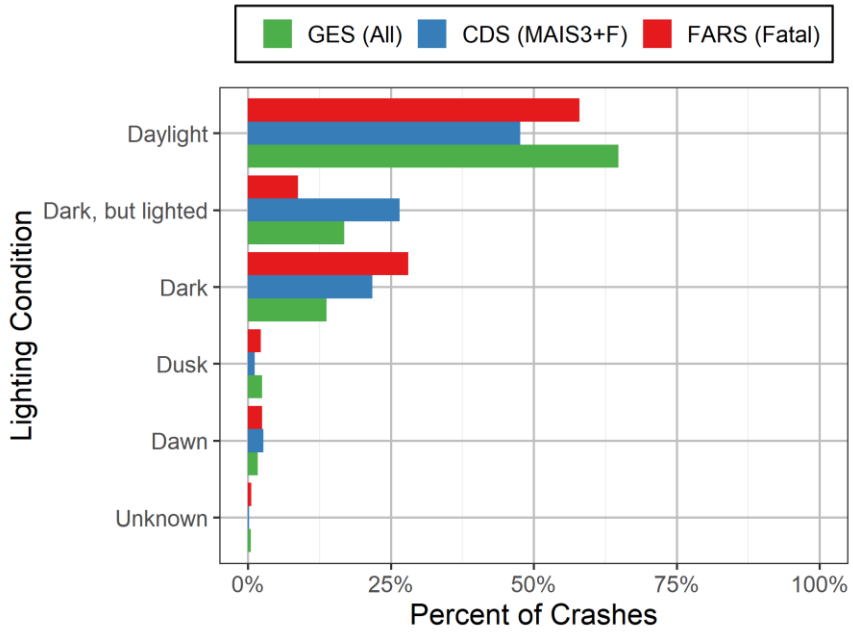

Figure 60. Distribution of lighting conditions in head-on crashes.

Most crashes occurred during typical clear days with dry roads (Figure 61 and Figure 62).

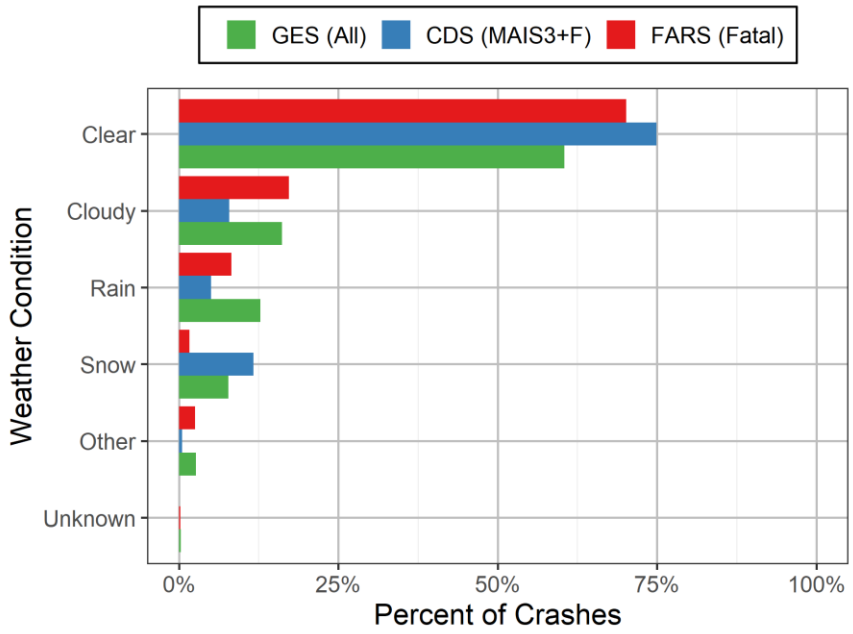

Figure 61. Weather conditions during head-on crashes.

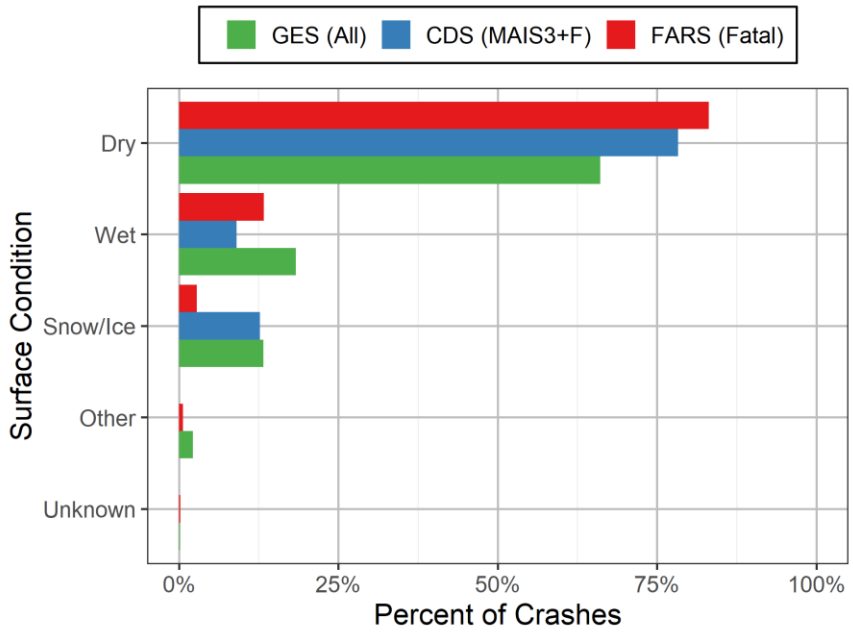

Figure 62. Surface conditions during head-on crashes.

In almost all head-on cases in FARS, NASS/CDS, and NASS/GES, there was either no evasive maneuver or the maneuver was unknown (Figure 63). Because of the lack of insight from these datasets, Chapter 4 will characterize the evasive actions using EDR information. Rollovers occur after less than 2% of all head-on crashes (Figure 64).

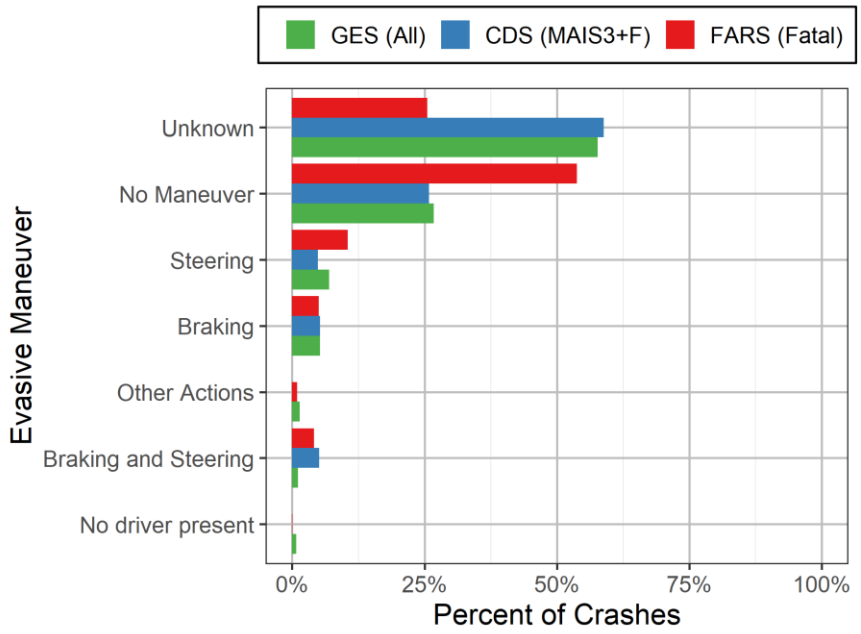

Figure 63. Distribution of evasive maneuvers for head-on crashes.

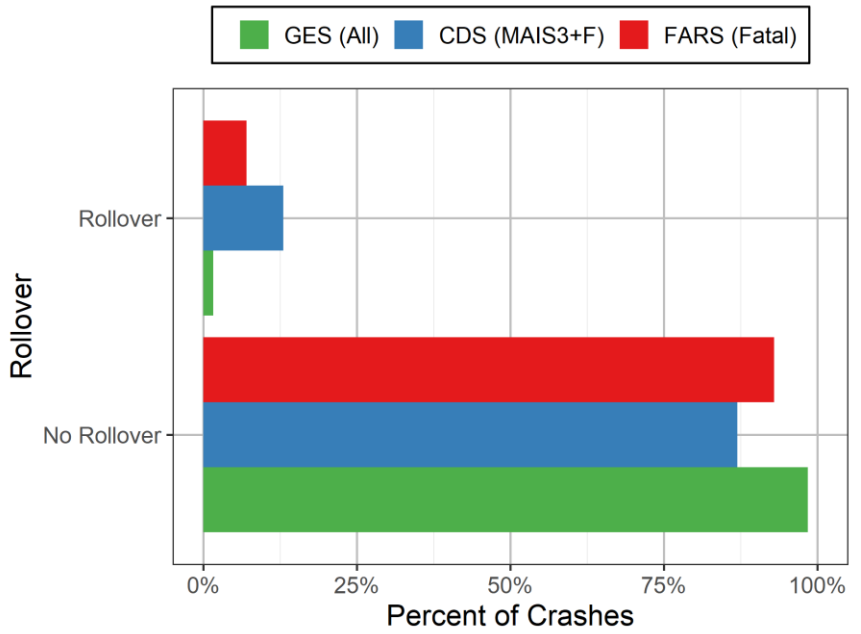

Figure 64. Occurrence of rollovers after head-on crashes.

The age distribution of drivers involved in head-on crashes is relatively evenly distributed between the ages of 25 and 70 years old (Figure 65). Fatally injured drivers tend to be older than the general driver population involved in these head-on crashes. Male drivers were more frequently involved in a head-on crash (Figure 66).

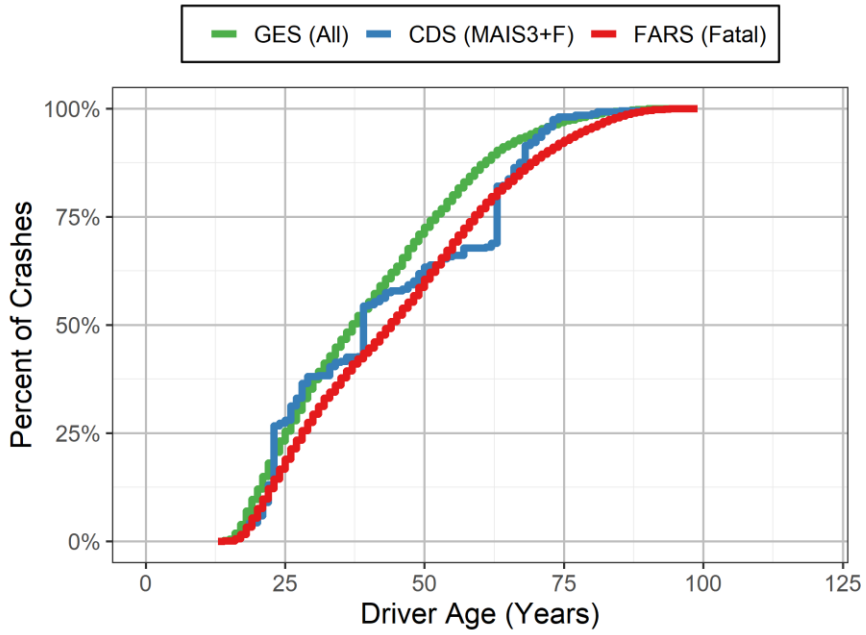

Figure 65. Age distribution of drivers involved in head-on crashes.

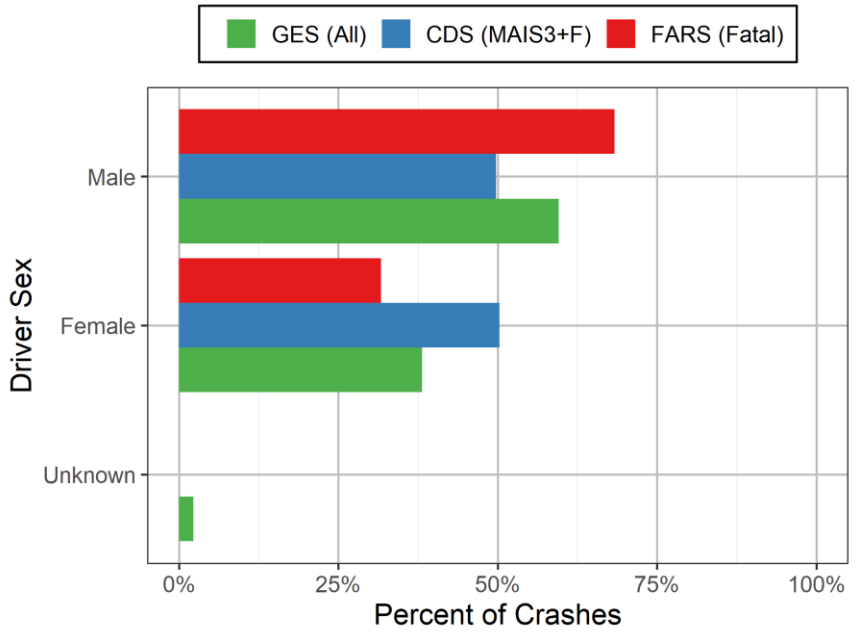

Figure 66. Sex of drivers involved in head-on crashes.

More severe crashes were overrepresented among cases that involved alcohol or other impairing drugs (Figure 67 and Figure 68). However, it should be noted that these counts are based on police assessment of alcohol or drug involvement and may not always rely on a test. This could bias the results toward none or unknown involvement.

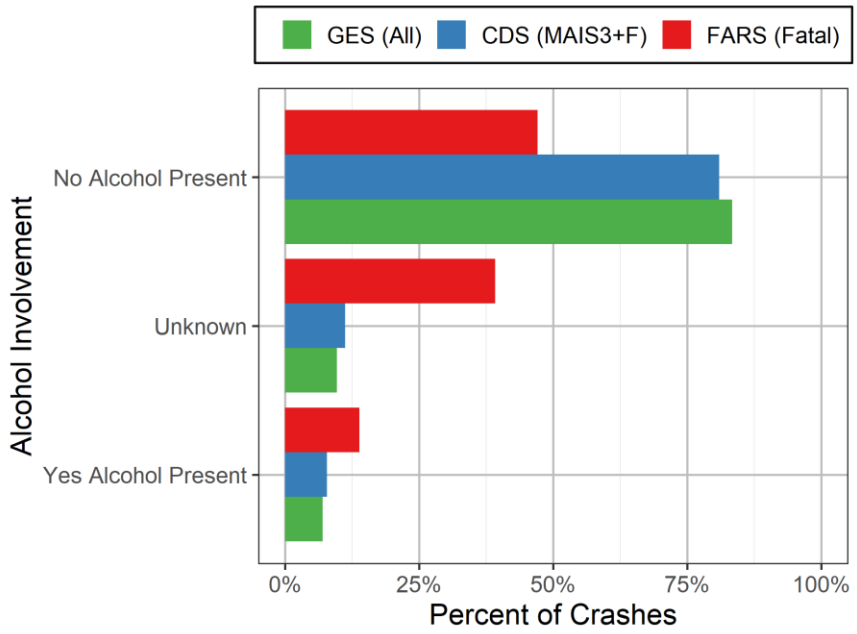

Figure 67. Percentage of head-on crashes involving alcohol.

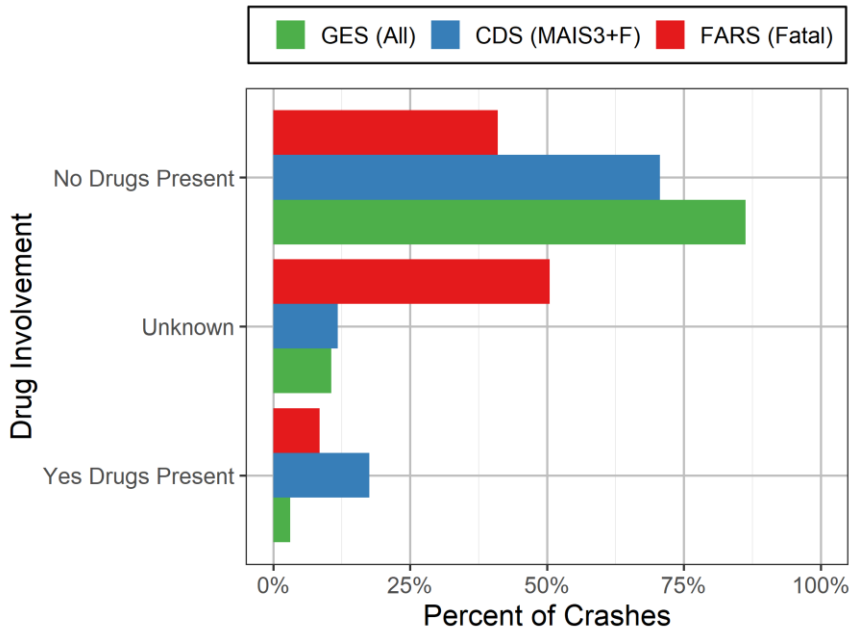

Figure 68. Percentage of head-on crashes involving other impairing drugs.

Before the centerline crossing event, nearly all drivers in a head-on crash were not attempting any maneuver such as turning on to a new road (Figure 69). The model year of vehicles in fatal head-on crashes is essentially the same as the model year of all DrOOL road departure crashes (Figure 70). CDS does not follow the same curve because NHTSA purposely sampled vehicles that were less than 10 years old.

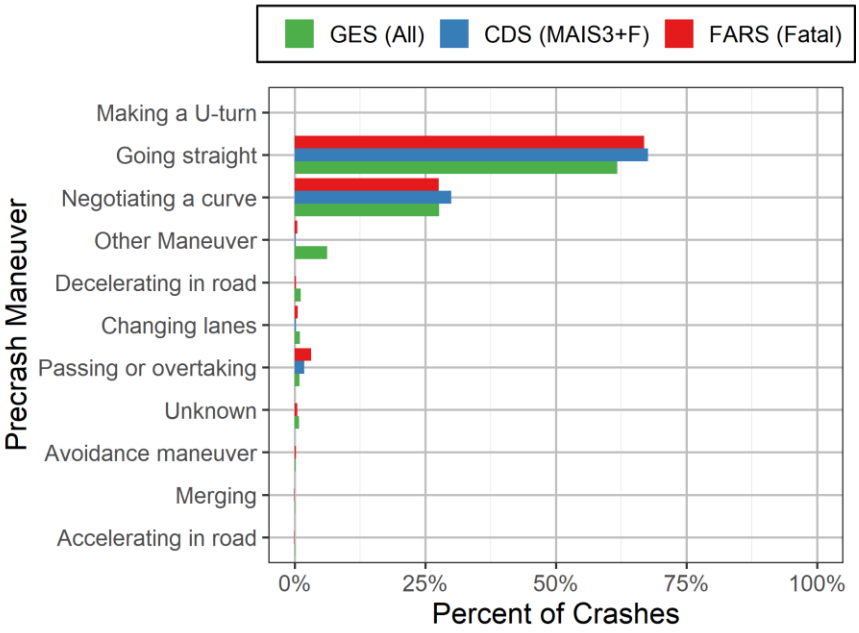

Figure 69. Distribution of driver maneuvers before the centerline crossing event.

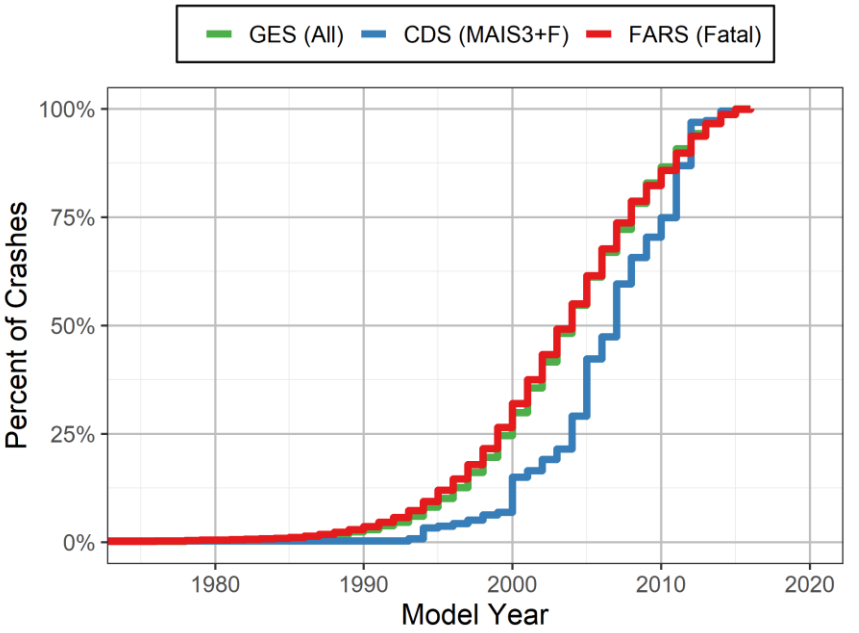

Figure 70. Model year distribution for vehicles involved in head-on crashes.

Nearly three-quarters of the occupants in head-on crashes are in the driver seat (Figure 71). Since most of these vehicles contain a single occupant, there is a drastic increase in the frequency of drivers after occupants reach licensing age (Figure 72). Similar to the driver age distribution, more severe crashes tended to have older occupants.

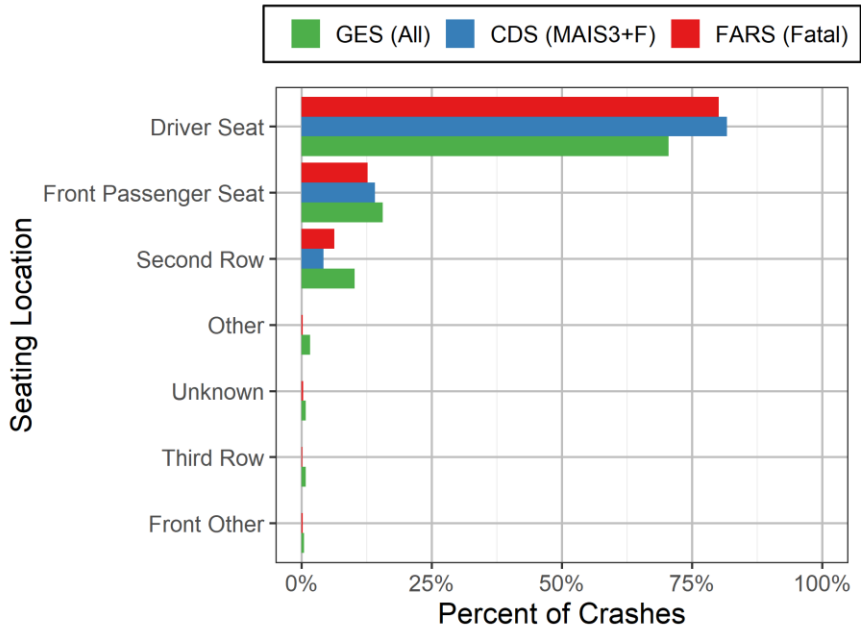

Figure 71. Distribution of occupant seating locations during head-on crashes.

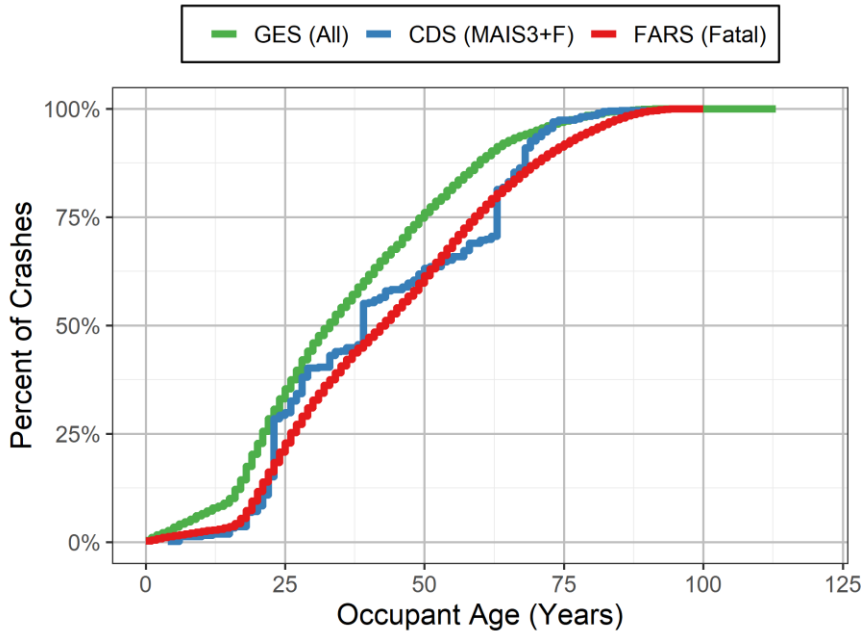

Figure 72. Age distribution of occupants involved in head-on crashes.

Moderate to fatally injured occupants were more likely to be unbelted during head-on crashes (Figure 73). Occupants were rarely ejected during head-on crashes (Figure 74).

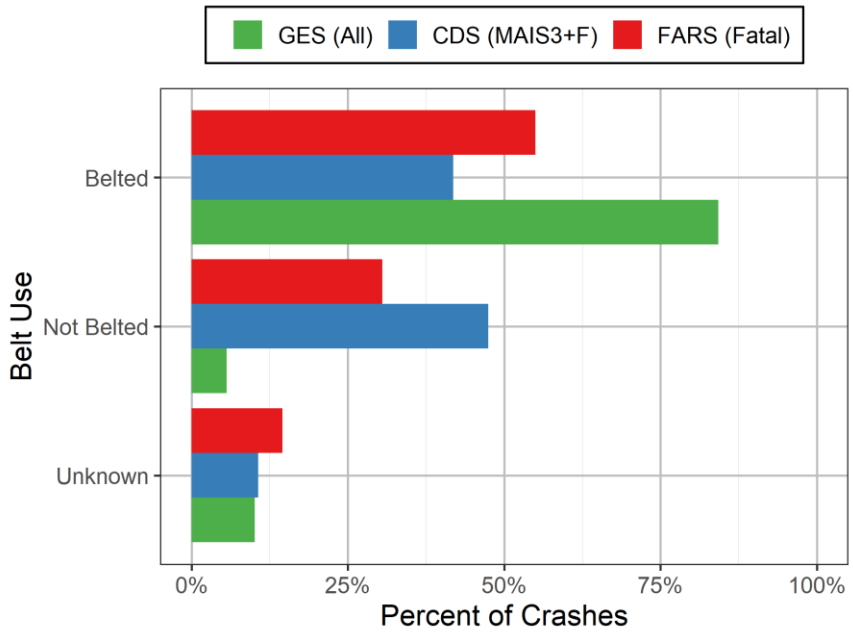

Figure 73. Distribution of occupant belt use during head-on crashes.

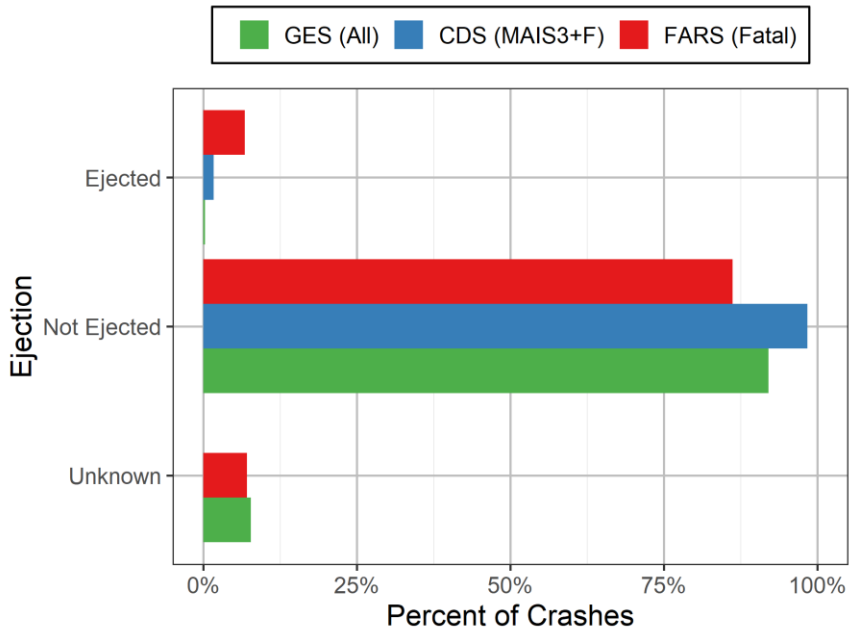

Figure 74. Occurrence of occupant ejection during head-on crashes.

Similar to the distribution for drivers, most of the occupants in head-on crashes were male (Figure 75).

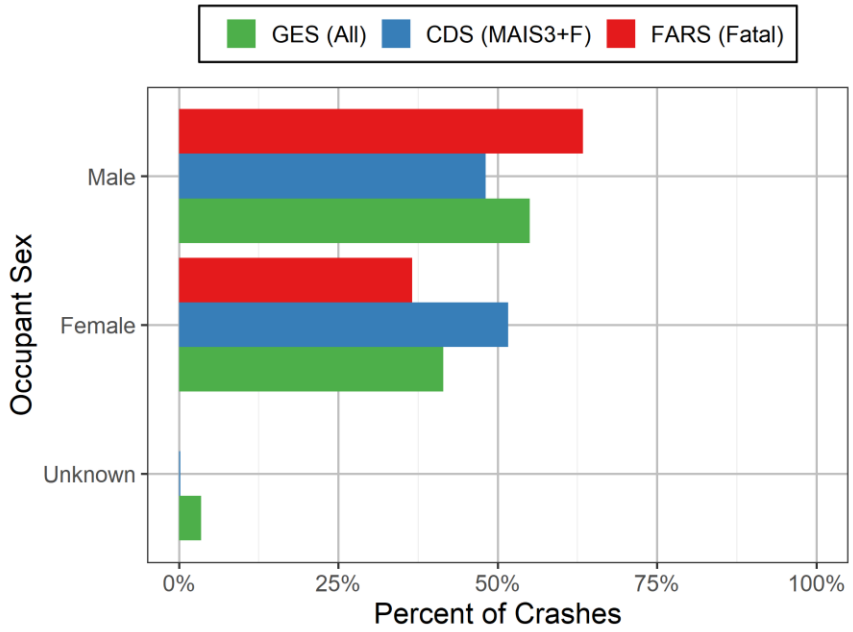

Figure 75. Distribution of occupant sex in head-on crashes

7.4 Conclusions

Most cross-centerline head-on crashes occur on straight two-lane roads on clear days. Older drivers are more likely to receive moderate to fatal injuries during the head-on crash. These crash datasets did not contain much information regarding driver evasive actions before head-on collision. This topic will be explored in more detail in Chapter 8 and in Chapter 11.

8 CHARACTERIZATION OF DRIVER EVASIVE ACTIONS IN HEAD-ON CRASHES

8.1 Purpose

The purpose of this chapter is to determine the evasive actions taken by the drivers and to develop a driver behavior model for both the encroaching and impacted drivers.

8.2 Approach

8.2.1 Data Selection

To be included in this study, NASS/CDS cases with supplemental data in the cross-centerline database must have EDR information available for either the encroaching or impacted vehicle. To ensure that the EDR event recorded corresponds to the impact described in the NASS/CDS case, only those cases in which the EDR either recorded an airbag deployment or had a delta-v greater than 8 kph were selected [4, 45]. When an airbag deploys, the data is locked into the EDR and cannot be overwritten by lower severity impacts. A delta-v of 8 kph is a significant crash, and it is unlikely that a more significant event not involving an airbag deployment could occur to overwrite the data. To ensure that the EDR events align with the NASS/CDS events, the first event in the NASS/CDS case must have the largest delta-v. This selection criteria is the same as that used by Scanlon to analyze intersection crashes [45]. The case selection criteria are summarized in Table 21. There were 157 vehicles with valid EDR information available. However, every EDR did not contain all the variables of interest.

Table 21. Case selection.

	Number of Encroaching Vehicles	Weighted Number of Encroaching Vehicles	Number of Impacted Vehicles	Weighted Number of Impacted Vehicles
NASS/CDS 2011-2015 Head-On	13,826	6,350,944	13,826	6,350,944
Cross-centerline Collision Database	181	58,219	183	58,222
EDR Valid	62	15,971	95	33,974
EDR Speed Available	62	15,971	94	33,240
EDR Braking Available	61	15,710	95	33,974
EDR Yaw Rate Available	10	2,394	17	5,043

8.2.2 Data Analysis

The analyses of the cross-centerline collisions were separated into two groups: the encroaching and impacted vehicle. The departure angle was measured from the scene diagram and was defined as the angle between the path of the vehicle center of gravity and the line tangent to the lane line at the first lane departure. For example, if the encroaching vehicle crosses multiple lanes before the centerline, the departure angle was measured at the first lane departure not at the centerline. The distance to impact from the first lane departure was measured as the straight-line distance from the point of departure to the point of impact.

The information recorded by EDRs vary by manufacturer and module type. All EDRs record five seconds of pre-crash information. However, the resolution of the measurements can vary from one sample to ten samples a second. Since the EDR module takes measurements at a specified interval, it likely does not record a measurement exactly at the time of impact [45]. A few EDRs do record a measurement at the moment of impact but it is not necessarily measured at the same period as the rest of the measurements. In our study, the impact speed was assumed to be the last measurement taken by the EDR. Therefore, the assumed impact time was no more than one sampling period from the actual impact time. The travel speed was assumed to be the first measured speed.

Each case was examined for evidence of braking or steering maneuvers. For the EDRs that recorded brake activation, the brake activation was used to determine whether the driver braked before the crash. However, brake activation does not indicate the magnitude of the deceleration. Therefore, the change in speed was divided by the brake duration to estimate the deceleration. The average deceleration was determined for both encroaching and impacted vehicles using a linear regression relating the change in velocity to the time spent braking. The deceleration was only computed during the consecutive measurements where the driver activated the brake leading up to the crash. Evasive steering was defined as a yaw rate greater than 4 deg/s [35] or a steering wheel angle of 17.5 degrees (Chapter 4). Drivers that performed an evasive braking action were assumed to be activating the brake at the last EDR measurement.

8.3 Results

The evasive maneuvers performed by the drivers and their frequency are summarized in Table 22. Steering was the most common driver response, followed by braking.

Table 22. Evasive maneuvers.

Evasive Action	Role	Action Performed	Cases Available	Percent of Cases	Action Performed (weighted)	Weighted Cases	Percent of Weighted Cases
Brake	Encroaching	29	61	47.5%	7,229	15,710	46.0%
	Impacted	76	95	80%	26,230	33,974	77.2%
	Total	105	156	67.3%	33,458	49,584	67.5%
Yaw	Encroaching	5	10	50.0%	1,878	2,394	78.4%
	Impacted	13	17	76.5%	4,056	5,043	80.4%
	Total	18	27	66.7%	5,934	7,437	79.8%

Our dataset included one case in which both the encroaching and impacted vehicles had yaw rate information from the EDRs. However, there were 11 cases where both vehicles had braking information. The majority of impacted vehicles did perform a braking maneuver before the crash (Table 23). In contrast, the majority of encroaching vehicles did not brake before impact.

Table 23. Evasive maneuvers for cases in which EDRs were available from both vehicles.

Evasive Action	Role	Action Performed	Cases Available	Percent of Cases	Action Performed (weighted)	Weighted Cases	Percent of Weighted Cases
Brake	Encroaching	3	11	27.3%	1,361	6,540	20.8%
	Impacted	9	11	81.8%	6,260	6,540	95.7%
Yaw	Encroaching	0	1	0.0%	0	75	0.0%
	Impacted	1	1	100.0%	75	75	100.0%

There were 18 cases representing 5,933 crashes with both steering and braking data. The majority of impacted drivers responded by steering and braking (Table 10). The impacted vehicle was more likely to respond by either braking or steering and braking than the encroaching vehicle.

Table 24. Combination of evasive maneuvers.

Evasive Action	Vehicle Role	Action Performed	Percent of Cases	Action Performed (weighted)	Percent of Weighted Cases
No Avoidance	Encroaching	4	40.0%	394	16.5%
	Impacted	0	0.0%	0	0.0%
	Total	4	22.2%	394	6.7%
Brake and Steer	Encroaching	3	30.0%	1,333	55.7%
	Impacted	11	64.7%	3,731	74.0%
	Total	14	77.8%	5,065	85.4%
Steer Only	Encroaching	2	20.0%	544	22.7%
	Impacted	2	11.8%	323	6.4%
	Total	4	22.2%	868	14.6%
Brake Only	Encroaching	1	10.0%	121	5.1%
	Impacted	4	23.5%	987	19.6%
	Total	5	27.8%	1,108	118.7%

8.4 Discussion

In the majority of cross-centerline crashes – 49.3% of encroaching vehicles and 31.2% of impacted vehicles – the vehicle was travelling faster than the speed limit (Figure 76). In 26 of the 62 cases, the encroaching vehicle was travelling more than 8 kph (5 mph) over the speed limit. The median travel speed was 59.6 kph for the encroaching vehicle and 46.7 kph for the impacted vehicle (Figure 77). Overall, the distributions of impact speeds are similar for both the encroaching and impacted vehicles.

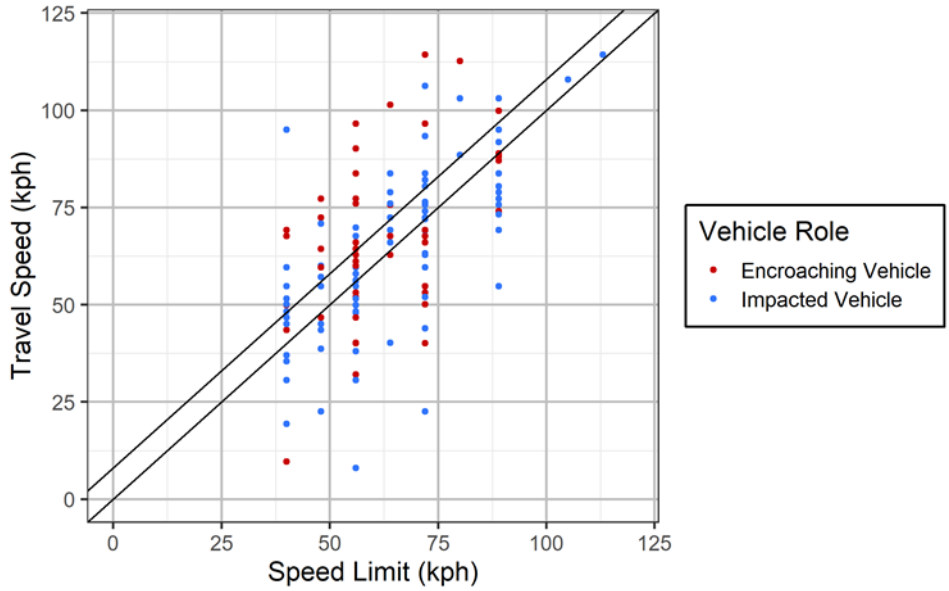

Figure 76. Vehicle speed compared to the posted speed limit. Cases above the lower line represent vehicles travelling faster than the posted speed limit. Cases above the upper line represent vehicles travelling more than 5 kph faster than the posted speed limit.

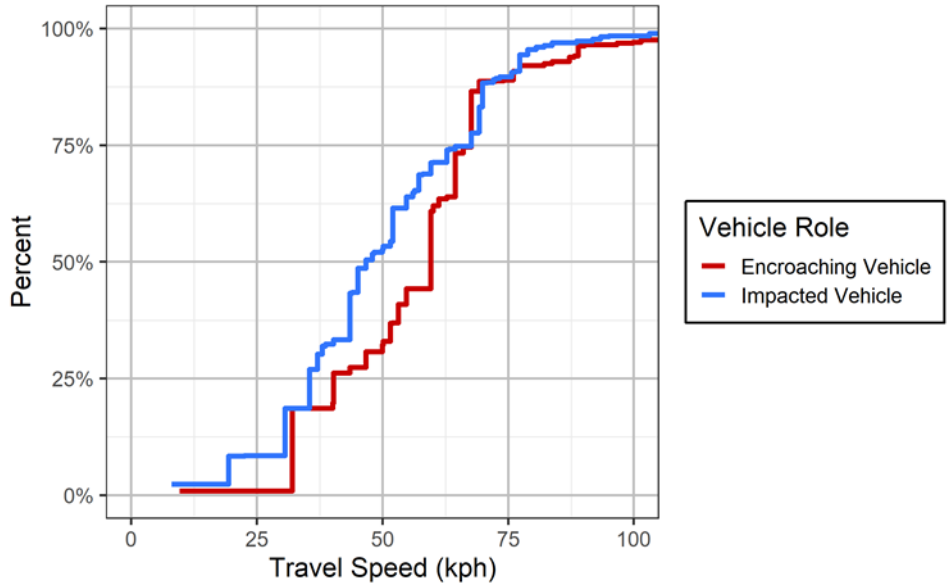

Figure 77. Distribution of travel speeds.

The median departure angle was 9°. The median departure angle was larger than the 0.4 to 0.6° reported from naturalistic driving studies [65]. This is likely due to the fact that all case in NASS/CDS are crashes, which is not the case in naturalistic data sets.

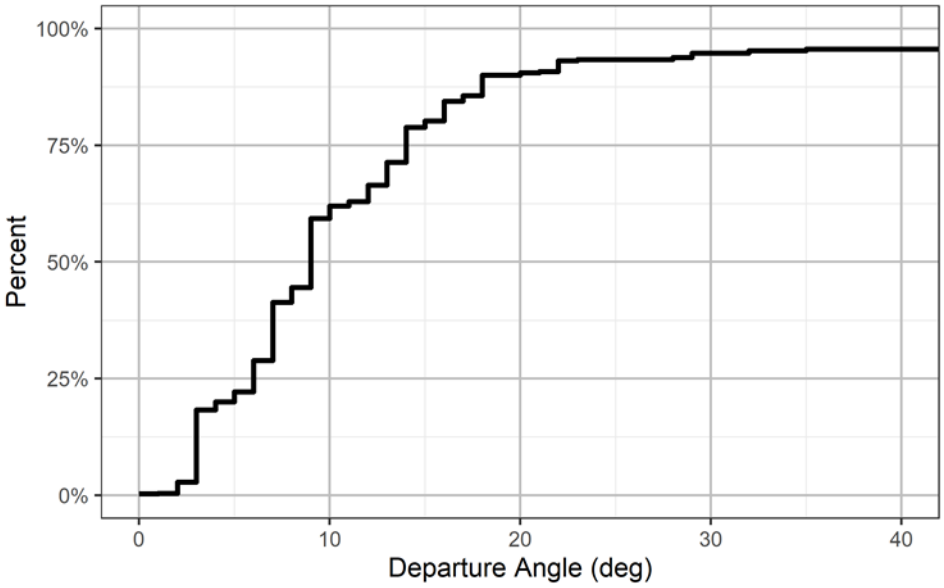

Figure 78. Distribution of departure angles.

Every encroaching vehicle that performed a steering maneuver before the impact, steered back toward their original lane of travel (Table 25). The impacted vehicle was more likely to steer but the direction of steering was not consistent. They most commonly turned to the right, which is away from the centerline. The encroaching vehicle performed a harder evasive steering maneuver with a median magnitude of 25 deg/s compared to only 11.7 deg/s by the impacted vehicle (Figure 79).

Table 25. The distribution of directions for vehicles that performed a steering maneuver.

Steering Direction	Role	Action Performed	Cases Available	Percent of Cases	Action Performed (weighted)	Weighted Cases	Percent of Weighted Cases
Left	Encroaching	0	5	0.0%	0	1,877	0.0%
	Impacted	5	13	38.5%	1,149	4,054	28.3%
Right	Encroaching	5	5	100.0%	1,877	1,877	100.0%
	Impacted	8	13	61.5%	2,905	4,054	71.7%

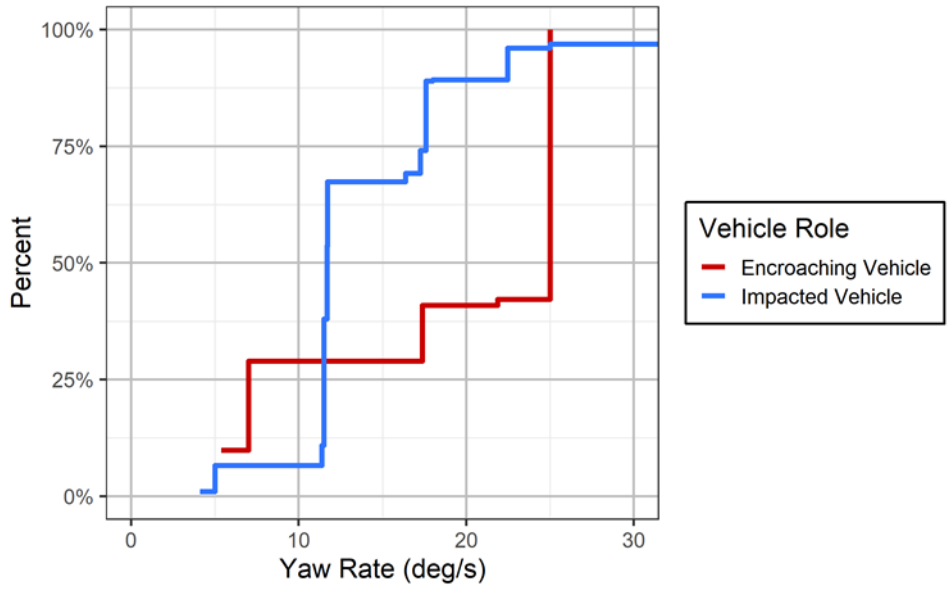

Figure 79. Distribution of the maximum yaw rates for 5 encroaching vehicles and 13 impacted vehicles that performed a steering maneuver.

The deceleration was computed using a linear regression of the amount of time the driver was braking as a function of the change in velocity. The average deceleration of the vehicle due to braking was 0.3 g (Figure 80). This is half of the 0.58 g evasive braking present in intersection crashes [45]. The evasive braking deceleration was much lower for cross-centerline crashes than road departure crashes, which may indicate less time to react. There was very little difference in the deceleration between the encroaching and impacted vehicles.

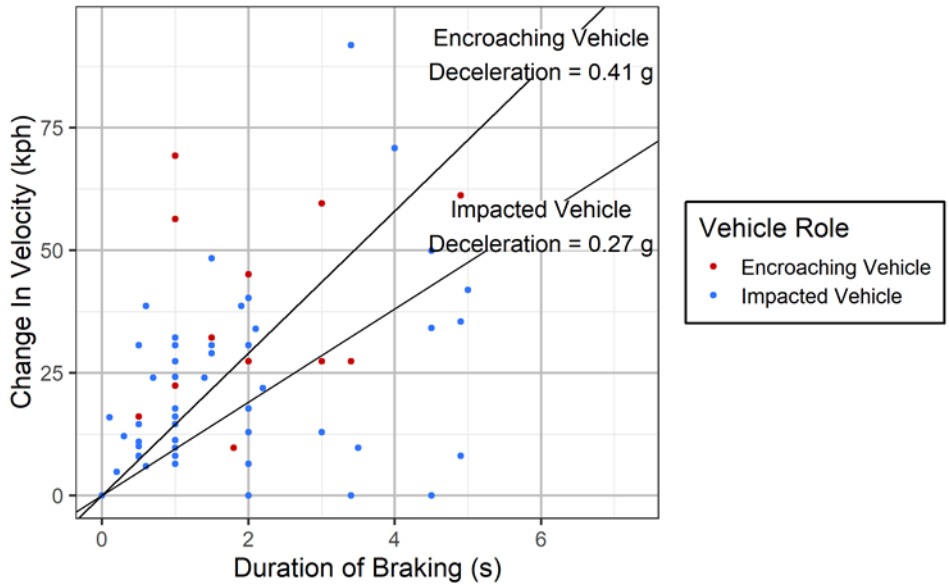

Figure 80. Vehicle deceleration from braking before impact for 29 encroaching vehicles and 76 impacted vehicles.

Of the vehicles that performed a braking maneuver before impact, the median brake duration was 1.0 s for the encroaching vehicle and 0.6 s for the impacted vehicle (Figure 81).

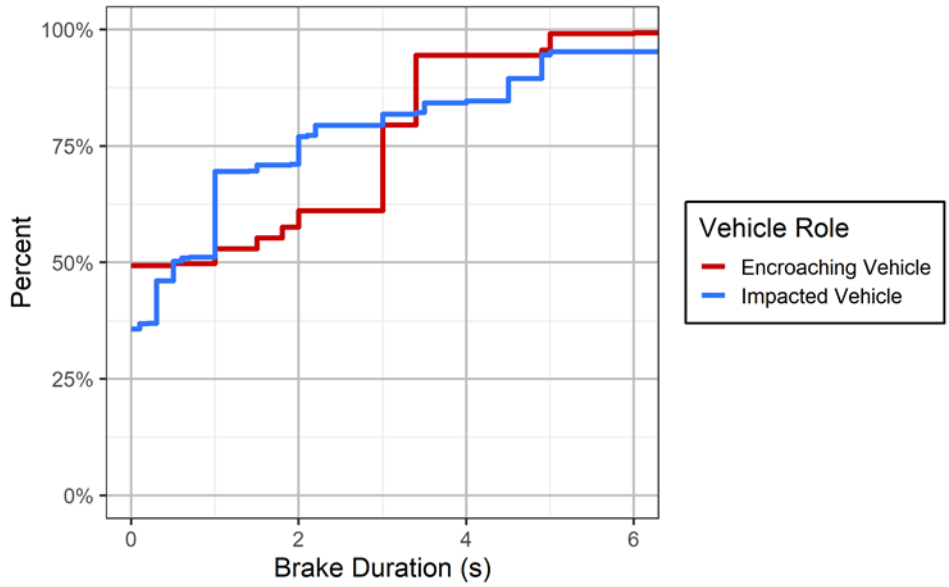

Figure 81. The distribution of braking duration for 29 encroaching vehicles and 76 impacted vehicles that performed a braking maneuver.

The distribution of vehicle decelerations during the final braking event is shown in Figure 82. The median deceleration was 0.56 g for the encroaching vehicle and 0.32 g for the impacted vehicle. The decelerations were computed as the change in velocity divided by the duration braking. This method led to a total six cases with a deceleration greater than 1g, which is not possible from braking alone. Therefore, there may be other factors involved allowing the vehicle to decelerate faster, such as an incline or an impact.

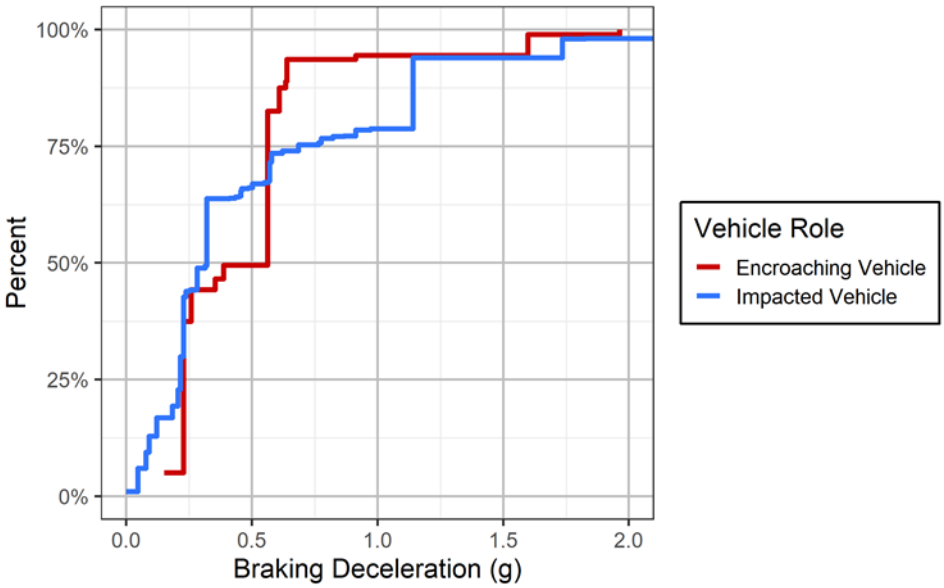

Figure 82. The distribution of deceleration during the final braking event for 29 encroaching vehicles and 76 impacted vehicles.

The median impact speed was 40.3 kph for the encroaching vehicle and 38.0 kph for the impacted vehicle (Figure 83). The median delta-v was 17.2 kph for the encroaching vehicle, which is about half of the impact speed (Figure 84). The median delta-v of 12.4 kph was lower for the impacted vehicle than the encroaching vehicle.

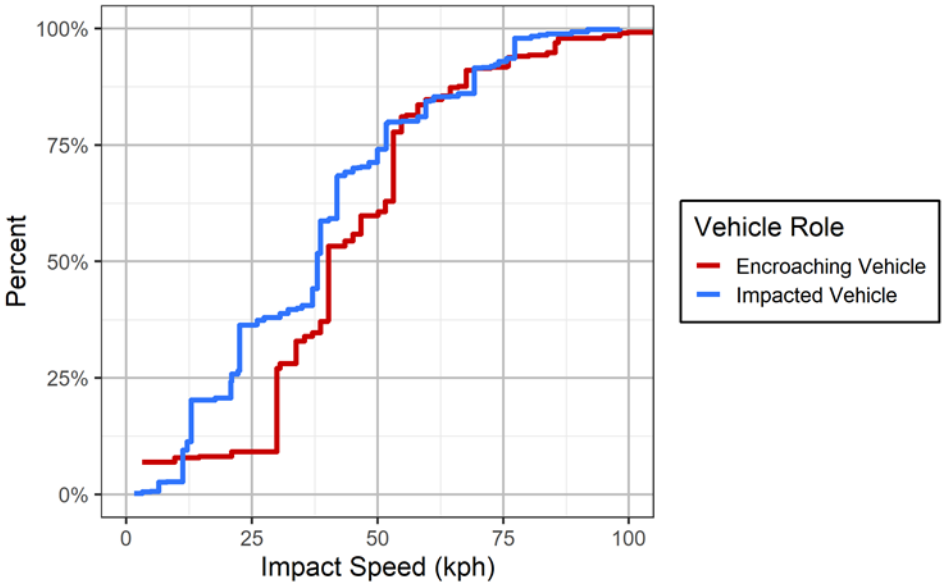

Figure 83. Distribution of single vehicle road departure impact speeds.

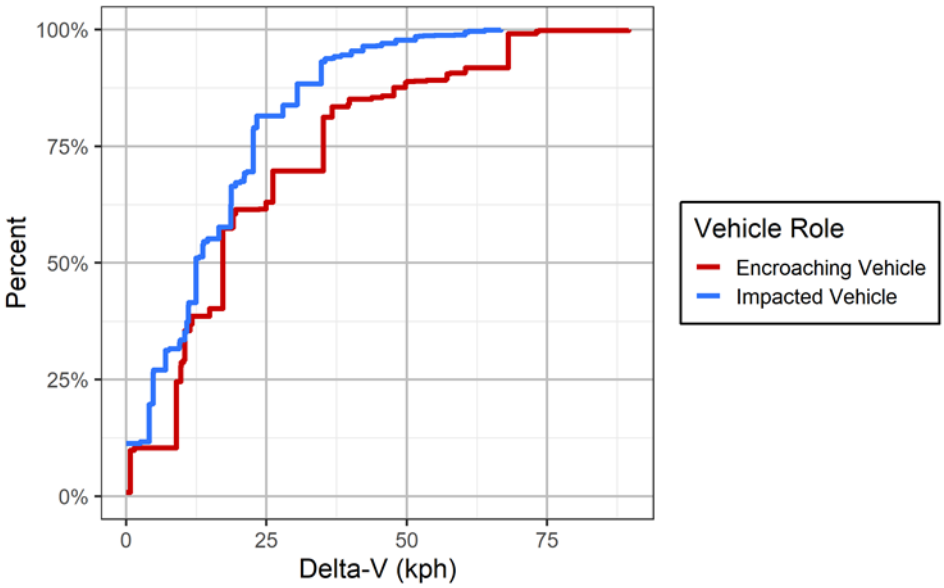

Figure 84. Distribution of single vehicle road departure crash impact delta-v.

All of the trajectories of the encroaching and impacted vehicles are shown in Figure 85. The origin is the point where the encroaching vehicle crosses the centerline. There is a large spread away from the origin because of the different road shapes. The majority of crashes occurred close to the centerline as seen by the points on the trajectories in Figure 86. Over 25% of cross-centerline crashes occurred within 1m of the centerline.

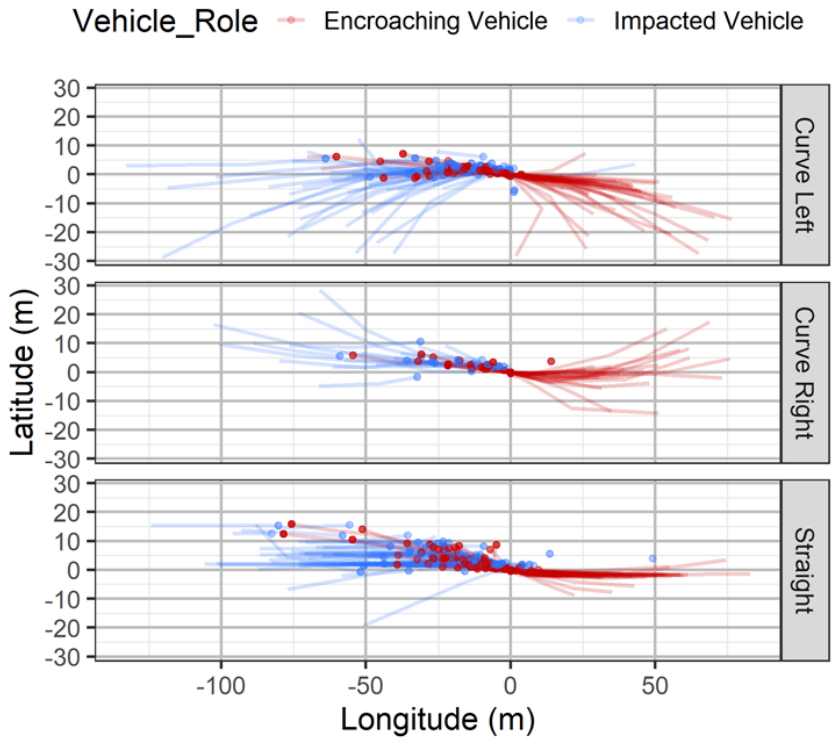

Figure 85. Trajectories of vehicles involved in cross-centerline vehicle-to-vehicle collisions.

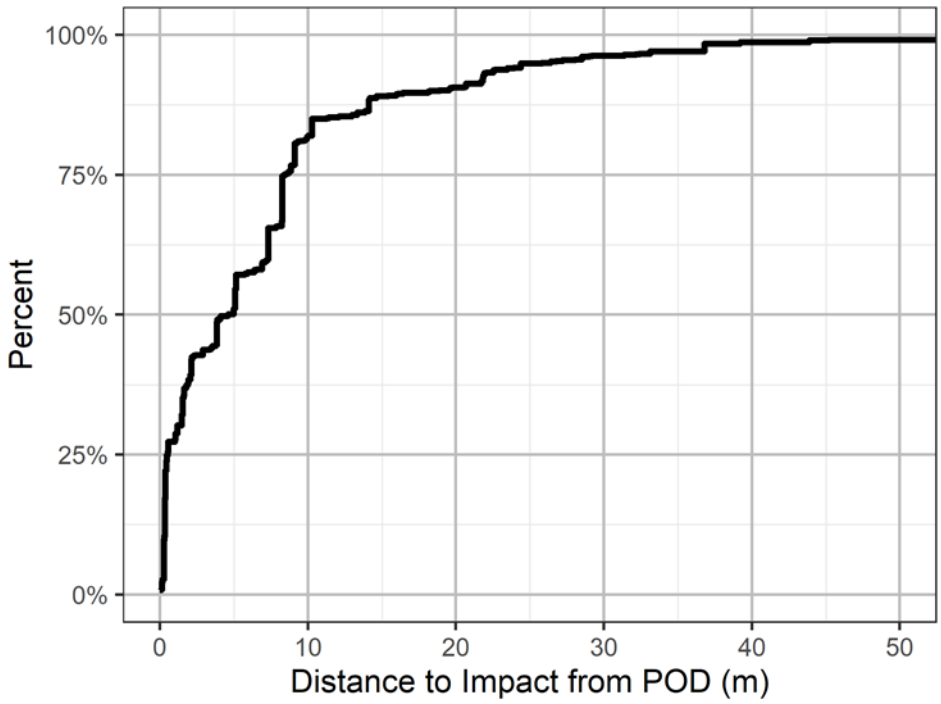

Figure 86. Distance from the point of departure to the impact location for the encroaching vehicle.

8.4.1 Case Study

One specific case analyzed was case number 550017440. In this case a 73-year-old female was driving a 2011 Chevrolet HHR through a construction zone on a rural two-lane highway (Figure 87). The vehicle departed the lane and impacted a 2010 Ford E-Series van driven by a 25-year-old female travelling the opposite direction. The driver of encroaching vehicle had a MAIS of 4 and the other driver had a MAIS of 2. The EDR information indicates that both vehicles were travelling about the same speed prior to the crash (Figure 88). The impacted vehicle saw the encroaching vehicle and reacted by both steering and braking simultaneously.

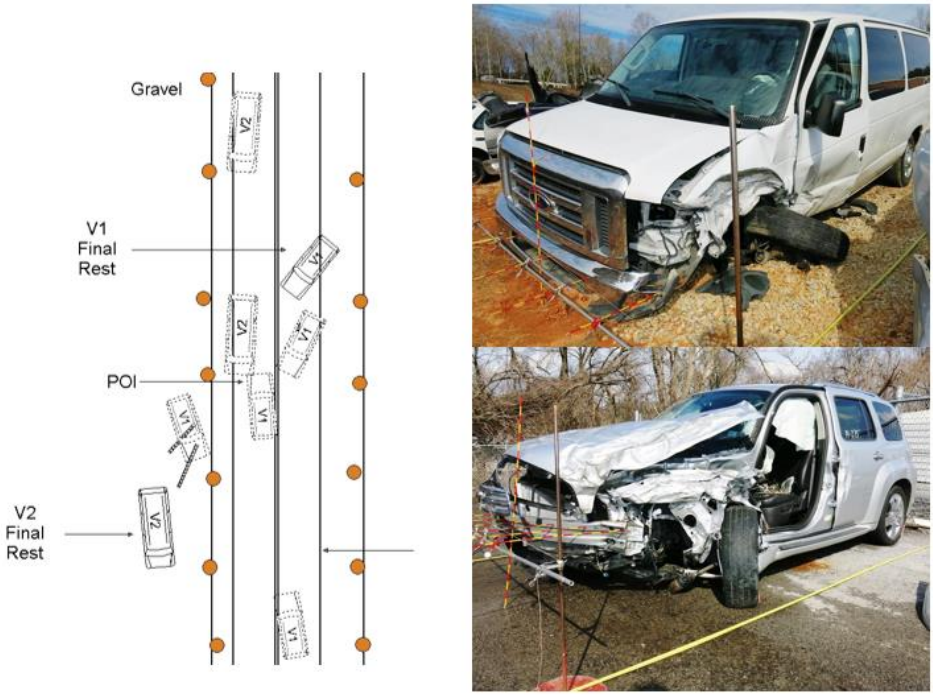

Figure 87. Case number 550017440. Chevrolet HHR (V1) departs lane and impacts a Ford E-Series van (V2).

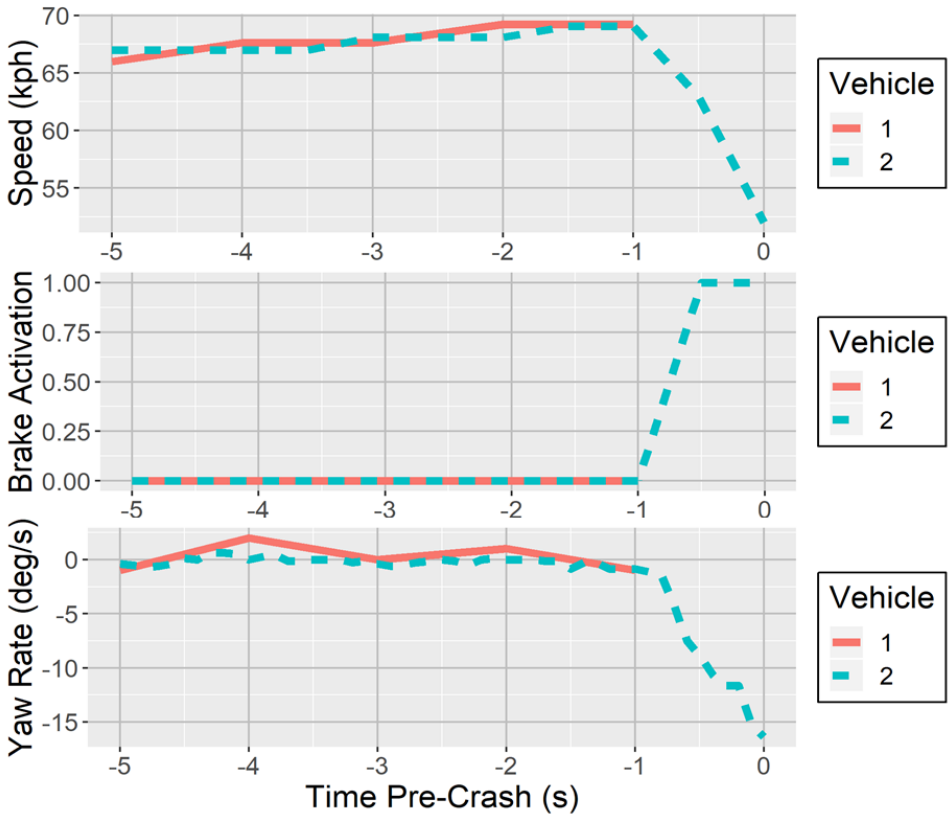

Figure 88. The EDR speed, braking, and yaw rate information for both vehicles.

8.5 Limitations

This study analyzed only those centerline departures that resulted in vehicle-to-vehicle collisions. Accordingly, conclusions cannot be made about what driver maneuvers are successful in avoiding a crash. With two drivers it is possible that the attempted maneuver by one influences the maneuver of the other driver. This study assumed that the two drivers responded independently due to the small sample of crashes with EDR information for both drivers.

Within this dataset, more EDRs recorded steering wheel angle than yaw rate. However, the threshold to indicate a steering maneuver based on steering wheel angle may not be accurate for all vehicles. The yaw rate resulting from a given steering wheel angle is highly dependent on the vehicle geometry such as the track width, the suspension, and the speed of the vehicle. However, a steering wheel angle of 17° would be higher than necessary to maintain lane position, which indicates a steering maneuver.

The majority of encroaching drivers responded to the centerline crossing by performing some steering maneuver. This method cannot exclude the possibility of non-evasive steering actions such as the driver falling asleep and causing the vehicle to cross the centerline. These results are also limited by the small number of cases that had the EDR steering or yaw rate data available. Because of the low sampling rate of EDR precrash data, the temporal error for the length of a braking or steering response can be up to 1 s. This is particularly large for cases when the drive responded just before impact. However, when the driver responds relative to an encroachment event will be explored in Chapter 11 using naturalistic driving data.

8.6 Conclusions

Overall, the impacted vehicle driver is much more likely to attempt an evasive maneuver the encroaching vehicle. Among the crashes where EDR information was available, all impacted vehicles attempted to perform an evasive action. The most common maneuver was braking. However, the drivers did not brake as hard as was possible. The encroaching vehicle tended to be travelling faster than the impacted vehicle. Additionally, over one quarter of cross-centerline vehicle-to-vehicle crashes occur within 1 m of the centerline.

9 ESTIMATED CRASH PREVENTION OF CROSS-CENTERLINE HEAD-ON CRASHES BY LDW

9.1 Purpose

The purpose of chapter 9 is to estimate the benefit of LDW/LDP systems in head-on crashes and to characterize the residual cross-centerline crash population after deployment of LDW/LDP systems.

9.2 Approach

9.2.1 Data Selection

NASS/CDS cross-centerline head-on crashes from 2011 to 2015 were selected for estimating the effectiveness of LDW/LDP systems. This is the most recent five years available in NASS/CDS. The VT cross-centerline crash database was used to provide the coded trajectory of the vehicle before the crash. The EDR pre-crash velocity data was used to determine the vehicle's speed at each point along the trajectory.

To be included in the study, the first event for the encroaching vehicle had to be the head-on crash in NASS/CDS (ACCTYPE = 50, 51). Additionally, the EDR needed to record either an airbag deployment or a delta-v greater than 8kph (5mph) for the encroaching vehicle [45]. The bag deployment locks the EDR data preventing subsequent events from overwriting EDR data. In cases where the airbag did not deploy, the 8 kph delta-v requirement increases the likelihood that the event stored in the EDR corresponds to the NASS/CDS case rather than a minor impact. A crash of at least 8 kph will produce significant damage and would be unlikely to be overwritten by a post-crash event, e.g., hitting a pothole while being towed from the scene. Finally, the EDR must have recorded values for the pre-crash velocity to be used in this study.

In our dataset, there were three cases in which the encroaching vehicle departed the road at least once before the head-on crash. In each of these cases, the encroaching vehicle departed the road to the right, overcorrected, crossed the centerline, and impacted a vehicle travelling in the opposite direction. The first intervention opportunity for this particular scenario involves activating the LDW or LDP system during the road departure rather than when the vehicle crosses the centerline. Therefore, the three cases where a road departure occurred before the cross-centerline crash were removed from the dataset. Although these cases were excluded from this study, it is still possible that implementing avoidance countermeasures may have mitigated or prevented the impact. The three removed cases are shown in Figure 89. Overall, there were 111 encroaching vehicles in the simulation dataset. After applying NASS/CDS sampling weights, this represents 35,677 real-world crashes used in this study (Table 26).

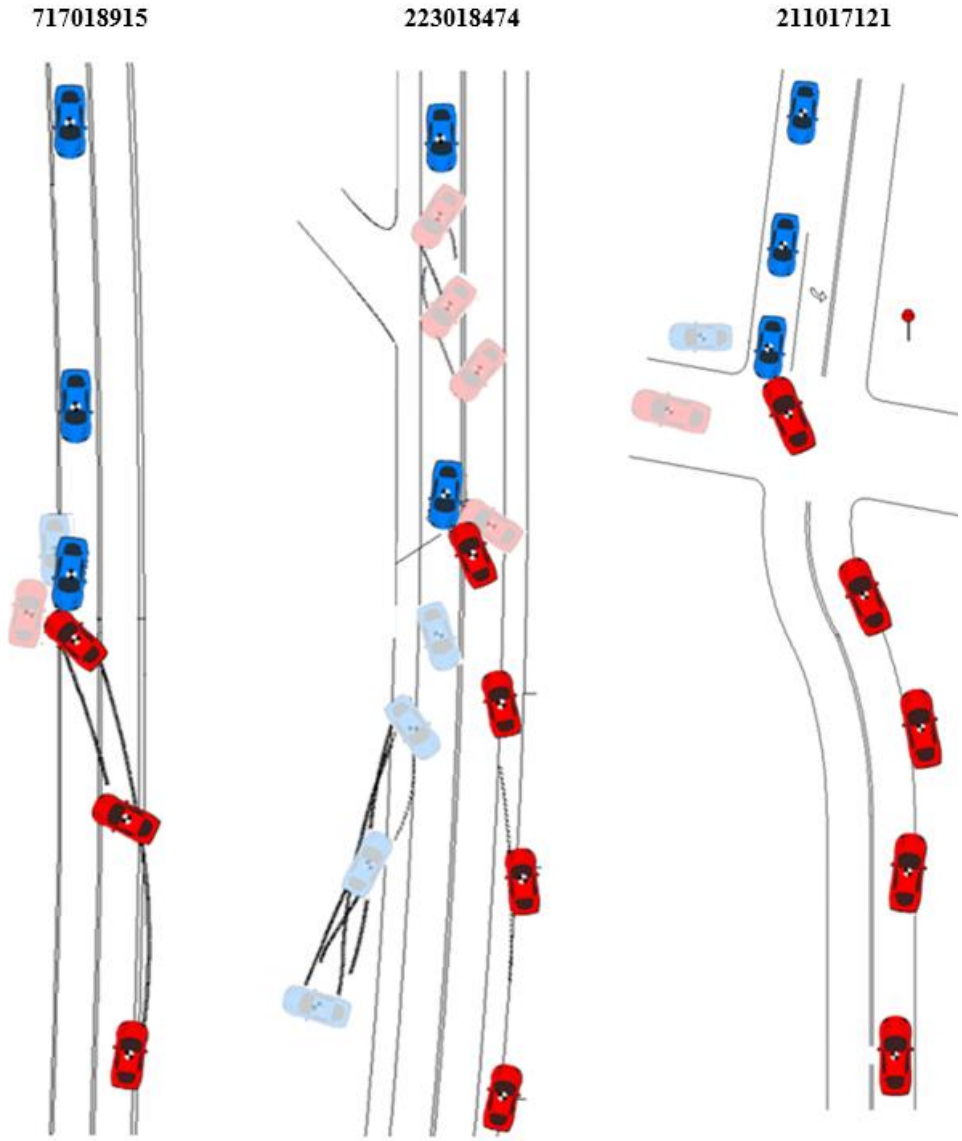

Figure 89. NASS/CDS scene diagrams of cross-centerline cases 717018915, 223018474, and 211017121. The encroaching vehicle departed from the right, overcorrected, and struck an oncoming vehicle. Translucent trajectory points occurred after the impact.

Table 26. Case selection criteria.

	Number of Cases	Weighted Cases
Vehicles with EDR information and in the cross-centerline database	183	58,298
Air bag deployment or delta-v > 8 kph	165	48,728
Valid pre-crash data	164	48,641
First event	164	48,641
Single departure cases	161	47,885
Remove large trucks	148	46,509
Valid crash delta-v	134	44,991
Valid pre-crash velocity	111	33,677

9.2.2 Crash Reconstruction

Often the EDR was only available in one of the vehicles involved in the cross-centerline head-on collision. To accurately model both vehicles in the crash, the speed of the vehicle without the EDR was reconstructed. Using the delta-v of one vehicle from the EDR, the mass of both vehicles, and the impact angle of both vehicles, the delta-v of the other vehicle was computed based on the conservation of momentum. The delta-v of the other vehicle was computed in both the x (Eq. 15) and y (Eq. 16) directions. This assumes that all of the vehicle motion was planar and there was no rotation of the vehicles from the impact. The mass of each vehicle was the sum of the curb weight and cargo weight reported in NASS/CDS.

$$\mathrm{m}_1\Delta v_{x1}\cos(\theta_1) + m_1\Delta v_{y1}\sin(\theta_1) = \mathrm{m}_2\Delta v_{x2}\cos(\theta_2) + m_2\Delta v_{y2}\sin(\theta_2) \quad (15)$$

$$-\mathrm{m}_1\Delta v_{x1}\sin(\theta_1) + m_1\Delta v_{y1}\cos(\theta_1) = -\mathrm{m}_2\Delta v_{x2}\sin(\theta_2) + m_2\Delta v_{y2}\cos(\theta_2) \quad (16)$$

The velocity of the vehicle after impact was approximated based on the linear distance (D) to the final rest position from the point of impact. The energy absorbed during that distance was estimated from a 0.2g deceleration along the distance to the final rest position (Eq. 17). This value was chosen to maximize the agreement between the predicted and actual impact velocities.

$$v_f = \frac{9.8}{0.2 * t}, where\ t = \sqrt{\frac{2D}{9.8 * 0.2}} \quad (17)$$

From the delta-v and the velocity immediately following the impact, the impact velocity was computed (Eq. 18).

$$v_i = v_f + \sqrt{\Delta v_x^2 + \Delta v_y^2} \quad (18)$$

Depending on which vehicle, encroaching, or impacted, contained the EDR information, the initial travel speed changed. For cases in which the impacted vehicle contained an EDR, the first recorded speed was assumed to be its travel speed. For cases in which the encroaching vehicle contained an EDR, the velocity measurements were mapped onto the vehicle trajectory assuming a linear acceleration between measurements [4]. The travel speed was the speed of the vehicle when its center of mass crossed the centerline.

The reconstructed delta-v for the vehicle without an EDR was compared with the WinSmash reconstructed delta-v [41]. Our reconstructed delta-v overestimated the WinSmash delta-v by about 17 percent on average (**Error! Reference source not found.**) because it does not account for the rebound v elocity of the vehicle and because it does not consider rotation of either vehicle. These assumptions were particularly highlighted by case 717020839 (**Error! Reference source not found.**), which had a r econstructed delta-v of 122 kph but a WinSmash delta-v of 55 kph. Our estimate was higher than the WinSmash because the small sedan experienced extreme deformation to the occupant compartment.

However, WinSmash underestimates the true crash delta-v by roughly 10%, which may indicate that our delta-v estimates are close to the true delta-v [42, 66].

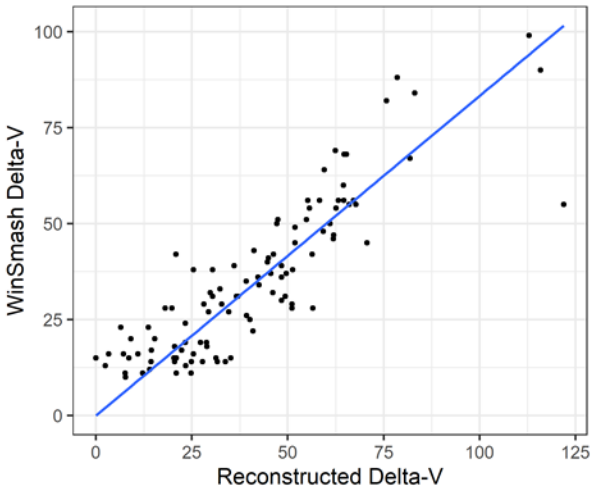

Figure 90. Validation of the delta-v reconstruction.

Figure 91. The large deformation experienced by the sedan in NASS/CDS case 717020839.

The impact velocity reconstructed from the delta-v was compared with the last recorded pre-crash velocity of the vehicle (Figure 92). A linear regression between the reconstructed and last pre-crash velocity determined that the predicted impact speed was on average 9.6% below the last pre-crash velocity with an r^2 value of 0.85. Because many EDRs do not record the exact impact velocity, the last recorded pre-crash velocity does not capture any decrease in speed due to braking before impact.

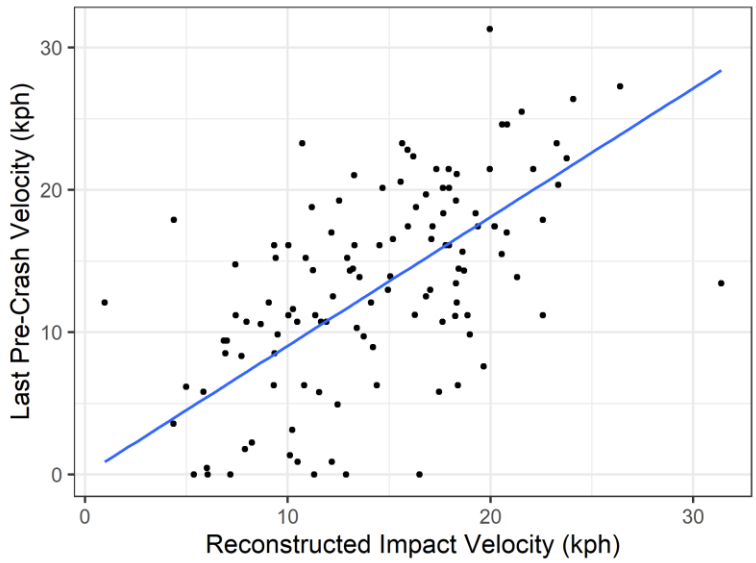

Figure 92. Validation of the delta-v reconstruction.

Depending on which vehicle (encroaching or impacted) contained the EDR information, the initial travel speed changed. For cases in which the impacted vehicle contained an EDR, the first recorded speed was assumed to be its travel speed. The encroaching vehicle was assumed to take no evasive action, which has been shown to be the case in 54% of cases [3]. Therefore, the travel speed of the encroaching vehicle was the same as the impact speed.

For cases in which the encroaching vehicle contained an EDR, the velocity measurements were mapped onto the vehicle trajectory assuming a linear acceleration between measurements [8]. The travel speed was the speed of the vehicle when its center of mass crossed the centerline.

9.2.3 Crash Environment

To accurately predict the benefits of LDW systems for cross-centerline head-on crashes, the environment where the crash occurred must also be modeled. The most important aspect of the crash environment was the road geometry. The individual road segments for each crash were retrieved from the cross-centerline database.

9.2.4 Vehicle Model

The vehicles dynamics before the crash were modeled using the same equations as in chapter 5.

The vehicles in the crash were represented by a rectangle with a length and width equivalent to the overall length and width from NASS/CDS of each vehicle. The vehicle dynamics were modeled as a point with a time step of 0.01s in Equations 19-24 and followed the global coordinate system in Figure 93.

$$a_{t+1} = a_t + Jerk_t \Delta t \quad (19)$$
$$v_{t+1} = v_t + a_t \Delta t \quad (20)$$
$$\dot{\Psi}_{t+1} = \dot{\Psi}_t + \ddot{\Psi}_t \Delta t \quad (21)$$
$$\Psi_{t+1} = \Psi_t + \dot{\Psi} \Delta t \quad (22)$$
$$x_{t+1} = x_t + v_t \Delta t \cos(\Psi_t) \quad (23)$$
$$y_{t+1} = y_t + v_t \Delta t sin(\Psi_t) \quad (24)$$

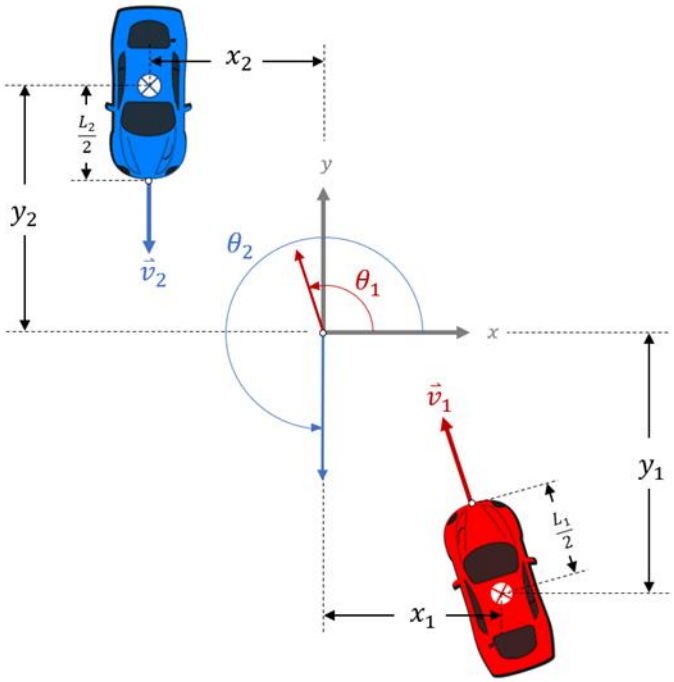

Figure 93. Global coordinate system: the origin of the coordinate system represents the location that the encroaching vehicle crossed the centerline.

The total force exerted by the tires was limited to the force available from friction. Therefore, any combination of steering and acceleration could not exceed 1g, as shown in Equation 25. If the 1g limit was exceeded, then the braking force was maintained, and the steering was scaled down such that the magnitude was equal to 1g.

$$9.8\mu > \sqrt{(a)^2 + \left(\dot{\Psi} v\right)^2}, where \quad (251)$$
$$\mu = friction\ coefficient\ (-)$$
$$a = longitudinal\ acceleration\ \left({}^{m}/_{s^2}\right)$$
$$\dot{\Psi} = yaw\ rate\ \left({}^{deg}/_{s}\right)$$
$$v = longitudinal\ velocity\ ({}^{m}/_{s})$$

9.2.5 Driver Model

Both the encroaching vehicle and impacted vehicle follow their original crash trajectory using the steering model shown in Chapter 5. The encroaching vehicle follows its original crash trajectory, but the impacted vehicle was simulated to follow the road by remaining centered in its lane. The vehicle steering

was controlled by a manually tuned proportional-integral-derivative (PID) controller with the following parameters: K_p = 743.5, K_i = 0.1, K_d = 0. The PID controller parameters were determined by manually tuning such that the error was reduced quickly (K_d), with minimal offset (K_i), and with minimal overshoot (K_d) to a right-angle turn. The PID controller was minimizing the distance between the predicted vehicle center in half a second to the intended path of the vehicle. The 0.5s look-ahead was used to more closely resemble how humans drive; drivers do not steer based on their current position but where they will be [67]. Additional length equal to 0.5s of travel was added to the end of the trajectory because the steering model looked ahead 0.5s.

9.2.5.1 Encroaching Vehicle

The encroaching vehicle follows its original crash trajectory. First, it starts at the reconstructed initial velocity. The driver applies a constant deceleration such that the vehicle would be travelling at the impact speed at the original impact location. When the LDW system activates, there is a reaction period during which the vehicle continues travelling as before until the driver reacts. Our model considered three different reaction times: 0.0s, 0.38s, and 1.36s. The 0.0s reaction time was intended to represent the LDP system, which can respond to the departure immediately [50], and the remaining two reaction times represent a fast and slow driver reaction time to either a haptic or audible warning [5].

Once the driver has reacted to the warning, there were two different braking magnitudes (0.0g and 0.41g) and three different maximum turning rates (0 deg/s, 11.4 deg/s, and 34.1 deg/s) based on EDR data [36]. The steering maneuver was governed by the PID controller, which tried to steer back into the original lane of travel. Thus, there were six different possible driver maneuvers (Table 27).

Table 27. Probability of every simulated encroaching vehicle evasive action.

	No Braking	Braking
No Steering	16.5%	5.1%
Light Steering	11.4%	27.8%
Heavy Steering	11.4%	27.8%

9.2.5.2 Impacted Vehicle

The impacted vehicle begins the simulation traveling at the reconstructed initial velocity. The impacted vehicle had a constant deceleration such that it would be traveling at the reconstructed impact velocity at the point of impact. The model assumed that the driver of the impacted vehicle was paying attention to the road and anticipated the encroachment of the other vehicle. Therefore, as soon as the encroaching vehicle touched the lane line, the driver of the impacted vehicle performed a braking maneuver with a magnitude of either 0.0g or 0.27g [36]. The driver was assumed to follow their intended path by remaining centered in their lane. This assumption was made because the intention of the average driver is to remain centered in their lane, and current autonomous driving technologies are focused on centering a

vehicle within its own lane. Thus, there were two possible driver options for the impacted vehicle (Table 28).

Table 28. Probability of every simulated impacted vehicle evasive action.

	No Braking	Braking
Lane Centering	6.4%	93.6%

9.2.6 LDW/LDP Algorithm

The LDW and LDP algorithms utilized were the same as in Chapter 5. The study was based on the analysis of 111 cross-centerline road departure crashes selected from the National Automotive Sampling System Crashworthiness Data System (NASS/CDS). Each case was then simulated with several variants of potential LDP and LDW systems to determine if the crash could be avoided. Our model investigated six hypothetical LDW systems and two hypothetical LDP systems. An LDW system warns the driver that the vehicle has inadvertently left the lane of travel, hopefully providing the driver enough time to respond. However, the effectiveness of LDW systems is limited by the reaction time of the driver (Figure 94). Lane departure prevention systems (LDP) remove this limitation by providing an immediate, automated steering response.

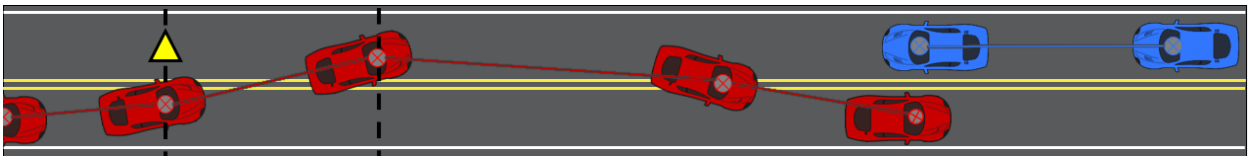

Figure 94. Visual representation of LDW and LDP systems. LDW systems alert the driver that the vehicle has departed its lane of travel. LDP operate similar to LDW systems, except the LDP system provides an immediate, automated steering response.

There were two simulated activation speeds for the LDW and LDP systems: a standard activation and an expanded activation (Table 29). Together, these systems represent the range of real LDW/LDP system TTC thresholds and activation speeds [60]. The standard system activated when the vehicle was travelling faster than 50 kph. This higher speed threshold is intended to prevent activations in locations, such as intersections and parking lots, where there may be many lane lines. The expanded activation system would deliver a warning at speeds over 20 kph if the driver was distracted and over 50 kph otherwise. Driver distraction data was determined by the CDS crash investigator for all 111 simulated cases in the study. If the investigator determined that the driver had “looked but not seen” then it was assumed that an HMI system would interpret that the driver is attentive. If the investigator was not sure if the driver was distracted, it was assumed that the driver was attentive. This assumption would give the driver the latest warning and highest activation speed, which is the less favorable system configuration. Of the 111 cross-centerline cases studied, there were 15 cases in which the driver of the encroaching vehicle was both distracted and travelling between 20 kph and 50 kph.

Table 29. Eight simulated LDW and LDP systems with different activation speeds and times.

System Design	Activation Speed	Activation TTLC
LDW	>50 kph	0.0 s before lane crossing
LDW with Expanded Speed	>20 if distracted >50 otherwise	0.0 s before lane crossing
Advanced LDW	>50 kph	0.5 s before lane crossing
Advanced LDW with Expanded Speed	>20 if distracted >50 otherwise	0.5 s before lane crossing
HMI LDW	>50 kph	1.2s before lane crossing if distracted 0.5 s before lane crossing otherwise
HMI LDW with Expanded Speed	>20 if distracted >50 otherwise	1.2 s before lane crossing if distracted 0.5 s before lane crossing otherwise
LDP	>50 kph	1.0 s before lane crossing
LDP with Expanded Speed	>20 if distracted >50 otherwise	1.0 s before lane crossing

9.2.7 LDW/LDP Effectiveness

The LDW effectiveness was determined by calculating the total possible permutations of LDW activation speeds, time to lane crossing (TTLC) of warning activation, reaction times, steering types, and braking types for both vehicles (Figure 7 and Figure 8); this resulted in a total of 16,539 simulations of cross-centerline collisions (Table 30). These simulations were performed on multiple CPU cores by a custom python script. Each simulation was weighted based on the frequency of each driver evasive action if the system was of the LDW model or weighted based on the case weight if the system was of the LDP model. A crash was predicted to be prevented with an LDW/LDP system if the vehicle continued driving without striking the opposing vehicle (Missed) or came to a stop (Stopped). A crash was predicted to not be prevented if both vehicles impacted each other (Crashed) or the vehicle took no evasive action and departed the road (Parted).

Table 30. Maneuvering responses for the encroaching and impacted vehicle.

	Encroaching Vehicle	Impacted Vehicle
Reaction Times	2 (0.38s, 1.36s)	1 (0s)
Steering Types	3 (0 deg/s, 11.4 deg/s, 34.1 deg/s)	1 (centered in lane)
Braking Types	2 (0g, 0.41g)	2 (0g, 0.27g)
Simulated Responses	12	2

9.3 Results

Each of the eight system types was analyzed, and a general system benefit was determined. The overall system benefit was defined to be the percentage of cases in which the system successfully avoided a crash, compared to the percentage of cases in which the crash still occurred. The baseline model was

defined as a vehicle without an LDW or LDP system in which the encroaching vehicle followed the original crash trajectory. The benefit of each system type is shown in Figure 95. The crash avoidance benefit of the LDW system increased for systems that delivered an earlier warning. LDP systems always activated at 1.0 s TTLC and reacted immediately, which produced a greater crash reduction than LDW systems. The expanded speed models had a higher benefit than the same model with a standard 50 kph activation speed because the system could activate at speeds above 20 kph if the driver is distracted.

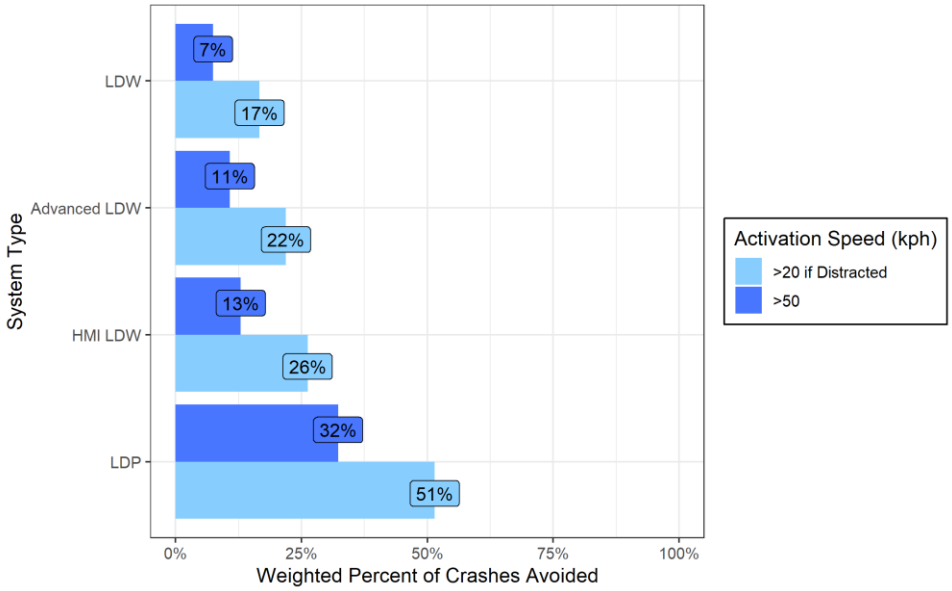

Figure 95. Weighted percent of crashes avoided for each system model and activation speed.

9.4 Discussion

The basic LDW model provided the smallest benefit since it activated much later than the other systems, a TTLC of 0.0s. For the base LDW system, the predicted crash benefit was 7% and more advanced LDP systems had predicted crash benefit up to 51%. The range of these benefits encompass estimates by Cicchino and Sternlund that combined the analysis LDW and LDP systems in road departure, sideswipe, and head-on crashes [9, 10] (Table 31).

Table 31. Summary of previous LDW studies with head-on crashes.

Study	Case Selection	LDW/LDP Injury Benefit
Cicchino 2018 [9]	Single vehicle road departure, head-on, sideswipe crashes in US	Reduction of minor injurious crashes 21% (LDW/LDP)
Sternlund 2017 [10]	Single vehicle road departure, head-on crashes on high-speed roads in Sweden	Reduction of minor injurious crashes 30% (LDW/LDP)
Present Study	Cross-centerline head-on crashes in the US	7%-17% (LDW) 32%-51% (LDP)

One difference this model is that the LDW system for this study only activates if the vehicle is travelling faster than 50 kph. No warning was delivered to the driver in 52% of cases because the encroaching vehicle was travelling below 50 kph. Since the current project's LDW system activates for less than half as many cases as the previous project, the benefits are significantly reduced. Of the 111 cross-centerline cases studied, there were 16 cases in which the driver of the encroaching vehicle was both distracted and travelling between 20 kph and 50 kph. After accounting for the NASS/CDS case weights, it was determined that the maximum additional benefit for the expanded activation speed is 20.0%. This benefit was almost entirely reached by the LDP system; The expanded speed system had a 19% benefit increase compared to the standard activation threshold.

The Advanced LDW system predicted a benefit of 11%, and the base HMI LDW system predicted a benefit of 13%. This is a 4% and 6% increase in benefit for each system, respectively, compared to the base LDW model. The previous study showed that the highest benefits are to be expected when driver reaction times are the slowest. The Advanced and HMI LDW systems, which activate at least 0.5 s before a lane crossing, effectively turn a long reaction time into a quicker reaction. If the driver is not distracted, then the Advanced LDW and HMI LDW systems both provide a warning at 0.5s TTLC. However, in the cases where the driver is distracted, the HMI LDW system will provide the much greater warning time of 1.2s TTLC. In our sample, 62% of drivers were distracted and would benefit from the earlier warning by the HMI LDW system. The LDP system with the expanded speed threshold, which could activate at 20 kph if the driver were distracted, had the highest overall benefit of 51%. For the LDP system, the vehicle responds immediately and automatically provides steering input without any driver input. The trends listed above conclude that a higher benefit is yielded when the LDW/LDP system is activated earlier and for a greater proportion of the cases.

Due to the nature of cross-centerline crashes, many road departure crashes were not avoided in the simulations because there was very little time for the driver to respond. The fastest driver reaction time (0.38s) and even an early warning of 0.5s TTLC often left very little time for the driver to steer or brake to avoid the object. The time available for the driver of the encroaching vehicle to respond is related to the distance from the departure to the impact location and the speed of the vehicle. Slower moving vehicles with larger distances to travel before impact will have more time to respond than fast moving vehicles with smaller distances to travel before impact. Figure 96 shows the simulation outcome based on the encroaching vehicle's speed and distance between the impact location and point of departure for the two different reaction times and activation speeds for the Advanced LDW system where the encroaching vehicle evasive action was no braking and heavy steering, and the impacted vehicle evasive action was braking. For the cases without the expanded activation speed, there was a clear boundary at 50 kph, below which the vehicle crashed in the simulation. In one cross-centerline case, 201408108 (marked on the figure), the encroaching

vehicle was travelling at 45 kph when crossing the lane line and avoided the crash, which appears to violate the threshold. However, Figure 96 represents the departure speed of the original crash, not when the system activated. For this case, at 0.5 s TTLC when the system activated, the vehicle was travelling over 50 kph.

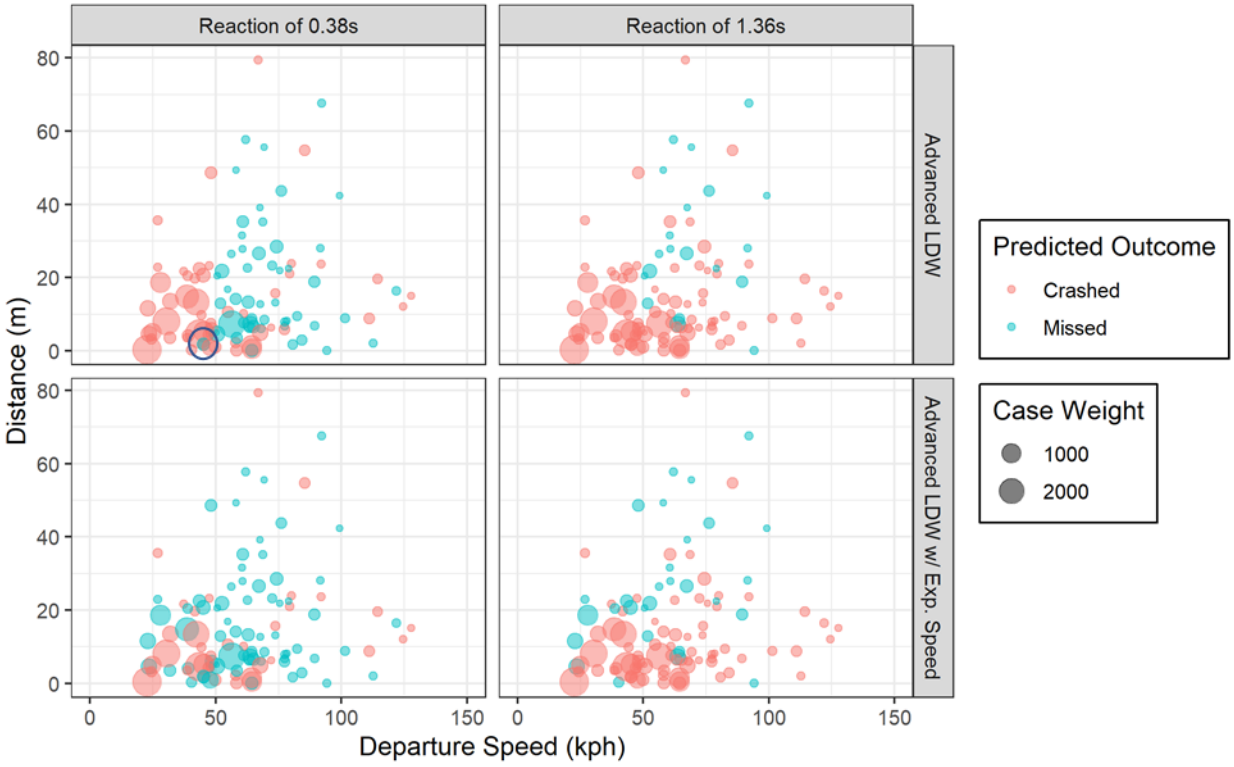

Figure 96. Crash outcome based on the departure speed and the straight-line distance to the impact point from the point of departure. The crash outcome is shown for each reaction time for Advanced LDW and Advanced LDW with Expanded Speed simulations. The encroaching driver model involved heavy steering (34.1 deg/s) and no braking (0.0 g), and the impacted driver model involved following the intended path and braking (0.27 g).

9.5 Residual Crashes

There were 43 cases that were not avoided despite an encroaching vehicle equipped with the LDP system with the lower activation threshold (Table 32). Almost all of these residual crashes occurred because the vehicle was travelling below the activation threshold for the LDP system. In only two cases did the LDP system activate and the vehicle was unable to avoid the crash.

Table 32. Types of residual crashes for an encroaching vehicle with the LDP system with the expanded activation threshold.

Crash Reason	Crashes	Percent	Weighted Crashes	Weighted Percent
Below Activation Threshold	41	36.9%	16,067	47.7%
Unable to Navigate Turn	2	1.8%	275	0.8%

9.5.1 No System Activation

All 41 cases in which the encroaching vehicle was travelling below the activation threshold collided with the impacted vehicle (Figure 97).

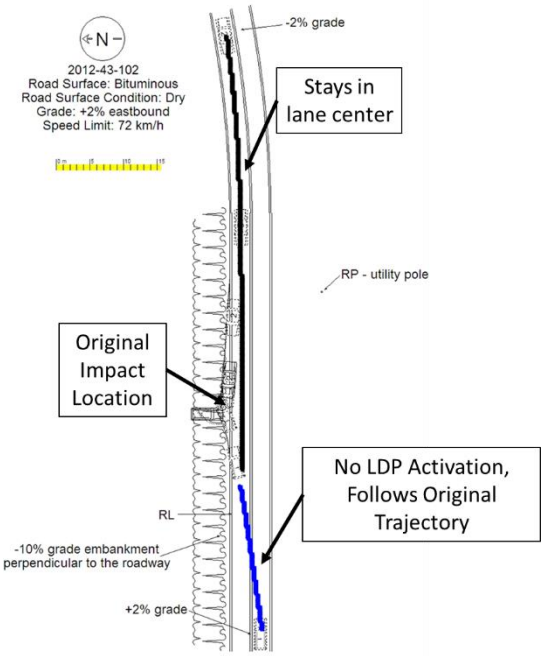

Figure 97. Example case 718017192 where the vehicle was travelling too slow to activate the LDP system.

9.5.2 Unable to Navigate Curve

There were two cases in which the LDP system did activate but was unable to return to the correct lane. Both of these cases occurred on curve right roads. One case, 777014859, the LDP system turned enough to avoid the collision with the impacted vehicle but could not navigate the curve in the road (Figure 98). This crash would have likely resulted in a single vehicle road departure with the LDP system. The other case, 971017553, which was unable to navigate the curve in the road, still contacted the opposing vehicle (Figure 99).

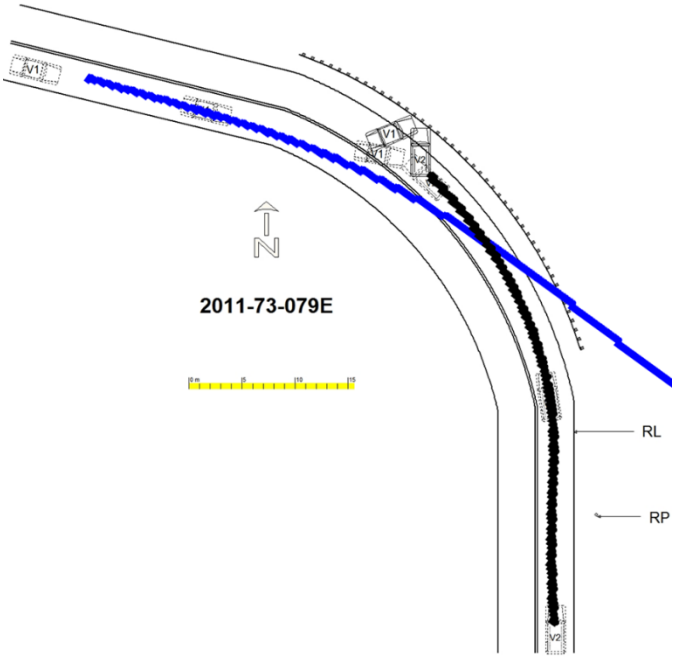

Figure 98. Example case 777014859 where the LDP system avoided the impacted vehicle but was unable to navigate the curve in the road.

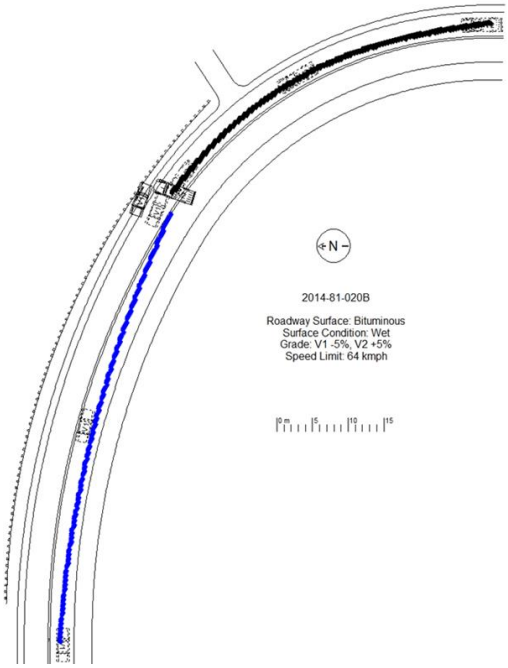

Figure 99. Example case 971017553 where the LDP system was unable to navigate the curve in the road and contacted the impacted vehicle.

9.6 Limitations

In many cases, an EDR was present for one of the involved vehicles. While the delta-v was recorded for one vehicle, the delta-v of the other vehicle was reconstructed. This reconstruction assumed that all the

vehicle motion was planar and there was no rotation of the vehicles from the impact, which may not always be the case for an oblique frontal crash.

Additionally, this model assumed that the driver of the impacted vehicle was fully attentive and anticipated the encroachment of the other vehicle because drivers in the impacted vehicle always performed an evasive action [36]. However, this may not be true if the driver of the impacted vehicle was also distracted, the road was curved, or the view was obstructed such that the encroaching vehicle approached from a blind turn. The driver of the impacted vehicle did not perform an evasive steering maneuver. Instead, the driver of the impacted vehicle braked and followed their intended path by remaining centered in their lane. These simulated behaviors are intended to represent reasonable and typical driver responses of the impacted and encroaching vehicles.

Our study excluded cases with multiple departures. Additionally, this study assumed that there were no other vehicles or objects to be avoided, which may increase the effectiveness estimates. Another limitation to the study was that the friction coefficient is assumed to be constant for every case. This would affect a select few cases where road conditions, such as rain and snow, decrease the turning/braking effects. This study did not account for the grade of the road which could alter the deceleration of the simulated vehicles. However, this effect is likely overcome by any braking performed by the driver.

The vehicle model limited the acceleration to 1 g. This represents the upper limit of the tire force available for a maneuver. Due to tire tread, the driving surface, and the shape of the vehicle, the actual tire force is likely much lower.

The driver distraction during the original crash was determined based on the CDS investigator. Driver distraction was often unknown and could be underreported during interviews with the driver. Unless the investigator indicated the driver was distracted, it was assumed that the driver was attentive. This is a conservative assumption since every modeled system would deliver the warning later or at higher activation speed.

There are a number of sources of error which present a challenge to identify the error on the benefit estimates for each system. These error sources include the CDS sampling error, vehicle location in the scene diagram, EDR temporal sampling error, EDR measurement error, distribution of driver maneuvers, and the error associated with the driver response time. Despite the assumptions necessary to compute the benefit estimates, the trends found when comparing the systems would be unaffected. Future studies could utilize a monte carlo simulation technique which would allow for the overall error to be estimated.

9.7 Conclusions

The purpose of this subtask was to estimate the safety benefits of an HMI system that supports an LDW/LDP system. For cross-centerline crashes, LDP systems with a 20 kph activation speed when the driver is distracted resulted in the highest benefit of 51% (compared to 32% for the same system with a higher activation speed). An Advanced LDW system with a lowered activation speed yielded a benefit of 22%. In comparison, the standard LDW system had a benefit of 17%. Finally, the HMI LDW system with lowered activation speeds was shown to have a benefit of 26%. Future iterations of this study should analyze if there is a significant change in crash prevention benefits if the trajectory of the impacted vehicle deviates from the center of their lane or if the impacted vehicle performs a steering evasive maneuver.

10 PREDICTING THE FUTURE OF CROSS-CENTERLINE HEAD-ON CRASHES

10.1 Purpose

The purpose of this chapter is to estimate the future reduction of DrOOL head-on crashes and injuries due to lane departure warning and lane departure prevention systems.

10.2 Methodology

10.2.1 Data Selection

There were 111 cases in the simulation dataset with 222 vehicles from chapter 9. After applying NASS/CDS sampling weights, this represented 33,677 crashes.

10.2.2 LDW/LDP Crash Benefits

The model predicted that LDW systems would prevent between 7% and 17% of cross-centerline head-on crashes. More advanced LDW systems were predicted to prevent up to 26% of cross-centerline crashes. LDP systems were more effective and were predicted to prevent 32% to 51 %% of cross-centerline head-on crashes. For any crash that was avoided in the model, the probability of injury was set to zero. Because the driver reacted to the warning system, the impact speed changed, which may have changed the probability of injury for simulations where a crash occurred.

10.2.3 Injury Model

The probability of front occupant injury for cross-centerline crashes was estimated using the injury model developed by Bareiss using NASS/CDS frontal crashes and was also utilized in Chapter 6 [61]. The logistic injury model has seven inputs: delta-v, belt use, sex, age, crash compatibility, BMI, and striking location (Table 33, Eq. 26). Delta-v and BMI were continuous covariates and all other injury model parameters were binary. Higher injury severity models lacked enough injured cases to construct a detailed model of occupant injury. The injury model was constructed based on the injury data of front seat occupants that were at least 12 years old and involved in a frontal crash with another vehicle. For cross-centerline crashes, the rear of a vehicle is not struck and therefore the striking location was zero for all cases. Of the 111 simulated cases, 101 cases involving 182 occupants contained all the information necessary to utilize the injury model and estimate the injury benefit. If the vehicle stopped or returned to the lane, the probability of an occupant sustaining a MAIS2+F injury was assumed to be zero. For crashed and parted simulation outcomes, the last velocity was assumed to be the impact velocity.

Table 33. Frontal impact injury model [61].

Variable	Parameter	Estimate	Standard Error	p-value
Intercept	--	-6.516	0.863	<0.001
Total Delta-V	Delta-V (kph)	0.090	0.019	<0.001
Belt Use	Belted	-0.769	0.396	0.054
Sex	Male	-0.891	0.333	0.008
Age	≥65	1.070	0.492	0.031
Crash Compatibility	Car Struck LTV	1.222	0.368	0.001
BMI	BMI (kg/m^2)	0.084	0.021	<0.001
Striking Location	Rear	-1.455	0.501	0.004

$$p(MAIS2+F) = \frac{1}{1+e^{-(\beta_0+\beta_1 DeltaV+\beta_2 Belted+\beta_3 Male+\beta_4 Over65+\beta_5 Compat+\beta_6 BMI+\beta_7 Rear)}} \quad (26)$$

10.2.4 Determine Delta-V

The delta-v was estimated based on the computed final velocity (Eq. 27-28). The final velocity was computed based on the mass of each vehicle (m_1, m_2), and the impact velocity of each vehicle (V_{1i}, V_{2i}). The coefficient of restitution (C_R) was assumed to be 1, which follows an assumption used in WinSmash [66]. Often, the two vehicles in cross-centerline crashes are not perfectly aligned and much of the energy is transferred into rotational energy. To match the actual crash injury outcomes with the predicted injury outcomes for the baseline configuration and account for any rotation after impact, 29.5% of the total delta-v was assumed to be longitudinal.

$$V_{1f} = \frac{m_1 V_{1i} + m_2 V_{2i} + m_2 C_R (V_{2i} - V_{1i})}{m_1 + m_2} \quad (272)$$

$$V_{2f} = \frac{m_1 V_{1i} + m_2 V_{2i} + m_1 C_R (V_{1i} - V_{2i})}{m_1 + m_2} \quad (283)$$

10.2.5 Estimating Injury Benefit and Population Attributed Risk

The population attributed risk, or injury benefit, for multiple covariates was computed following Bruzzi's methodology, which applies the logistic model to the population with countermeasures [62]. For each simulated system configuration, the estimated number of injuries was computed using Equation 29 below. The standard errors from the logistic model were used in the calculation to compute 95th percentile confidence intervals of all estimates. The estimated injury reduction for each system configuration was computed relative to the predicted number of injured occupants in the baseline configuration.

$$Predicted\ Injuries = \sum_{i=1}^{111} Probability\ of\ Injury * Case\ Weight \quad (29)$$

10.2.6 Future Fleet Prediction

The annual number of crashes in the US is related to the annual vehicle miles traveled (VMT), which is an estimate of exposure. In 2015, there was an estimated 3.1 trillion miles traveled in the US and

increases by about one percent each year [45]. Based on a 1% annual increase, the future annual VMT was estimated (Figure 50).

To predict the number of crashes that will occur in the future, the crash rate, the number of crashes per VMT, was assumed to remain constant. The annual crash rate for head-on crashes was computed based on the average annual number of crashes in NASS/CDS 2010 to 2015. There were on average 24,177 head-on crashes (acctype = 50,51) annually involving at least one passenger vehicle that did not rollover. The estimated crash rate for head-on crashes was 7.9 crashes per billion VMT. The ratio of MAIS2+F injured front seat occupants was computed using the same methodology. In NASS/CDS, if the vehicle's model year was greater than 10 years old, a full investigation was not performed. This means that the occupants of these old vehicles are missing injury information. To account for these injured occupants, it was assumed that the ratio of injured occupants to total occupants remained constant between the known and unknown occupants. For head-on crashes, there were 59,648 known front seat occupants at least 12 years old with 9,620 injured occupants resulting in an injury rate of 16.1%. Overall, there was an estimated 8,469 occupants injured in head-on crashes. The estimated injured occupant rate for head-on crashes was 2.8 injured occupants per billion VMT.

The predicted number of future road departure and cross-centerline head-on crashes is dependent on the penetration of LDW systems into the US fleet. The fleet penetration of LDW was estimated by HLDI in 2018 [64] (Figure 51).

The crash reduction was computed as the product between the annual VMT, crash rate, LDW effectiveness, and the probability that the vehicle had LDW (Eq. 30). The same process was used to estimate the number of MAIS2+F injured front seat occupants (Eq. 31). In NASS/CDS, if the vehicle's model year was greater than 10 years old, a full investigation was not performed. This means that the occupants of these old vehicles are missing injury information. To account for these injured occupants, it was assumed that the ratio of injured occupants to total occupants remained constant between the known and unknown occupants.

$$Predicted\ Crashes = VMT * Crash\ Rate * LDW\ Eff_c * P(LDW)_i \quad (30)$$

$$Predicted\ MAIS2+F\ Injured\ Occupants = VMT * Injury\ Rate * LDW\ Eff_i * P(LDW)_i \quad (31)$$

10.3 Results

The 101 simulated crashes used to predict the reduction in MAIS 2+F injured persons contained 182 occupants of which 54 occupants sustained at least one MAIS2+F injury. This represents 6,380 MAIS 2+F injured occupants in road departure crashes nationally. For the baseline system, which represents the original crash outcome, the injury model predicted 6,320 MAIS 2+F injured occupants (Table 34). The expanded activation speed systems had a small increase in injured occupant reduction compared to the base

system. The injury reduction is modest since the additional crashes prevented with the expanded activation threshold are at low impact velocities and have a lower probability of an MAIS2+F injured occupant.

Table 34. Predicted effectiveness for LDW/LDP systems in cross-centerline crashes.

Simulation	Percent Crash Reduction	MAIS 2+F Injured Occupants with CI	Percent MAIS 2+F Injured Occupant Reduction with CI
Baseline	0%	6,320 ± 680	0.0%
LDW	7.5%	4,970 ± 200	21.4% ± 9.0%
LDW with Expanded Speed	16.7%	4,380 ± 190	30.7% ± 8.0%
Advanced LDW	10.8%	4,560 ± 200	27.8% ± 8.3%
Advanced LDW with Expanded Speed	21.9%	3,790 ± 180	40.1% ± 7.0%
HMI LDW	13%	4,490 ± 200	29.0% ± 8.2%
HMI LDW with Expanded Speed	26.2%	3,390 ± 170	46.4% ± 6.3%
LDP	32.3%	3,070 ± 500	47.3% ± 9.7%
LDP with Expanded Speed	51.5%	1,670 ± 390	73.7% ± 6.8%

Using the 51.5% crash effectiveness of LDP for head-on crashes, an estimated 29.3% of crashes will be prevented in 2025 (Figure 100). The predicted number of MAIS2+F injuries was reduced by 35.0% by 2025 (Figure 101).

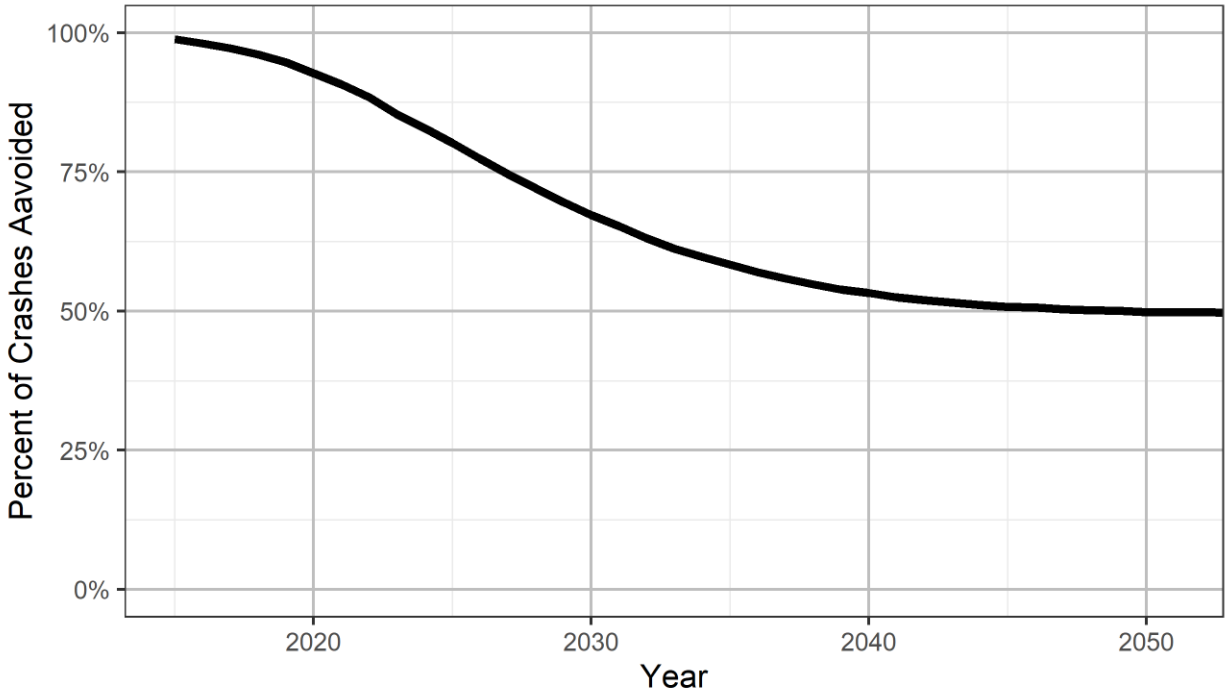

Figure 100. Predicted percent of cross-centerline head-on crashes avoided by LDP.

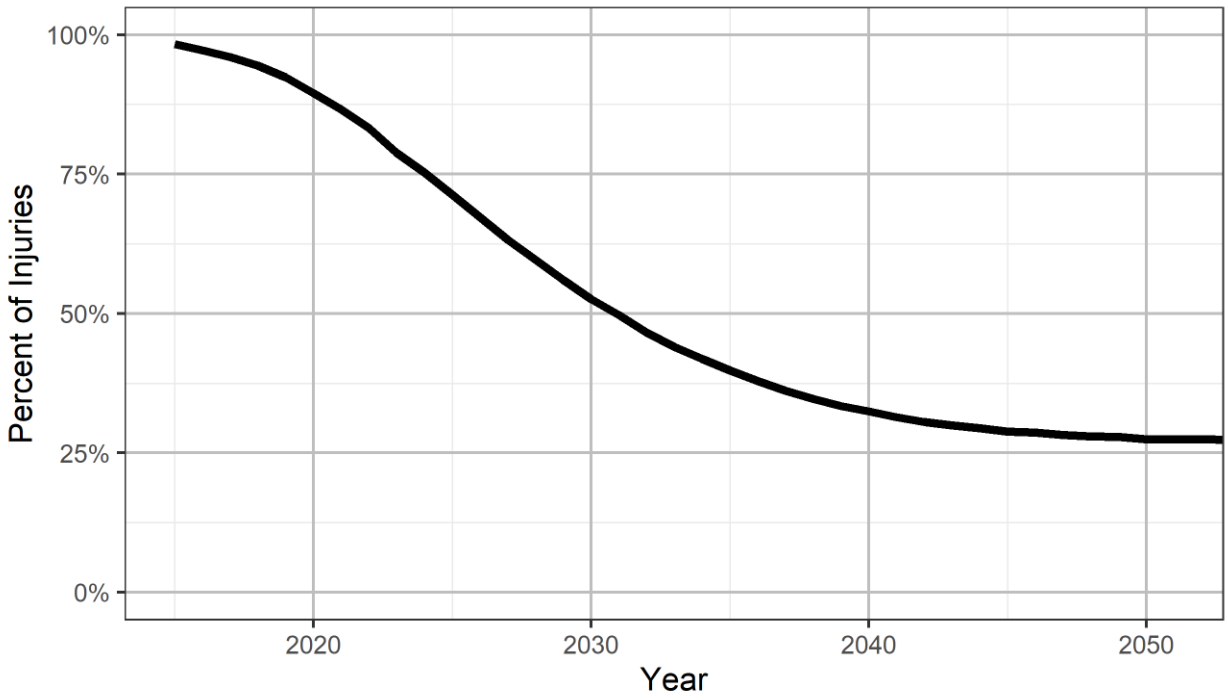

Figure 101. Predicted percent of MAIS2+F injured occupants in cross-centerline head-on crashes prevented by LDP.

In 2025, there will be an estimated 21,429 head-on crashes with LDP resulting in 6,680 MAIS2+F injured occupants assuming an increasing VMT (Figure 102 and Figure 103)

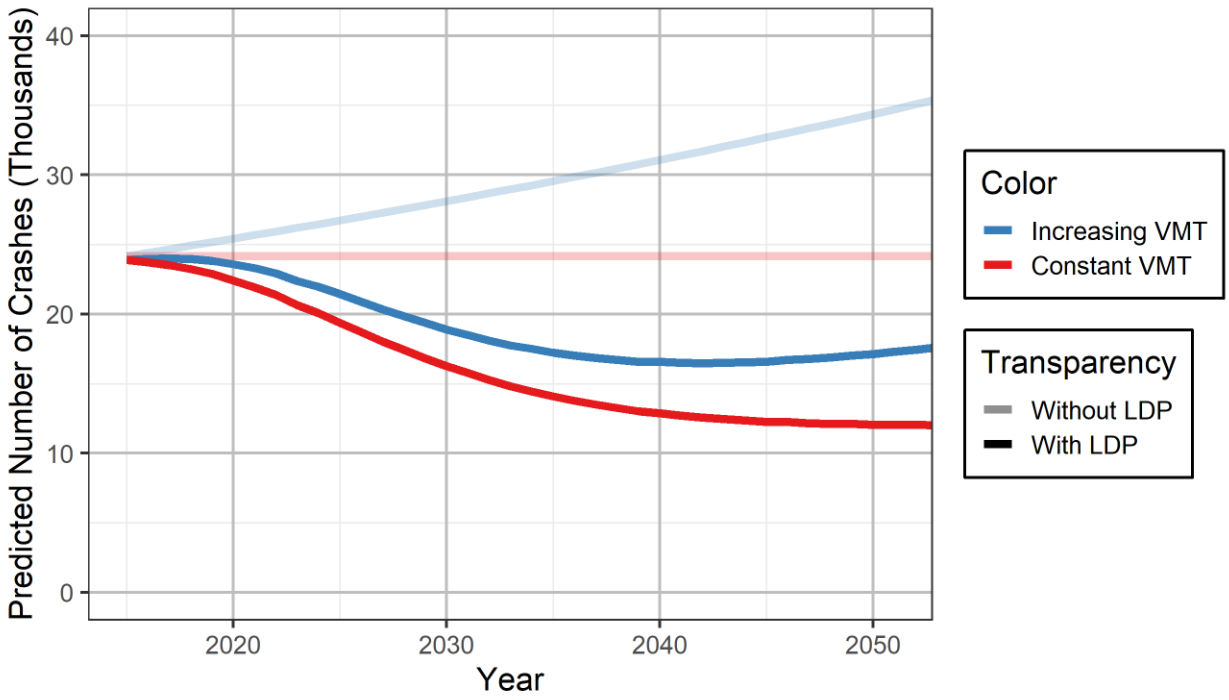

Figure 102. Predicted number of cross-centerline head-on crashes.

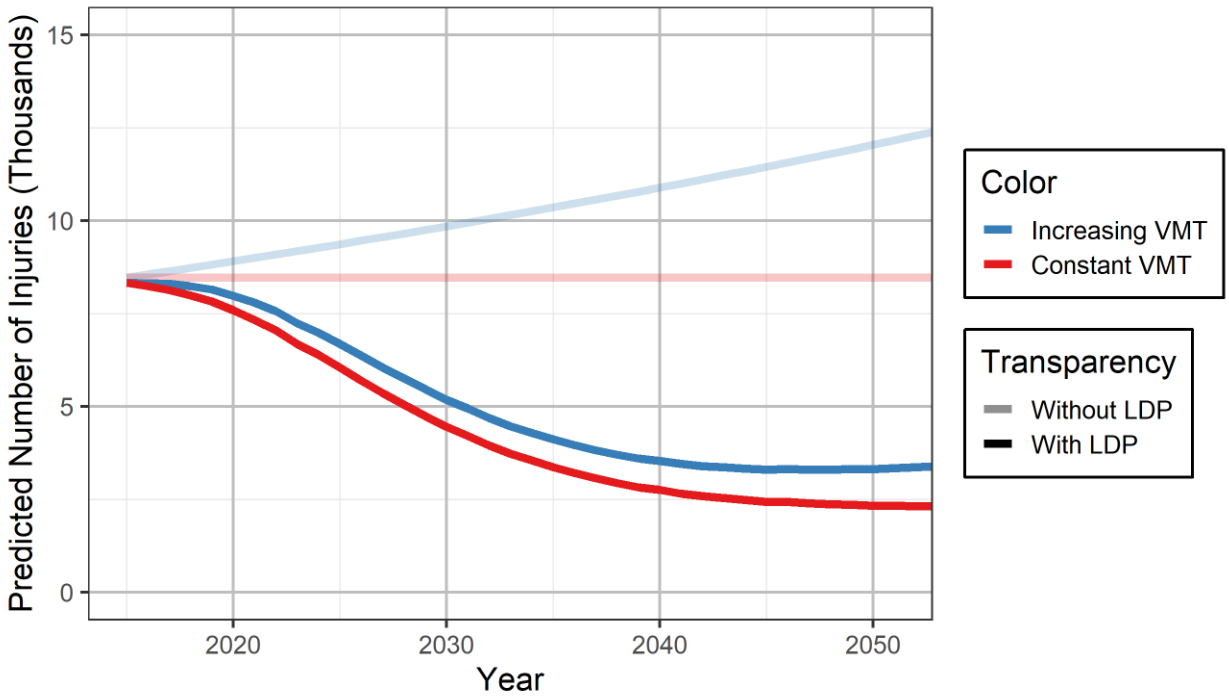

Figure 103. Predicted number of MAIS2+F injured occupants in cross-centerline head-on crashes.

10.4 Discussion

The introduction of LDP systems that can activate before crossing the centerline has the potential to greatly reduce the number of head-on crashes and their resulting injuries. The crash and injury prediction for increasing VMT was always higher than for a constant VMT because it was assumed that the number of crashes increases with VMT. This relationship predicts that the increase in crashes will surpass the benefit from LDP systems entering the fleet in 2048 and the number of head-on crashes and resulting injuries will begin to increase. Continued development of cross-centerline prevention systems will be necessary to reduce the number of crashes after 2048.

Our model assumed that every vehicle has the LDW/LDP system turned on and that every driver responded to the warning. The cross-centerline model assumed that the encroaching vehicle only performed a braking maneuver. Both models assumed that each of the possible driver responses were equally likely to occur. Future versions of the model will incorporate a more realistic driver model based on EDR data.

10.4.1 Validation

The CISS dataset from 2017 to 2019 was used to identify DrOOL road departure crashes to understand how the future predictions compare over this short time frame. For reference, the average crashes and injured occupants in CDS from 2011 to 2015, which was used as the initial point for the prediction model, and the values from CDS in 2015 are provided as reference (Table 35). Since CISS has

a slightly different sample population, NHTSA provided a new variable in 2019 that allows a CDS equivalent population to be determined. After 2017, the estimated crashes in CISS are lower than the predicted values but in 2017 and 2019 the estimated injuries are nearly identical to the predicted values. This could be because the sampled CISS cases are more likely to have known occupant injury outcomes because they resampled if the injuries in recent vehicles were unknown. The large variance in CISS cases makes it challenging to compare with the prediction since it is unlikely that the actual number of head-on crashes would be reduced by 50% in only 2 years.

Table 35. Comparison of CISS 2017 to 2019 to the predicted head-on crashes and injured occupants.

Case Year	CDS/CISS (Actual)		Prediction (Constant VMT)		Prediction (Increasing VMT)	
	Crashes	MAIS2+F Injuries	Crashes	Crashes	MAIS2+F Injuries	Crashes
2010-2015	24,177	8,469	24,177	8,469	24,177	8,469
2015	24,848	15,158	-	-	-	-
2016	-	-	23,990	8,374	24,232	8,458
2017	27,863	8,824	23,790	8,272	24,273	8,440
2018	18,329	14,376	23,516	8,132	24,235	8,381
2019	14,317	8,232	23,166	7,955	24,117	8,281
2019 (CDS Equivalent)	14,317	8,232	23,166	7,955	24,117	8,281

10.4.2 Limitations

The injury model predictions are largely dependent on the delta-v of the frontal crash. The delta-v estimation assumed that the coefficient of restitution was 1, which follows an assumption used in WinSmash [66]. Often, the two vehicles in cross-centerline crashes are not perfectly aligned and much of the energy is transferred into rotational energy. To match the actual crash injury outcomes with the predicted injury outcomes for the baseline configuration and account for any rotation after impact, 29.5% of the total delta-v was assumed to be longitudinal.

In the simulations, the driver would not intervene during the automated steering by the LDP system. In some real LDP systems, the system deactivates if the driver provides steering input or pedal application. The LDW/LDP systems were simulated in isolation and did not consider any possible interactions with other active safety systems on the same vehicle such as AEB.

These predictions assumed that the VMT, the number of crashes, the number of injuries in head-on crashes, in the absence of LDW/LDP systems, only increases by 1% each year. This methodology cannot account for sudden changes to the transportation habits of Americans due to events such as world-wide pandemics. This methodology also assumed that the best simulated system, LDP with expanded activation,

would follow the LDW market penetration curve. More advanced systems, like this one, would likely arrive later to the market than LDW systems and LDW systems would be phased out.

10.5 Conclusions

LDW was predicted to reduce the number of front occupant injuries by 21% to 31% for cross-centerline head-on crashes. LDP systems performed much better and could prevent up to 74% of injured front seat occupants in head-on crashes. Cross-centerline head-on crashes had better injury outcomes than road departure crashes since both the encroaching and impacted vehicles had the opportunity to mitigate the crash. in 2025, there will be an estimated 29% reduction in head-on crashes due to the introduction of LDP.

11 UNDERSTANDING DRIVER RESPONSE IN CROSS-CENTERLINE EVENTS

11.1 Purpose

In a future with advanced driver assist systems (ADAS), there is the potential for a vehicle to cross the centerline and become an imminent threat to a vehicle with an ADAS. The purpose of this chapter is to develop a decision framework for an ADAS based on the braking and steering PRT of a human driver in an unanticipated crash scenario. This study also sought to understand the relationship between the driver's PRT, the type of response, and the urgency of the scenario.

11.2 Methodology

11.2.1 Case Selection

SHRP 2 identified 42 crash or near-crash events in which an oncoming vehicle encroached into the lane of the subject vehicle. Each of the 42 cross-centerline encroachment scenarios were manually reviewed, and 17 met all the selection criteria (Table 36). Three cases were removed because the subject vehicle was in a parking lot rather than on a road. Another, two cases were removed because the subject vehicle was at an intersection and changing roadways. Ten cases were removed because the road did not have a centerline to mark the start of the event. Three cases were removed since the oncoming vehicle did not cross the centerline, and there was no threat to the subject vehicle. Three cases that occurred in the rain and at night were removed because significant glare prevented the researchers from identifying the lane-crossing initiation. There were an additional three cases that were removed because the lane crossing could have been anticipated by the driver. In the first, the encroaching vehicle was overtaking a slower vehicle and the maneuver was visible for nearly six seconds. In the second case, the encroaching vehicle was an emergency vehicle with the lights and siren active. Thus, the driver could have reasonably anticipated the vehicle due to the siren before the emergency vehicle was visible. The third case involved a large truck where only the rear wheel of the trailer crossed the centerline, and the front of the truck did not depart. This case was removed because the presence of the large truck on a tight turn may have initiated the driver's response rather than the actual encroachment. One final case was removed because the time-series acceleration and yaw rate data were unavailable during the encroachment event.

Table 36. SHRP 2 Case selection criteria.

Cumulative Criteria	Remaining Cases
SHRP 2 event categorized as oncoming vehicle encroachment	42
Subject vehicle on a roadway	39
Subject vehicle cannot be changing roadway	37
Road must have a centerline	27
Oncoming vehicle must cross centerline	24
Front-facing video cannot be obscured by glare	21
Event must be unanticipated	18
Event time-series data must be available	17

11.2.2 Determining Driver PRT

The driver's PRT is dependent on the urgency of the situation [37]. In the current study, the length of the event in each of the selected cases was used as a measure of the urgency of the scenario. Presumably, scenarios in which the driver had more time to respond were less urgent. The length of the event and the driver PRT were calculated based on three key points during the crash or near-crash event (Figure 104). Using the forward-facing video, the start of the event was defined as the timestamp when the encroachment was visible. In most cases, this was the moment when the encroaching vehicle first contacted the centerline. In encroachment reveal scenarios when traversing a turn or hill, the first identifiable moment that the oncoming vehicle was in the lane of the subject vehicle was used. Similarly, in night scenarios, the brightness of the headlights was used to indicate the encroachment (Figure 105). The end of event key point was defined as the timestamp when the encroaching vehicle was no longer in the view of the forward-facing camera.

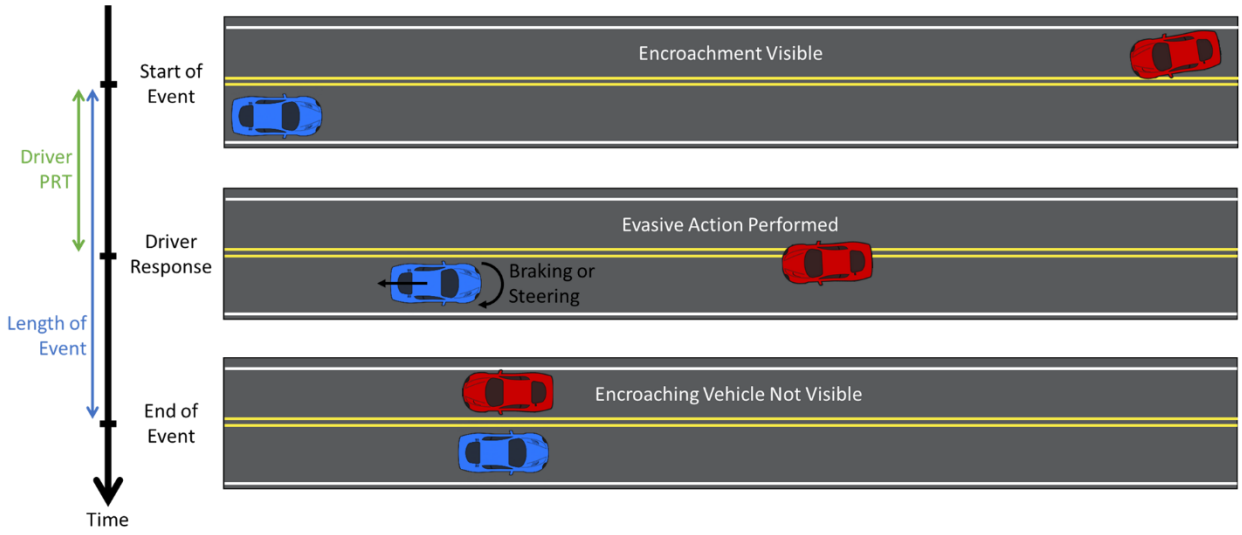

Figure 104. Visual representation of the driver PRT and length of event measurements based on the three key time points.

Figure 105. 19174663 Before (left) and after (right) crossing event for scenarios at night based on headlight brightness.

The driver response key point was determined separately for braking and steering maneuvers. Driver braking was determined using the longitudinal acceleration of the vehicle and the activation of the brake pedal. The longitudinal acceleration was normalized to the longitudinal acceleration 200 ms before the event started to account for cases in which hills were being traversed. The first record of an acceleration less than -0.1 g with the brake pedal activated was considered the start of the braking maneuver. This threshold ensured that the vehicle was decelerating due to braking rather than other external factors such as the grade of the road. If brake pedal activation was unavailable, then the longitudinal acceleration alone was used to identify the start of the braking maneuver (Figure 106).

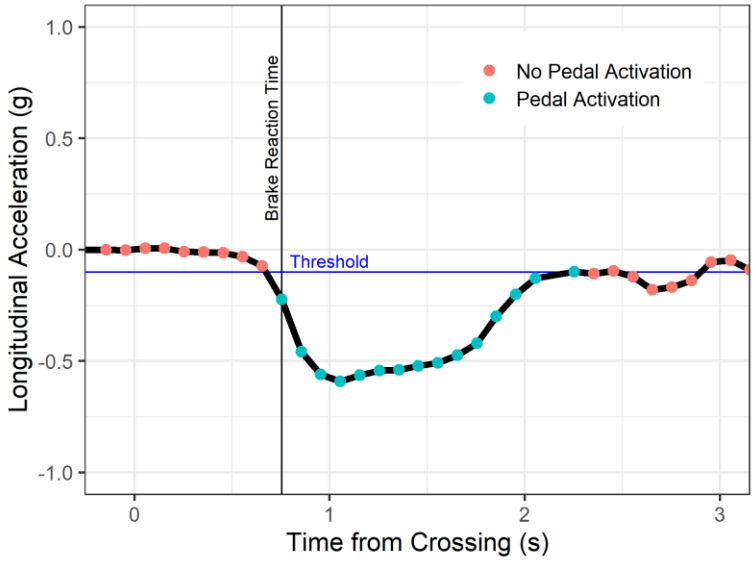

Figure 106. Example acceleration of the subject vehicle with the brake pedal status at each time point. The maneuver threshold of -0.1 g is marked in blue.

The start of evasive steering actions was determined from the information recorded by the yaw rate sensors. The yaw rate was normalized to the yaw rate 200 ms before the event started to account for cases

in which there were curved roads. To be considered an evasive steering action, the yaw rate during the event must have exhibited an N-shape with a peak magnitude greater than 2 deg/s as utilized by Dingus et al. (2016) to identify evasive steering actions during naturalistic driving [35]. The driver steering reaction time based on the yaw rate was the first record with a magnitude greater than 2 deg/s (Figure 107).

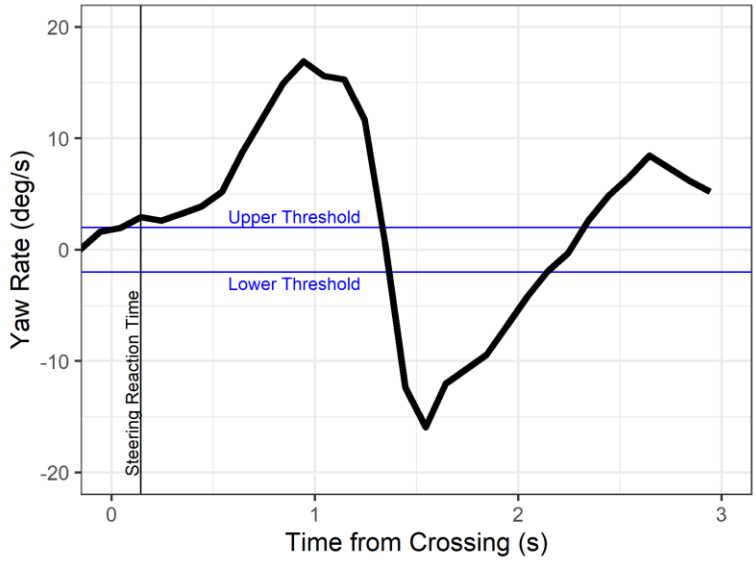

Figure 107. Example yaw rate of the subject vehicle during an evasive maneuver. The maneuver threshold of 2 deg/s is marked in blue.

In each case, the driver's PRT was computed separately for braking and steering maneuvers. To understand if there was a difference in the driver's PRT for braking and steering maneuvers, a two-sample t-test was performed with a significance level of 0.05. The null hypothesis was that the driver steering PRT was no different than the driver braking PRT. Specifically, the average driver braking PRT was compared to the average driver steering PRT.

To understand how the time of the event influenced the reaction time and type, the time to contact (TTC) was estimated at the start of the encroachment event. The TTC at the encroachment event was defined as the distance to the contact point divided by the vehicle velocity at the start of the event (Eq. 32). The distance to the contact point was estimated numerically using trapezoidal integration of acceleration and velocity during the event (Eq. 33-34). The TTC provides a consistent metric for the time the driver had to respond to the encroachment if they did not perform an evasive action.

$$TTC\ (s) = \frac{distance}{initial\ velocity} \tag{32}$$

$$velocity = \sum \frac{\Delta a}{2} * \Delta t \tag{33}$$

$$distance = \sum \frac{\Delta velocity}{2} * \Delta t \tag{34}$$

11.3 Results

There were 11 cases in which the driver both activated the brakes and performed a steering maneuver (Table 37). There were four cases in which the driver activated the brakes, but no steering maneuver was detected. There were also two cases in which the use of a steering maneuver was unknown, one with brake activation and one without. Each of the 11 drivers that performed a steering maneuver, moved to the right, away from the encroaching vehicle. During the steering maneuver, the vehicle may have entered the shoulder, but did not depart the roadway.

Table 37. Distribution of the combinations of driver evasive actions.

	Brake Activation	No Brake Activation
Steering Maneuver	11	0
No Steering Maneuver	4	0
Unknown	1	1

The average steering response time measured by yaw rate activation of 0.39 s was faster than the average braking response time 0.84 s (Figure 108) and was statistically significant (p = 0.031).

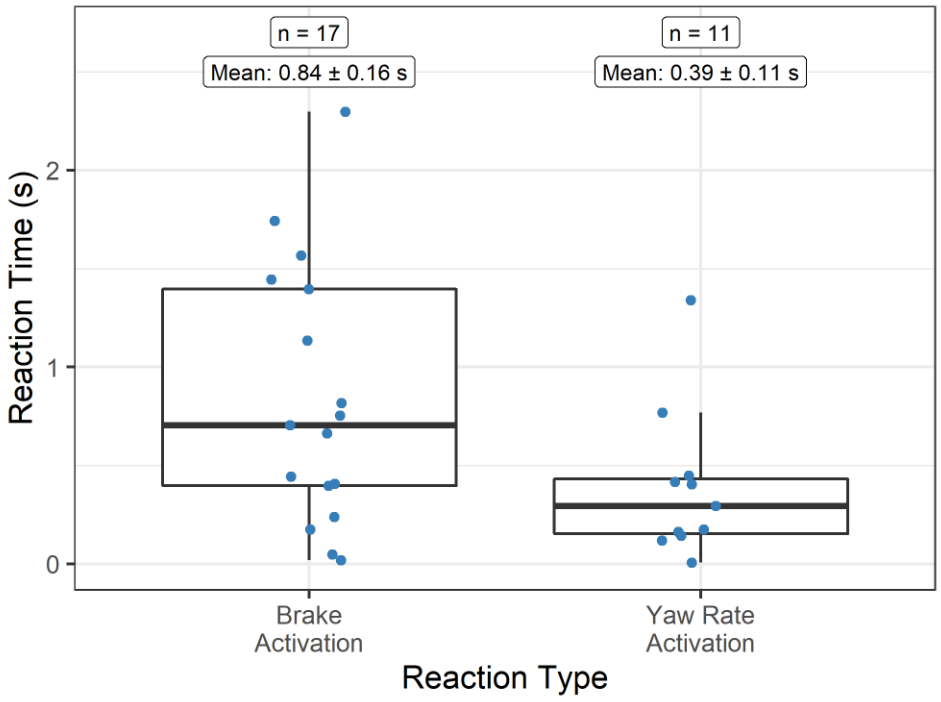

Figure 108. Average reaction time with the accompanying standard error.

TTC on the 17 cases analyzed ranged from 0.21 s to 3.35 s, with a median value of 1.06 s. Each driver's PRT was also plotted against their TTC (Figure 109). When the TTC was less than 1.17 s, the driver more frequently performed a steering evasive action before braking in 70% of cases and braked first in only 20% of cases. There was a single case in which the driver applied the brakes and performed a steering action simultaneously. Conversely, when the TTC was greater than 1.17 s, the first driver evasive

action was always to brake before steering. The response time was shorter when there was less time for the driver to respond. Drivers were more likely to steer when there was relatively less time to react to the encroaching vehicle (Figure 109). Given a driver responds to an encroachment event, the TTC at the start of the event accounted for 48% of the variability in the driver's PRT (Eq. 35).

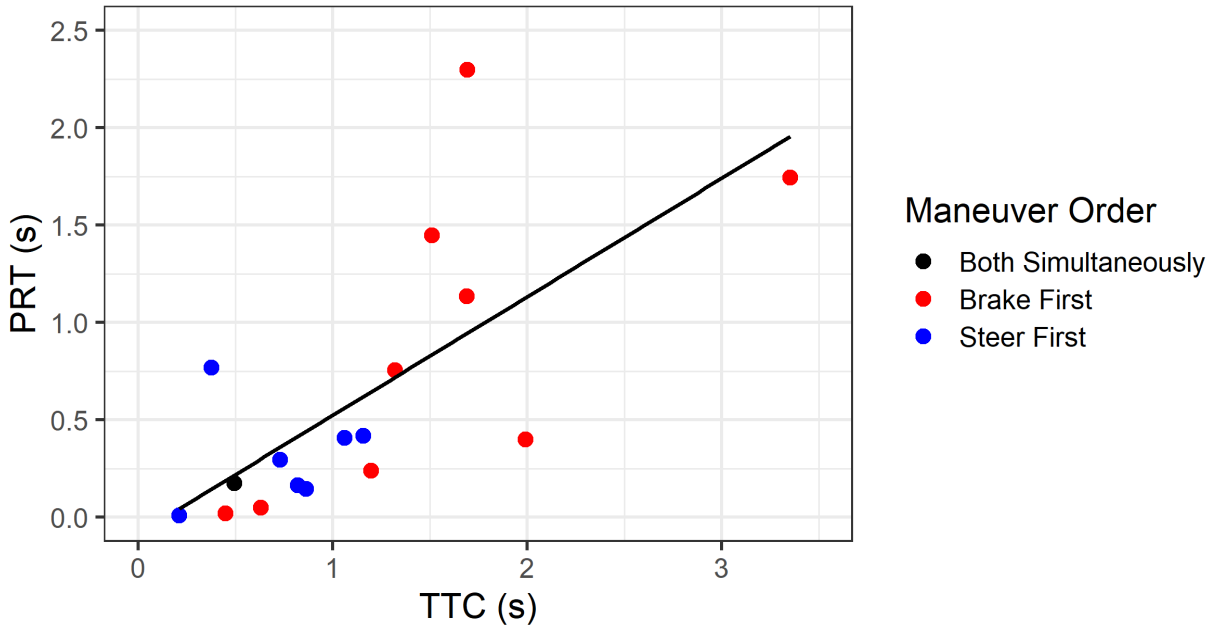

Figure 109. The first driver PRT compared to the TTC at the start of the event.

$$PRT\ (s) = -0.085 + 0.608 * TTC(s), r^2 = 0.484 \quad (35)$$

11.4 Discussion

This study used real cross-centerline events captured during naturalistic driving to measure PRT and TTC. The data showed a few clear trends. The first was that most drivers provided both a braking and steering reaction to the cross-centerline encroachment. This was generally consistent with previous studies that tracked both braking and steering reactions to unanticipated roadway hazards [29]. The current study also found that the steering reaction occurred significantly earlier (by approximately one-half second) than the braking reaction. This finding is somewhat consistent with the analysis of a left turn across path hazard by D'Addario and Donmez [31], though the PRT was much greater and the difference between braking and steering was smaller in the previous work. These differences in absolute PRT values are likely due to the differences in driver expectancy and urgency of various hazards [33].

Following that, one area in which the current research clearly diverged from the previous studies mentioned earlier in which drivers reacted to some type of unanticipated hazard was that the PRTs of the

current study were much faster. The most logical explanation for this is that the current study utilized naturalistic driving with real-world reactions to a truly unanticipated hazard as opposed to staged hazards or simulators. It is admittedly very challenging for researchers to replicate the threats imposed by real-world hazards, so the SHRP 2 database presents a rare opportunity to accurately capture the responses of drivers to these situations. The results of this study provide new benchmarks for PRT values used in the reconstruction of vehicle crashes with unanticipated hazards.

The current study also revealed a more nuanced finding, namely that drivers encountering a hazard with a shorter TTC reacted differently than when faced with a longer TTC. For shorter TTC events, steering was more likely than braking. From a human factors perspective, with the driver's hands already on the wheel and steering inputs provided more regularly during driving than accelerator/brake inputs, it is intuitive to think that steering is a quicker, more natural reaction to an urgent scenario (i.e. shorter TTC) [33, 68]. For less urgent situations (i.e., longer TTC), it is likely that drivers are slowing down to allow for more time to evaluate the encroachment scenario and calculate the optimal evasive action. This finding, and the associated PRT and TTC values, may be particularly useful in the field of vehicle accident reconstruction, especially when considering what expected and typical driver reactions would be in response a cross-centerline encroachment or other similarly rare, unanticipated road hazard.

Understanding of driver's PRT is critical for the improvement of current advanced driver-assistance systems. These systems are intended to augment the driver's natural response to critical precrash scenarios. For example, forward collision warning and lane departure warning systems provide warnings to the driver in an effort to elicit a response before a frontal collision or a road departure occurs [4, 59]. These systems may be more effective for distracted drivers because the warning can direct their attention to the situation sooner than in the absence of the warning. However, one of the main limitations of these systems is that the driver response may not occur soon enough to avoid the collision [50]. Newer advanced driver-assistance systems, such as automatic emergency braking and lane departure prevention systems, can automatically provide either a braking or steering input faster than the driver in potential crash scenarios, which increases the effectiveness of these systems [50, 59]. These systems are designed to respond when a crash is imminent to reduce the chance of a false activation and provide the driver with more time to respond. In these cross-centerline scenarios, ADAS should have a predictable, human-like response to avoid the crash to not disrupt or confuse the human driver in the opposing vehicle. A predictable response could also promote the occupant confidence in the ability of the system to perform safe maneuvers [69]. Based on this study, ADAS should modify the response from braking to evasive as the TTC increases in cross-centerline encroachment scenarios. If an evasive steering action is performed, the vehicle should move to the right, away from the encroaching vehicle, without departing the road.

Accurate measurement of the driver's PRT during naturalistic driving is critical for the development of future highly automated vehicles (HAVs), which provide both longitudinal and lateral control of the vehicle. Current, Society of Automotive Engineers (SAE) Level 2 HAVs are not expected to be the operator of the vehicle [70]. The intent is that the driver will operate the vehicle by constantly monitoring the environment and providing input in emergency situations. The PRT of the driver is an important factor because the driver must be able to respond to unexpected scenarios since a SAE Level 2 vehicle is not necessarily designed to respond. At the next level of automation, SAE Level 3, the vehicle is operating itself, and the occupant does not need to monitor the environment. However, situations may occur in which the automated system must "handover" control back to a human driver [70]. These "handover" scenarios can be categorized based on the urgency, predictability, and criticality of the scenario [71]. The most urgent, unexpected scenarios are the primary area of concern for SAE Level 3 vehicles because an inattentive driver may take significantly longer than the time available to provide input during handover scenarios [72]. Because the initial driver response was found to change from steering to braking for scenarios with a TTC above 1.17 seconds in the current study, that threshold may provide a foundation for differentiating various levels of urgency in unexpected crash scenarios. In addition, this study may support automated braking during "handover" maneuvers if the TTC is greater than 1.17 seconds.

11.5 Limitations

This study assumed that the driver was able to first identify the encroachment at the same moment the researchers identified based on the forward-facing video. This assumption may have increased the measured PRT of drivers who visualized the encroachment later in the event. This study also defined the start of a braking response to be when the deceleration exceeded 0.1 g and the start of the steering response to be when the yaw rate exceeded 2 deg/s. While this consistent threshold is helpful for comparing the PRT across cases, the time for the vehicle to respond to the driver input is still present [33]. In addition, these thresholds may not capture any minor evasive actions that did not reach 0.1 g deceleration or a yaw rate greater than 2 deg/s. Based on the forward-facing video, there were three drivers who appeared to perform a subtle steering maneuver, but the maneuver magnitude was too small to be captured by the 2 deg/s steering threshold. Those three cases were not considered evasive actions based on the yaw rate threshold despite being in response to the encroachment event.

This study did not analyze effect of driver distractions or driver age on the driver's PRT. Driver PRT and crash risk has been shown to be drastically increased when the driver is distracted or engaged in secondary tasks [32, 35, 73, 74] as well as for elderly drivers [33]. Within the current study sample, six drivers were distracted or engaged in a secondary task during the encroachment event based on the information coded in SHRP 2. Two drivers were using a cellular phone during the event. One driver was

talking to another occupant. One driver was singing and dancing to music, and another driver was adjusting the radio. One other driver was distracted by something out the window and was not looking ahead. Due to such a sample size, this study did not have the statistical power to analyze the effects of driver age or distraction.

11.6 Conclusions

The driver steering PRT of 0.39 s was statistically lower than the braking PRT of 0.84 s in response to centerline crossing events involving approaching vehicles. The current study found that as the TTC of the encroachment event increased, the driver PRT increased and the driver was more likely to brake before steering. Not only does this study support previous findings that the urgency of an unexpected crash scenario can influence driver PRT, but it also indicates that urgency can influence the type of driver response.

12 CHARACTERIZATION OF ROLLOVER CRASHES

12.1 Purpose

The objective of chapter 12 was to determine the frequency of and characterize rollover crashes in the U.S. vehicle fleet. By understanding the nature of rollover crashes, potential countermeasures can be identified to prevent these crashes from occurring.

12.2 Approach

12.2.1 Data Selection

All recorded rollover crashes that occurred between 2011 and 2015 were extracted from NASS/GES, NASS/CDS, and FARS. These three databases cover a large range of crash severities from police reported crashes (GES), and moderate to fatal injurious crashes (CDS), to fatal crashes (FARS).

Control loss road departure crashes account for 34% of all rollovers in the US (Figure 110). While rollovers after a DrOOL account for a larger proportion of rollover crashes, these rollovers could be mitigated from the LDW/LDP systems analyzed in previous chapters. Therefore, the following analysis focuses on rollovers that occur after a control loss road departure.

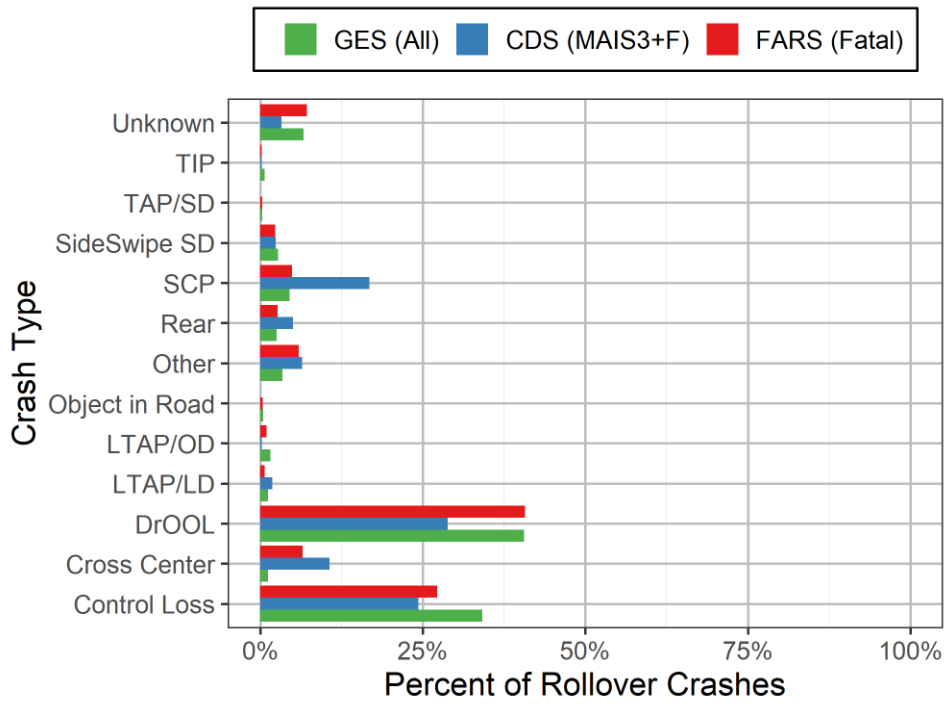

Figure 110. Distribution of crash types for crashes containing a rollover.

12.2.2 Analyzed Parameters

For every rollover crash in each database, twenty-seven factors were analyzed from four main characteristics: road/environment, vehicle, driver, and occupants (Table 38). The road/environment

characteristic was analyzed for each case since every vehicle and occupant in the crash interacts with a road/environment. The vehicle characteristics analysis was restricted to those vehicles that rolled over during the crash. The roof strength from IIHS safety tests was matched to vehicles in NASS/CDS based on the make, model, and year of each vehicle. The driver characteristics analysis only considered the drivers of the vehicles that rolled over. Only occupants of passenger cars that rolled over were analyzed.

Table 38. Data elements for in-depth characterization.

	Characteristic	Factors	Data Source
Crash Causation	Road/Environment	Speed Limit	All
		Road Alignment	All
		Number of Lanes	All
		Weather Condition	All
		Surface Condition	All
		Roadway Lighting	All
	Driver	Avoidance Maneuver	All
		Demographics (age, sex)	All
		Alcohol Involvement	All
		Drug Involvement	All
		Pre-crash Avoidance Maneuvers	All
Injury Causation	Vehicle	Rollover Location	CDS
		Rollover Type	CDS
		Rollover Distance	CDS
		Number of Quarter Turns	CDS
		ESC	CDS
		Model Year	All
		Roof Strength	CDS
		Roof Displacement	CDS
		Airbags	CDS
	Occupants	Demographics (age, sex)	All
		Belt Use	All
		Ejection	All
		Seat Location	All

Table 39. Number of analyzed cases across each of the datasets.

Dataset	Population	Injury Severity	Weighted Crashes (unweighted)	Weighted Occupants (unweighted)
NASS/GES	All Police-Reported DrOOL Crashes	All	331,512 (4,507)	489,115 (6,976)
NASS/CDS	Tow-Away DrOOL Crashes	MAIS 3+F	5,584 (86)	6,374 (100)
FARS	DrOOL Crashes with a Fatally Injured Occupant	Fatal	10,126	11,084

12.3 Results

Rollover crashes were most common on 55 mph roads (Figure 111). Unlike DrOOL and head-on crashes, fatal rollovers do not have a relationship with speed limit. Most rollover crashes occurred on straight road sections (Figure 112).

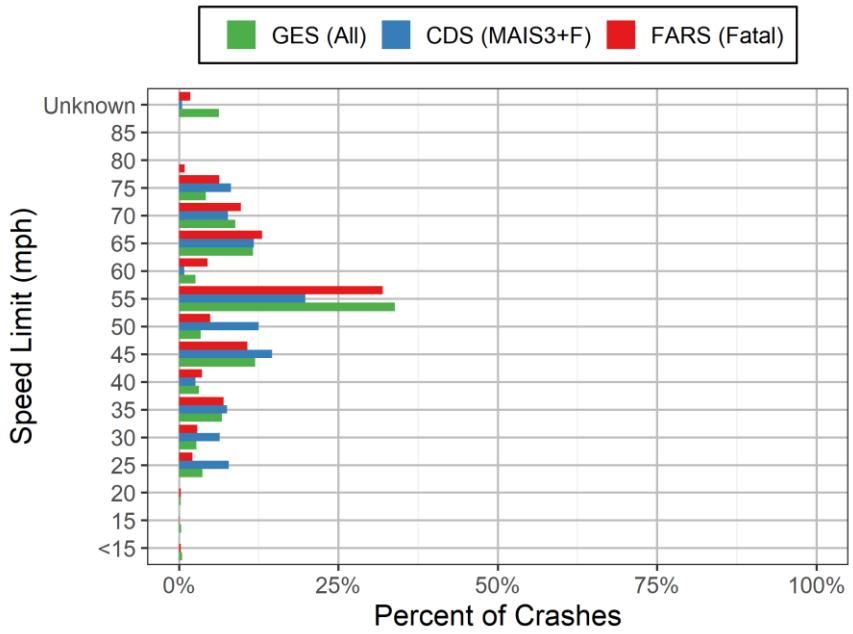

Figure 111. Distribution of speed limits for rollover crashes.

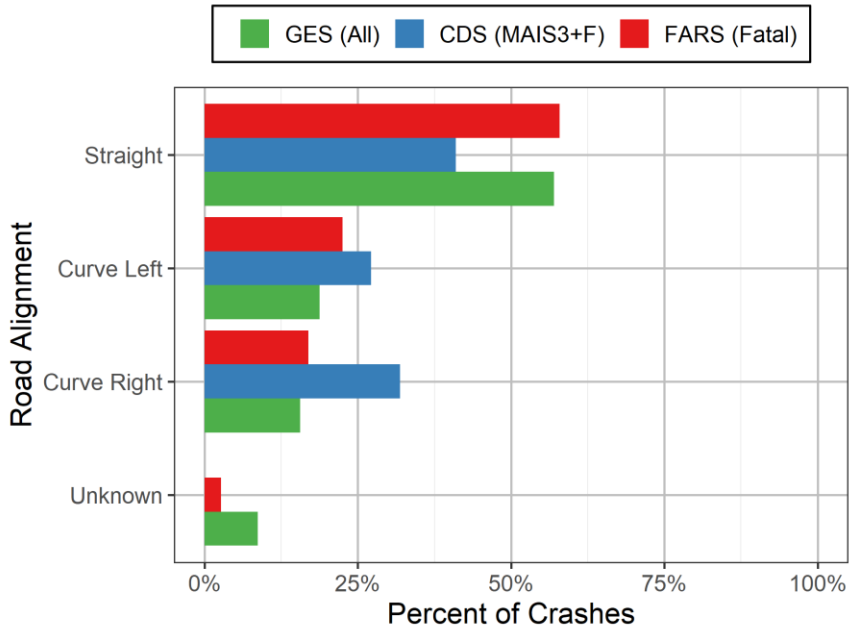

Figure 112. Distribution of road alignment for rollover crashes.

Two lane roads were the most common location of control loss rollover crashes but these roads are also one of the most common roadway types in the US (Figure 113). Following the NASS/CDS definition,

this counts all lanes on undivided roads and the lanes in the same direction for divided roads. Fatal rollover crashes were as common at night in the dark as during the day (Figure 114).

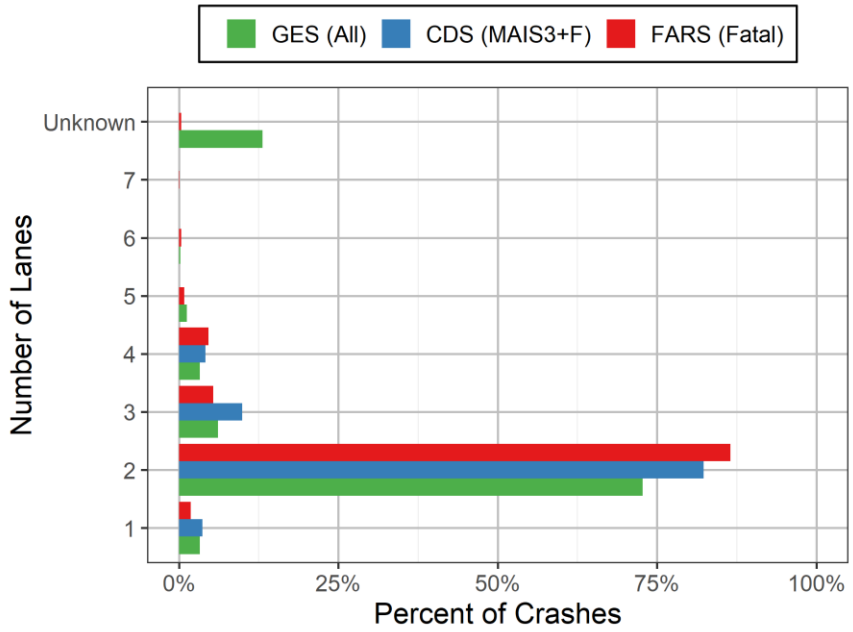

Figure 113. Distribution of lanes for rollover crashes.

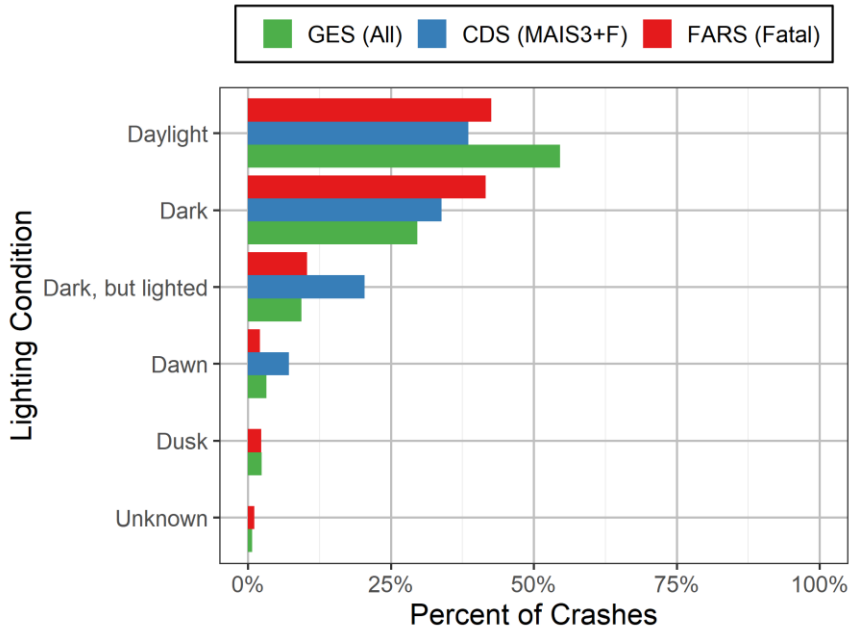

Figure 114. Distribution of lighting conditions for rollover crashes.

Most rollover crashes occurred on clear days with dry roads (Figure 115 and Figure 116). In addition, moderate to fatal rollover crashes were overrepresented on these clear days with dry roads.

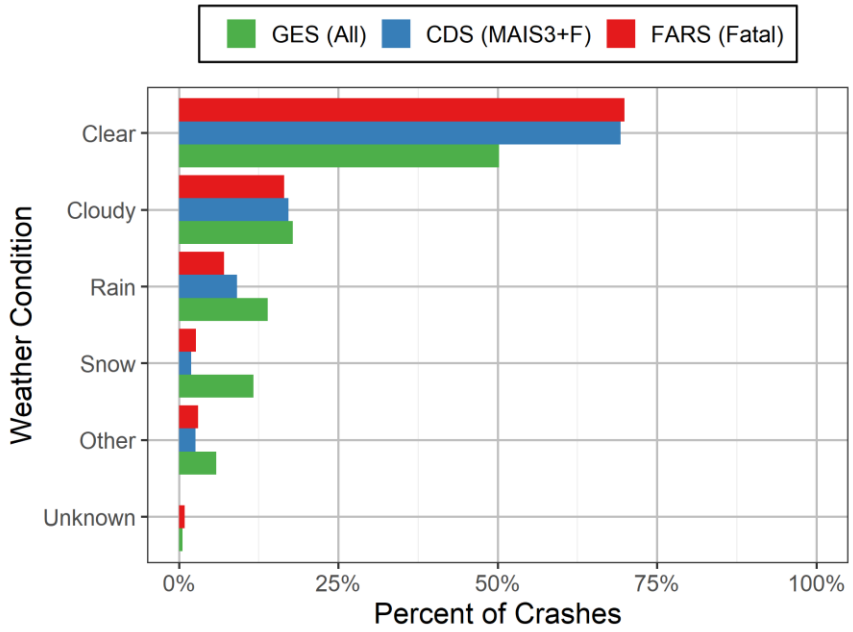

Figure 115. Distribution of weather conditions during rollover crashes.

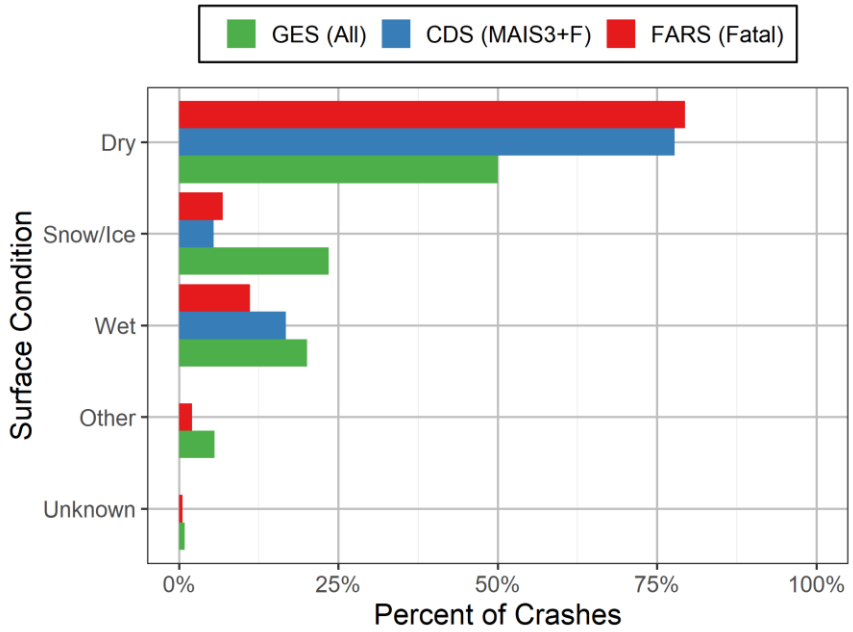

Figure 116. Distribution of surface conditions during rollover crashes

Before losing control of the vehicle, nearly all drivers were not attempting any maneuver such as turning on to a new road (Figure 117). After the control loss, most drivers performed a steering maneuver if an evasive action could be determined (Figure 118). This may indicate that drivers were attempting to regain control of the vehicle before the rollover occurred.

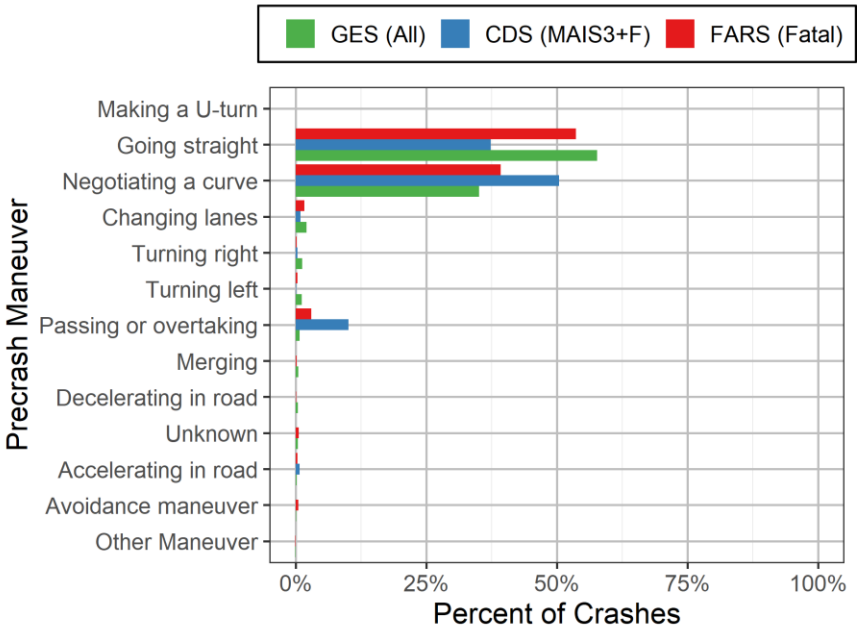

Figure 117. Distribution of maneuvers before the loss of control rollover.

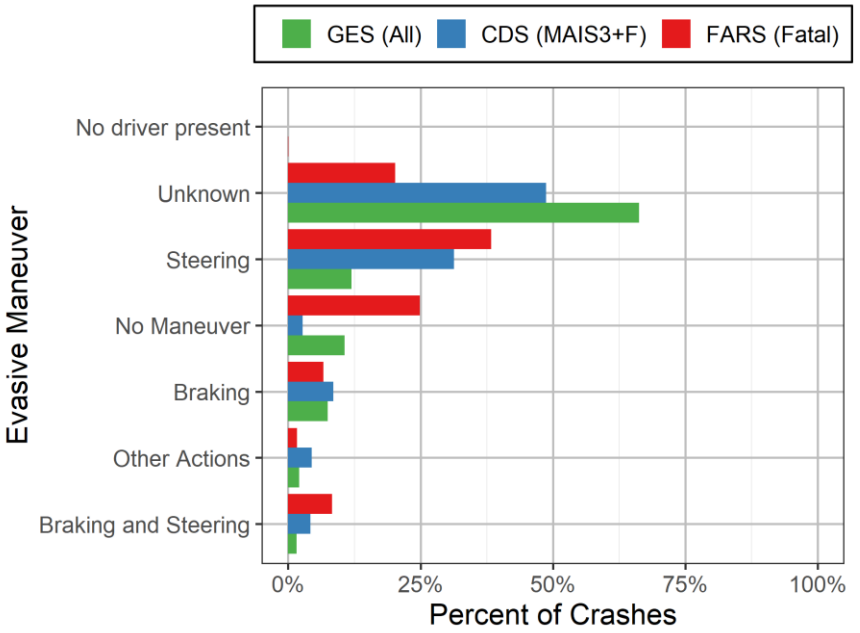

Figure 118. Distribution of evasive actions after control loss before the rollover.

Most drivers in rollover crashes were relatively young; 41% of drivers were at most 25 years-old (Figure 119). More severe crashes tended to have older drivers, which may indicate that older drivers are more susceptible to serious injuries. Most of the drivers were male (Figure 120).

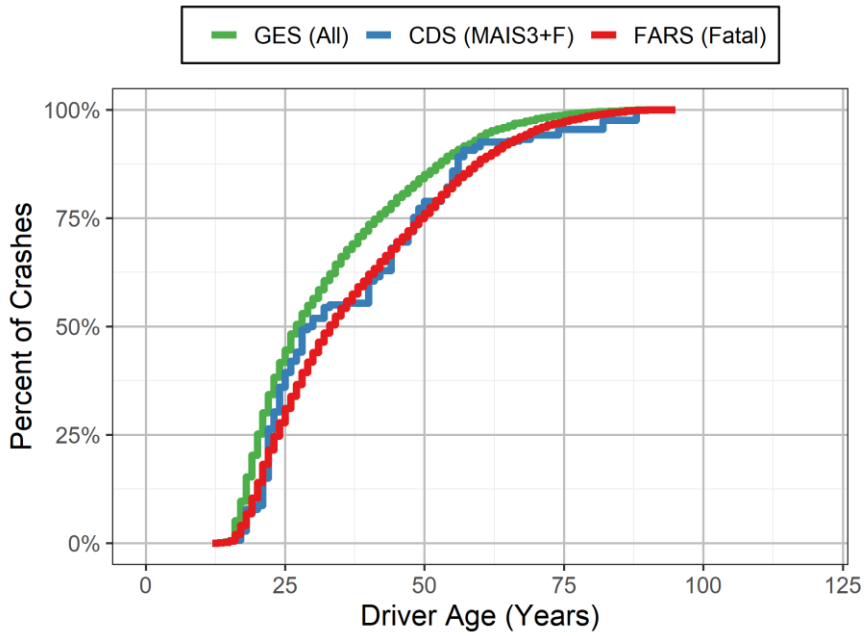

Figure 119. Distribution of driver age in rollover crashes.

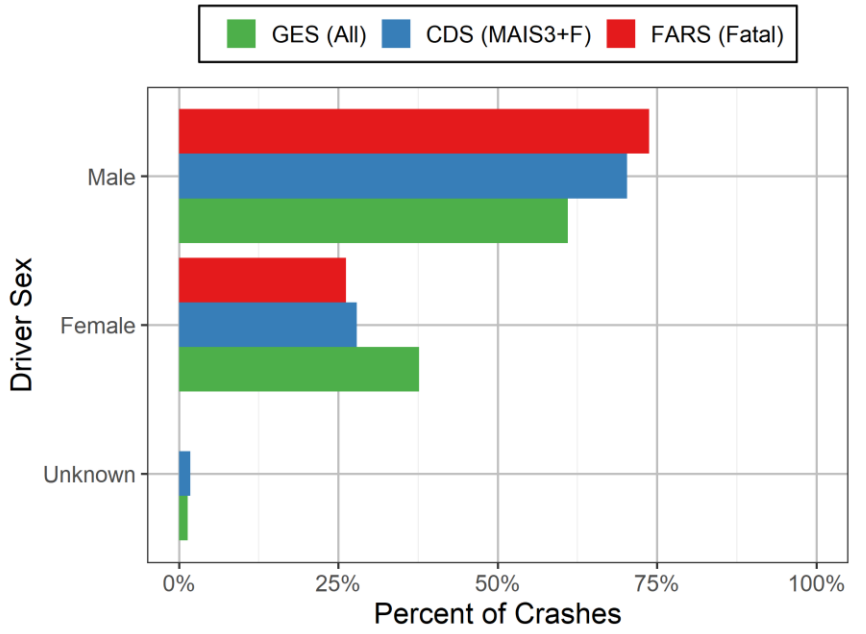

Figure 120. Distribution of driver sex in rollover crashes.

Moderate to fatal crashes were overrepresented among cases that involved alcohol or other impairing drugs (Figure 121 and Figure 122). However, it should be noted that these counts are based on police assessment of alcohol or drug involvement and may not always rely on a test. This could bias the results toward none or unknown involvement.

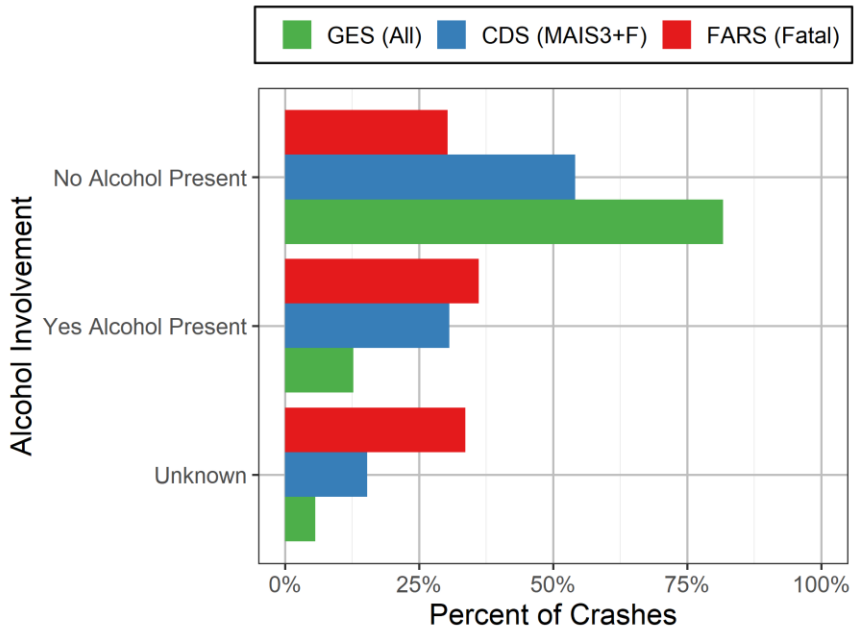

Figure 121. Involvement of alcohol in rollover crashes.

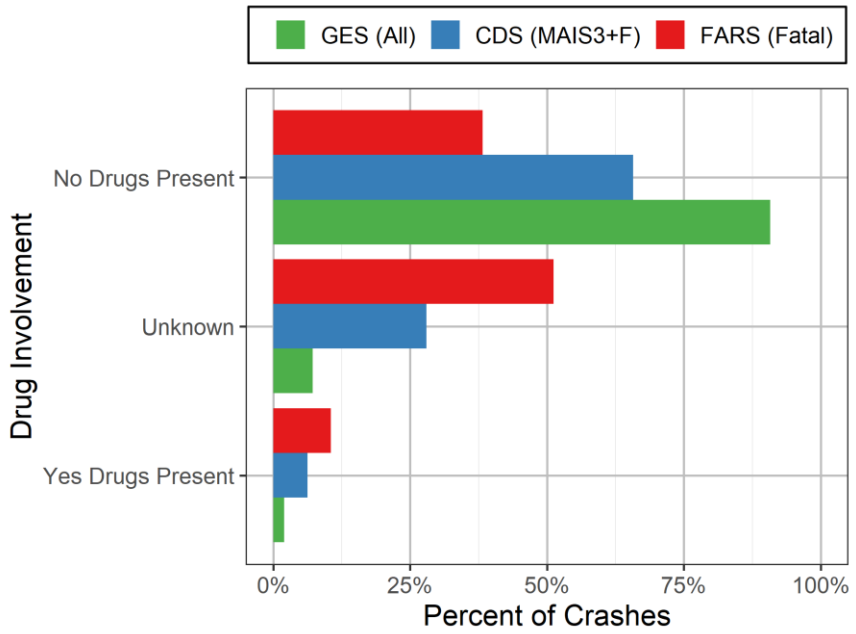

Figure 122. Involvement of drugs in rollover crashes.

The vehicle model year in all rollover crashes and fatal rollover crashes are very similar (Figure 123). CDS does not follow the same curve because NHTSA purposely sampled vehicles that were less than 10 years old. Nearly three-quarters of the occupants in rollover crashes are in the driver seat (Figure 124).

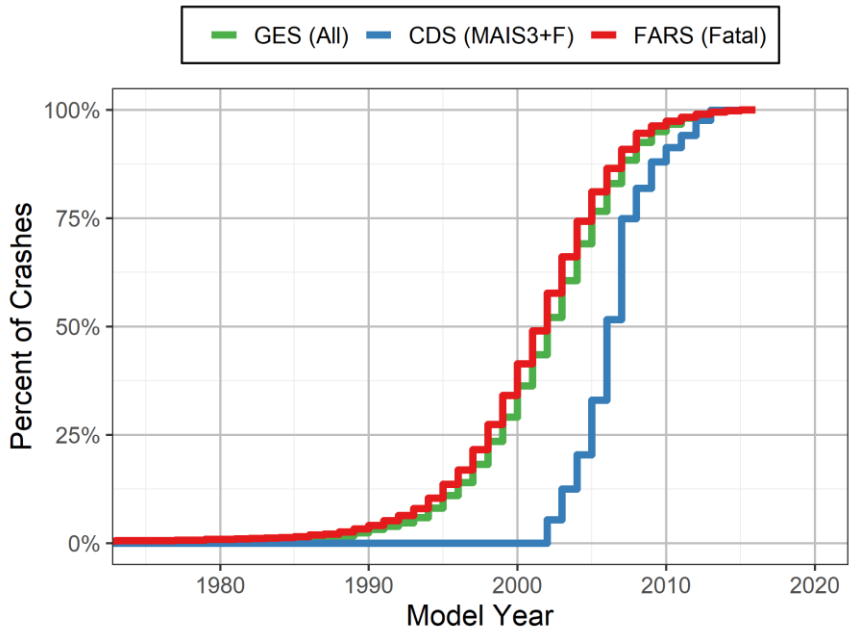

Figure 123. Distribution of vehicle model year in rollover crashes.

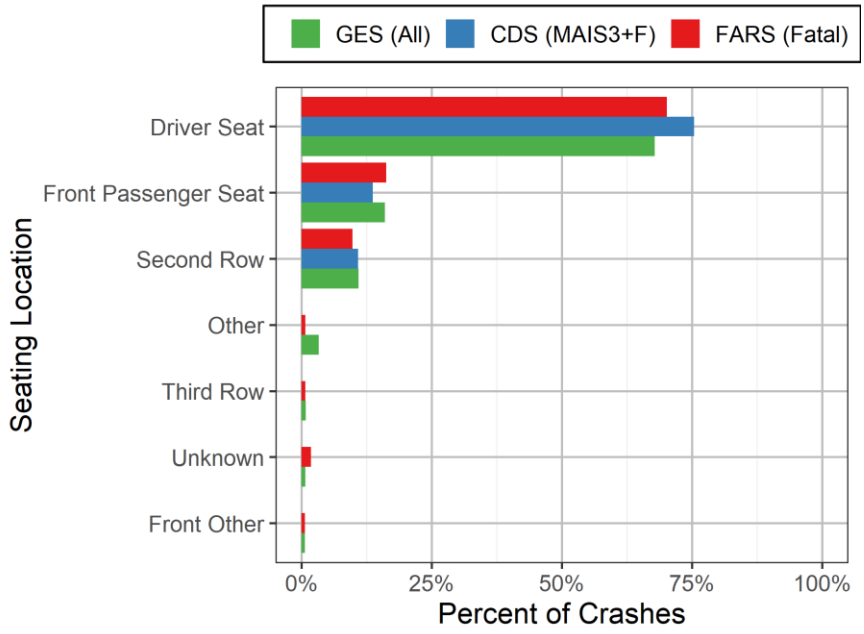

Figure 124. Distribution of rollover occupant seating location.

Since most of these crashes involve a single occupant, there is a drastic increase in the age distribution after occupants reach licensing age (Figure 125). Similar to the driver age distribution, more severe crashes tended to have older occupants. Most of the occupants in rollover crashes were male (Figure 126).

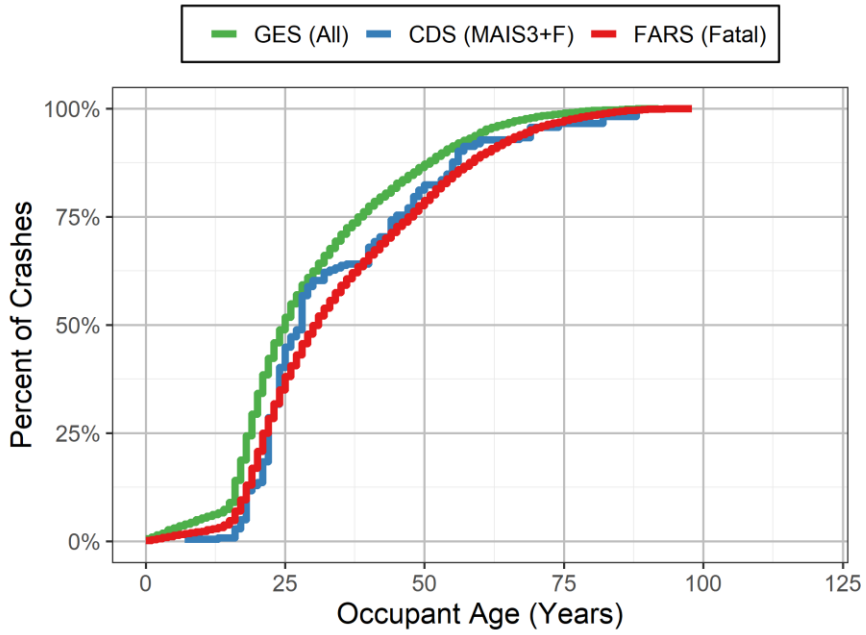

Figure 125. Ag distribution of occupants in rollover crashes.

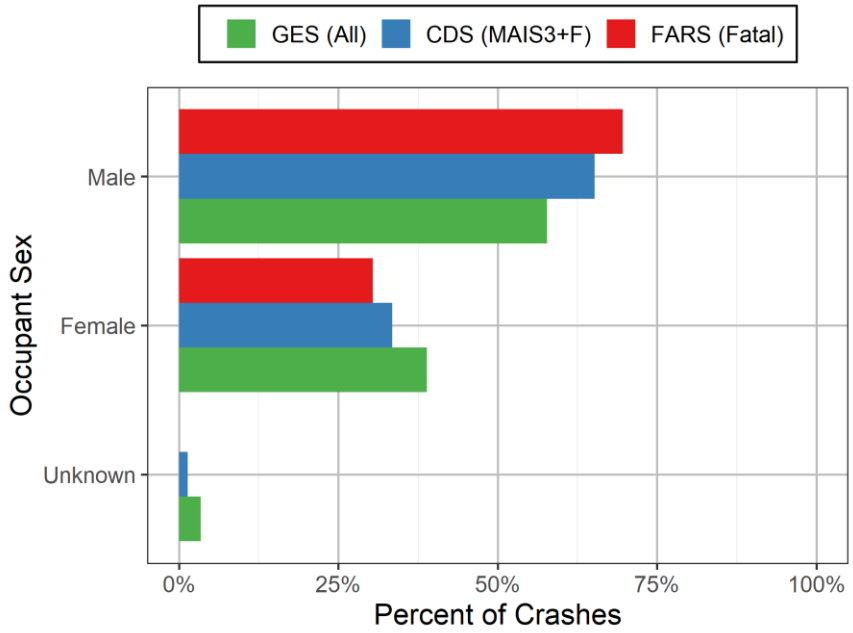

Figure 126. Sex distribution of occupants in rollover crashes.

Fatal and MAIS 3+F injured occupants were overrepresented among unbelted occupants and ejected occupants in rollover crashes (Figure 127 and Figure 128).

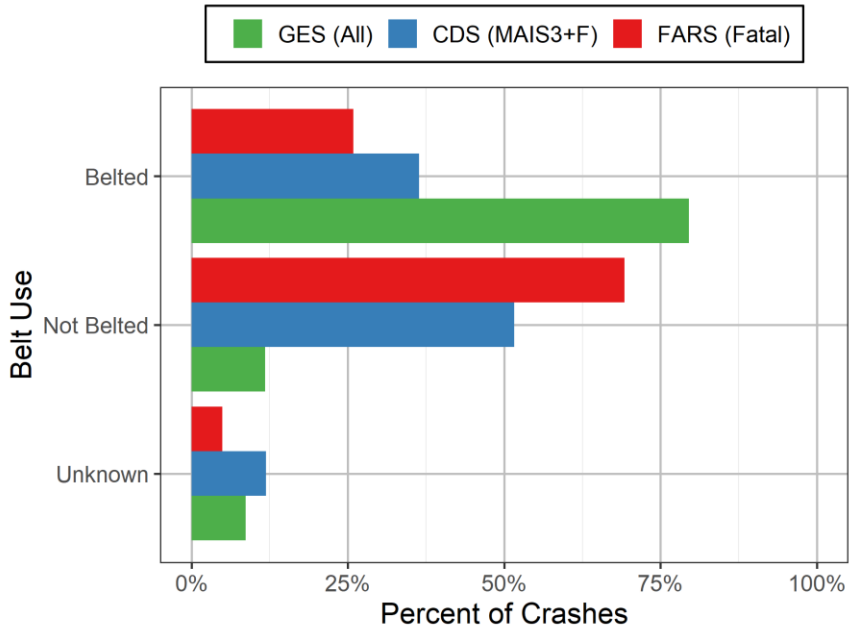

Figure 127. Distribution of occupant belt use in rollover crashes.

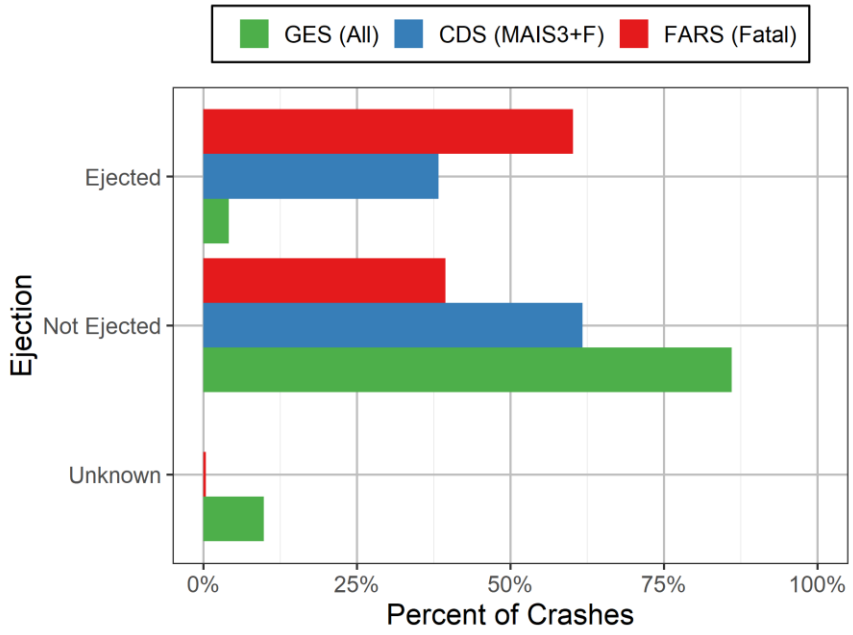

Figure 128. Distribution of ejected occupants in rollover crashes.

Very few belted occupants in rollover crashes were ejected from the vehicle (Figure 129). Most of the ejected occupants were unbelted.

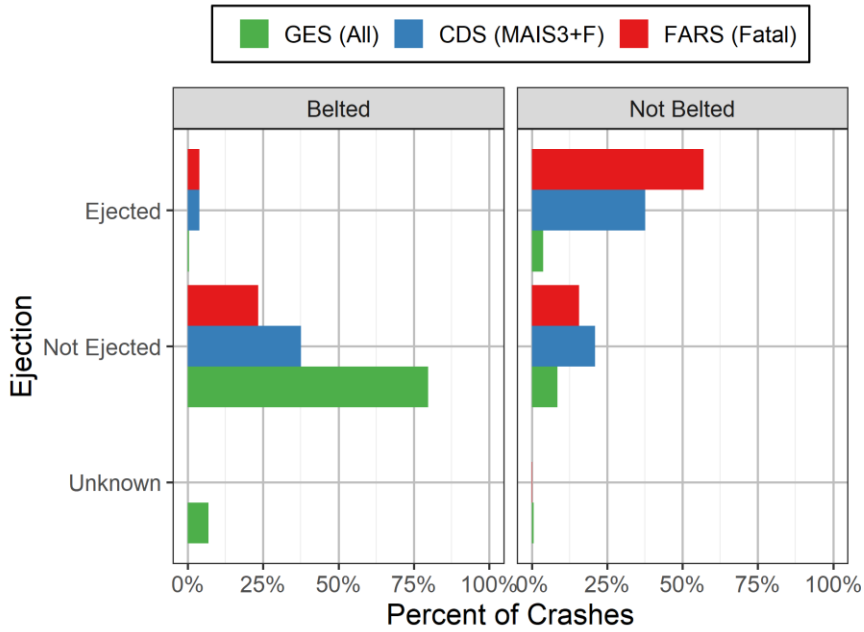

Figure 129. Distribution of ejected occupants given their belt use in rollover crashes.

The most common type of rollover was a trip-over (Figure 130). Trip-over rollovers occur when the lateral motion of the vehicle is prevented, which causes the vehicle to "trip" and initiate the rollover. Bounce-over rollovers, the second most common rollover, occur when a vehicle contacts a fixed-objects and the resulting vehicle rotation initiates the rollover.

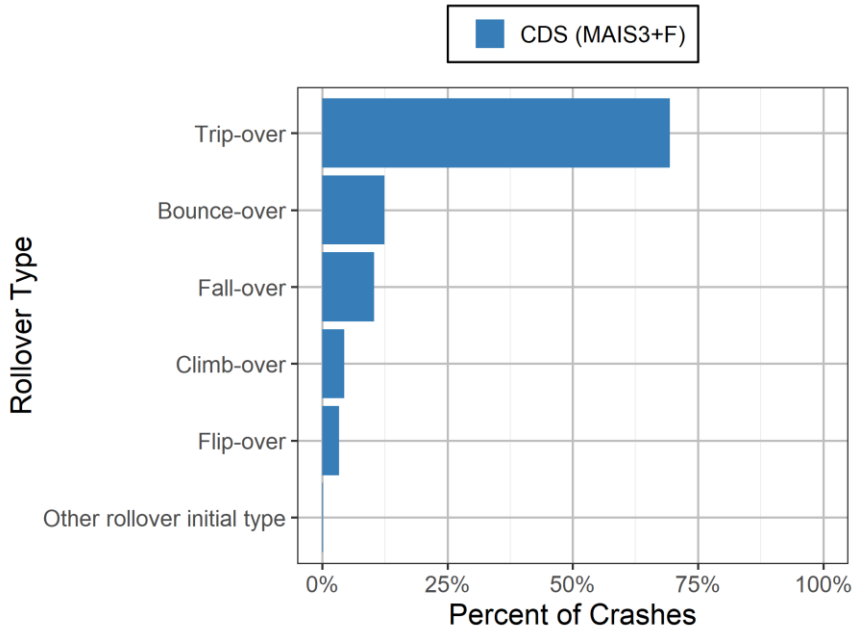

Figure 130. Distribution of rollover type.

Because these are single vehicle control loss rollover crashes, the rollover almost always occurs along the roadside (Figure 131). ESC was a standard feature in roughly 10% of the vehicles in rollover crashes (Figure 132).

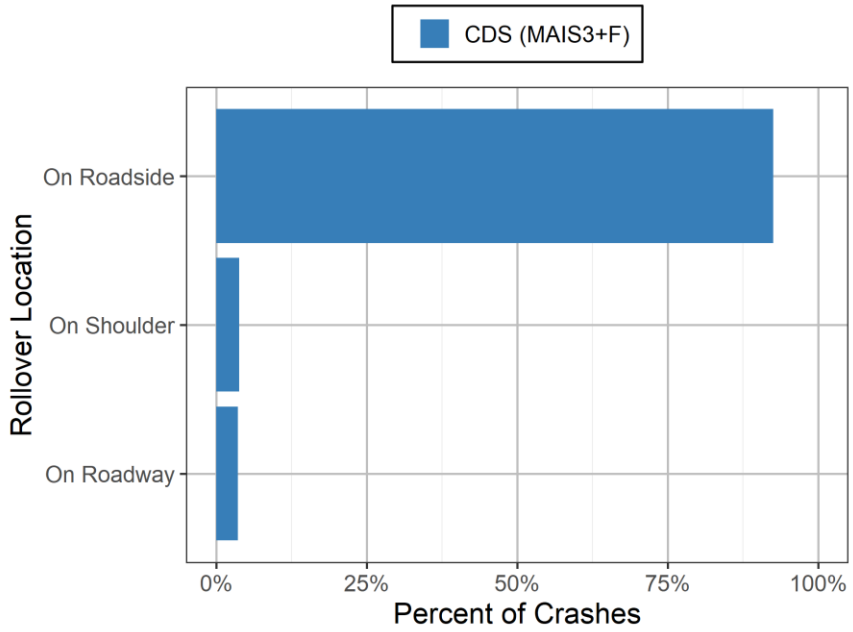

Figure 131. Distribution of rollover location.

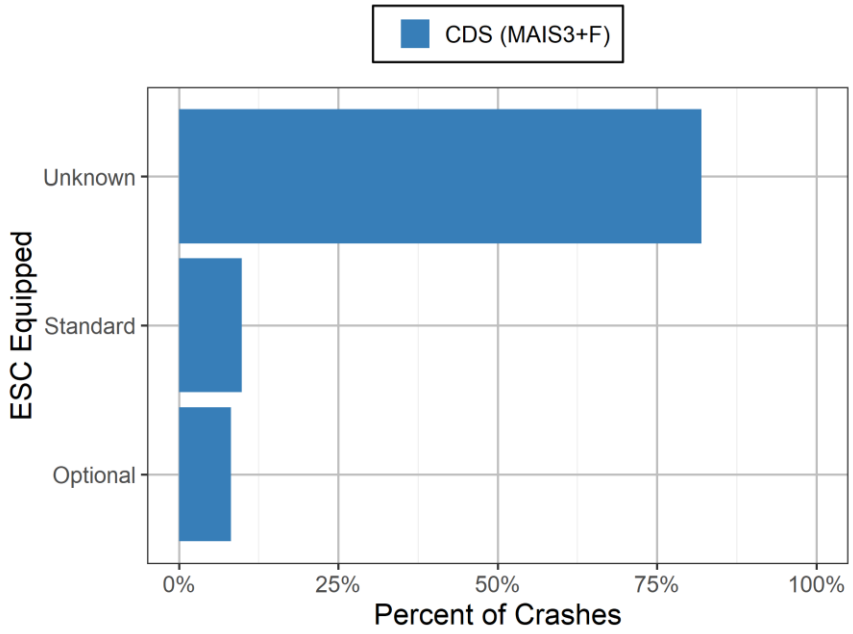

Figure 132. Distribution of ESC equipped vehicles in rollover crashes.

Vehicle rollovers are often quantified based on the number of quarter turns that occur during the rollover. Even quarter turns occurred more frequently than odd quarter turns because resting on the roof or the wheels is a more stable configuration than either side of the vehicle (Figure 133). The median roll distance was 19 m (Figure 134).

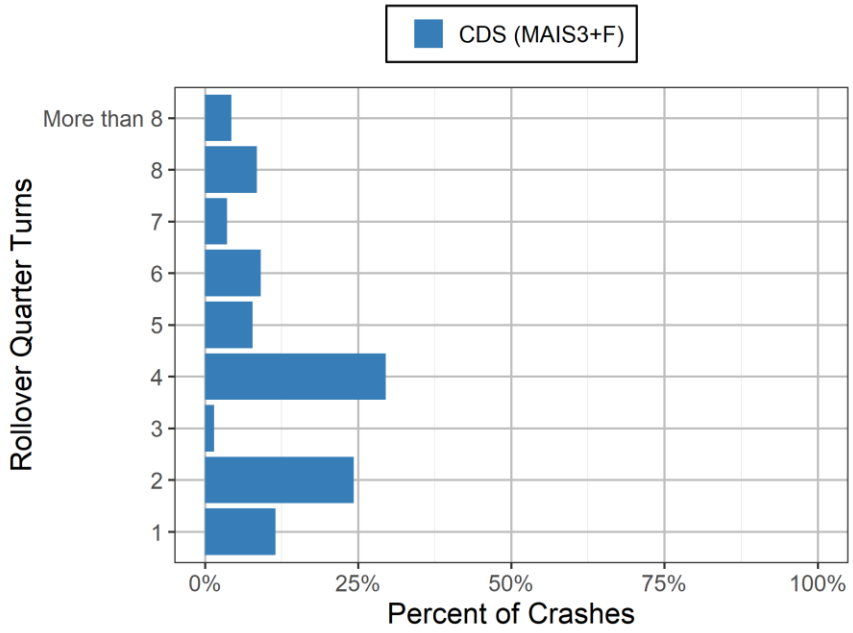

Figure 133. Distribution of rollover quarter turns.

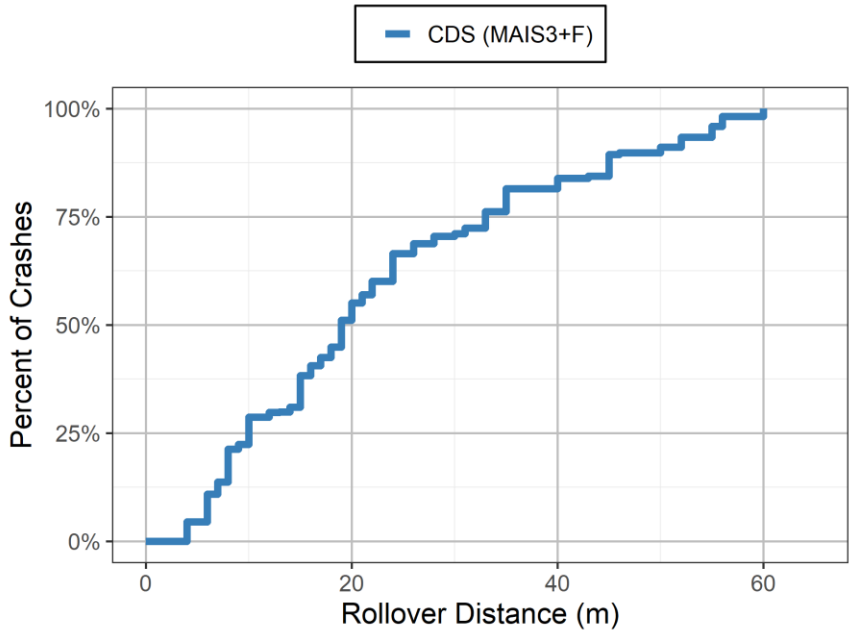

Figure 134. Distribution of rollover distance.

Based on the IIHS and NHTSA roof SWR tests, vehicles involved in rollovers most commonly had a roof SWR of 3 or 4 (Figure 135). Most vehicles experienced less than 15 cm of roof displacement from the rollover crash (Figure 136).

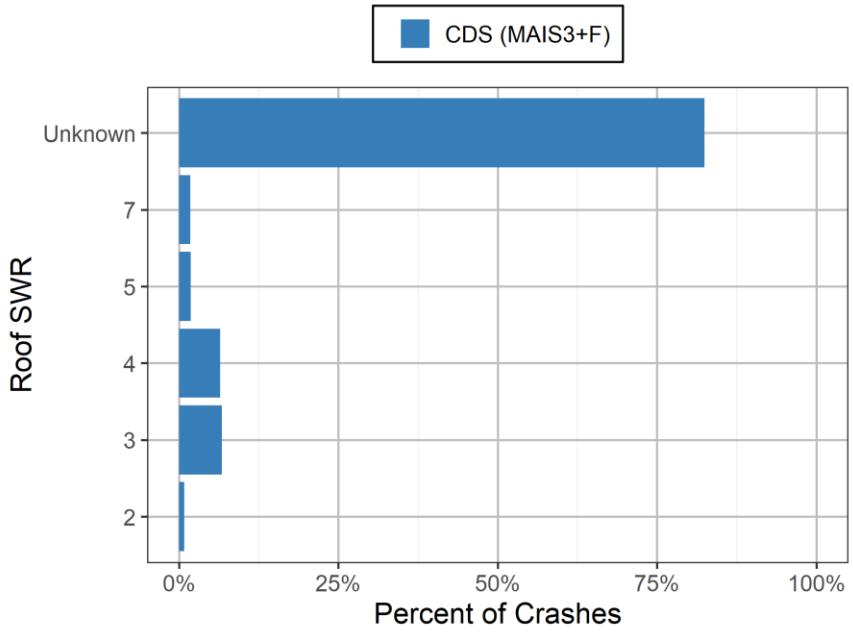

Figure 135. Distribution of vehicle roof SWR.

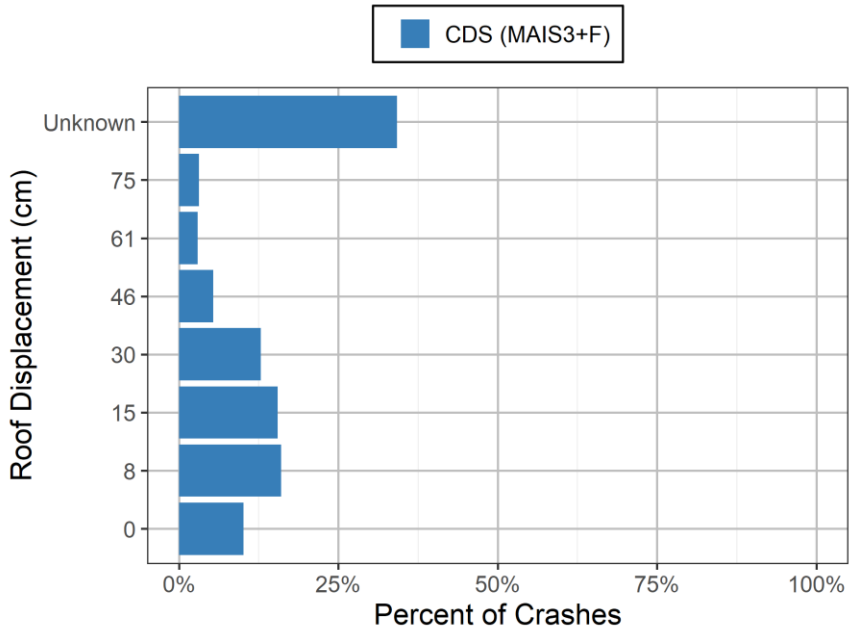

Figure 136. Distribution of roof displacement from a rollover crash.

A side airbag was deployed in 22% of control loss rollover crashes (Figure 137). Many vehicles within the sample were not yet equipped with side curtain airbags as a method to comply to FMVSS 226[75].

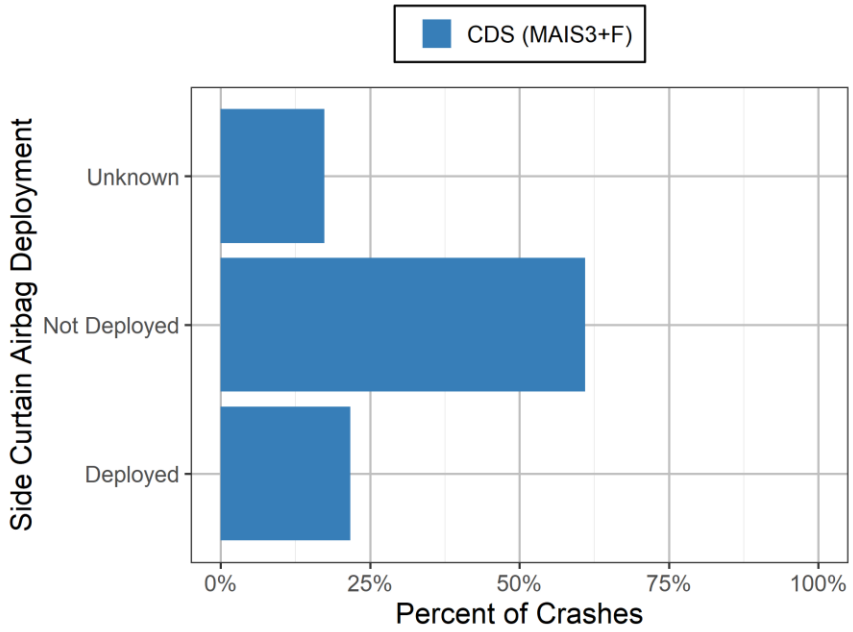

Figure 137. Distribution of side airbag deployment during rollover crashes.

12.4 Conclusions

Most control loss rollovers occur on straight two-lane roads on clear days. Younger drivers and male drivers are more commonly involved in these rollover crashes than older drivers or female drivers. However, older drivers are more likely to be fatally injured in the event of a rollover. The primary countermeasure for control loss rollover crashes is ESC but ESC does not prevent all rollover crashes. In the event of a rollover crash, passive safety systems, such as the strength of the roof, side curtain airbags and seat belts, are designed to protect the occupants. Belted occupants were much less likely to be ejected from the vehicle. The following chapters will quantify the effect of ESC and the passive safety systems for rollover crashes.

13 ROLLOVER CRASH INJURY MODEL

13.1 Purpose

Unlike planar crashes such as frontal crashes, a severity indicator such as delta-v does not exist, making them difficult to characterize. Because many factors are involved in rollover injuries, a seemingly severe rollover crash may have only minor injuries. The purpose of this chapter is to develop an occupant injury model for rollover crashes.

13.2 Approach

13.2.1 Merging NASS/CDS with Vehicle Data

This rollover injury model will incorporate the ESC availability by make and model from the IIHS vehicle dataset and roof SWR from both the IIHS vehicle dataset and the NHTSA component test database. Because the frame of a vehicle does not necessarily change from year to year and corporate twins, the SWR data was assumed to be unchanged for multiple model years of the same make and model. For example, a 2004 Chevrolet Silverado was one of the tested vehicles in the NHTSA component test dataset. Since the frame was not redesigned from model years 1999 to 2006, the roof SWR was assumed to be applicable for all 1999 to 2006 Chevrolet Silverado light trucks. Additionally, the GMC Sierra is a corporate twin of the Chevrolet Silverado. Thus, all 1999 to 2006 GMC Sierra light trucks share the same roof SWR. For SWR from the IIHS vehicle dataset, there were a few make/model/model years that changed frames during production: 2010 Ford Fusion; 2011 Ford Edge; 2011 Lincoln MKX; 2013 Ford Fusion. For these vehicle make/model/model year combinations, there were two reported strength to weight ratios. For each of these cases, the vehicle was assumed to be manufactured before the change date, and thus had the lower, more conservative SWR.

The vehicle identifier notation used by IIHS differs from the notation used in NASS/CDS. For example, the Toyota 4runner has a different notation in the two databases: the IIHS data referred to it as a 4Runner, but NASS-CDS referred to it as a 4-Runner. To match SWR to vehicles found in NASS-CDS, a cross-reference table was developed that paired the IIHS and CDS notation for each make and model. This cross-reference table unified the SWR from IIHS and NHTSA while accounting for vehicle redesigns and corporate twins. For NHTSA tests performed on both sides of the vehicle, the average SWR measurement was used. For vehicles with IIHS and NHTSA SWR measurements, the IIHS value was used since represented the majority of the combined data. The SWR and ESC availability was then merged into NASS/CDS using the notation matching table by make model and model year.

13.2.2 Data Selection

This study focused on rollover crashes within the NASS/CDS case years 2006 to 2015. Any cases with a case weight greater than 5,000 were removed from our case set. To isolate injuries caused by the rollover, only pure rollovers were investigated. A pure rollover was defined by the following criteria similar to that of Kahane [76]:

- The first event was a rollover or all events prior to the rollover must be contact with a curb, the ground, a fence, a bush or shrub, or an object, which fell from a vehicle.
- The rollover was the last event in the crash.

This study only analyzed drivers and right front passengers. Any rollover vehicles with any other front seat occupants, e.g., as an occupant in the middle seat, were excluded since they could interact with the occupants of interest. Any occupants under the age of 12 were excluded from the study. Beginning in the 2010 case year, NASS/CDS changed the criteria for the full investigation of a crash, which includes obtaining the occupant injury information, to only investigate vehicles which were less than or equal to ten years old at the time of the crash. For consistency across all case years, vehicles had to be at most ten years old at the time of the crash to be included in the dataset. Since a logistic model for ejection and injury will be constructed, there cannot be any missing values among their respective covariates.

The ejection model utilized occupant ejection status, occupant belt use, roll direction, and the vehicle SWR. For the 14 vehicles that appeared in both the NHTSA component test database and the IIHS database, the roof SWR measured by IIHS was used. The measured roof SWR was assumed to be the same between NHTSA and IIHS tests despite having different loading rates. The number of cases that satisfy the selection criteria for the ejection model is summarized in Table 40.

Table 40. Ejection model data selection.

Selection Criteria	Cases	Weighted Cases	Vehicles	Weighted Vehicles	Occupants	Weighted Occupants
NASS/CDS	82,755	43,623,355	149,037	78,962,085	212,567	104,389,167
Case Years 2006-2015	41,900	20,899,060	76,752	38,354,340	106,445	49,176,156
Weight ≤5000	41,506	16,386,843	76,032	30,232,471	105,558	39,179,559
Rollover Vehicles	6,341	1,639,226	6,341	1,639,226	10,351	2,403,055
All Other Events were Minor	1,542	503,297	1,542	503,297	2,737	762,890
Last Event was Rollover	1,442	481,793	1,442	481,793	2,654	727,221
Driver or Right Front Passenger only	1,226	415,831	1,226	415,831	1,674	521,663
Age ≥ 12 years	1,206	404,021	1,206	404,021	1,634	502,436
LTV/Passenger Car	1,206	404,021	1,206	404,021	1,634	502,436
Vehicle ≤ 10 years old at time of crash	813	258,071	812	258,071	1,109	324,508
Ejection Known	771	240,048	771	240,048	1,056	303,381
Belt Use Known	771	240,048	771	240,048	1,056	303,381
Roll Direction Known	701	220,343	701	220,343	953	275,009
Vehicle SWR Known	347	105,137	347	1055,137	467	126,526
Unbelted Occupants	77	13,187	77	13,187	89	14,897

The injury model uses the probability of ejection as one of the covariates. Therefore, in addition to needing the injury information, occupant BMI, occupant age, number of half turns, and vehicle type, the occupant belt status, rollover direction, and roof SWR were also needed to construct the injury model. The number of cases that satisfy the selection criteria for the injury model is summarized in Table 41.

Table 41. Injury model data selection.

Selection Criteria	Cases	Weighted Cases	Vehicles	Weighted Vehicles	Occupants	Weighted Occupants
NASS/CDS	82,755	43,623,355	149,037	78,962,085	212,567	104,389,167
Case Years 2006-2015	41,900	20,899,060	76,752	38,354,340	106,445	49,176,156
Weight ≤5000	41,506	16,386,843	76,032	30,232,471	105,558	39,179,559
Rollover Vehicles	6,341	1,639,226	6,341	1,639,226	10,351	2,403,055
All Other Events were Minor	1,542	503,297	1,542	503,297	2,737	762,890
Last Event was Rollover	1,442	481,793	1,442	481,793	2,654	727,221
Driver or Right Front Passenger only	1,226	415,831	1,226	415,831	1,674	521,663
Age ≥ 12 years	1,206	404,021	1,206	404,021	1,634	502,436
LTV/Passenger Car	1,206	404,021	1,206	404,021	1,634	502,436
Vehicle ≤ 10 years old at time of crash	813	258,071	812	258,071	1,109	324,508
Injury Information Available	753	231,245	753	231,245	1,021	285,407
Belt Use Known	753	231,245	753	231,245	1,021	285,407
Occupant Age Known	753	231,245	753	231,245	1,021	285,407
Number of Half Turns Known	686	211,316	686	211,316	921	256,712
Roll Direction Known	684	211,148	684	211,148	919	256,544
Vehicle SWR Known	342	102,134	342	102,134	456	120,180
Occupant BMI Known	299	89,015	299	89,015	395	103,917

13.2.3 Covariate Definitions

In this study, occupants were considered an ejected occupant only if they were completely ejected from the vehicle [23]. Partially ejected occupants were not considered ejected since they remained inside the vehicle. Light trucks were defined as vehicles with a NASS/CDS body type between 30 and 39. The number of half turns was defined as the number of inversions experienced by the vehicle during the rollover. Therefore, a rollover with 1 quarter turn would have 0 half turns and a rollover with 5 quarter turns would have 2 half turns.

A nearside rollover is an event in which the first quarter turn is on the door adjacent to the occupant. Conversely, a far-side rollover is an event in which the first quarter turn is on the door not adjacent to the occupant. Since a nearside or far-side rollover is dependent on the occupant seating position, the driver and right front passenger experience the opposite type of rollover (Figure 138).

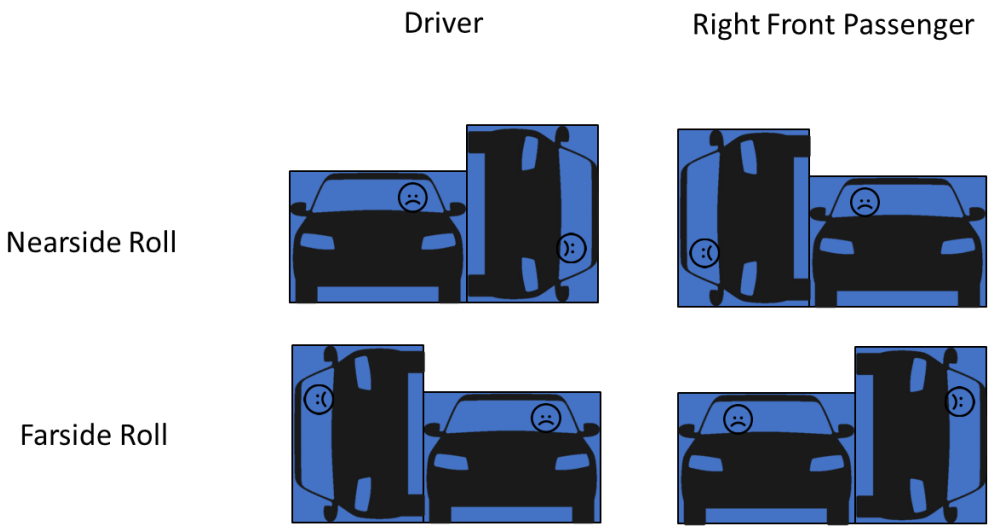

Figure 138. Nearside and Farside Roll Definition.

13.2.4 Logistic Model

13.2.4.1 Ejection Model

Of the 1,056 occupants representing 303,381 weighted occupants with ejection and belt status known, only 7 occupants representing 383 weighted occupants were ejected from the vehicle. Belted occupants that were ejected accounted for only 0.1% of occupants in our dataset. Thus, when predicting the probability of ejection, the probability of ejection was assumed to be zero for belted occupants. To evaluate other covariates, the injury model was constructed for unbelted occupants only. The distribution of ejected occupants among relevant variables is shown in Table 42.

Table 42. Distribution of ejections among the variables used in the logistic regression.

Population	Ejected Occupants	Number of Occupants	Ejected Occupants (Weighted)	Number of Occupants (Weighted)
Half Turns				
0 (1 quarter turn)	1	2	5	74
1	6	18	638	3,987
2	15	33	1,622	4,272
3	8	18	643	1,674
4	8	12	442	3,883
5	2	2	76	76
6	1	3	35	132
Side Airbag Deployment				
Deployed	3	7	140	610
Did not Deploy	38	81	3,322	13,488
Roof SWR				
1	12	18	783	1,189
2	24	50	2,463	9,727
3	4	15	181	1,659
4	0	3	0	1,418
5	1	2	35	105
Model Year				
1990 – 1999	5	7	262	997
2000 – 2009	35	75	3,166	11,538
2010 - 2016	1	6	35	1,563
Roll Direction				
Near-side	16	45	761	9,292
Far-side	25	43	2701	4,806
Seat Position				
Driver	34	67	3,134	12,028
Right Front Passenger	7	21	328	2,069
Vehicle Type				
Car	9	27	279	3,855
Light Truck	17	31	2,084	3,878
SUV	13	26	872	6,040
Van	2	4	227	326
Total	41	88	3,462	14,897

13.2.4.2 Injury Model

Almost all occupants who were ejected from the vehicle sustained a MAIS 2+F injury (Table 43). Therefore, ejection was one of the most important predictors of injury. The probability of ejection was computed for each case based on the ejection model and occupant belt use. Belted occupants were assumed to have a zero probability of ejection. The injury model used the number of half turns, occupant age, occupant BMI, whether the vehicle was a light truck, and the probability of ejection to predict the probability of the occupant sustaining a MAIS 2+F injury.

Table 43. Distribution of injuries among the variables used in the logistic regression.

Population	MAIS2+F Injuries	Number of Occupants	MAIS2+F Injuries	Weighted Number of Occupants
Belt Use				
Belted	74	326	10,030	93,212
Unbelted	51	69	4,614	10,705
Half Turns				
0 (1 quarter turn)	4	19	200	8,483
1	18	105	2,450	38,354
2	42	142	5,932	33,335
3	29	80	3,046	10,082
4	25	36	2,514	7,993
5	3	7	303	5,313
6	3	5	139	298
7	1	1	59	59.1
Ejection				
Complete Ejection	33	34	2,595	2,758
Partially Ejected	19	24	2,214	2,728
Not Ejected	71	335	9,724	98,320
Unknown	2	2	111	111
Side Airbag Deployment				
Deployed	12	27	1,447	3,953
Did not Deploy	110	364	12,982	99,101
Unknown	3	4	2214	863
Roof SWR				
1	30	88	3,014	17,109
2	65	223	7,105	65,746
3	22	54	3,185	11,736
4	5	20	1,136	7,175
5+	3	10	204	2,150
Model Year				
1990 – 1999	9	21	1,095	5,571
2000 – 2009	109	353	13,142	91,941
2010 - 2016	7	21	406	6,404
Roll Direction				
Near-side	67	223	8,440	67,699
Far-side	58	172	6,204	36,218
Seat Position				
Driver	97	296	12,181	88,850
Right Front Passenger	28	99	2,462	15,066
Vehicle Type				
Car	38	141	2,864	37,365
Light Truck	47	109	6,629	30,682
SUV	31	124	4,655	31,899
Van	9	21	495	3,971

Population	MAIS2+F Injuries	Number of Occupants	MAIS2+F Injuries	Weighted Number of Occupants
Occupant Age				
14-19	14	65	1,287	13,782
20-29	41	126	3,881	39,745
30-39	20	67	2,858	11,312
40-49	22	56	2,501	18,404
50-59	10	37	1,474	10,013
60-69	10	26	2,213	8,435
70-79	5	14	220	1,934
80-89	3	4	210	191
Occupant BMI				
Obese (> 30 kg/m^2)	43	117	5,385	22,190
Not Obese (<30 kg/m^2)	82	278	9,258	81,726
Total	125	14,644	395	103,917

Numerous other factors were found to not be significant predictors of ejection or injury during the model construction. The number of turns, vehicle type, ESC equipped, lateral skidding, occupant sex, occupant age, and occupant BMI were not significant predictors of occupant ejection. Lateral skidding, ESC equipped, occupant sex, were not significant predictors of injury.

13.2.5 Model Validation

The injury model was validated using the "leave-one-out cross-validation" methodology (Figure 139). The leave-one-out cross-validation was performed as follows: the logistic regression model was trained on the entire dataset except for one case. For the remaining test case, the trained model was used to predict the probability of injury. The predicted number of injuries was defined as the probability of injury times the case weight. The observed number of injuries was defined as zero if the occupant was uninjured and the case weight if the occupant was injured. The residual error was the difference between the observed number of injuries and the predicted number of injuries for each test case. The average relative error was defined as the sum of the residual errors divided by the actual number of injuries.

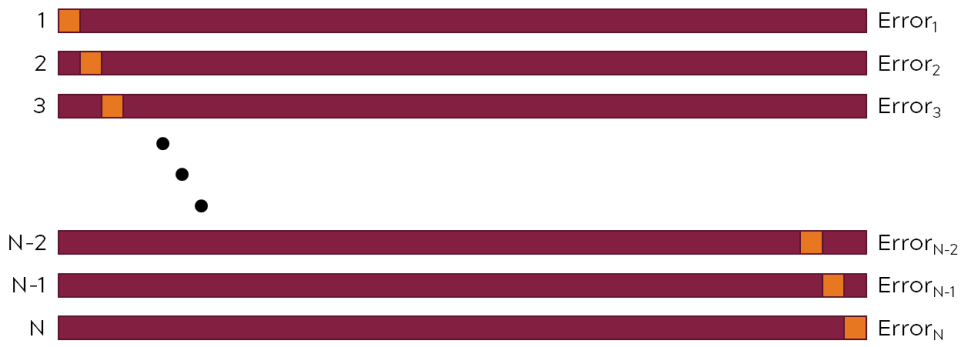

$$Error_i = Predicted_i - Actual_i$$

$$Relative\ Error = \frac{\sum_{i=1}^{N} Error_i}{\sum_{i=1}^{N} Actual_i}$$

Figure 139. Leave-one-out cross-validation methodology.

The ability of the model to correctly predict injury was evaluated using a receiver operating characteristic (ROC) curve. A ROC curve compares the false positive rate to the true positive rate at each probability of injury. An ideal model, which perfectly predicts injury, has an area under the curve (AUC) equal to 1. A model that randomly predicts injury would have an AUC equal to 0.5.

In addition, CISS 2017 to 2019 cases, following the same selection criteria, were used as a validation dataset for the rollover ejection and injury models. This dataset was composed of 118 rollover crashes representing 35,191 real-world crashes.

13.3 Results

13.3.1 Ejection Model

The logistic regression model for ejection was developed for the 89 unbelted front seat occupants using primarily passive safety measures (Table 44). Belted occupants were assumed to have zero probability of being ejected from the vehicle. An occupant in vehicle with a higher roof SWR has a lower probability of being ejected from the vehicle (Table 5). An occupant in a far-side rollover is more likely to be ejected from the vehicle. Based on the leave-one-out cross validation, the rollover ejection model under-predicted the number of ejections by only 2.5%.

Table 44. Logistic regression for probability of ejection.

	Estimate	Std. Error	p-value
Intercept	1.785	1.563	0.26
Far-side Rollover	2.817	0.691	0.006
Roof SWR	-1.581	0.546	<0.001

An odds ratio was also calculated for the ejection model (Table 45). Based on the ejection model, each unit increase in roof SWR reduced the odds of ejection by 5 times (Figure 140). Far side rollovers increased the odds of ejection by over 16 times.

Table 45. Odds ratio of ejection for a unit increase in each variable.

Variable	Odds Ratio
Far-side Rollover	16.73 ± 12.53
Roof SWR	0.21 ± 0.14

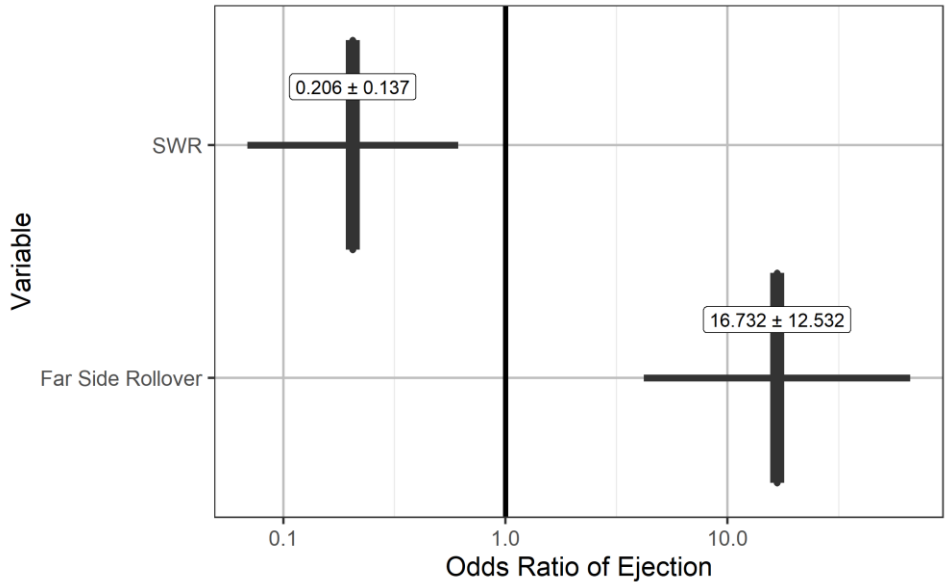

Figure 140. Odds ratios of ejection for a unit increase in each variable.

13.3.2 Injury Model

The logistic regression model for MAIS 2+F injury was computed using the records of 395 drivers and right front passengers (Table 46). As expected, the more vehicle rollover half turns, the greater the risk of occupant injury. Older occupants were at a greater risk of injury than younger occupants. Occupants of light trucks were at an increased risk of injury compared to other passenger vehicle types. However, unlike other passenger vehicles, the injury risk for occupants of light trucks increases slightly with each additional half turn. Occupants with a greater risk of being ejected from the vehicle were much more likely to sustain an MAIS2+F injury.

Table 46. Logistic regression for probability of a MAIS2+F injury, traditional model.

	Estimate	Std. Error	p-value
Intercept	-5.976	0.765	<0.001
Age	0.031	0.011	0.006
Ejection Probability	4.557	0.947	<0.001
Half Turns	1.047	0.228	<0.001
Light Truck	2.843	0.770	<0.001
Obese	1.054	0.466	0.026
Half Turns: Light Truck	-0.985	0.257	<0.001

Using the logistic regression coefficients above, the odds ratio was computed for each variable (Figure 141). Front seat occupants were 2.8 times more likely to be injured for each half turn rolled. For each additional year old, the occupant's odds of injury increased by 1.03 times. Obese occupants (BMI >

30 kg/m^2) were 2.87 times more likely to sustain a MAIS2+F injury in a pure rollover. If the vehicle was a light truck, the odds of injury increased by 17 times when not including the interaction with half turns. For light trucks, the odds of injury increased only 0.2 times for each additional half turn. Due to the interaction effects between the vehicle type and the number of half turns, the probability of MAIS2+F injury was computed for a 45-year-old, non-obese, belted occupant in either a light truck or other passenger vehicle (Table 47). Occupants of light trucks have a higher probability of injury then other passenger vehicles for rollovers with few half turns. However, occupants of light trucks have a much lower probability of injury than other passenger vehicles for rollovers with many half turns.

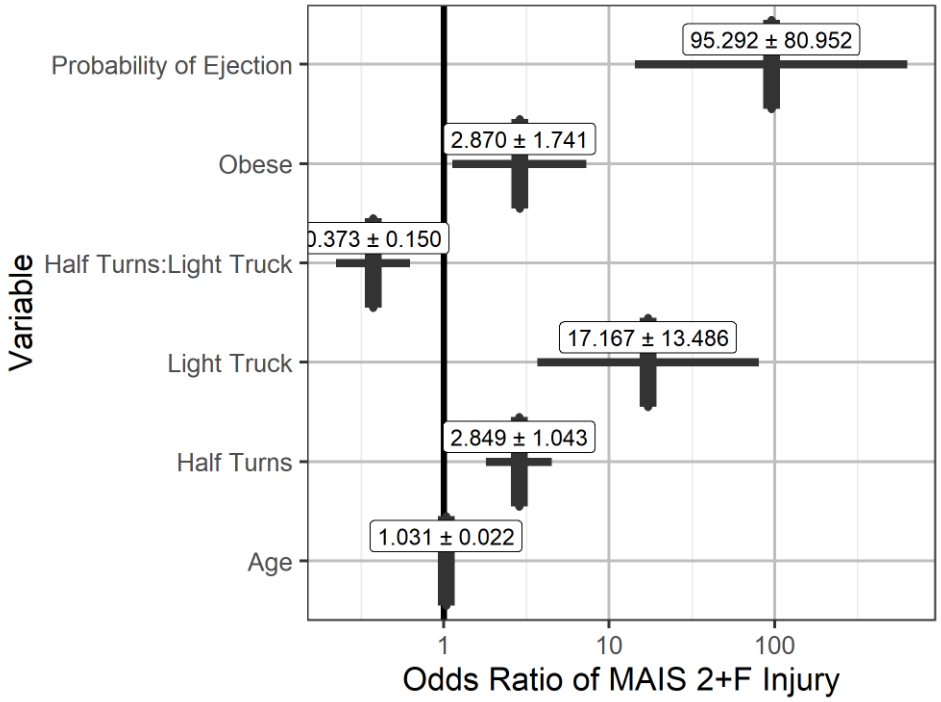

Figure 141. Odds ratio of MAIS2+F injury for a unit increase in each variable.

Table 47. Probability of MAIS2+F injury of a 45-year-old, non-obese, belted occupant based on the vehicle type and the number of half turns.

Half Turns	Light Trucks	All Other Passenger Vehicles
0	15.0%	1.0%
1	15.8%	2.8%
2	16.6%	7.6%
3	17.5%	19.1%
4	18.4%	40.3%
5	19.3%	65.8%
6	20.3%	84.6%
7	21.3%	93.9%

13.4 Validation

Based on the leave-one-out cross validation, the ejection model under-predicted the number of ejections by 2.5% and the rollover injury model under-predicted the number of injuries by 12.3%. The AUC of the injury model was 0.829 (Figure 142).

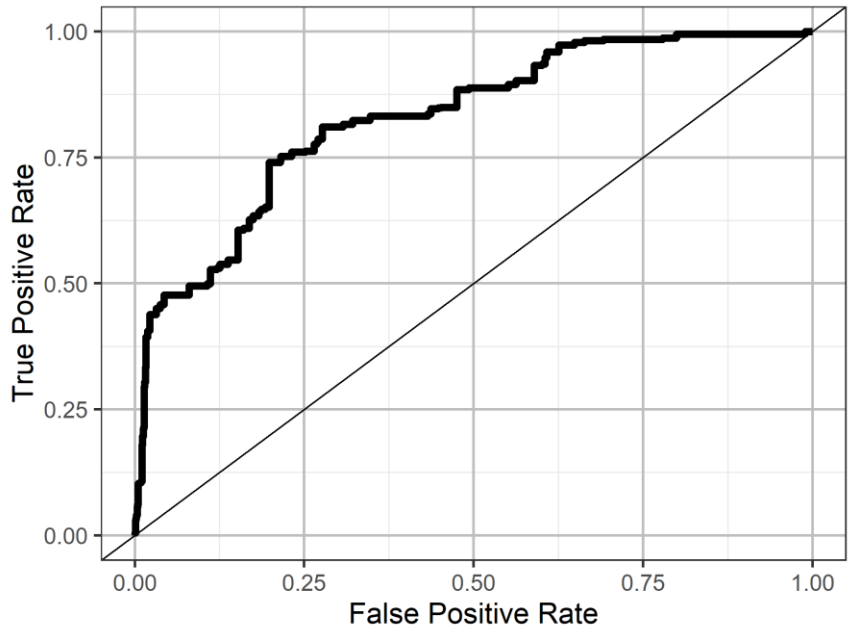

Figure 142. Receiver-Operator curve for injury model.

The predicted number of ejected occupants matched the actual number of ejected occupants during rollover pure crashes in CISS 2017 to 2019. The predicted value for MAIS2+F injured occupants was lower than the actual value estimated in CISS but it is within the 95% confidence intervals.

Table 48. Comparison between the estimated and actual number of ejected and MAIS2+F injured occupants in pure rollover crashes.

	Ejected Occupants (95% CI)	MAIS2+F Injured Occupants (95% CI)
CISS Estimation	254 ± 261	2,655 ± 809
Model Prediction	300 ± 200	3,400 ± 300

13.5 Discussion

Much of the passive safety in rollover events is designed to prevent the occupant from being ejected from the vehicle. Ejected occupants almost always sustain an MAIS2+F injury (Table 4). Belt use was the most significant factor in predicting ejection given that almost no belted occupants were ejected. This agrees with Funk et al, who also showed that belt use is the best indicator of ejection [4]. Our study used roof SWR as a predictor of ejection since a stronger roof should prevent ejection paths from opening. Roof SWR was

used instead of roof displacement since it is unrelated to the severity of the crash. In agreement with Funk, occupants in a far-side rollover were more likely to be ejected from the vehicle.

Similar to Funk et al., ejection was used as a predictor variable for AIS 3+ injuries since this is one of the primary modes of injury [5]. In both models, injury risk increased with each additional vehicle inversion and with the occupant's age. Occupants of light trucks were at an increased risk of MAIS2+F injury for lower half turns while Funk et al. did not find any significance at the MAIS3+F injury level. The decreased risk of light truck occupants for many half turns was attributed to the fact that 16.6% of light trucks had 5 or more half turns (Table 49). In contrast, less than 1% of all other passenger vehicles had 5 or more half turns. This difference led to the interaction between light trucks and half turns. The interaction variable indicates that occupants of light trucks have larger odds of injury than other passenger vehicles for rollovers with 2 or fewer half turns. Rollovers with larger numbers of half turns, occupants of light trucks had lower odds of injury than other passenger vehicles. With an increased sample size, it may be more accurate to construct two separate models depending on the vehicle type.

Table 49. Distribution of the number rollover half turns based on the vehicle type.

Half Turns	Light Trucks	All Other Passenger Vehicles
0	5.6%	9.2%
1	30.4%	39.6%
2	36.3%	30.3%
3	6.7%	10.9%
4	4.3%	9.1%
5	16.4%	0.4%
6	0.2%	0.3%
7	0.0%	0.0%

Flannagan constructed a similar model to Funk et al., however, she used both belt use and ejection in the rollover injury model [6]. Since belted occupants are almost never ejected from the vehicle, and both roof SWR and side curtain airbags aim to prevent occupants from being ejected, combining all of the passive safety features into a probability of ejection covariate removes these interactions. Roof deformation was not included as a factor of the injury risk because it would be confounded with the number of half turns as a severity measure.

The model is unable to predict the effect of side curtain airbags since there are so few cases with a side curtain airbag. A larger, newer dataset that contains more vehicles with side curtain airbags, which are compliant with FMVSS 226, would be able to quantify their effect.

13.5.1 Limitations and Assumptions

To increase the number of vehicles with a known SWR, measurements from both IIHS and NHTSA were used. Although the two organizations use slightly different displacement rates to measure the roof SWR, it was assumed that there was no difference between their measured values. This seemed reasonable

based on the 14 vehicle models with a roof SWR measured by both IIHS and NHTSA. The roof SWR measured by IIHS tended to be higher than the roof SWR measured by NHTSA (Figure 143). Due to the similarity between the test methods used by IIHS and NHTSA, it is not surprising that the average difference of 0.31 between the IIHS and NHTSA measurements of roof SWR was small. For example, the 2006 Honda Civic had a roof SWR of 4.5 as measured by NHTSA and a roof SWR of 4.48 as measured by IIHS. The largest difference was the GMC Canyon, which had an average roof SWR of 1.94 as measured by NHTSA and 2.86 as measured by IIHS. However, NHTSA tested a 2-door cab while IIHS tested a 4-door cab, which is expected to have a higher roof SWR. In cases with both a NHTSA and IIHS roof SWR, the IIHS measurement was used because most of the vehicles in the dataset only had IIHS roof SWR measurements.

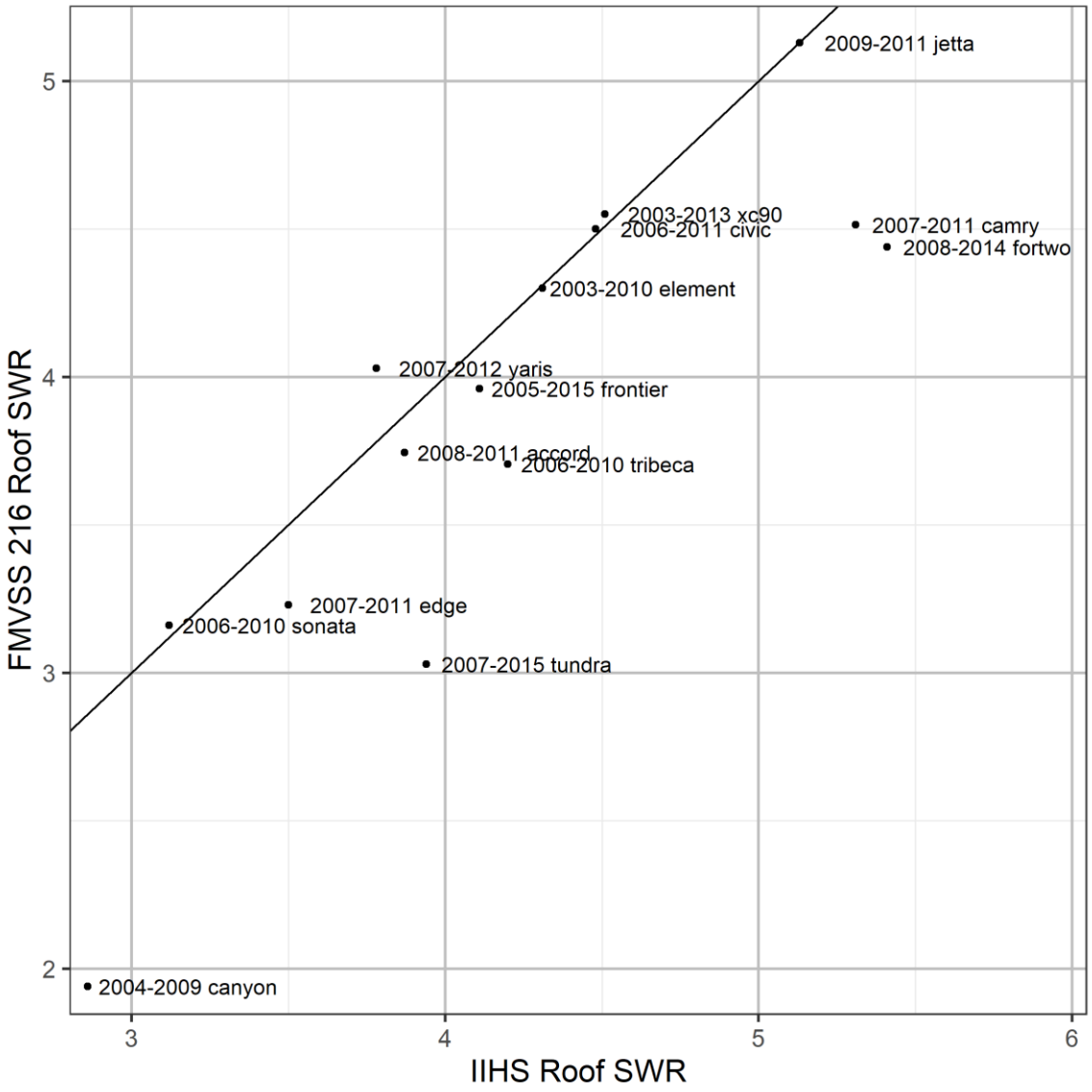

Figure 143. Comparison between the roof SWR measured by IIHS and NHTSA. The solid line represents perfect agreement between the measurements.

13.6 Conclusions

MAIS 2+F injuries sustained by front seat occupants during a first event rollover crash were predicted using five parameters: occupant age, occupant BMI, vehicle class, the number of half turns and the probability of ejection. The probability of ejection was assumed to be zero for belted occupants. The probability of ejection for unbelted occupants was predicted based on the roof SWR and the rollover direction. There were not enough cases to determine the effect of side curtain airbags on ejection. Based on leave-one-out cross validation, the rollover injury model under-predicted the number of injuries by 12.3%. Overall, our injury model agrees with previous studies and allows the benefits of the passive safety systems to be isolated.

14 ESTIMATED BENEFIT OF ESC FOR ROLLOVER CRASH

14.1 Purpose

The purpose of this chapter is to estimate the control loss rollover crash reduction due to the introduction of ESC.

14.2 Approach

14.2.1 Data Selection

This study utilized the most recent 10 years of NASS/CDS data, case years 2006 to 2015. Cases with weights greater than 5000 were removed, as those higher weighted cases would skew the analysis in favor of those particular cases [77]. The analysis was restricted to cases in which the vehicle rolled over. The target population for ESC was limited to crashes where the crash scenario was control loss. Control loss crashes were defined by the variable "acctype" and included types 2 and 7, which are single vehicle control loss. Since LDW/LDP systems can prevent rollovers as a result of DrOOL road departures, the target population only included control loss crashes that did not overlap with another active safety system. For example, a vehicle may leave the road, then lose control before impacting a tree. This case may be prevented with LDW before the control loss and therefore, was not included in the ESC target population. Rear end crashes were used as the control group in our quasi-induced exposure calculation, as the number of vehicles with ESC overall is not known, and rear end crashes would not benefit from ESC. Control data selection parameters are in Table 50. Target population data selection parameters are in Table 51.

Table 50. Control data selection.

Criteria	Cases	Weighted Cases	Vehicles	Weighted Vehicles
NASS/CDS 2006-2015	41,900	20,899,060	76,752	38,354,340
Weight <= 5,000	41,506	16,386,843	76,032	30,232,471
Rear – End Crashes	6,968	3,801,501	6,968	3,801,501

Table 51. Target population data selection criteria.

Criteria	Cases	Weighted Cases	Vehicles	Weighted Vehicles
NASS/CDS 2006-2015	41,900	20,899,060	76,752	38,354,340
Weight <= 5,000	41,506	16,386,843	76,032	30,232,471
Rollover Vehicles (rollover >0)	5,623	1,484,590	5,676	1,494,845
Control Loss (acctype = 2 or 7)	5,850	2,230,283	5,850	2,230,283
Control Loss Rollover	2,132	627,861	2,312	627,861

14.2.2 Calculation of Effectiveness

The effectiveness of ESC was defined as the proportion of crashes prevented by the introduction of ESC. The vehicles were considered "equipped" with ESC if and only if ESC was standard in that vehicle.

If ESC was optional in a vehicle, the vehicle was considered "not equipped" with ESC. The number of crashes must be scaled by either the number of vehicles or the number of miles driven to account for differences in exposure between groups (Eq. 36). However, the number of vehicles with or without ESC is unknown. Therefore, the quasi-induced exposure method was used as an alternative method for computing the effectiveness.

$$Effectiveness = 1 - \frac{(\#\ of\ Target\ crashes\ with\ ESC)\left(Exposure\ \frac{w}{o}ESC\right)}{\left(\#\ of\ Target\ crashes\frac{w}{o}ESC\right)(Exposure\ with\ ESC)} \quad (36)$$

The quasi-induced exposure method estimates the change in risk when the actual exposure is unknown based on an independent parameter [78]. Because the number of vehicles with ESC was unknown, the effectiveness of ESC for all control loss crashes, all rollover crashes, and control loss that resulted in rollovers were estimated using the quasi-induced exposure method (Eq. 37). It was assumed that ESC has no effect on rear end crashes. Therefore, rear crashes were used as the comparison population, which remains unchanged by the presence of ESC. If the ratio of crashes with ESC is smaller than the ratio of crashes without ESC than some portion of crashes were prevented by the introduction of ESC.

$$Effectiveness = 1 - \frac{(\#\ of\ Target\ crashes\ with\ ESC)\left(\#of\ Rear\ End\ crashes\frac{w}{o}ESC\right)}{\left(\#of\ Target\ crashes\frac{w}{o}ESC\right)(\#\ of\ Rear\ End\ crashes\ with\ ESC)} \quad (37)$$

14.3 Results

The quasi-induced exposure method for estimating effectiveness yielded a 50.6% effectiveness of ESC in preventing crashes within the target population of control loss rollovers from occurring (Table 52).

Table 52. Estimated Effectiveness of ESC for the three test populations.

Population	Crashes with ESC	Crashes without ESC	Rear Crashes with ESC	Rear Crashes without ESC	Effectiveness
All Control Loss Crashes	93,848	2,136,435	377,188	3,424,312	60.1%
All Rollovers	122,437	1,372,409	377,188	3,424,312	19.0%
Target Population (Control Loss Rollovers)	26,601	601,260	377,188	3,424,312	59.8%

14.4 Discussion

Most of the vehicles in NASS/CDS from 2006 to 2015 did not have ESC because they were older vehicle models. ESC was required in all light vehicles manufactured after September 1, 2011 by FMVSS 126 [79]. However, as shown in Figure 144 automakers began introducing ESC many years before this required date. The majority of vehicles in NASS/CDS manufactured after 2010 were equipped with ESC.

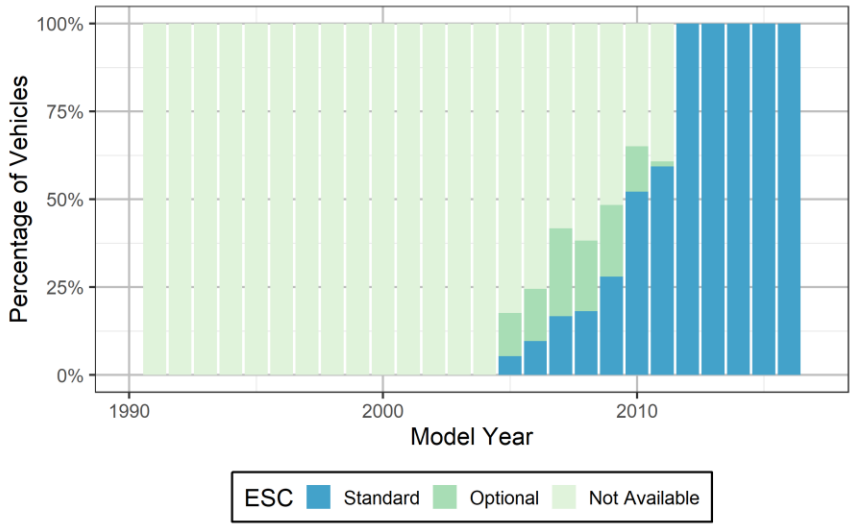

Figure 144. ESC prevalence by model year in all NASS/CDS 2006-2015 vehicles based on IIHS ESC availability data.

The prevalence of ESC in vehicles in NASS/CDS increased in each of the case years from 2006-2015 (Figure 145). The increase in ESC prevalence was due to older vehicles without ESC leaving the fleet and newer vehicles with ESC entering the US vehicle fleet. ESC adoption is expected to reach 85% in the US fleet by 2025 [80].

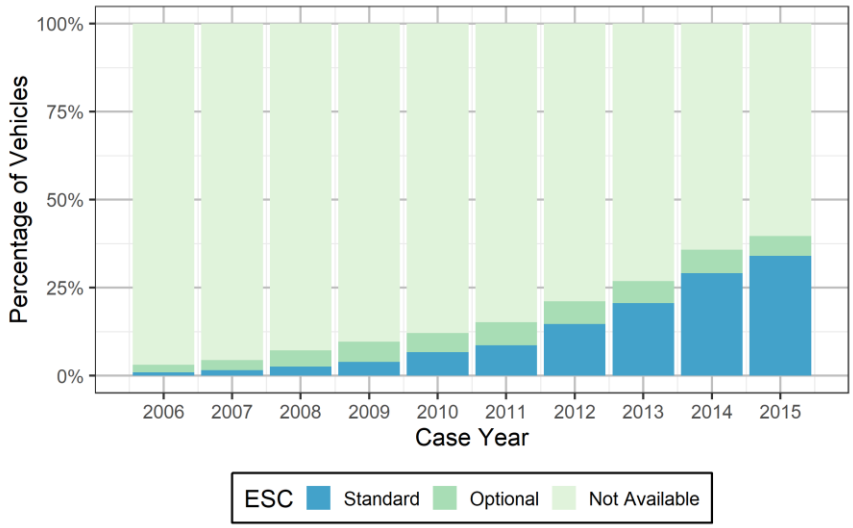

Figure 145. ESC prevalence among all vehicles in NASS/CDS 2006-2015 per case year based on IIHS ESC availability data.

14.4.1 Comparison with Previous Studies

Using the quasi-induced exposure method for estimating effectiveness, this study compared the number of crashes that occurred with ESC with what would have been expected based on the number of crashes that occurred without ESC. For all control loss crash scenarios, the estimated effectiveness was 60.1%. This is very similar to the estimated effectiveness of 56.2% on wet roads computed by Lie [20].

ESC was estimated to be able to prevent 59.8% of rollover crashes that were the result of control loss. This is similar to the effectiveness of ESC in preventing all control loss crashes as expected. The effectiveness of ESC among all rollover crashes was 19.0%, which is about a third of the reduction of rollover crashes due to control loss. ESC would be expected to have little effect on preventing other crash scenarios, such as intersection crashes that resulted in a rollover. The estimate for ESC effectiveness in rollovers was much lower than the 69% estimated by Erke, and 74% by Farmer [16, 17]. However, this estimate of ESC effectiveness for control loss rollovers were within the 95% confidence interval of both of these studies.

14.4.2 ESC May Not Always Prevent Rollovers

The estimate of ESC effectiveness for rollover crashes is about 60%. While high, this also implies that ESC did not prevent rollovers in all cases resulting from control loss. Those cases that were not prevented were analyzed as potential targets for further improvements to ESC (Figure 146).

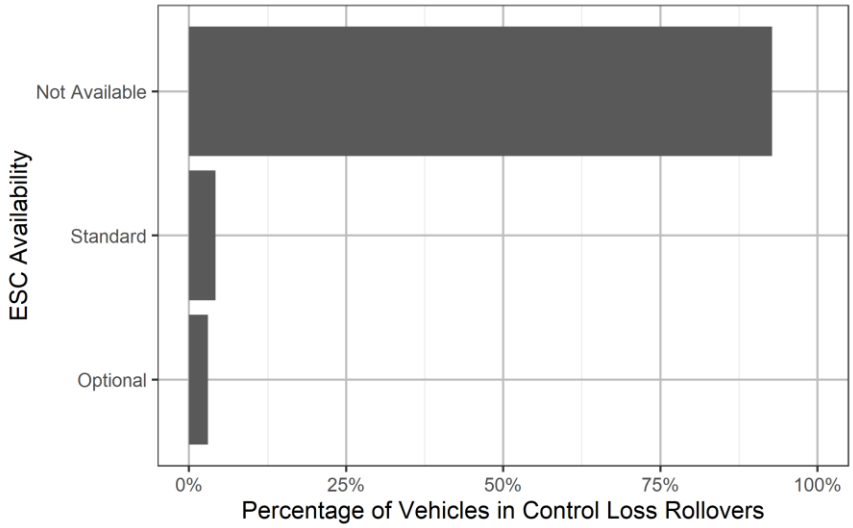

Figure 146. Distribution of ESC availability on vehicles in the target population based on IIHS ESC availability data.

There were 69 cases in which the vehicle had ESC but still lost control and overturned. The pre-impact stability of those cases was analyzed, which showed that ESC reduced the frequency of lateral skidding control loss rollovers, but not tracking or longitudinal skidding rollovers (Figure 147). This is consistent with the operation of ESC, which can apply brakes to individual wheels to ensure that the vehicle travels in the direction specified by the driver. If a vehicle is tracking or skidding longitudinally, ESC will likely not engage. Interestingly, 34.3% of weighted control loss rollovers had an unknown pre-impact stability. ESC may change the nature of the rollover crashes and make it more difficult to determine the pre-impact stability.

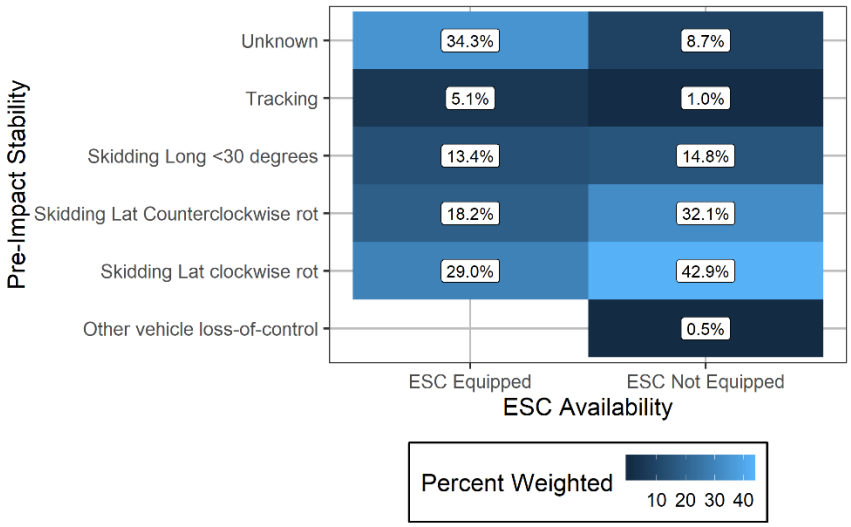

Figure 147. Distribution of Pre-Impact Stability with and without ESC.

For vehicles with ESC, 25% of the lateral skidding control loss rollover crashes occurred due to traveling too fast during bad road conditions (3.3% for wet/water, 21.8% for snow/slush/ice/frost, etc.). Another 38.2% of crashes had a critical pre-crash event of traveling off the road (Table 53). ESC may be less effective in situations in which the tire friction is low such as when the road conditions are poor, or the vehicle is no longer on the road. Additionally, if a vehicle leaves the road, they might overcorrect, resulting in departing on the other side of the road.

Table 53. Critical Pre-Crash Event vs. Road Surface Condition for Loss of Control Rollovers that Included Lateral Skidding.

	Dry	Snow/Slush/ Ice/Frost	Wet/Water	Total
Vehicle Traveling Off the Edge of the Road	40.0%	0.0%	1.3%	41.3%
Not LOC or This Vehicle Traveling	1.0%	4.5%	0.0%	5.5%
LOC: Traveling too Fast for Conditions	25.7%	16.9%	3.6%	46.2%
LOC: Poor Road Conditions	3.0%	1.6%	1.2%	5.8%
LOC: Other Cause	1.2%	0.0%	0.0%	1.2%
Total	70.9%	23.0%	6.1%	100%

14.5 Limitations

The quasi-induced exposure method does have some limiting assumptions as it is an estimate of the effectiveness that does not require the prevalence of ESC to be known. ESC was assumed to have no influence on rear end crashes. ESC tends to be present in newer vehicles. Therefore, it was assumed that there was no difference in new vehicles, which would affect the occurrence of either rollover or rear end crashes. As more active safety systems such as automatic emergency braking systems become more prevalent, the quasi-induced method using rear end crashes as a comparison may become inaccurate.

14.6 Conclusions

ESC is a highly effective means of preventing loss of control, and of particular relevance to this study, is highly effective in preventing rollovers caused by loss of control. ESC was estimated to prevent 59.8% of control loss crashes that resulted in a rollover and 19.0% of all rollover crashes. The vast majority of vehicles with ESC equipped crashed due to travelling too fast during poor road conditions or traveling off the edge of the road.

15 PREDICTING THE FUTURE BENEFIT OF ROLLOVER COUNTERMEASURES

15.1 Purpose

The purpose of chapter 15 is to predict the number of MAIS2+F injured occupants that will occur in the future, assuming all vehicles have ESC and passive safety countermeasures such as side curtain airbags and strong roofs.

15.2 Methods

15.2.1 Data Selection

The 395 occupants used to predict the rollover reduction for 100% deployment of side curtain airbags, ESC, and strong roofs were selected the same as in Chapter 12.

15.2.2 Estimating Strong Roof Benefit

For each of the 395 occupants in the dataset, the probability of ejection and probability of injury was computed using the ejection and injury models. The probability of ejection and injury was then recomputed for cases that had a SWR less than 4 assuming they had a SWR of 4[62]. The difference in ejection and injury due to the introduction of side curtain airbags was characterized.

15.2.3 Estimating Side Curtain Benefit

For each of the 395 occupants in the dataset, the probability of ejection and probability of injury was computed using the ejection and injury models. The probability of ejection and injury was then recomputed for cases that had a side curtain airbag applicable ejection. Side airbag applicable ejections were when an occupant was ejected through the sides of the vehicle not through the windshield, roof, or other opening. It was assumed that FMVSS 226 compliant side curtain airbags would completely eliminate these ejections and thus have zero probability of ejection. The difference in ejection and injury due to the introduction of side curtain airbags was characterized.

15.2.4 Estimating Combined Countermeasure Injury Reduction

For each control loss rollover crash occupant, the probability of an MAIS2+F injury was computed for nine different scenarios: the eight possible vehicle configurations of ESC, strong roofs, and side curtain airbags, and an ideal fleet with every safety feature and all occupants belted. The baseline fleet prediction consisted of the same active and passive safety systems as the original crash. The probability of ejection was assumed to be zero if the occupant was belted in the crash. Additionally, for the populations with side curtain airbags, the probability of ejection was assumed to be zero if the occupant was ejected through the sides of the vehicle in the original crash. Otherwise, the probability of ejection was determined based on the SWR and whether the occupant experienced a far-side rollover according to the ejection model (Chapter

13). The probability of the occupant sustaining a MAIS 2+F injury was determined by the injury model developed in Chapter 13.

Some rollover crashes would be prevented due to ESC but not all vehicles in the baseline fleet had ESC. Thus, the estimated 59.8% effectiveness of ESC from Chapter 14 in preventing control loss rollover crashes was used to predict if the crash would have occurred if the vehicle had been equipped with ESC. It was assumed that all vehicles with ESC equipped that had a rollover crash in the baseline fleet would also have a rollover crash in the future fleet and ideal fleet. Thus, the probability of a control loss crash was 1 if the vehicle had ESC equipped originally. However, if the vehicle did not have ESC, the probability a crash would occur was equal to 1 – Effectiveness of ESC or 40.2% (Figure 148).

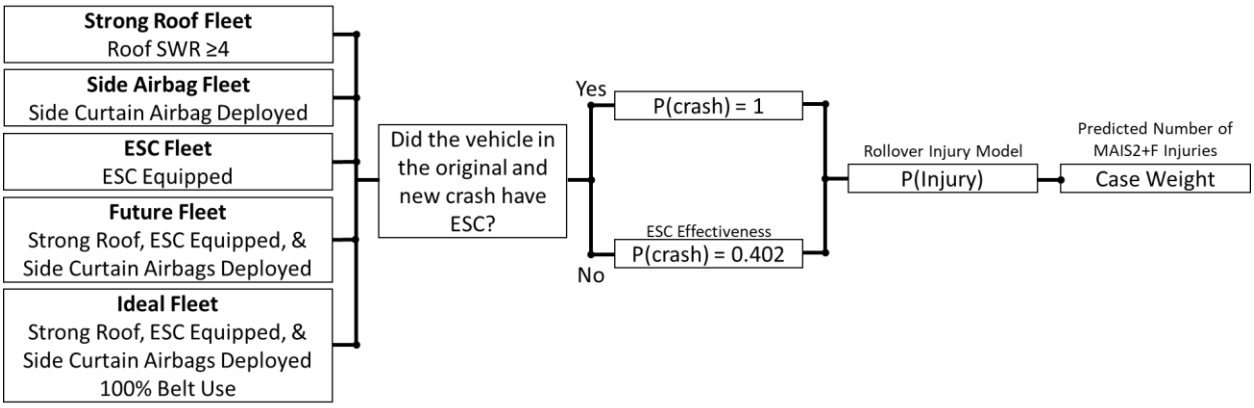

Figure 148. Flowchart of Injury Prediction in 2025 for each occupant.

The predicted number of MAIS2+F injured occupants was computed based on the sum of the probability of the crash occurring multiplied by the occupant's probability of injury (Eq. 38). Since the rollover countermeasures used in this study were already on the market in 2015, the fleet has some crash and injury reduction. To predict how many crashes and injured occupants were prevented, the probability of ejection and injury was estimated for a no countermeasure fleet. This fleet assumed that every vehicle had no ESC, no side curtain airbags and a SWR equal to 2. A SWR equal to 2 was selected since it is between 1.5, the minimum roof SWRs mandated by NHTSA until 2012, and 3 the minimum roof SWR mandated by NHTSA since 2012. The overall reduction in crashes and injured occupants was computed relative to the no countermeasures population using the weighted values [62]. The total number of predicted MAIS2+F injured occupants was computed for the baseline (2015) fleet, no countermeasure fleet, ESC fleet, strong roof fleet, side curtain airbag fleet, ESC and strong roof fleet, ESC and side curtain airbag fleet, strong roof and side curtain airbag fleet, future fleet with all countermeasures, and the ideal future fleet with all countermeasures and 100% belt use.

$$MAIS2+F\ Injured\ Drivers = \sum_{i=case} Weight_i * P(Crash)_i * P(Injury)_i \qquad (38)$$

15.2.5 Determining the Strong Roof Fleet Penetration

The prevalence of strong roofs (SWR ≥4) by model year was approximated based on the prevalence in NASS/CDS. For all passenger vehicles in NASS/CDS 2006-2015 with a sampling weight less than 5000, the proportion of vehicles in a given model year with a strong roof was computed (Figure 149). Vehicles with an unknown roof SWR were excluded from this proportion.

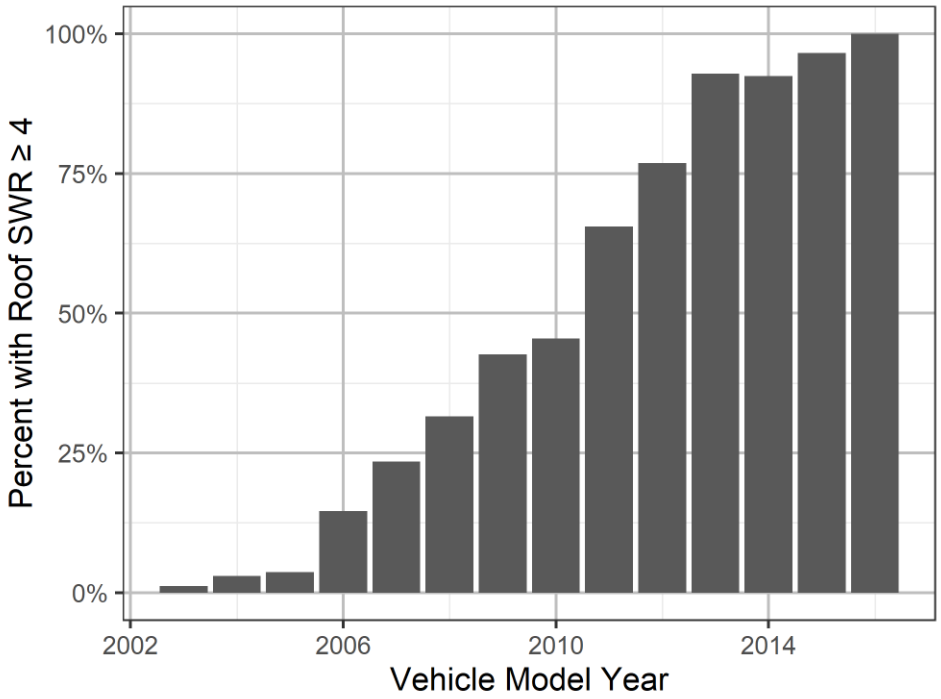

Figure 149. Proportion of vehicles with a strong roof by model year.

The fleet age distribution was assumed to be the same for a given case year (Figure 150). The proportion of vehicles with a strong roof for a given year remained constant. The product between these two distributions yields the distribution of strong roofs for the given case year. The integral of all vehicles with strong roofs for a given case year yields the fleet penetration. This method is also known as the cross-correlation between the age distribution and the proportion of vehicles with strong roofs across multiple case years.

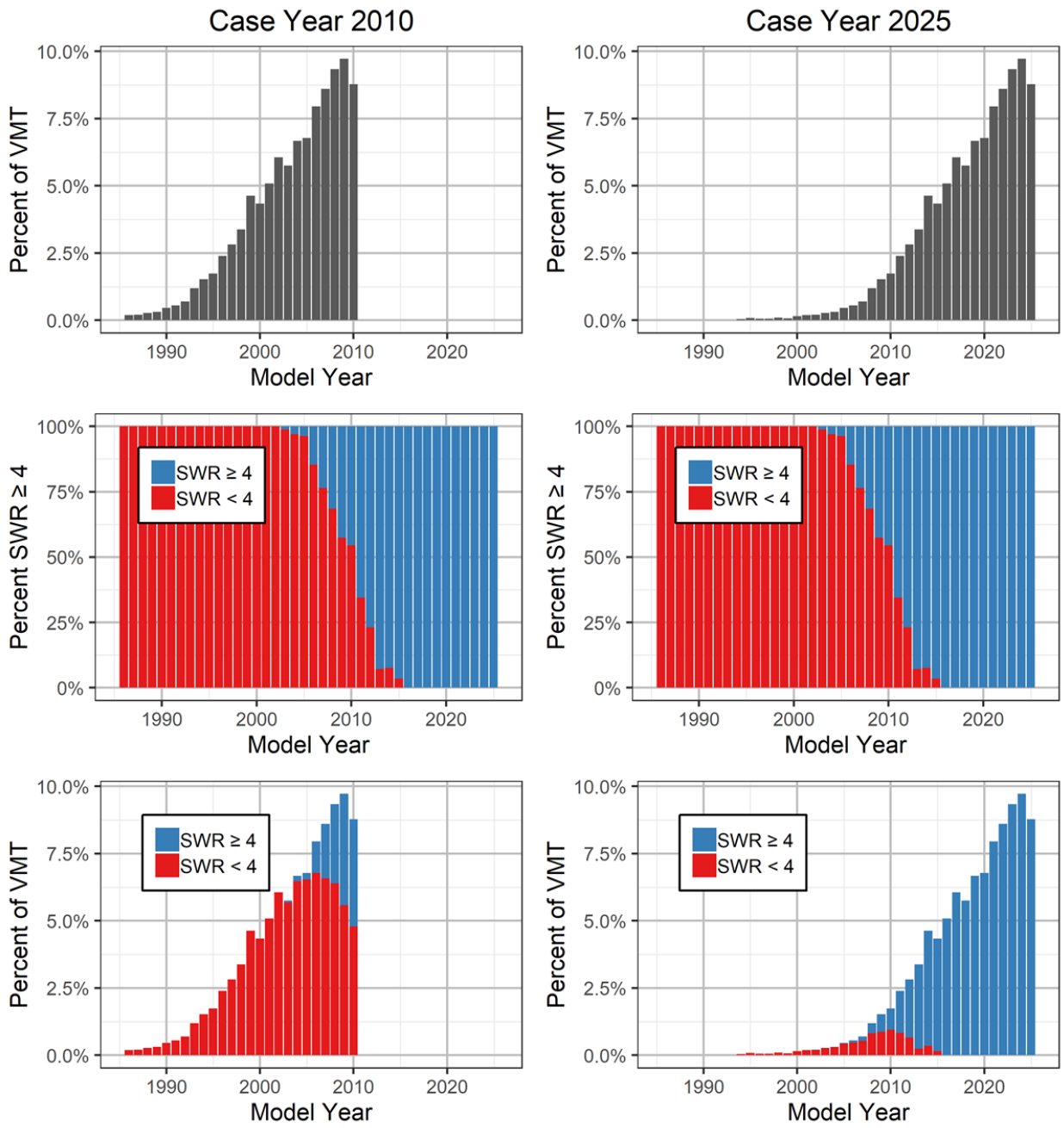

Figure 150. Comparison between the prevalence of strong roofs in the fleet in 2010 compared to 2025. The product between the age distribution (top), and the proportion of vehicles with a strong roof (middle) yielded the prevalence of strong roofs in the given case year (bottom).

15.2.6 Determining the Side Curtain Airbag Penetration

The prevalence of side curtain airbags by model year was approximated based on the prevalence of deployed side airbags among 812 vehicles in pure rollover crashes in NASS/CDS. Vehicles without airbag information were removed from the dataset. Additionally, if there were less than ten vehicles (unweighted) in a given model year, the proportion of vehicles with side airbag curtains was excluded.

There were 730 vehicles with known side curtain airbag deployment known. These vehicles were used to develop a binomial model of side curtain airbag market penetration (Figure 151). Vehicles newer than model year 2016 were assumed to have side curtain airbags to comply with FMVSS 226. Vehicles older than model year 2000 were assumed to not have side curtain airbags.

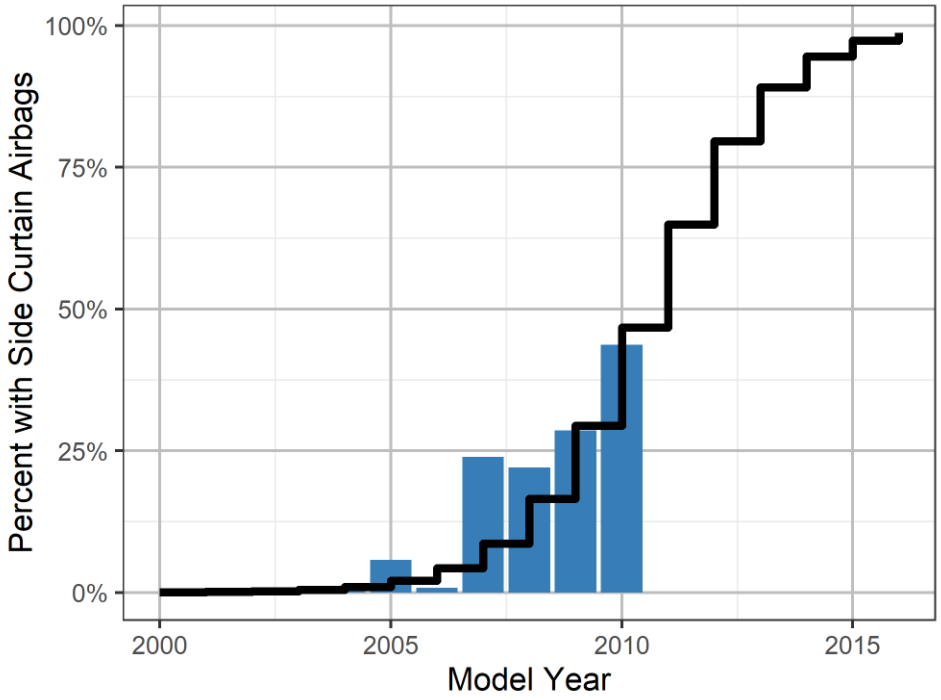

Figure 151. Proportion of vehicles with side curtain airbags by model year.

The fleet penetration of side airbags was computed using the same cross-correlation methodology as for roof SWR (Figure 152).

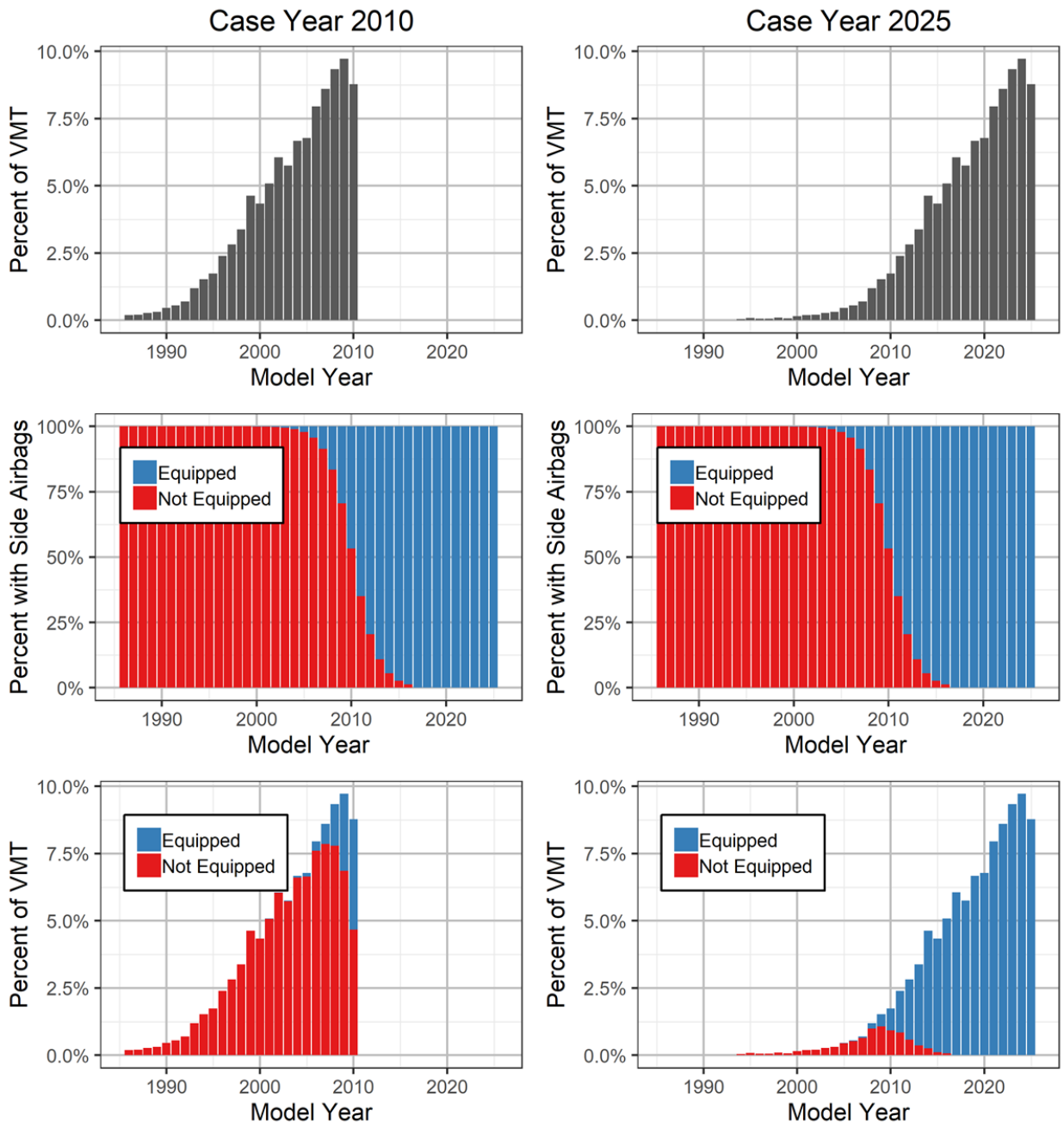

Figure 152. Comparison between the prevalence of side curtain airbags in the fleet in 2010 compared to 2025. The product between the age distribution (top), and the proportion of vehicles with a side curtain airbag (middle) yielded the prevalence of side curtain airbags in the given case year (bottom).

15.2.7 Prediction of Injured Occupants in the future

Since ESC, side curtain airbags, and side curtain airbags have all begun to reach the market at different times and affect injury outcomes in different ways, their benefit must be evaluated for every combination of these safety features (Figure 153). A given vehicle could have any of the following

configurations: none, ESC only, side curtain airbags only, strong roof only, ESC and strong roof only, side curtain airbags and strong roof only, ESC and side curtain airbags only, and all three safety features. Based on the market penetration curves for strong roofs, side curtain airbags, and ESC, the probability that a vehicle has a given combination of rollover countermeasures can be computed (Eq. 39). For example, in 2025, an estimated 86.2% of vehicles will be equipped with ESC, 92.2% of vehicles will be equipped with strong roofs, and 91.6% of vehicles will be equipped with side curtain airbags. Therefore, based on Equation 1, an estimated 72.8% of vehicles would be equipped with ESC, strong roofs, and side curtain airbags in 2025.

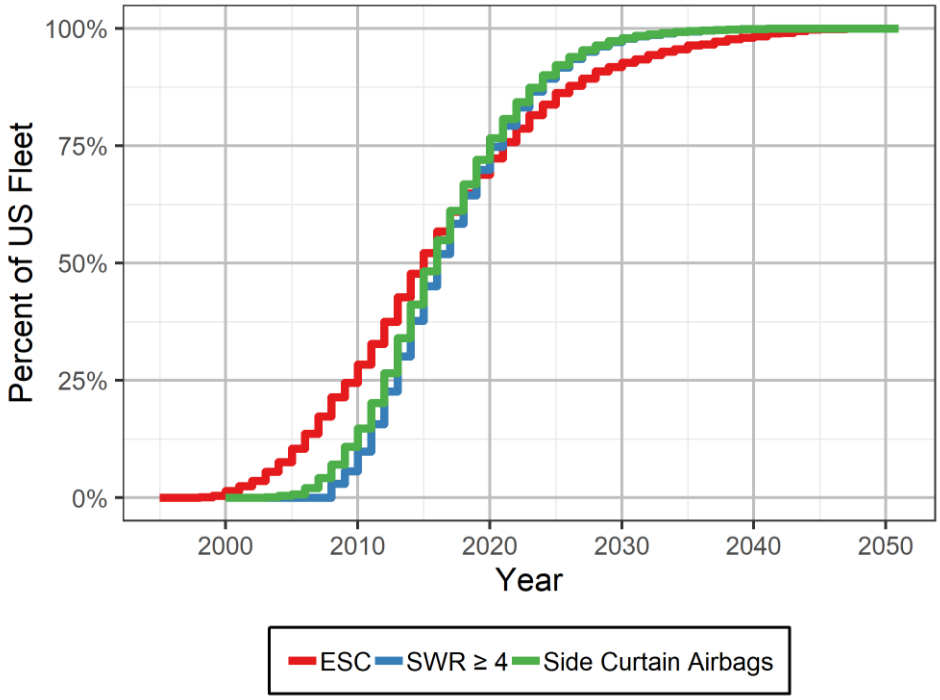

Figure 153. Fleet penetration of ESC [81], strong roofs, and side curtain airbags.

$$p(all|2025) = p(ESC|2025) * p(Strong\ Roof|2025) * p(Side\ Curtain\ Airbag|2025) \quad (39)$$

The number of crashes generally increases with any increase in the number of vehicle miles travelled (VMT). Based on the number of rollover crashes that occurred in NASS/CDS 2015, the estimated crash and injury benefit in the baseline fleet, and the VMT in 2015, the rollover crash rate was estimated. The annual VMT increases by approximately 1% each year. The following predictions for the rollover crash and injury reduction is given for both a static and increasing VMT (Figure 50).

The annual crash rate for control loss rollover crashes was computed based on the number of crashes in NASS/CDS from 2010 to 2015. However, ESC prevalence increased almost 4 times over that period from 13.6% to 52.1% of vehicles. This change was accounted for by computing the estimated number of crashes that would have occurred that year if no vehicles had ESC equipped (Eq. 40). The

estimated number of crashes if no vehicles had ESC equipped was averaged over the 6-year period from 2010 to 2015.

$$crashes\,{}^{W}/_{O}\,ESC = \frac{crashes}{1 - (ESC\ Penetration) * (ESC\ Effectiveness)} \quad (40)$$

Then the average number of crashes was adjusted to the predicted number of crashes based on the market penetration of ESC (Eq. 41). There were on average 46,561 control loss rollover crashes in 2015. The estimated crash rate for road departure crashes was 15.0 crashes per billion VMT.

$$Crashes\ in\ 2015 = Avg\ Crashes\,{}^{W}/_{O}\,ESC * \big(1 - (Penetration) * (Effectiveness)\big) \quad (41)$$

In NASS/CDS, if the vehicle's model year was greater than 10 years old, a full investigation was not performed. This means that the occupants of these old vehicles are missing injury information. To account for these injured occupants, the ratio of injured occupants to total occupants was assumed to remain constant between the known and unknown occupants. For control loss rollover crashes, there were 30,246 known front seat occupants at least 12 years old with 3,784 injured occupants resulting in an injury rate of 12.5%. Overall, there was an estimated 5,792 occupants injured in control loss rollover crashes. The estimated injured occupant rate for control loss rollover crashes was 1.9 injured occupants per billion VMT.

15.3 Results

Based on the ejection model, the odds of an occupant being ejected from the vehicle decrease by over 5 times for each additional unit increase in SWR. Since ejection is a primary method of injury during a rollover crash, a reduction in ejection probability relates to a reduction in injury probability. There was a total of 66 occupants in vehicles that had a roof SWR less than four and were unbelted. These occupants would receive a reduction in the probability of ejection and injury by increasing the roof SWR. The change in the probability of ejection and probability of injury was computed with the same roof SWR and a SWR equal to 4 for the 66 occupants (Figure 154). The probability of ejection was decreased by an average of 26.5 percentage points for these occupants. The probability of injury was decreased by an average of 28.8 percentage points for these occupants. Increasing the SWR to 4 eliminated an estimated 2,163 ejections and 1,900 MAIS2+F injuries from our sample. This accounted for an 80% reduction in ejections and a 13% reduction in MAIS2+F injuries.

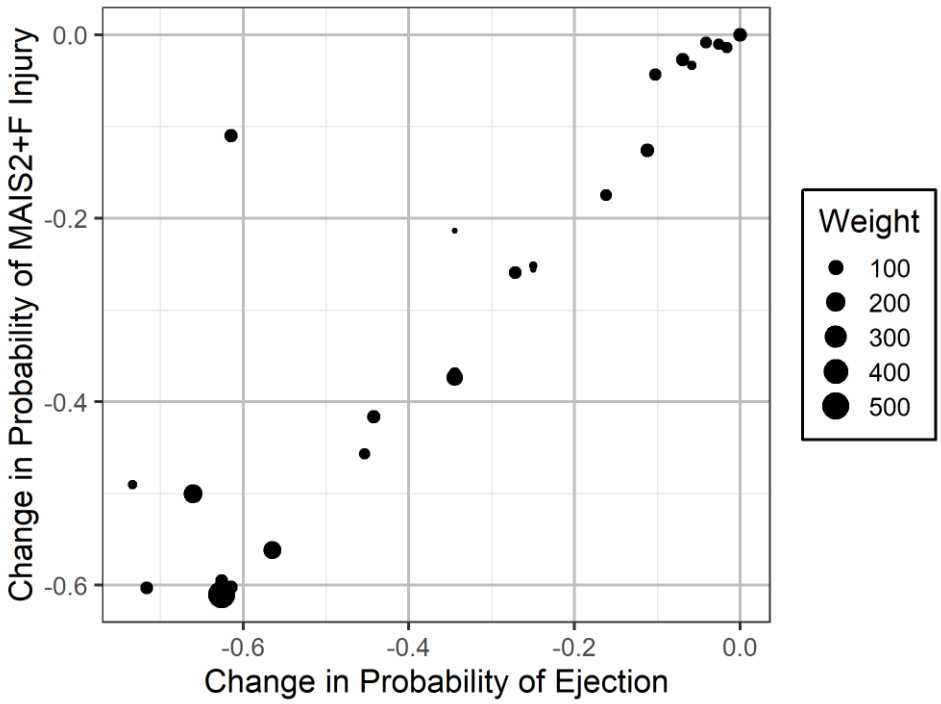

Figure 154. Change in probability of ejection and injury with the introduction of side curtain airbags.

There was a total of 43 occupants that experienced a side airbag applicable ejection. Only 26 of these occupants were unbelted to take advantage of the introduction of side curtain airbags. The change in the probability of ejection and probability of injury was computed with and without side curtain airbags (Figure 155). The probability of ejection was decreased by an average of 44.6 percentage points for these 26 occupants. The probability of injury was decreased by an average of 36.5 percentage points for these 26 occupants. Adding side curtain airbags eliminated an estimated 1,140 ejections and 971 MAIS2+F injuries from our sample. This accounted for a 42% reduction in ejections and a 6.6% reduction in MAIS2+F injuries.

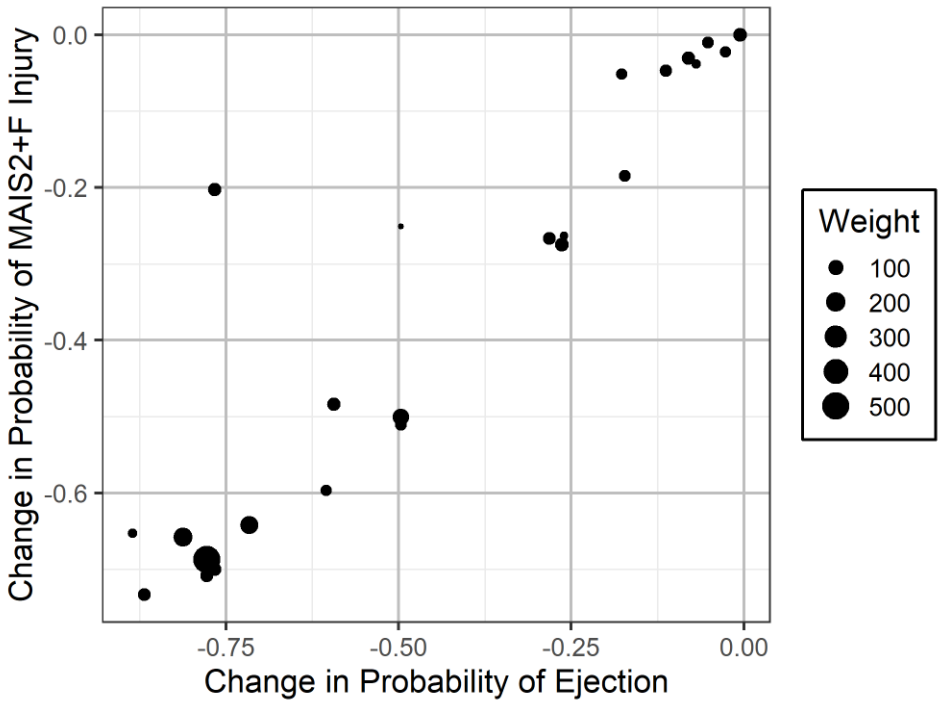

Figure 155. Change in probability of ejection and injury with the introduction of side curtain airbags.

The predicted number of injured occupants from rollover crashes is shown in Table 54. In the future fleet, when all vehicles on the road will be equipped with ESC, strong roofs, and side curtain airbags, the predicted number of drivers injured during control loss rollover crashes was reduced by 59.60%. In the ideal fleet, in which all vehicles had ESC, strong roofs and side curtain airbags, the predicted number of drivers injured would decrease by 60.20% of the baseline fleet.

Table 54. Results of predicted MAIS2+F injured front seat passengers in control loss rollovers.

Population	Actual Baseline Occupants Injured	Predicted Occupants Injured (95% CI)	Percent Reduction in Occupants Injured (95% CI)
No Countermeasure Fleet No Side Airbags Roof SWR = 2 ESC not Equipped Current Belt Use	10,200±1,000	10,200±1,000	0.0%
Baseline Fleet (Predicted) Current Side Airbags Current Roof Strength Current ESC Equipment Current Belt Use	10,200±1,000	9,440±935	7.39±13%
Side Airbag Equipped Fleet All Side Airbag Equipped Current Roof Strength Current ESC Equipment Current Belt Use	10,200±1,000	8,960±935	12.10±13%
Side Airbag Equipped + Strong Roof Fleet All Side Airbag Equipped All Strong Roofs Current ESC Equipment Current Belt Use	10,200±1,000	8,240±905	19.20±12%
Side Airbag Equipped + ESC Equipped Fleet All Side Airbag Equipped Current Roof Strength All ESC Equipped Current Belt Use	10,200±1,000	4,500±606	55.90±7%
Strong Roof Fleet Current Side Airbags All Strong Roofs Current ESC Equipment Current Belt Use	10,200±1,000	8,340±906	18.20±12%
Strong Roof + ESC Equipped Fleet Current Side Airbags All Strong Roofs All ESC Equipped Current Belt Use	10,200±1,000	4,170±567	59.10±7%
ESC Equipped Fleet Current Side Airbags Current Roof Strength All ESC Equipped Current Belt Use	10,200±1,000	4,690±606	54.00±8%

Population	Actual Baseline Occupants Injured	Predicted Occupants Injured (95% CI)	Percent Reduction in Occupants Injured (95% CI)
Future Fleet All Side Airbag Equipped All Strong Roofs All ESC Equipped Current Belt Use	10,200±1,000	4,120±567	59.60±7%
Ideal Fleet All Side Airbag Equipped All Strong Roofs All ESC Equipped All Occupants Belted	10,200±1,000	4,060±558	60.20±7%

Since ESC had penetrated 52.1% of the US fleet in 2015 and prevented some crashes, ESC was estimated to prevent 36.4% of control loss rollover crashes (Figure 156). In 2025, the number of control loss rollover crashes is expected to be reduced by 51.5%. ESC was predicted to prevent 60.2% of control loss rollover crashes in 2050.

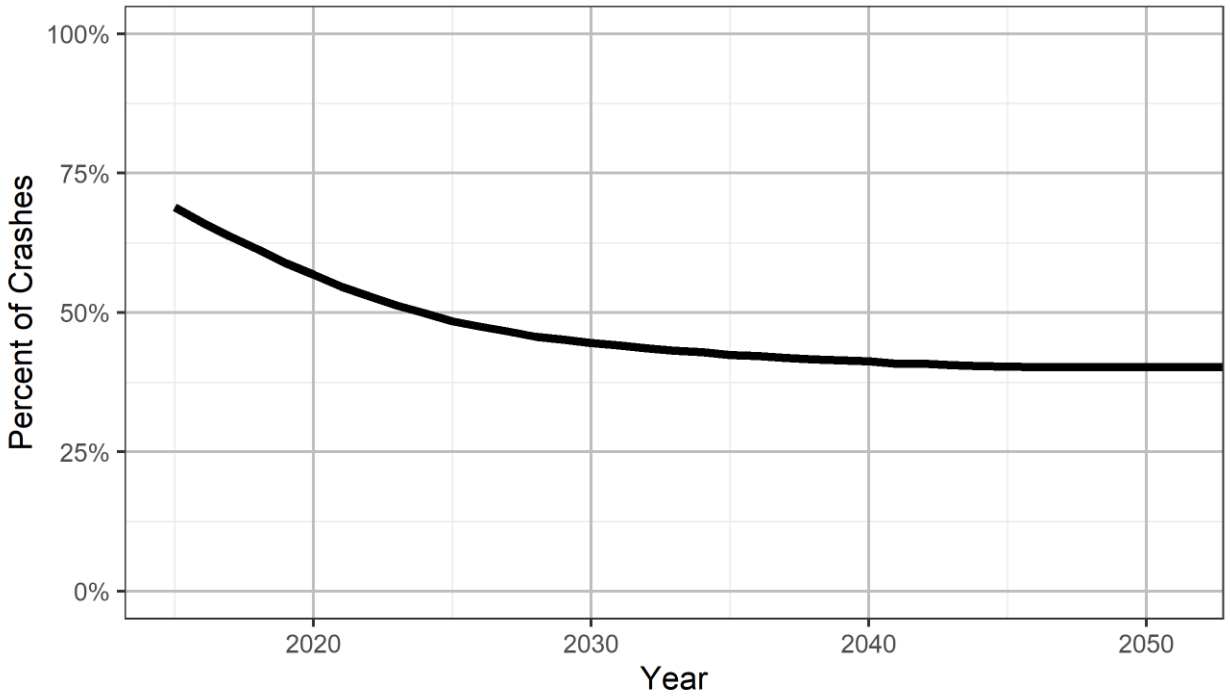

Figure 156. Percent of control loss rollover crashes avoided by ESC.

The number of injured occupants in 2015 from rollover crashes was predicted to be rapidly reduced in the future (Figure 157). By 2025, there was expected to be a 53.6% reduction in MAIS3+F injured occupants from rollover crashes and a 59.6% reduction by 2050.

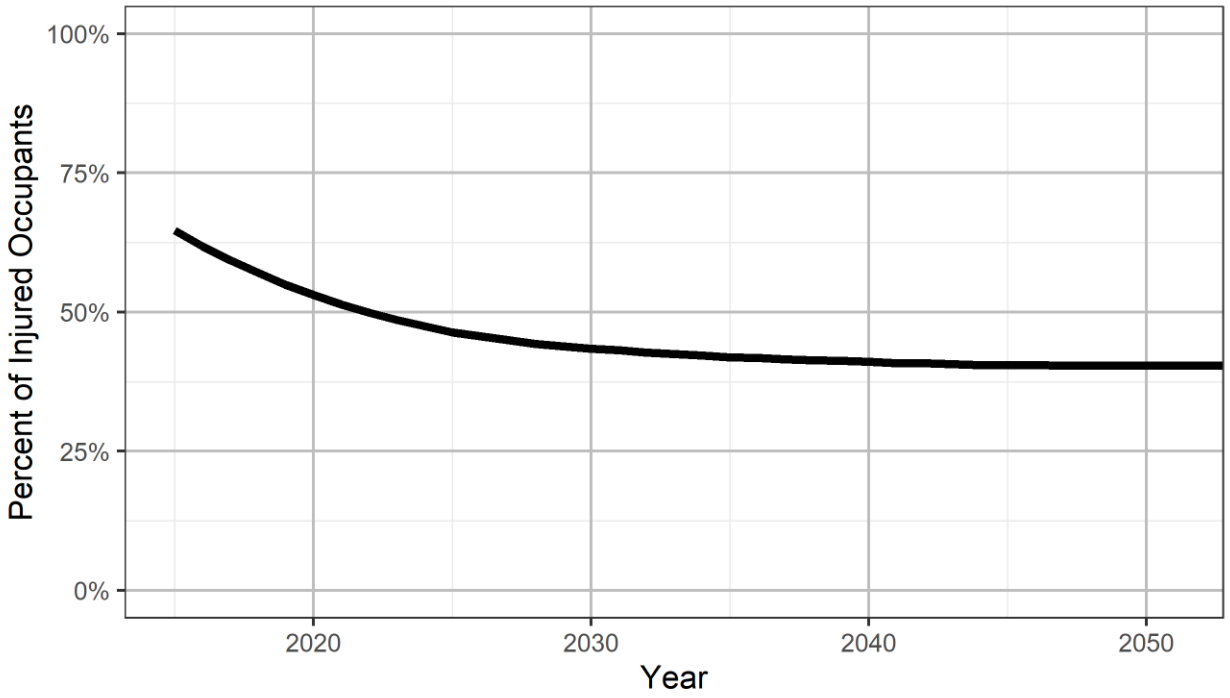

Figure 157. Percent of MAIS2+F injured occupants in control loss rollover crashes prevented due to ESC, side curtain airbags and strong roofs.

The estimated control loss rollover crash rate in 2015 was 18.7 control loss rollover crashes per billion VMT. The predicted number of control loss rollover crashes will decrease until about 2030, while ESC is still penetrating the fleet (Figure 158). From then on, ESC is present in almost every vehicle in the fleet, so the number of control loss rollover crashes increases with the annual VMT.

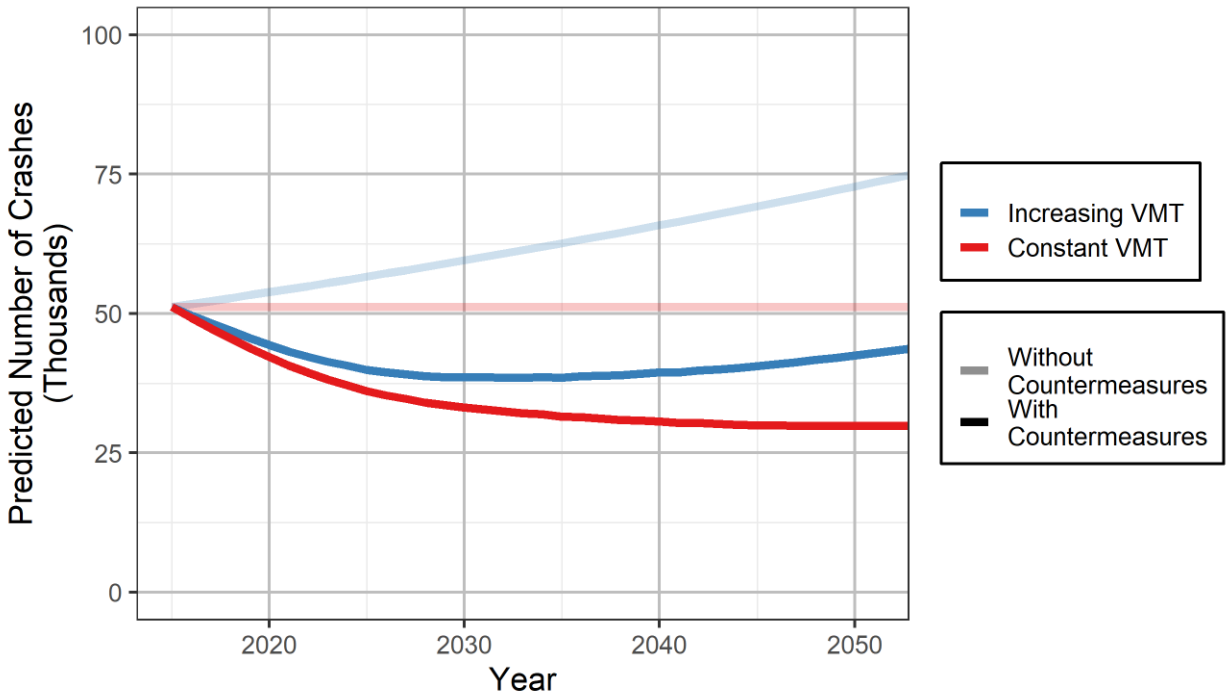

Figure 158. Control loss rollover crash reduction due to ESC.

The estimated rollover MAIS2+F injury rate in 2015 was 0.73 MAIS2+F injured occupants per billion VMT. About 1,780 MAIS2+F injured occupants were predicted in 2025 due to control loss rollover crashes (Figure 159).

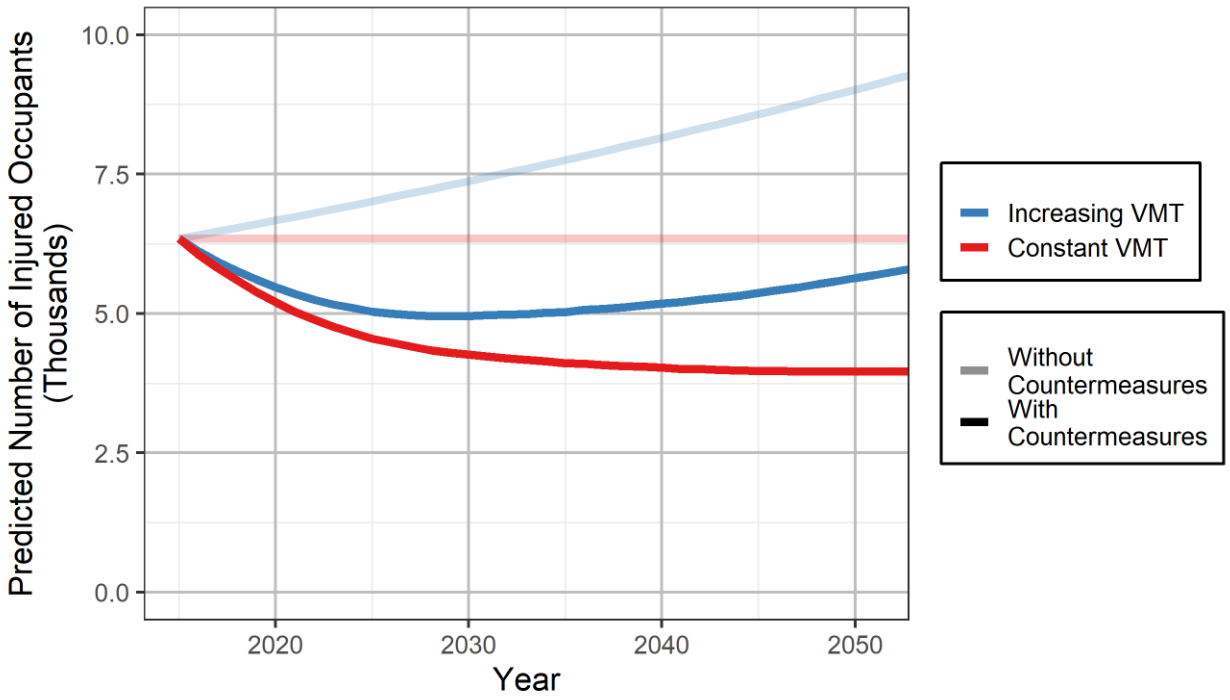

Figure 159. Control loss rollover crash injury reduction due to ESC, side curtain airbags, and strong roofs.

15.4 Discussion

Belt use was the most significant factor in predicting ejection, which largely predicts injury. In our weighted sample of over 300,000 occupants in a pure rollover, only 383 belted occupants were completely ejected. This effect greatly overshadows the effect of having an increased roof SWR. For this reason, the ejection model was constructed based on unbelted occupants alone. Strong roofs were most effective for unbelted occupants in far-side rollovers. For example, in case 782012643, the unbelted, 18-year-old occupant of a 2000 Jeep Cherokee with a roof SWR of 1.55 and without side airbags or ESC was in a far-side rollover with 3 half turns. The occupant was ejected and injured as a result of this rollover crash. The model predicted a probability of ejection of 89.6% and a probability of injury of 85.8%. By only increasing the roof SWR to 4, the probability of ejection was reduced to 15.2% and the probability of injury was reduced to 16.9%. This is the most drastic decrease observed in the dataset since the occupant was unbelted, and the vehicle had a very low SWR originally. In cases with a belted occupant, increasing the SWR did not changed the probability of injury.

The benefit of stronger roofs for unbelted by occupants may not be as large for vehicles equipped with side curtain airbags since both countermeasures aim to keep the occupant in the vehicle. There were not enough cases in our dataset to estimate the effect of side curtain airbags. A larger, newer dataset that contains more vehicles with strong roofs and side curtain airbags would be able to better quantify the interaction.

NASS/CDS and CISS do not differentiate between side impact airbags and side curtain airbags. To estimate the how many vehicles had side curtain airbags, it was assumed that any side airbags that deployed during the rollover were side curtain airbags and any that did not deploy were not side curtain airbags. NHTSA's evaluation of side curtain rollover airbags used the same assumption because NASS/CDS does not specify the type of side airbag [8]. It is important to note that the FMVSS 226 side curtain airbag requirement began phase-in in 2013. All passenger vehicles were not required to have side curtain airbags until 2016. Therefore, most of the side airbags that deployed during the rollovers in this study were not necessarily compliant with FMVSS 226. For the benefits estimation, FMVSS 226 compliant side curtain airbags were assumed to eliminate ejections out the sides of the vehicle.

To estimate the market penetration, the age distribution was assumed to remain the same each case year. This assumption may introduce significant error if external factors such as an economic recession occur before 2050. Additionally, NASS/CDS was assumed to be representative of the SWR of all passenger vehicles in the US fleet to estimate the proportion of vehicles with a strong roof for a given case year. More importantly, NASS/CDS is sampled to be representative of all vehicles involved in a tow-away crash in the US, which is the target population of this study.

Roughly 25% of all injured drivers were either ejected or partially ejected from the vehicle. Thus, drivers with a seat belt are much less likely to be injured. With seat belts properly used, all ejected drivers are predicted to be prevented in control loss rollovers.

The 54% reduction in injured front seat occupants in a control loss rollover crash due to ESC alone is larger than the 44.4% estimated reduction in serious to fatal injury crashes by Lie et al [10]. Our estimate focused on control loss rollover crashes. Therefore, this study was expected to predict a larger reduction in injured occupants than Lie et al.

15.5 Validation

The CISS dataset from 2017 to 2019 was used to identify DrOOL road departure crashes to understand how the future predictions compare over this short time frame. For reference, the average crashes and injured occupants in CDS from 2011 to 2015, which was used as the initial point for the prediction model, and the values from CDS in 2015 are provided as reference (Table 55). Since CISS has a slightly different sample population, NHTSA provided a new variable in 2019 that allows a CDS equivalent population to be determined. In 2017 and 2018, the predicted number of crashes is similar to the actual number of control loss crashes in CISS. Within that same time period, the number of MAIS2+F injured occupants in CISS increased by almost 4,000 while the number of rollover crashes only increased by about 3,000. The following case year, 2019, CISS estimated almost 30,000 more control loss rollover crashes and almost 7,000 more MAIS 2+F injuries. The large variance in CISS cases makes it challenging

to compare with the prediction since it is unlikely that the actual number of control loss rollover crashes would have nearly doubled in one year. Similarly, it is unlikely that the number of MAIS 2+F injured occupants would increase by 59% from 2017 to 2018. Prior to 2019, the predicted number of crashes were within 14% of the control loss rollover crashes in CISS.

Table 55. Comparison of CISS 2017 to 2019 to the predicted control loss rollover crashes and injured occupants.

Case Year	CDS/CISS (Actual)		Prediction (Constant VMT)		Prediction (Increasing VMT)	
	Crashes	MAIS2+F Injuries	Crashes	MAIS2+F Injuries	Crashes	MAIS2+F Injuries
2010-2015	51,205	6,342	51,205	6,342	51,205	6,432
2015	50,279	7,664	-	-	-	-
2016	-	-	49,159	6,062	49,656	6,123
2017	41,395	6,605	47,291	5,816	48,251	5,934
2018	42,940	10,477	45,556	5,598	46,950	5,770
2019	75,990	17,208	43,777	5,388	45,573	5,609
2019 (CDS Equivalent)	74,644	17,208	43,777	5,388	45,573	5,609

15.6 Limitations

The probability that a control loss rollover crash was prevented assumed that all vehicles with ESC had ESC enabled. Additionally, it assumed that any passenger vehicle with ESC as an optional feature did not have it equipped. Both of these assumptions underestimate the effectiveness of ESC for control loss crashes. Therefore, the estimated injury reductions due to ESC are likely lower than the actual injury reduction in the future.

In 2025, all vehicles were assumed to be equipped with FMVSS 226 compliant rollover airbags for ejection mitigation. Because little data on the field performance of the airbags is available at this point, it was assumed that they would have the same effectiveness as being belted.

15.7 Conclusions

In 2025, assuming that all cars are equipped with ESC, side airbags, and strong roofs, there is an estimated 53.6% decrease in MAIS2+F injured occupants occurring due to loss of control rollover crashes. In the future fleet, the combined effectiveness of strong roofs, side curtain airbags, and ESC is estimated to be 59.6%. While ESC provides benefit by preventing rollover crashes, the passive safety systems, such as seat belts, side curtain airbags, and stronger roofs, primarily prevent occupant injury by preventing the occupant ejection from the vehicle.

16 CONLUSIONS AND CONTRIBUTION TO THE FIELD OF AUTOMOTIVE SAFETY

The focus of this dissertation is to evaluate vehicle-based countermeasures, such as lane departure warning and electronic stability control, to prevent or mitigate single vehicle road departure crashes, cross-centerline head-on crashes, and single vehicle rollover crashes. This evaluation was completed through three sections of the dissertation corresponding to the three crash modes investigated. The following conclusions will summarize the findings from each section.

16.1 DrOOL Road Departure Crashes

Road departure crashes are one of the most dangerous crash modes. From 2007 to 2011, drift-out-of-lane road departure crashes accounted for one-third of all crash fatalities despite accounting for less than 10% of all crashes [2]. Most DrOOL road departure crashes occur on straight, 2-lane roads on clear days. Male drivers are more likely to be involved in these crashes. Older drivers are more likely to be fatally injured in the event of a DrOOL road departure crash. Analysis of real-world DrOOL road departure crashes revealed two potential challenges for road departure countermeasures. First, over 20% of the analyzed DrOOL road departure crashes resulting in an MAIS 2+F injury occurred at road locations without a lane line. Missing lane lines may make it challenging to for some early LDW systems to identify a departure event. More advanced LDW/LDP systems may use the road edge as an indicator for lane position to prevent this issue. Second, among those same crashes, 40% of the departure locations had no shoulder and the median clear zone width along the roadside was only 2.5 m. The lack of a shoulder combined with a small clear zone may reduce the chances of the vehicle recovering back onto the roadway.

Another challenge for LDW systems is that their effectiveness is dependent on the evasive actions of the driver. To understand how drivers could respond to an LDW, the driver evasive actions in 97 real road departure crashes were characterized in Chapter 3 using event data recorders. In 16 road departure crashes where both braking and steering information was available, half of the drivers steered in an attempt to return to the road and another 30% braked while performing a steering maneuver. This distribution is an indication for how drivers may respond to a LDW system in a road departure crash scenario. Over half of the analyzed crashes had less than a second elapse from the departure to the impact. Due to the lower coefficient of friction with most roadside materials and very little time to reduce the vehicle speed, steering may be a more effective evasive action for preventing DrOOL road departure crashes. LDW systems, which rely on driver input, may not be limited by the evasive action since 80% of drivers provide some steering input.

Previous studies have shown that the main factor limiting LDW and LDP effectiveness is the time available to avoid the impact [4, 50]. Real-world DrOOL road departure crashes were simulated with LDW/LDP systems to estimate the overall effectiveness of these systems. The simulated systems covered a range of current designs and hypothetical designs which can activate earlier before departure or at lower speeds. The simulations revealed two trends for LDW/LDP effectiveness in road departure crash scenarios: systems that activated earlier and systems that activated at lower speeds were predicted to prevent more crashes. At 15% crash reduction, the least effective system was the LDW system that activated at speeds over 50 kph when the vehicle crossed the lane line. Because the system activated comparatively late, many drivers could not react before the crash occurred. In contrast, the LDP system, which activated immediately at a 1.0 s TTLC, was able to prevent about 40% of crashes. The number of prevented crashes increased to 67% if the LDP system could activate at lower speeds when the driver was distracted. These trends highlight the importance for future LDW and LDP systems to activate at a higher TTLC and at lower speed thresholds.

However, even with the best system, a third of these road departure crashes still occurred. Over half of these residual cases occurred because the vehicle was not travelling fast enough to activate the system. This further reinforces the importance to develop LDW/LDP systems that can activate at lower speeds. However, these systems with lower activation speeds must differentiate lines in intersections and parking lots from intersections. In addition, the LDW/LDP systems should work to optimize the delivery of the warning to prevent too frequent system activation that could lead to drivers disabling the system [82].

The reduction of occupants sustaining at least a moderate injury due to LDW/LDP systems was primarily due to the crash avoidance. The LDW system tended to have a higher injury benefit than crash benefit because many drivers applied the brakes which reduced the occupant injury risk. The basic LDW system was predicted to prevent up to 17% of moderately injured occupants while LDP systems were predicted to prevent up to 60% of moderately injured occupants. Similar to the crash prevention, the injury reduction revealed the same two trends: systems that activated earlier and systems that activated at lower speeds were predicted to prevent more occupants from sustaining moderate to fatal injuries.

The results of these simulations assumed that every vehicle was equipped with the analyzed LDW/LDP system. However, LDW systems are not expected to reach near complete market penetration until 2050 [64]. The market penetration and LDP effectiveness were combined to provide a context for when the benefits from LDP systems will begin to impact the number of road departure crashes and resulting injured occupants. In 2025, there will be an estimated 107,851 road departure crashes with LDP resulting in 13,229 MAIS2+F injured occupants assuming an increasing VMT. Due to increases in the annual VMT, the predicted number of road departure crashes will eventually increase when LDP systems near complete market penetration. While this study estimates the minimum number of road departure

crashes will occur in 2045, it is likely that future improvements to LDW/LDP systems, as well as other lane keeping ADAS will further reduce the number of road departure crashes.

16.2 Cross-Centerline Head-On Crashes

DrOOL cross-centerline head-on crashes consist of a vehicle unintentionally crossing the centerline and colliding with a vehicle traveling the opposite direction. Head-on collisions are particularly dangerous due to the large deceleration experienced upon impact since the vehicles were moving in opposite directions. Head-on crashes comprise only 4% of non-intersection crashes but account for 49% of fatalities in non-intersection crashes [3]. Most cross-centerline head-on crashes occur on straight two-lane roads on clear days. Older drivers are more likely to receive moderate to fatal injuries during the head-on crashes.

Similar to road departure crashes, the LDW system effectiveness in head-on crashes is limited by the response of the driver. The driver evasive actions for 62 encroaching vehicles and 95 impacted vehicle were characterized using EDR data from the Virginia Tech EDR database and coded trajectories from the Cross-Centerline Database. In 18 vehicles where both braking and steering information was available the majority of impacted vehicles preformed either braking alone or a combination of braking and steering. For the encroaching vehicle, the driver performed either steering alone or a combination of braking and steering. Unlike the encroaching vehicle, every impacted vehicle driver attempted some evasive maneuver before the crash. Because nearly every impacted vehicle driver attempts a braking maneuver, and most encroaching vehicle drivers attempt a steering maneuver, the effectiveness of LDW/LDP systems may not be drastically affected by the evasive action but instead could be restricted by the time available to react.

Real-world head-on crashes were simulated with LDW/LDP systems to estimate the crash effectiveness of these systems. The simulated systems covered a range of current designs and hypothetical designs which can activate earlier before departure or at lower speeds. Identical to road departure crashes, the simulations revealed two trends for LDW/LDP effectiveness in head-on crash scenarios: systems that activated earlier and systems that activated at lower speeds were predicted to prevent more crashes. At a 7% crash reduction, the least effective system was the LDW system that activated at speeds over 50 kph when the vehicle crossed the lane line. Because the system activated comparatively late, many drivers could not react before the crash occurred. In contrast, the LDP system, which activated immediately at a 1.0 s TTLC, was able to prevent 32% of crashes. The number of prevented crashes increased to 51% if the LDP system could activate at lower speeds when the driver was distracted. These trends highlight the importance for future LDW and LDP systems to activate at a higher TTLC and at lower speed thresholds.

However, even with the best LDP system, half of all head-on crashes are predicted to still occur. The LDP system did not activate in all but two of the remaining/residual crashes due to the activation threshold. This further reinforces the importance to develop LDW/LDP systems that can activate at lower

speeds. However, these systems with lower activation speeds must differentiate lines in intersections and parking lots from intersections. In addition, the LDW/LDP systems should work to optimize the delivery of the warning to prevent too frequent system activation that could lead to drivers disabling the system [82].

The reduction of occupants sustaining at least a moderate injury due to LDW/LDP systems was primarily due to the crash avoidance. Both the LDW and the LDP systems tended to have a higher injury benefit than crash benefit because many drivers applied the brakes which reduced the occupant injury risk. The basic LDW system was predicted to prevent up to 21% of moderately injured occupants while LDP systems were predicted to prevent up to 74% of moderately injured occupants. Similar to the crash prevention, the injury reduction revealed the same two trends: systems that activated earlier and systems that activated at lower speeds were predicted to prevent more occupants from sustaining moderate to fatal injuries.

The results of these simulations assumed that every vehicle was equipped with the analyzed LDW/LDP system. However, LDW systems are not expected to reach near complete market penetration until 2050 [64]. The market penetration and LDP effectiveness were combined to provide a context for when the benefits from LDP systems will begin to reduce the number of head-on crashes and resulting injured occupants. In 2025, there will be an estimated 21,429 head-on crashes with LDP resulting in 6,680 MAIS2+F injured occupants assuming an increasing VMT. Due to increases in the annual VMT, the predicted number of head-on crashes will eventually increase when LDP systems near complete market penetration. While this study estimates the minimum number of road departure crashes will occur in 2042, it is likely that future improvements to LDW/LDP systems, as well as other lane keeping ADAS will further reduce the number of head-on crashes.

While future ADAS systems may not cross the centerline, they will likely encounter a cross-centerline encroachment from an oncoming vehicle. To form a frame-work for the timing of possible evasive actions, the PRT and response type of drivers in real cross-centerline encroachment scenarios were analyzed. Based on 17 cases, the driver steering PRT was, on average, 0.39s and faster than the driver braking PRT of 0.84s. The PRT and the type of response were dependent on the urgency of the scenario. When the driver had very little time to react, the response was often a fast steering maneuver. In contrast, the driver PRT was longer in less urgent scenarios, and the driver applied the brakes prior to any steering maneuver. ADAS encountering a cross-centerline event should modify their initial response from evasive braking to steering as the TTC decreases to promote the occupant confidence in the ability of the system to perform safe maneuvers [69].

16.3 Control Loss Rollover Crashes

In 2017, 30.4% of passenger vehicle crash fatalities involved a vehicle rollover [1]. Ejection is a key contributor to occupant injury with over 40% of the fatalities in rollovers due to occupant ejection. However, not every fatally injured occupant involved in a rollover was ejected from the vehicle. Another confounding factor is that the vehicle may collide with fixed objects or other vehicles in addition to the rollover. Most control loss rollovers occur on straight two-lane roads on clear days. Younger drivers and male drivers are more commonly involved in these rollover crashes than older drivers or female drivers. However, older drivers are more likely to be fatally injured in the event of a rollover. The primary countermeasure for control loss rollover crashes is ESC but ESC does not prevent all rollover crashes. In the event of a rollover crash.

Since ESC already has a significant presence in the US fleet, the benefit of ESC in control-loss rollover crashes could be estimated with existing crash data. The number of control loss rollover crashes and rear-end crashes where the vehicle was equipped with ESC was compared to those same crash types where the vehicle was not equipped with ESC. This quasi-induced exposure method estimates that 50.6% of control loss rollover crashes have been prevented by ESC. While high, this also implies that ESC did not prevent rollovers in all cases resulting from control loss. There were 69 cases in which the vehicle had ESC but still lost control and overturned. For vehicles with ESC, 25% of the lateral skidding control loss rollover crashes occurred due to traveling too fast during bad road conditions and another 38.2% of crashes had a critical pre-crash event of traveling off the road. ESC may be less effective in situations in which the tire friction is low such as when the road conditions are poor, or the vehicle is no longer on the road.

In cases where a rollover crash still occurs, passive safety systems, such as the strength of the roof, side curtain airbags and seat belts, are designed to protect the occupants. A novel rollover injury model was constructed which incorporates the reduction of occupant ejection due to seat belts and stronger roofs while accounting for the occupant age, BMI, vehicle type, and number of quarter turns. Belted occupants were almost never ejected from the vehicle. Assuming a similar effectiveness for side airbags, there is a predicted 12% reduction in the number of occupants sustaining MAIS 2+F injuries. Stronger roof designs, with a SWR of at least 4, are estimated to prevent up to 18% of number of occupants sustaining MAIS 2+F injuries by reducing the likelihood of occupant ejection.

ESC, strong roofs and side curtain airbags, are continually being introduced into the US fleet and are already equipped in many vehicles on the road. The market penetration and effectiveness of each of these countermeasures were combined to provide a context for when the benefits from rollover systems will be outpaced by the increase in annual VMT. The predicted number of control loss rollover crashes will decrease until about 2030, while ESC is still penetrating the fleet. About 1,780 MAIS2+F injured occupants were predicted in 2025 due to control loss rollover crashes.

17 PUBLICATION SUMMARY

The research presented in or in support of this dissertation has been in many peer-reviewed publications, presented at conferences, or publication is anticipated in the near future. The following lists summarize these publications and manuscripts.

17.1 Journal Publications

1. Riexinger LE, Sherony R, Gabler HC, (2019). "Residual Road Departure Crashes After Full Deployment of LDW and LDP Systems." *Traffic and Injury Prevention.* DOI: 10.1080/15389588.2019.1603375
2. Riexinger LE, Gabler HC, (2020). "Expansion of NASS/CDS for Characterizing Run-Off-Road Crashes". *Traffic Injury Prevention.* DOI: 10.1080/15389588.2020.1798942

17.2 Conference Publications

1. Riexinger LE, Johnson NS, Gabler HC, "A Corridor-Based Procedure for Determining Longitudinal Barrier Length of Need", Proceedings of the 100th Transportation Research Board Annual Meeting, Washington, DC (January 2021).
2. Riexinger LE, Gabler HC, "Expansion for NASS/CDS for Characterizing Run-Off-Road Crashes", 64th Annual Proceedings of the Association for the Advancement of Automotive Medicine, (October 2020).
3. Riexinger LE, Gabler HC, "Development of the NCHRP 17-43 Roadway Departure Database", Proceedings of the 99th Transportation Research Board Annual Meeting, Washington, DC (January 2020).
4. Riexinger LE, Sherony R, Gabler HC, "A Preliminary Characterization of Driver Evasive Manoeuvres in Cross-Centerline Vehicle-to-Vehicle Collisions", Proceedings of the 2019 International Research Council on Biomechanics of Injury Europe Conference, Florence, Italy (September 2019)
5. Riexinger LE, Sherony R, Gabler HC, "Residual Road Departure Crashes After Full Deployment of LDW and LDP Systems", Proceedings of the 26th Enhanced Safety of Vehicles Conference, Eindhoven, Netherlands (June 2019)
6. Riexinger LE, Sherony R, Gabler HC, "Has Electronic Stability Control Reduced Rollover Crashes?", SAE Paper 2019-01-1022 (April 2019). DOI: 10.4271/2019-01-1022
7. Almannaa MH, Bareiss M, Riexinger LE, Guo F, "Are Individuals with Arthritis More Likely to be Involved in a Crash?", Proceedings of the 98th Transportation Research Board Annual Meeting, Washington, DC (January 2019)
8. Riexinger LE, Gabler HC, "Preliminary Characterization of Road Departure Impact Conditions Using Event Data Recorders", Proceedings of the 98th Transportation Research Board Annual Meeting, Washington, DC (January 2019)
9. Riexinger LE, Gabler HC, "A Preliminary Characterization of Driver Manoeuvres in Road Departure Crashes", Proceedings of the 2018 International Research Council on Biomechanics of Injury Europe Conference, Athens, Greece (September 2018)

10. Riexinger LE, Sherony R, Gabler HC, "Methodology for Estimating the Benefits of Lane Departure Warnings Using Event Data Recorders," SAE Paper 2018-01-0509 (April 2018). DOI: 10.4271/2018-01-0509

17.3 Conference Abstracts

1. Riexinger LE, Sherony R, Gabler HC, "Predicted Benefit of Lane Departure Warning for Cross-Centerline Head-On Crashes using a Multi-Vehicle Dynamics Model," *6th Annual Proceedings of the Association for the Advancement of Automotive Medicine, Student Symposium,* Madrid, Spain (October 2019)
2. Riexinger LE, Gabler HC, "Incidence and Fatal Injury Outcomes in Rollover Crashes", *Proceedings of the 2018 Biomedical Engineering Society Conference,* Atlanta, GA (October 2018)
3. Riexinger LE, Sherony R, Gabler HC, "Estimated Benefits of Lane Departure Warning and Prevention Systems Based on EDR Crash Information," *62nd Annual Proceedings of the Association for the Advancement of Automotive Medicine, Student Symposium,* Nashville, TN (October 2018)

17.4 Anticipated Publications

1. Riexinger LE, Johnson SN, Gabler, HC, "A Corridor-Based Procedure for Determining Longitudinal Barrier Length of Need", *Transportation Research Record.* (Accepted, Under Review).
2. Riexinger LE, Fortenbaugh DM, "Quantifying Perception Response Time to Unanticipated Encroachments Using Naturalistic Driving Data". *Accident Analysis and Prevention*. (Submitted, Under Review).
3. Riexinger LE, King S, Sherony R, Gabler HC, "Quantifying Occupant Injury Risk in Rollover Crashes: A Rollover Injury Model".
4. Riexinger LE, King S, Sherony, R, Gabler HC, "Future Benefit of Current Active and Passive Countermeasures for Rollover Crashes".
5. Riexinger LE, Galloway AJ, Gopiao JB, Sherony R, Gabler HC, "The Benefit of Advanced Lane Departure Countermeasures for Real-World Cross-Centerline and Road Departure Crashes".

18 REFERENCES

[1] National Highway Traffic Safaety Administration. (2019). *DOT HS 8112 806, Traffic Safety Facts 2017*.

[2] K. D. Kusano and H. C. Gabler, "Comprehensive target populations for current active safety systems using national crash databases," *Traffic Injury Prevention,* vol. 15, no. 7, pp. 753-761, 2014, doi: 10.1080/15389588.2013.871003.

[3] K. D. Kusano and H. C. Gabler, "Characterization of opposite-direction road departure crashes in the united states," *Transportation Research Record,* vol. 2377, no. 1, pp. 14-20, 2013.

[4] L. E. Riexinger, R. Sherony, and H. C. Gabler, "Methodology for Estimating the Benefits of Lane Departure Warnings Using Event Data Recorders," in *SAE World Congress Experience*, Detroit, USA, April 2018 2018: SAE International, doi: 10.4271/2018-01-0509.

[5] K. Suzuki and H. Jansson, "An analysis of driver's steering behaviour during auditory or haptic warnings for the designing of lane departure warning system," *JSAE review,* vol. 24, no. 1, pp. 65-70, 2003, doi: 10.1016/S0389-4304(02)00247-3.

[6] L. E. Riexinger and H. C. Gabler, "A Preliminary Characterisation of Driver Manoeuvres in Road Departure Crashes," in *IRCOBI Conference*, Athens, Greece, September 2018 2018.

[7] K. D. Kusano, H. Gabler, and T. I. Gorman, "Fleetwide safety benefits of production forward collision and lane departure warning systems," *SAE International Journal of Passenger Cars-Mechanical Systems,* vol. 7, no. 2014-01-0166, pp. 514-527, 2014.

[8] J. M. Scanlon, K. D. Kusano, R. Sherony, and H. C. Gabler, "Potential safety benefits of lane departure warning and prevention systems in the US vehicle fleet," in *International Conference on Enhanced Safety of Vehicles (ESV)*, June 2015 2015.

[9] J. B. Cicchino, "Effects of lane departure warning on police-reported crash rates," *Journal of Safety Research,* vol. 66, pp. 61-70, 2018, doi: 10.1016/j.jsr.2018.05.006.

[10] S. Sternlund, J. Strandroth, M. Rizzi, A. Lie, and C. Tingvall, "The effectiveness of lane departure warning systems—A reduction in real-world passenger car injury crashes," *Traffic injury prevention,* vol. 18, no. 2, pp. 225-229, 2017, doi: 10.1080/15389588.2016.1230672.

[11] T. O. T. F. f. R. Safety, *Roadside design guide*. AASHTO, 2011.

[12] D. A. Noyce and V. V. Elango, "Safety evaluation of centerline rumble strips: crash and driver behavior analysis," *Transportation Research Record,* vol. 1862, no. 1, pp. 44-53, 2004.

[13] B. N. Persaud, R. A. Retting, and C. A. Lyon, "Crash reduction following installation of centerline rumble strips on rural two-lane roads," *Accident Analysis & Prevention,* vol. 36, no. 6, pp. 1073-1079, 2004.

[14] M. Ray, C. Carrigan, C. Plaxico, S. Miaou, and T. Johnson, "Roadside Safety Analysis Program (RSAP) Update. National Cooperative Highway Research Program Project 22-27," *Transportation Research Board, Washington DC,* 2012.

[15] American Association of State Highway and Transportation Officials, *Manual for Assessing Safety Hardware*. AASHTO, 2009.

[16] C. M. Farmer, "Effect of electronic stability control on automobile crash risk," *Traffic injury prevention,* vol. 5, no. 4, pp. 317-325, 2004.

[17] A. Erke, "Effects of electronic stability control (ESC) on accidents: A review of empirical evidence," *Accident Analysis & Prevention*, vol. 40, no. 1, pp. 167-173, 2008/01/01/ 2008, doi: https://doi.org/10.1016/j.aap.2007.05.002.
[18] J. N. Dang, "Preliminary results analyzing the effectiveness of electronic stability control (ESC) systems," US Department of Transportation, National Highway Traffic Safety Administration, 2004.
[19] Y. E. Papelis, G. S. Watson, and T. L. Brown, "An empirical study of the effectiveness of electronic stability control system in reducing loss of vehicle control," *Accident Analysis & Prevention*, vol. 42, no. 3, pp. 929-934, 2010.
[20] A. Lie, C. Tingvall, M. Krafft, and A. Kullgren, "The effectiveness of electronic stability control (ESC) in reducing real life crashes and injuries," *Traffic injury prevention*, vol. 7, no. 1, pp. 38-43, 2006.
[21] K. H. Digges and A. M. Eigen, "Crash attributes that influence the severity of rollover crashes," *Progress in Technology*, vol. 101, pp. 299-308, 2004.
[22] C. Conroy *et al.*, "Rollover crashes: predicting serious injury based on occupant, vehicle, and crash characteristics," *Accident Analysis & Prevention*, vol. 38, no. 5, pp. 835-842, 2006.
[23] J. R. Funk, J. M. Cormier, C. E. Bain, J. L. Wirth, E. B. Bonugli, and R. A. Watson, "Factors affecting ejection risk in rollover crashes," in *Annals of Advances in Automotive Medicine/Annual Scientific Conference*, 2012, vol. 56: Association for the Advancement of Automotive Medicine, p. 203.
[24] J. R. Funk, J. M. Cormier, and S. J. Manoogian, "Comparison of risk factors for cervical spine, head, serious, and fatal injury in rollover crashes," *Accident Analysis & Prevention*, vol. 45, pp. 67-74, 2012.
[25] Association for the Advancement of Automotive Medicine, "The Abbreviated Injury Scale 2005 Update 2008," 2008.
[26] C. A. Flannagan *et al.*, "Comparing motor-vehicle crash risk of EU and US vehicles," *Accident Analysis & Prevention*, vol. 117, pp. 392-397, 2018.
[27] D. A. Krauss, *Forensic aspects of driver perception and response*. Lawyers & Judges Publishing Company, 2015.
[28] P. L. Olson and M. Sivak, "Perception-response time to unexpected roadway hazards," *Human factors*, vol. 28, no. 1, pp. 91-96, 1986.
[29] N. D. Lerner, "Brake perception-reaction times of older and younger drivers," in *Proceedings of the human factors and ergonomics society annual meeting*, 1993, vol. 37, no. 2: SAGE Publications Sage CA: Los Angeles, CA, pp. 206-210.
[30] N. L. Broen and D. P. Chiang, "Braking response times for 100 drivers in the avoidance of an unexpected obstacle as measured in a driving simulator," in *Proceedings of the Human Factors and Ergonomics Society Annual Meeting*, 1996, vol. 40, no. 18: SAGE Publications Sage CA: Los Angeles, CA, pp. 900-904.
[31] P. D'Addario and B. Donmez, "The effect of cognitive distraction on perception-response time to unexpected abrupt and gradually onset roadway hazards," *Accident Analysis & Prevention*, vol. 127, pp. 177-185, 2019.
[32] J. Gao and G. A. Davis, "Using naturalistic driving study data to investigate the impact of driver distraction on driver's brake reaction time in freeway rear-end events in car-following situation," *Journal of safety research*, vol. 63, pp. 195-204, 2017.

[33] M. Green, "" How long does it take to stop?" Methodological analysis of driver perception-brake times," *Transportation human factors*, vol. 2, no. 3, pp. 195-216, 2000.
[34] G. J. Andersen and C. W. Sauer, "Optical information for car following: The driving by visual angle (DVA) model," *Human factors*, vol. 49, no. 5, pp. 878-896, 2007.
[35] T. A. Dingus *et al.*, "The 100-car naturalistic driving study, Phase II-results of the 100-car field experiment," Virginia Tech Transportation Institute, April 2006 2006.
[36] L. E. Riexinger, R. Sherony, and H. C. Gabler, "A Preliminary Characterisation of Driver Evasive Manoeuvres in Cross-Centreline Vehicle-to-Vehicle Collisions," presented at the International Research Consortium on the Biomechanics of Injury Florence, Italy, 2019.
[37] G. Markkula, J. Engström, J. Lodin, J. Bärgman, and T. Victor, "A farewell to brake reaction times? Kinematics-dependent brake response in naturalistic rear-end emergencies," *Accident Analysis & Prevention*, vol. 95, pp. 209-226, 2016.
[38] National Highway Traffic Safety Administration. "Fatality Analysis Reporting System." National Highway Traffic Safety Administration. ftp://ftp.nhtsa.dot.gov/FARS/ (accessed.
[39] National Highway Traffic Safety Administration. "National Automotive Sampling System General Estimates System." National Highway Traffic Safety Administration. ftp://ftp.nhtsa.dot.gov/GES/ (accessed.
[40] National Highway Traffic Safety Administration. "National Automotive Sampling System Crashworthiness Data System." National Highway Traffic Safety Administration. ftp://ftp.nhtsa.dot.gov/NASS/ (accessed.
[41] D. Sharma, S. Stern, J. Brophy, and E. Choi, "An overview of NHTSA's crash reconstruction software WinSMASH," in *Proceedings of the 20th International Technical Conference on Enhanced Safety of Vehicles*, Lyon, France, 2007.
[42] C. E. Hampton and H. C. Gabler, "Evaluation of the accuracy of NASS/CDS Delta-V estimates from the enhanced WinSmash algorithm," in *Annals of Advances in Automotive Medicine/Annual Scientific Conference*, Las Vegas, USA, 2010, vol. 54: Association for the Advancement of Automotive Medicine, p. 241.
[43] H. C. Gabler, C. Hampton, and N. Johnson, *Development of the WinSMASH 2010 Crash Reconstruction Code*. U.S. Department of Transportation, National Highway Traffic Safety Administration (NHTSA), 2012.
[44] National Highway Traffic Safety Administration. "Crash Investigation Sampling System." National Highway Traffic Safety Administration. ftp://ftp.nhtsa.dot.gov/CISS/ (accessed.
[45] J. M. Scanlon, K. D. Kusano, and H. C. Gabler, "Analysis of driver evasive maneuvering prior to intersection crashes using event data recorders," *Traffic Injury Prevention*, vol. 16, no. sup2, pp. S182-S189, 2015, doi: 10.1080/15389588.2015.1066500.
[46] K. D. Kusano and H. C. Gabler, "Characterization of lane departure crashes using event data recorders extracted from real-world collisions," *SAE International journal of passenger cars-mechanical systems*, vol. 6, no. 2013-01-0730, pp. 705-713, 2013.
[47] Virginia Tech. *National Cooperative Highway Research Program 17-43: Long-Term Roadside Crash Data Collection Program*. [Online]. Available: https://apps.trb.org/cmsfeed/TRBNetProjectDisplay.asp?ProjectID=1637
[48] L. E. Riexinger and H. C. Gabler, "Expansion of NASS/CDS for characterizing run-off-road crashes," *Traffic Injury Prevention*, pp. 1-5, 2020, doi: 10.1080/15389588.2020.1798942.

[49] L. E. Riexinger and H. C. Gabler, "Characterization of Road Departure Impact Conditions Using Event Data Recorders," presented at the Transportation Research Board 98th Annual Meeting, Washington, DC, 2019.
[50] L. E. Riexinger, R. Sherony, and H. Gabler, "Residual Road Departure Crashes After Full Deployment of LDW and LDP Systems," *Traffic injury prevention*, 2019, Art no. 19-0121.
[51] T. A. Dingus *et al.*, *Naturalistic driving study: Technical coordination and quality control* (no. SHRP 2 Report S2-S06-RW-1). 2015.
[52] C. K. Layman, M. A. Perez, T. Sugino, and J. Eggert. *Research of Driver Assistant System*, VTTI, doi: doi:10.15787/VTT1/DEDACT.
[53] National Highway Traffic Safety Administration. *Component Test Database*. [Online]. Available: https://www-nrd.nhtsa.dot.gov/database/VSR/com/QueryTest.aspx
[54] National Highway Traffic Safety Administration, "FMVSS 216, Upgrade Roof Crush Resistance," ed: Preliminary Regulatory Impact Analysis, Office of Regulatory Analysis and Evaluation, 2005.
[55] Insurance Institute For Highway Safety. "Vehicle Safety Ratings." Insurance Institute For Highway Safety. https://www.iihs.org/iihs/ratings (accessed August, 2018).
[56] Insurance Institute For Highway Safety, "Crashworthiness Evaluation Roof Strength Test Protocol (Version III)," Insurance Institute for Highway Safety, Ruckersville, VA, 2016, vol. III.
[57] Federal Highway Administration. *National Household Travel Survey*. [Online]. Available: https://nhts.ornl.gov
[58] M. W. Hancock and B. Wright, "A policy on geometric design of highways and streets," *American Association of State Highway and Transportation Officials: Washington, DC, USA*, 2013.
[59] K. D. Kusano and H. C. Gabler, "Safety benefits of forward collision warning, brake assist, and autonomous braking systems in rear-end collisions," *IEEE Transactions on Intelligent Transportation Systems*, vol. 13, no. 4, pp. 1546-1555, 2012.
[60] K. D. Kusano and H. C. Gabler, "Comparison of expected crash and injury reduction from production forward collision and lane departure warning systems," *Traffic injury prevention*, vol. 16, no. sup2, pp. S109-S114, 2015.
[61] M. Bareiss, "Effectiveness of Intersection Advanced Driver Assistance Systems in Preventing Crashes and Injuries in Left Turn Across Path/Opposite Direction Crashes in the United States," Virginia Tech, 2019.
[62] P. Bruzzi, S. B. Green, D. P. Byar, L. A. Brinton, and C. Schairer, "Estimating the population attributable risk for multiple risk factors using case-control data," *American journal of epidemiology*, vol. 122, no. 5, pp. 904-914, 1985.
[63] Federal Highway Administration, "Highway Statistics 2015: Public Road Mileage, Lane-Miles, and VMT," no. Chart VMT-422C, 2015. [Online]. Available: https://www.fhwa.dot.gov/policyinformation/statistics/2015/vmt422c.cfm.
[64] Highway Loss Data Institute, "Predicted Availability and Fitment of Safety Features on Registered Vehicles—A 2018 Update," *HLDI Bulletin*, vol. 35, no. 27, September 2018 2018.
[65] T. Johnson, "Fleetwide Models of Lane Departure Warning and Prevention Systems in the United States," Biomedical Engineering Master of Science, Biomedical Engineering and Mechanics, Virginia Tech, 2017. [Online]. Available: https://vtechworks.lib.vt.edu/handle/10919/74981

[66] P. Niehoff and H. C. Gabler, "The accuracy of WinSmash delta-V estimates: the influence of vehicle type, stiffness, and impact mode," in *Annual Proceedings/Association for the Advancement of Automotive Medicine*, 2006, vol. 50: Association for the Advancement of Automotive Medicine, p. 73.
[67] S. Datentechnik, "PC-Crash Operating and Technical Manual Version 11.1," MEA Forensic, 2017.
[68] J. M. Hankey, "Unalerted emergency avoidance at an intersection and possible implications for ABS implementation," 1997.
[69] F. Ekman, M. Johansson, L.-O. Bligård, M. Karlsson, and H. Strömberg, "Exploring automated vehicle driving styles as a source of trust information," *Transportation research part F: traffic psychology and behaviour*, vol. 65, pp. 268-279, 2019.
[70] *Taxonomy and Definitions for Terms Related to Driving Automation Systems for On-Road Motor Vehicles*, Society of Automotive Engineers On-Road Automated Vehicle Standards Committee, Warrendale, PA, 2014.
[71] C. Gold, F. Naujoks, J. Radlmayr, H. Bellem, and O. Jarosch, "Testing scenarios for human factors research in level 3 automated vehicles," in *International conference on applied human factors and ergonomics*, 2017: Springer, pp. 551-559.
[72] S. Trask, M. Stewart, T. Kerwin, and S. Midlam-Mohler, "Effectiveness of Warning Signals in Semi-Autonomous Vehicles," SAE Technical Paper, 0148-7191, 2019.
[73] J. Atwood, F. Guo, G. Fitch, and T. A. Dingus, "The driver-level crash risk associated with daily cellphone use and cellphone use while driving," *Accident Analysis & Prevention*, vol. 119, pp. 149-154, 2018.
[74] T. A. Dingus *et al.*, "Driver crash risk factors and prevalence evaluation using naturalistic driving data," *Proceedings of the National Academy of Sciences*, vol. 113, no. 10, pp. 2636-2641, 2016.
[75] *Federal Motor Vehicle Safety Standards 226: Ejection Mitigation*, National Highway Traffic Safety Administration, 2011.
[76] National Highway Traffic Safety Administration. (2014). *DOT HS 811 822, Updated Estimates of Fatality Reduction by Curtain and Side Airbags in Side Impacts and Preliminary Analyses of Rollover Curtains*.
[77] D. W. Kononen, C. A. Flannagan, and S. C. Wang, "Identification and validation of a logistic regression model for predicting serious injuries associated with motor vehicle crashes," *Accident Analysis & Prevention*, vol. 43, no. 1, pp. 112-122, 2011.
[78] J. Cuthbert, "An extension of the induced exposure method of estimating driver risk," *Journal of the Royal Statistical Society. Series A (Statistics in Society)*, pp. 177-190, 1994.
[79] National Highway Traffic Safety Administration, "Electronic Stability Control Systems for Light Vehicles," *Federal Motor Vehicle Safety Standards 126*, 2007.
[80] Highway Loss Data Institute, "Predicted Availability of Safety Features on Registered Vehicles—An Update," *HLDI Bulletin*, vol. 31, no. 15, September 2014 2014.
[81] Highway Loss Data Institute, "Predicted Availability of Safety Features on Registered Vehicles—A 2016 Update," *HLDI Bull.*, pp. 32 (16): 1–13, 2016.
[82] C. Flannagan *et al.*, "Large-scale field test of forward collision alert and lane departure warning systems," 2016.